Lecture Notes for PHY 521

James M. Lattimer

Dept. of Physics & Astronomy
State University of New York at Stony Brook

Chapter 1.
General Introduction

1.1. Luminosity, Flux and Magnitude

The luminosity L is an integral of the specific flux F_λ, the amount of energy at wavelength λ traversing a unit area per unit time:

$$L = 4\pi R^2 \int_0^\infty F_\lambda d\lambda. \tag{1.1.1}$$

Here R is the effective stellar radius. In the absence of any absorption between a star and the Earth, the incident energy flux is

$$f_\lambda = F_\lambda \left(\frac{R}{r}\right)^2, \tag{1.1.2}$$

where r is the distance to the star. In practice what is measured at the Earth's surface is modified by the transmissivity through the atmosphere A_λ and by the efficiency of the telescope E_λ whose collecting area is πa^2:

$$b = \pi a^2 \int_0^\infty f_\lambda A_\lambda E_\lambda d\lambda. \tag{1.1.3}$$

b is the apparent brightness. The transmissivity is affected by the viewing angle.

Historically, astronomers measure brightness using magnitudes. Hipparchus denoted the brightest naked eye stars magnitude 1 and the dimmest magnitude 6. The response of the eye is logarithmic. By international agreement, the difference of 5 magnitudes is equivalent to a factor of 100:

$$\frac{b_1}{b_2} = 100^{(m_2-m_1)/5} = 10^{.4(m_2-m_1)} = 2.512^{m_2-m_1}. \tag{1.1.4}$$

m refers to a star's apparent magnitude.

A star's intrinsic brightness, or luminosity, is related to a star's apparent brightness through the inverse square law and a normalization. By convention, this relation is

$$\frac{B}{b} = \left(\frac{r}{10\ \mathrm{pc}}\right)^2, \tag{1.1.5}$$

where B is the absolute brightness. Therefore,

$$M = m + 5 - 5\log\frac{r}{\mathrm{pc}}. \tag{1.1.6}$$

Since any detector has varying efficiency as a function of wavelength, one generally makes a bolometric correction to go from the recorded flux to the actual flux:

$$BC = 2.5 \log \frac{\text{incident energy flux}}{\text{recorded energy flux}}. \tag{1.1.7}$$

Then, the absolute bolometric magnitude M_b can be defined as

$$M_b = -2.5 \log \frac{L}{L_\odot} + 4.72, \tag{1.1.8}$$

where $L_\odot \simeq 3.9 \times 10^{33}$ erg s^{-1}.

1.2. Distances

The four most-used units of length in astronomy are the solar radius ($R_\odot$), astronomical unit (AU), light year, and parsec (pc):

- $R_\odot \simeq 7 \times 10^{10}$ cm
- 1 AU $= 1.5 \times 10^{13}$ cm
- 1 lt. yr. $= 9.3 \times 10^{17}$ cm
- 1 pc $= 3.1 \times 10^{18}$ cm $= 3.26$ lt. yr. $= 1$ AU/tan $1''$

The astronomical unit is based on the mean distance of the Earth from the Sun, a light year is the distance light travels in one year, and the parsec is the distance of a star whose apparent angular parallactic shift in three months is 1 second of arc.

1.3. Temperature

The **effective stellar temperature** is defined by

$$L = 4\pi R^2 \sigma T_{eff}^4. \tag{1.3.1}$$

Here, the radiation constant σ is defined by the integral

$$\sigma \equiv T^{-4} \int I_\lambda d\lambda = T^{-4} \int \frac{2\pi c^2 h}{\lambda^5} \frac{1}{e^{ch/\lambda k_B T} - 1} d\lambda = \frac{2\pi^4 k_B^4}{15 c^2 h^3} = 5.67 \times 10^{-5} \text{erg cm}^{-2}\text{s}^{-1}\text{deg}^{-4}. \tag{1.3.2}$$

The quantity $I_\lambda = \pi B_\lambda$ is the specific intensity of radiation at the wavelength λ, and B_λ is the Planck distribuion. We could equivalently define

$$I_\nu = \frac{2\pi h \nu^3}{c^2} \frac{1}{e^{h\nu/k_B T} - 1} = \pi B_\nu. \tag{1.3.3}$$

The energy density of radiation in thermodynamic equilibrium is

$$u = 4\pi \int B_\nu d\nu = 4\pi \int B_\lambda d\lambda = aT^4, \tag{1.3.4}$$

$$a = \frac{4\sigma}{c} = \frac{8\pi^5 k_B^4}{15c^3h^3} = 7.565 \times 10^{-15} \text{erg cm}^{-3}\text{deg}^{-4}. \tag{1.3.5}$$

Thus, the effective temperature is obtained by matching the total power output of the star to a blackbody spectrum.

One can also try to match the shape of the spectra. One example is to look at the position of the peak of the spectrum. For a blackbody, this is

$$\lambda_{max} = \frac{hc}{5k_BT} = \frac{0.29 \text{ cm K}}{T}. \tag{1.3.6}$$

Matching this to the peak of the observed spectrum is one estimate of the **color temperature**. Usually, broadband spectral brightnesses or magnitudes can give good estimates of the stellar temperature. Frequently used broadband magnitudes are U, B and V, corresponding to the ultraviolet, blue and visual bands. The **color index** is the difference of two of these, $B - V$, and is often used instead of the stellar temperature to classify stars..

The **excitation temperature** is established from the observed relative populations of excited states in the stellar atmosphere. Since the gases in the atmosphere are Boltzmann gases (i.e., no interactions or degeneracy) in approximate thermal equilibrium, the relative population of two states i and j is given by the Saha equation

$$\frac{n_i}{n_j} = \frac{g_i}{g_j} e^{(\epsilon_i - \epsilon_j)/k_BT}, \tag{1.3.7}$$

where g refers to the statistical weights of the states. For example, for a non-magnetized atomic state, $g_i = 2J_i + 1$ where J is the angular momentum. For hydrogen, $\epsilon_n = -13.6 \text{ eV}/n^2$ and $g_n = 2n^2$.

For states of ionization, the same principles apply, except that a third species, the electron, is involved. The **ionization temperature** is established with the Saha equation

$$\frac{n_{i+1}n_e}{n_i} = \frac{G_{i+1}g_e}{G_i} \frac{(2\pi m_e k_B T)^{3/2}}{h^3} e^{-\chi_i/k_BT}. \tag{1.3.8}$$

The ionization potential is χ_i. The statistical weights for each ionic state are sums over all the levels of that state:

$$G_i = g_{i,0} + g_{i,1}e^{-\epsilon_{i,1}/k_BT} + g_{i,2}e^{-\epsilon_{i,2}/k_BT} + \ldots \tag{1.3.9}$$

1.4. Spectral Types

There is a correlation between conditions at the stellar surface and the spectral features observed. Originally, astronomers concocted a spectral typing based on the alphabet. However, the original 20-odd classes have been combined into the following scheme: O, B, A, F, G, K, M (*Oh, be a fine girl, kiss me* is a mnemonic dating from the mid-twentieth century to remember this.) These are in order from the hottest stars ($T \simeq 50,000$ K) to the coolest ones ($T \simeq 2200$ K). Some details of each type are:

- Class O ($T > 25,000$ K), ionized He dominates, other atoms with high ionization potential.
- Class B ($11,000$ K $< T < 25,000$ K, Balmer H and neutral He dominate, ionized C, O.
- Class A (7500 K $< T <$ 11,000 K, H and ionized Mg dominate, but ionized Fe, Ti, Ca, &c become more important at lower temperatures.
- Class F (6000 K $< T <$ 7500 K, ionized metals
- Class G (5000 K $< T <$ 6000 K, netural metals, molecular CN, CH (Sun is G2)
- Class K (3500 K $< T <$ 5000 K, molecular bands, neutral metals
- Class M (2200 K $< T <$ 3500 K, complex molecular oxide bands, TiO

1.5. Physical Properties of Stars

Masses of stars can be determined in cases where the stars are in binaries. Kepler's Law

$$\frac{M_1 + M_2}{M_\odot} = \left(\frac{a}{\mathrm{AU}}\right)^2 \left(\frac{\mathrm{year}}{P}\right)^3 \tag{1.5.1}$$

where M_1, M_2 are the stellar masses, and a and P are the semimajor axis and period of the orbit. When spectral lines from one star are observed, the period is found from the period of the Doppler shifts; the magnitude of the shifts yields the stellar velocity times the sine of the inclination angle. The size of the orbit can thus be inferred. Individual masses can be determined in cases where two sets of spectral lines appear and the inclination angle can also be established. The quantity $M_\odot = 1.989 \times 10^{33}$ g is the solar mass. A correlation (MS) exists between the stellar mass and luminosity, with $L \propto M^n$, where $n \simeq 3$.

Hydrostatic equilibrium and the classical perfect gas law implies that a star's central pressure P_c, density ρ_c and temperature T_c are related by

$$P_c \sim \frac{GM\rho_c}{R}, \qquad P_c \sim \rho_c T_c, \tag{1.5.2}$$

so that $T_c \sim GM/R$. If $T_c \sim T_{eff}$, the relation $\rho_c \sim M/R^3$ yields

$$L \sim R^2 T_{eff}^4 \sim M^4 R^{-2}. \tag{1.5.3}$$

On the other hand, the energy generation rate for the H burning reactions varies roughly as $\rho^2 T^5$, which means that integrated over the stellar volume

$$L \sim \int_0^R \rho^2 T^5 dr^3 \sim \rho_c^2 T_c^5 R^3 \sim M^7 R^{-8}. \tag{1.5.4}$$

These relations combined imply that $R \sim M^{1/2}$ and $L \sim M^3$.

Radii of stars are more difficult to measure. Interferometric techniques have yielded sizes of some stars, but otherwise size estimates rely on the Planck blackbody formula $L = 4\pi R^2 \sigma T_{eff}^4$. However, stars are not blackbodies, and stellar atmosphere models must be constructed to determine reliable effective temperatures. The radius of the Sun is

$R_\odot = 6.96 \times 10^{10}$ cm. Radii of main sequence stars range from 0.3 – 20 times that of the Sun, but red giants like Betelgeuse have radii greater than 300 $R_\odot$, and white dwarfs like Sirius B have radii of order 0.02 $R_\odot$.

1.6. Stellar Energetics

The order of magnitude binding energy of the Sun is

$$\Omega = -GM^2/R = -4 \times 10^{48} \text{ erg}. \tag{1.6.1}$$

If this energy was liberated at its present rate, the sun would live for a time

$$\tau = -\Omega/L \approx 10^{15} \text{ s} = 3 \times 10^7 \text{ yr}. \tag{1.6.2}$$

It is known, however, that the Sun is 150 times older. In fact, the energy to power the Sun comes from nuclear reactions converting H into He, which convert a fraction of its rest mass into energy. This is now observationally established because of the detection of neutrinos, produced when neutrons are converted to protons, from the Sun. The total rest mass energy of the Sun is

$$M_\odot c^2 \simeq 2 \times 10^{54} \text{ erg} \tag{1.6.3}$$

which is enough to power the Sun for 5×10^{20} s or 1.6×10^{13} yr. In fact, nuclear reactions in the Sun only convert 0.007 of the rest mass into energy, and only the inner 10% of the Sun will convert its H to He. Thus the estimated solar lifetime is 1.1×10^{10} yrs.

The lifetimes of other stars can be estimated from $L \sim M^3$: The available energy in a star is proportional to M, so the stellar lifetime $\tau \sim M/L \sim M^{-2}$.

The estimate $T_c \approx GM/R$ leads to the estimate that, for the Sun, $T_c \simeq 10^7$ K. Therefore, the average thermal energy of protons at the solar center is

$$k_B T = 8.62 \times 10^{-8} T \text{ keV/K} \simeq 1 \text{ keV}. \tag{1.6.4}$$

But the Coulomb barrier between two positively charged protons is

$$V = \frac{e^2}{r} = \frac{1.44 \text{ MeV} - \text{fm}}{r}. \tag{1.6.5}$$

Since the proton radius is of order 1 fm, how can protons of energy 1 keV penetrate a 1 MeV barrier? The answer is by quantum mechanical tunneling.

1.7. The Hertzsprung-Russel Diagram

Astronomers discovered at the beginning of the twentieth century that plotting the observed luminosities of stars versus their temperatures or colors yielded highly significant correlations. Most stars lie on a narrow swath known as the Main Sequence, going from high L and high T to small L and small T. These stars burn H into He. Another group of stars has much greater L for the T than main sequence stars; these are generally known as

red giants, and obviously have very large radii (up to 10000 $R_\odot$). There is another group with the opposite tendancy; these have very small radii (of order Earth-like radii, 0.001 $R_\odot$), and are called white dwarfs. These different groupings represent stars at different points in their evolution. Red giants are stars near the end of their lives, and white dwars are their final dying embers.

Stellar evolution can be easily observed using the HR diagram. Clusters contain stars presumably formed at nearly the same time and all stars within the cluster are at nearly the same distance from the Sun. The most masive and luminous stars have relatively short lifetimes, so they should move off the main sequence first. Once the luminosity of one star in the cluster is determined, the luminosities of all the stars are then known. The observed "turn-off" luminosity provides an age for the cluster, which is the main-sequence lifetime of a star whose mass has that luminosity.

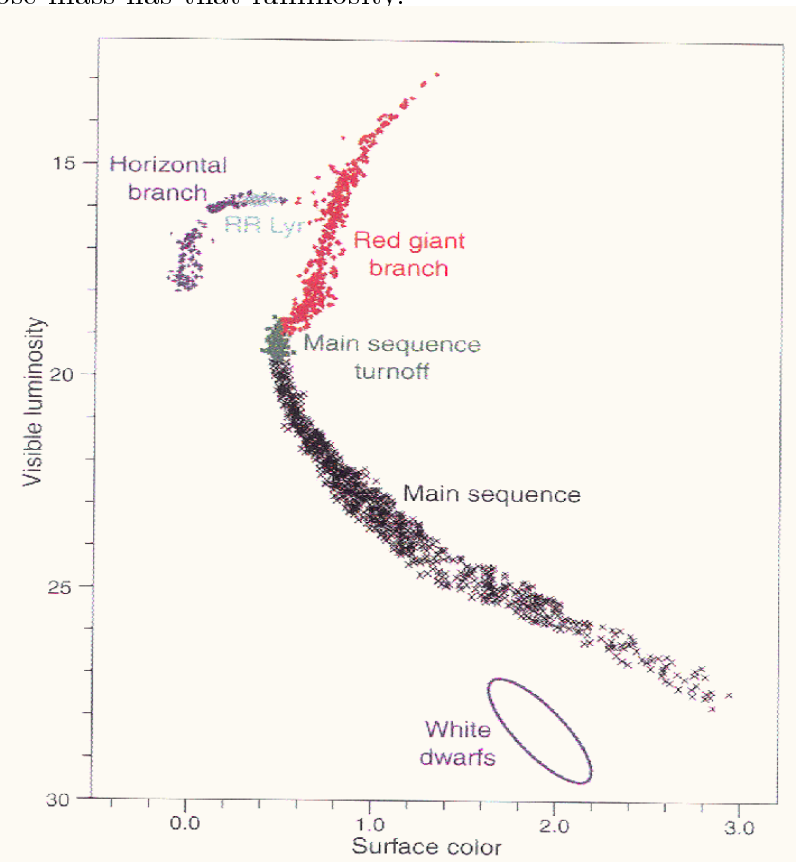

Fig. 2. A schematic color-magnitude diagram for a typical globular cluster (*33*) showing the location of the principal stellar evolutionary sequences. This diagram plots the visible luminosity of the star (measured in magnitudes) as a function of the surface color of the star (measured in B-V magnitude). Hydrogen-burning stars on the main sequence eventually exhaust the hydrogen in their cores (main sequence turnoff). After this, stars generate energy through hydrogen fusion in a shell surrounding an inert hydrogen core. The surface of the star expands and cools (red giant branch). Eventually the helium core becomes so hot and dense that the star ignites helium fusion in its core (horizontal branch). A subclass is unstable to radial pulsations (RR Lyrae). When a typical globular cluster star exhausts its supply of helium, and fusion processes cease, it evolves to become a white dwarf.

There are two different types of stellar clusters: galactic clusters which are loose associations of hundreds to thousands of stars, and globular clusters which are tight groupings of hundreds of thousands of stars. Galactic clusters are relatively young, with ages ranging

from millions to billions of years, but globular clusters are uniformly about 10 billion years old. Chemical compositions of cluster stars are also different: galactic cluster stars have abundances similar to that of the Sun, in which the mass fraction of elements heavier than He is a few percent, but stars in globular clusters have heavy element mass fractions of hundredths of a percent. The difference in galactic distributions, abundances and motions of the two types of clusters has resulted in the identification of two major populations of stars: Type I, stars formed recently like the Sun, and Type II, stars formed when the Galaxy was formed or even before.

1.8. Stellar Evolution and Nucleosynthesis

The chemical changes in a star are what produce stellar evolution. Stars with a homogeneous composition, as a function of mass, will occupy a narrow band in the H-R diagram strikingly similar to the main sequence. Stars with an abrupt chemical inhomogeneity can form a different sequence, one that occupies the red giant region. This occurs when about 10% of the star has a heavy core. The burning of H to He slowly generates the heavy core. Observations are well-fit by structures with both chemical inhomogeneities and a degenerate or partially degenerate core/non-degenerate envelope configuration. Some of these structures are prone to pulsational instabilities, observed as regular variabilities in temperature and luminosity. Finally, completely degenerate stellar structures form a third sequence that resembles the white dwarf branch. Therefore, stellar structure has to be understood before stellar evolution can be discussed.

Nucleosynthesis is the natural by-product of stellar evolution. The most bound nucleus is Fe, and slowly nuclear reactions in stars strive toward nuclei with the greatest binding. For the most part, however, the heavy elements produced in stars are trapped within unless the star can be disrupted. Low-mass stars, unless they are in close binaries, have little opportunity of disruption. However, high mass stars, and low-mass stars in close binaries, can undergo supernova explosions in which the star is partially or totally disrupted, accompanied by a tremendous release of energy: in photonic emissions and kinetic energy, and, in some cases, neutrinos. Supernovae involving white dwarfs (products of low-mass stellar evolution) in binaries are thermonuclear detonations which totally expell all the stellar material, while gravitational collapse of the cores of massive stars lead to neutron star (and black hole) formation accompanied by the expulsion of the star's massive envelope. These explosions also provide a natural method of enriching the chemical composition of the interstellar medium with heavy elements, leading to galactic chemical evolution. The pathways for creating elements heavier than Fe, which are less bound again, have to go through an extensive neutron or proton capture environment whose sites are still debated. It could be in gravitational collapse supernovae, in the envelopes of certain red giants or novae, or in the breakup of neutron stars themselves.

Chapter 2.
Statistical Mechanics

2.1. Classical Statistical Mechanics

A macrostate has N particles arranged among m volumes, with $N_i (i = 1 \ldots m)$ particles in the ith volume. The total number of allowed microstates with distinguishable particles in the macrostate is

$$W = \frac{N!}{\prod_i^m N_i!}\,; \quad \ln W = \ln N! - \sum_i^m \ln N_i!\,.$$

For a large number of particles, use Stirling's formula

$$\ln N! = N \ln N - N\,.$$

$$\ln W = N \ln N - N - \sum_i^m \left(N_i \ln N_i - N_i\right)\,.$$

The optimum configuration is the macrostate with the largest possible number of microstates, which is found by maximizing W, subject to the constraint that the total number of particles N is fixed ($\delta N = 0$). In addition, we require that the total energy be conserved. If w_i is the energy of the ith state, this is

$$\delta\left(\sum_i^m w_i N_i\right) = \sum_i^m w_i \delta N_i = 0\,.$$

With these constraints, the maximization is

$$\delta\left[\ln\left(W - \alpha\sum_i^m N_i - \beta\sum_i^m w_i N_i\right)\right] = 0\,.$$

$$\sum_i^m \left[\ln N_i - \alpha - \beta w_i\right]\delta N_i = 0\,.$$

$$N_i = \alpha e^{\beta w_i} = \alpha e^{-w_i/kT}\,,$$

which is the familiar Maxwell-Boltzmann, or classical, distribution function, if β is equated to $1/k_B T$. The quantity α is found from the total particle number $N = \sum N_i$ and will thus depend on the form of w_i.

2.2. Quantum Statistical Mechanics

In the quantum mechanical view, only within a certain phase space volume are particles indistinguishable. The minimum phase space volume is of order h^3. The number of microstates per macrostate is

$$W = \prod_i W_i \, .$$

where W_i is the number of microstates per cell of phase space of volume h^3. Note we have to consider both the particles and the compartments into which they are placed. If the ith cell has n compartments, there are n sequences of N_i+n-1 items to be arranged. There are $n(N_i+n-1)!$ ways to arrange the particles and compartments, but we have overcounted because there are $n!$ permutations of compartments in a cell, and $N_i!$ permutations of particles in a cell (just as in the classical case). Thus

$$W = \prod_i \frac{n\,(N_i+n-1)!}{N_i! n!} = \prod_i \frac{(N_i+n-1)!}{N_i!\,(n-1)!} \, .$$

Optimizing this, we find

$$\begin{aligned} \delta \ln W =& \delta \sum_i [(n+N_i-1)\ln(n+N_i-1) - N_i \ln N_i \\ & - (n-1)\ln(n-1) - \ln \alpha N_i - \beta w_i N_i] \\ =& \sum_i \left[\ln \frac{n+N_i-1}{N_i} - \ln\alpha - \beta w_i \right] \delta N_i = 0 \, , \end{aligned}$$

or

$$N_i = (n-1)\left(\alpha e^{w_i/kT} - 1 \right)^{-1} \, .$$

The occupation probability is $N_i/n \simeq [\alpha \exp(w_i/k_B T) - 1]^{-1}$. This is appropriate for the case when there is no limit to the number of particles that can be put into a compartment, *i.e.*, for bosons. For photons, particle number conservation does not apply, and $\alpha \equiv 1$.

Fermions obey the Pauli exclusion principle, and only 2 particles can be put into a compartment, where 2 is the spin degeneracy. Thus, phase space is composed of $2n$ half-compartments, either full or empty. There are no more than $2n$ things to be arranged and therefore no more than $(2n)!$ microstates. But again, we overcounted. For N_i filled compartments, the number of indistinguishable permutations is $N_i!$, and the number of indistinguishable permutations of the $2n - N_i$ empty compartments is $(2n-N_i)!$. In this case, we therefore have

$$W = \prod_i \frac{(2n)!}{N_i!\,(2n-N_i)!} \, .$$

As before, we optimize:

$$\begin{aligned} \delta \ln W =& \delta \sum_i [2n\ln(2n) - (2n-N_i)\ln(2n-N_i) \\ & - \ln\alpha N_i - \beta w_i N_i] \\ =& \sum_i \left[\ln \frac{2n-N_i}{N_i} - \ln\alpha - \beta w_i \right] \delta N_i = 0 \, , \end{aligned}$$

or

$$N_i = 2n\left(\alpha e^{w_i/k_BT} + 1\right)^{-1} .$$

The occupation probability is $N_i/(2n) = [\alpha \exp(w_i/(k_BT) + 1]^{-1}$.

The quantity $\ln \alpha$ for all statistics can be associated with the negative of the degeneracy parameter μ/T, where μ is the chemical potential of the system. The classical case is the limit of the fermion or boson case when $\alpha \to \infty$, since in this case the ± 1 in the denominator of the distribution function does not matter. In the boson case, also, $\alpha \geq 1$ since $w_i > 0$ and $N_i > 0$. Bosons become degenerate when $\alpha \to 1$. For photons, $\alpha = 1$. In the fermion case, there is no restriction on the value of α, and fermions become degenerate when $\alpha \to -\infty$. The value of α is determined by conservation of particle number: $N = \sum N_i$.

2.3. Thermodynamics

The internal energy U is

$$U = TS - PV + \sum_i \mu_i N_i$$

and the first law is

$$dU = TdS - PdV + \sum_i \mu_i dN_i \, .$$

This implies

$$VdP - SdT - \sum_i N_i d\mu_i = 0 \, .$$

The Helmholtz F and Gibbs G free energies are

$$F = U - TS \, ; \qquad G = \sum_i \mu_i N_i \, .$$

$$dF = -SdT - PdV + \sum_i \mu_i dN_i \, ; \quad dG = VdP - SdT + \sum_i dN_i \, .$$

The thermodynamic potential $\Omega = -PV$ obeys

$$d\Omega = -SdT - PdV - \sum_i N_i d\mu_i \, .$$

The following are useful thermodynamic relations:

$$\left.\frac{\partial U}{\partial S}\right|_{V,N_i} = T \qquad \left.\frac{\partial U}{\partial V}\right|_{S,N_i} = -P \qquad \left.\frac{\partial U}{\partial N_i}\right|_{S,V,N_{j\neq i}} = \mu_i$$

$$\left.\frac{\partial F}{\partial T}\right|_{V,N_i} = -S \qquad \left.\frac{\partial F}{\partial V}\right|_{T,N_i} = -P \qquad \left.\frac{\partial F}{\partial N_i}\right|_{T,V,N_{j\neq i}} = \mu_i$$

$$\left.\frac{\partial \Omega}{\partial T}\right|_{V,\mu_i} = -S \qquad \left.\frac{\partial \Omega}{\partial V}\right|_{T,\mu_i} = -P \qquad \left.\frac{\partial \Omega}{\partial \mu_i}\right|_{T,V,\mu_{j\neq i}} = -N_i$$

Then $\left.\partial P/\partial T\right|_{V,\mu_i} = S/V$ and $\left.\partial P/\partial \mu_i\right|_{T,V,\mu_{j\neq i}} = N_i/V$.

2.4. Statistical Physics of Perfect Gases—Fermions

The energy of a non-interacting particle is related to its rest mass m and momentum p by the relativistic relation

$$E^2 = m^2c^4 + p^2c^2. \tag{2.4.1}$$

The occupation index is the probability that a given momentum state will be occupied:

$$f = \left[1 + \exp\left(\frac{E-\mu}{T}\right)\right]^{-1} \tag{2.4.2}$$

for fermions, where $\mu = \partial\epsilon/\partial n|_s$ is the chemical potential and ϵ is the energy density. When the particles are interacting, E generally contains an effective mass and a potential contribution. μ corresponds to the energy change when 1 particle is added to or subtracted from the system. The entropy per particle is s. We will use units such that k_B=1; thus $T = 1$ MeV corresponds to $T = 1.16 \times 10^{10}$ K. The number and internal energy densities are given, respectively, by

$$n = \frac{g}{h^3}\int f d^3p; \qquad \epsilon = \frac{g}{h^3}\int E f d^3p \tag{2.4.3}$$

where g is the spin degeneracy ($g = 2j + 1$ for massive particles, where j is the spin of the particle, i.e., $g = 2$ for electrons, muons and nucleons, $g = 1$ for neutrinos). The entropy can be expressed as

$$ns = -\frac{g}{h^3}\int \left[f \ln f + (1-f)\ln(1-f)\right] d^3p \tag{2.4.4}$$

and the thermodynamic relations

$$P = n^2 \frac{\partial\left(\epsilon/n\right)}{\partial n}\bigg|_s = Tsn + \mu n - \epsilon \tag{2.4.5}$$

gives the pressure. Incidentally, the two expressions (Eqs. (2.4.4) and (2.4.5)) are generally valid for interacting gases, also. We also note, for future reference, that

$$P = \frac{g}{3h^3}\int p\frac{\partial E}{\partial p} f d^3p. \tag{2.4.6}$$

Thermodynamics gives also that

$$n = \frac{\partial P}{\partial \mu}\bigg|_T; \qquad ns = \frac{\partial P}{\partial T}\bigg|_\mu. \tag{2.4.7}$$

Note that if we define degeneracy parameters $\phi = \mu/T$ and $\psi = (\mu - mc^2)/T$ the following relations are valid:

$$P = -\epsilon + n\frac{\partial\epsilon}{\partial n}\bigg|_T + T\frac{\partial P}{\partial T}\bigg|_n; \quad \frac{\partial P}{\partial T}\bigg|_\phi = ns + n\phi; \quad \frac{\partial P}{\partial T}\bigg|_\psi = ns + n\psi. \tag{2.4.8}$$

In many cases, one or the other of the following limits may be realized: extremely degenerate ($\phi \to +\infty$), nondegenerate ($\phi \to -\infty$), extremely relativistic ($p >> mc$), non-relativistic ($p << mc$).

2.4.1. Non-relativistic

In this case, one expands Eq. (2.4.3) in the limit $p << mc$. Defining $x = p^2/(2mT)$ and $\psi = (\mu - mc^2)/T$, one has

$$n = \frac{g\,(2mT)^{3/2}}{4\pi^2\hbar^3}\int_0^\infty \frac{x^{1/2}dx}{1+e^{x-\psi}} \equiv \frac{g\,(2mT)^{3/2}}{4\pi^2\hbar^3}F_{1/2}\,(\psi) \tag{2.4.9}$$

$$\epsilon = nmc^2 + \frac{gT\,(2mT)^{3/2}}{4\pi^2\hbar^3}F_{3/2}\,(\psi)\,. \tag{2.4.10}$$

Here, F_i is the usual Fermi integral which satisfies the recursion

$$\frac{dF_i\,(\psi)}{d\psi} = iF_{i-1}\,(\psi)\,. \tag{2.4.11}$$

$$P = \frac{2}{3}\left(\epsilon - nmc^2\right); \qquad\qquad s = \frac{5F_{3/2}\,(\psi)}{3F_{1/2}\,(\psi)} - \psi. \tag{2.4.12}$$

Fermi integrals for zero argument satisfy

$$F_i\,(0) = \left(1-2^{-i}\right)\Gamma\,(i+1)\,\zeta\,(i+1)\,, \tag{2.4.13}$$

where ζ is the Riemann zeta function. Note that $F_i(0) \xrightarrow[i\to\infty]{} i!$. $F_i(\psi)$ may be expanded around $\psi = 0$ with

$$F_i\,(\psi) = F_i\,(0) + iF_{i-1}\,(0)\,\psi + \frac{i\,(i-1)}{2}F_{i-2}\,(0)\,\psi^2 + \cdots. \tag{2.4.14}$$

Since $F_0(\psi) = \ln(1+e^\psi)$, Fermi integrals with integer indices less than 0 do not exist. The recursion Eq. (2.4.11) can be employed to define non-integer negative indices, however.

i		$F_i(0)$	i		$F_i(0)$
-7/2		0.249109	3/2		1.152804
-5/2		0.2804865	2		1.803085
-3/2		-1.347436	5/2		3.082586
-1/2		1.07215	3	$7\pi^4/120$	5.682197
0	ln(2)	0.693147	4		23.33087
1/2		.678094	5	$31\pi^6/252$	118.2661
1	$\pi^2/12$	0.822467			

a. **Non-degenerate and non-relativistic**: In this limit, using the expansion

$$F_i(\psi) = \Gamma(i+1) \sum_{n=1}^{\infty} \frac{(-1)^{n+1} e^{n\psi}}{n^{i+1}}, \qquad \psi \to -\infty \tag{2.4.15}$$

we find

$$n = g \left(\frac{mT}{2\pi\hbar^2}\right)^{3/2} e^{\psi}, \qquad P = nT, \qquad s = 5/2 - \psi. \tag{2.4.16}$$

b. **Degenerate, non-relativistic**: In this limit, we use the Sommerfeld expansion

$$F_i(\psi) = \frac{\psi^{i+1}}{i+1} \sum_{n=0}^{\infty} \frac{(i+1)!}{(i+1-2n)!} \left(\frac{\pi}{\psi}\right)^{2n} C_n, \qquad \psi \to \infty \tag{2.4.17}$$

Some values for the constants C_n are $C_0 = 1, C_1 = 1/6, C_2 = 7/360$, and $C_3 = 31/15120$. We find

$$\begin{aligned} n =& \frac{g(2m\psi T)^{3/2}}{6\pi^2\hbar^3} \left[1 + \frac{1}{8}\left(\frac{\pi}{\psi}\right)^2 + \cdots\right], \\ P =& \frac{2n\psi T}{5} \left[1 + \frac{1}{2}\left(\frac{\pi}{\psi}\right)^2 + \cdots\right], \\ s =& \frac{\pi^2}{2\psi} + \cdots. \end{aligned} \tag{2.4.18}$$

2.4.2. Extremely relativistic

This case corresponds to setting the rest mass to zero. Eqs. (2.4.3) and (2.4.5) become

$$\begin{aligned} n =& \frac{g}{2\pi^2}\left(\frac{T}{\hbar c}\right)^3 F_2(\phi), \\ P =& \frac{\epsilon}{3} = \frac{gT}{6\pi^2}\left(\frac{T}{\hbar c}\right)^3 F_3(\phi), \\ s =& \frac{4F_3(\phi)}{3F_2(\phi)} - \phi. \end{aligned} \tag{2.4.19}$$

The above limiting expressions for the Fermi integrals may be used in these expressions.

a. **Extremely relativistic and non-degenerate**: Use of the expansion Eq. (2.4.15) results in

$$\begin{aligned} n =& \frac{g}{\pi^2}\left(\frac{T}{\hbar c}\right)^3 e^{\phi}, \\ P =& nT, \qquad s = 4 - \ln\left[\frac{\pi^2 n}{g}\left(\frac{\hbar c}{T}\right)^3\right] = 4 - \phi. \end{aligned} \tag{2.4.20}$$

b. **Extremely relativistic and extremely degenerate**: The expansion Eq. (2.4.17) gives

$$\begin{aligned} n =& \frac{g}{6\pi^2}\left(\frac{\mu}{\hbar c}\right)^3\left[1+\left(\frac{\pi}{\phi}\right)^2+\cdots\right], \\ P =& \frac{n\mu}{4}\left[1+\left(\frac{\pi}{\phi}\right)^2+\cdots\right], \\ s =& \frac{\pi^2}{\phi}+\cdots \end{aligned} \tag{2.4.21}$$

2.4.3. Extremely degenerate

This case corresponds to $\phi >> 0$. It is useful to define the Fermi momentum p_f for which the occupation index $f = 1/2$, i.e., where $\mu = E_f = \sqrt{m^2c^4 + p_f^2c^2}$. In terms of the parameter $x = p_f/mc$, we have

$$\mu = mc^2\sqrt{1+x^2}. \tag{2.4.22}$$

In the case $\phi \to \infty$, Eq. (2.4.2) becomes a step function, with $f = 1$ for $E \le \mu$; $f = 0$ for $E > \mu$.

$$\begin{aligned} n &= \frac{8A}{mc^2}x^3, \\ P &= A\left[x\left(2x^2-3\right)\sqrt{1+x^2}+3\sinh^{-1}x\right], \\ \epsilon - nmc^2 &= A\left[3x\left(2x^2+1\right)\sqrt{1+x^2}-8x^3-3\sinh^{-1}x\right], \\ s &= 0, \end{aligned} \tag{2.4.23}$$

where $A = (gmc^2/48\pi^2)(mc/\hbar)^3$.

2.4.4. Non-degenerate

This case coresponds to $\phi << 0$. Because pair creation is often important in this case, we delay detailed discussion of limiting formulae for a later section. If pairs are neglected, results may be expressed in terms of Bessel functions:

$$\begin{aligned} n &= \left(\frac{mc}{\hbar}\right)^3\frac{T}{3mc^2}e^{\phi}K_2\left(mc^2/T\right), \\ P &= nT, \\ \epsilon - nmc^2 &= \left(\frac{mc}{\hbar}\right)^3\frac{T}{3}e^{\phi}[-K_1\left(mc^2/T\right)+ \\ &\qquad \left(3T/mc^2-1\right)K_2\left(mc^2/T\right)], \\ s &= 4-\frac{mc^2}{T}\frac{K_1\left(mc^2/T\right)}{K_2\left(mc^2/T\right)}-\phi. \end{aligned} \tag{2.4.24}$$

2.5. General Comments About Fermions

Fermions become relativistic under non-degenerate conditions when $T > mc^2$ ($T > 5 \times 10^9$ K for electrons) for any density, and, under degenerate conditions, when $p_f c > mc^2$ ($\rho Y_e > 2 \times 10^6$ g cm^{-3} for electrons) for any temperature. Here, ρ is the baryon density, and the number of electrons per baryon is Y_e. $n(\equiv n_e) = \rho N_o Y_e$. N_o is Avogadro's number.

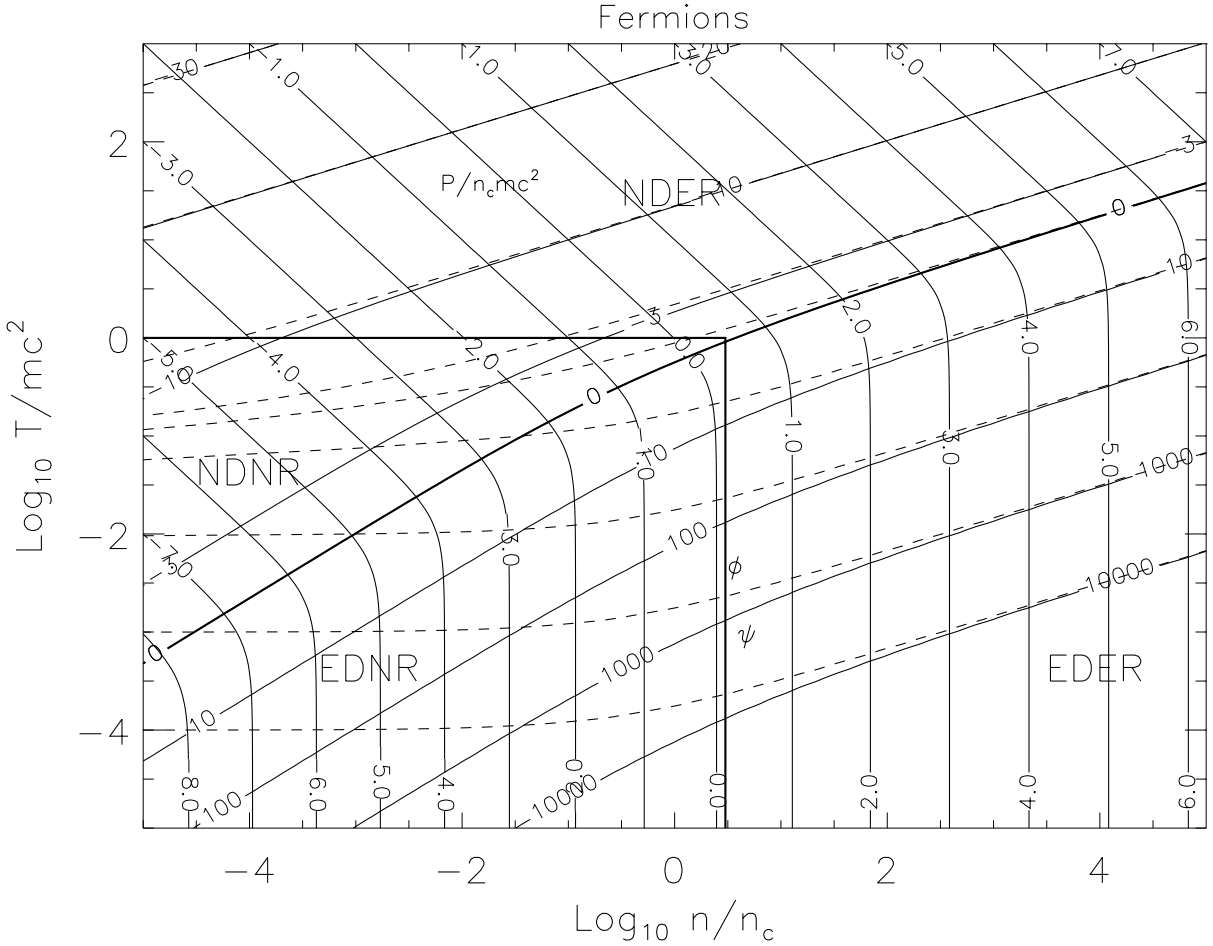

Figure 2.5.1: Thermodynamic quantities for a fermion gas. Contours moving from lower left to upper right are ψ (solid) and ϕ (dashed). Pressure contours go from upper left to lower right.

$\psi \simeq 0$ demarks the degenerate and non-degenerate regions under all relativity conditions.

$$n = g\frac{(2mT)^{3/2}}{4\pi^2\hbar^3}F_{1/2}(0)\,;$$

$$\rho Y_e \simeq 2 \times 10^6 \left(\frac{T}{5 \times 10^9 \text{ K}}\right)^{3/2} \text{ g cm}^{-3} \quad \text{non} - \text{relativistic};$$

$$n = \frac{g}{2\pi^2}\left(\frac{T}{\hbar c}\right)^3 F_2(0)\,;$$

$$\rho Y_e \simeq 2 \times 10^6 \left(\frac{T}{5 \times 10^9 \text{ K}} \right)^3 \text{ g cm}^{-3} \qquad \text{relativistic}$$

separate the degenerate from the non-degenerate regions.

Interacting baryons are far more complicated. At subnuclear densities ($\rho < \rho_o \equiv 2.7 \times 10^{14}$ g cm^{-3}) they cluster into nuclei with internal densities near ρ_o. The nuclei themselves are dilute, comprising a non-degenerate, non-relativistic gas, but with a strong Coulombic (lattice) interaction. At very high temperatures, the nuclei dissociate. Above ρ_o, nuclear interactions and degeneracy effects dominate. Baryons become relativistic at a density $(m_{baryon}/m_{electron})^3$ times higher than the electrons, or about 10^{16} g cm^{-3}. This is above the transition density to quark matter. At these densities, quarks can be approximated as a perfect gas due to asymptotic freedom.

2.6. Fermion–Antifermion particle pairs

Under conditions found in the evolution of very massive stars, the temperature may be high enough to produce electron-positron pairs, while the electrons are non-relativistic. During gravitational collapse a degenerate neutrino-antineutrino gas forms when densities large enough to trap neutrinos on dynamical time scales are reached ($\rho > 10^{12}$ g/cm^3). For particle-antiparticle pairs in equilibrium, $\mu_+ = -\mu_-$. The *net difference* of particles and anti-particles and the *total* pressure are

$$\begin{aligned} n =& n_+ - n_- = \frac{4\pi g}{h^3} \int_0^\infty p^2 \left[\frac{1}{1 + e^{(E-\mu)/T}} - \frac{1}{1 + e^{(E+\mu)/T}} \right] dp, \\ P =& P_+ + P_- = \frac{4\pi g}{3h^3} \int p^3 \frac{\partial E}{\partial p} \left[\frac{1}{1 + e^{(E-\mu)/T}} + \frac{1}{1 + e^{(E+\mu)/T}} \right] dp. \end{aligned} \tag{2.6.1}$$

Thus, when pairs are included, and n is positive, $\mu \equiv \mu_+$ must be positive, i.e., there will not be cases involving extreme non-degeneracy. However, pairs will never be important whenever $\mu/T >> 0$, that is, under extremely degenerate conditions. With the substitutions $x = pc/T$, $z = mc^2/T$, we may write

$$\begin{aligned} n &= \frac{g}{2\pi^2} \left(\frac{T}{\hbar c} \right)^3 \sinh\phi \int_0^\infty \frac{x^2}{\cosh\phi + \cosh\sqrt{z^2 + x^2}} dx, \\ P &= \frac{gT}{6\pi^2} \left(\frac{T}{\hbar c} \right)^3 \int_0^\infty \frac{x^4}{\sqrt{z^2 + x^2}} \left[\frac{\cosh\phi + e^{-\sqrt{z^2+x^2}}}{\cosh\phi + \cosh\sqrt{z^2 + x^2}} \right] dx. \end{aligned} \tag{2.6.2}$$

2.6.1. Extremely relativistic case: $\mu >> mc^2$ or $T >> mc^2$

This case is appropriate for neutrinos. With $\mu = \mu_+ = -\mu_-$, i.e., $z \to 0$,

$$\begin{aligned} n = n_+ - n_- &= \frac{g}{2\pi^2}\left(\frac{T}{\hbar c}\right)^3 \left[F_2\left(\frac{\mu}{T}\right) - F_2\left(-\frac{\mu}{T}\right)\right] \\ &= \frac{g}{6\pi^2}\left(\frac{\mu}{\hbar c}\right)^3 \left[1 + \left(\frac{\pi T}{\mu}\right)^2\right]; \\ \epsilon/3 = P = P_+ + P_- &= \frac{gT}{6\pi^2}\left(\frac{T}{\hbar c}\right)^3 \left[F_3\left(\frac{\mu}{T}\right) + F_3\left(-\frac{\mu}{T}\right)\right] \\ &= \frac{g\mu}{24\pi^2}\left(\frac{\mu}{\hbar c}\right)^3 \left[1 + 2\left(\frac{\pi T}{\mu}\right)^2 + \frac{7}{15}\left(\frac{\pi T}{\mu}\right)^4\right]; \\ s &= \frac{gT\mu^2}{6n\left(\hbar c\right)^3}\left[1 + \frac{7}{15}\left(\frac{\pi T}{\mu}\right)^2\right]. \end{aligned} \tag{2.6.3}$$

These expressions are *exact*. The exponential terms ignored in the Sommerfeld expansion of the $+\mu/T$ Fermi integral are exactly canceled by those of the $-\mu/T$ Fermi integral. The pair Fermi integral

$$G_i\left(\eta\right) \equiv F_i\left(\eta\right) + \left(-1\right)^{i+1} F_i\left(-\eta\right) \qquad i \geq 0$$

obeys the same recursion formula as $F_i(\eta)$ for $i \geq 1$.

$n(\mu)$ is a cubic in μ, which can be inverted:

$$\mu = r - q/r, \qquad r = \left[\left(q^3 + t^2\right)^{1/2} + t\right]^{1/3}, \tag{2.6.4}$$

where $t = 3\pi^2(\hbar c)^3 n/g$ and $q = (\pi T)^2/3$. For $T \to \infty$, one has $\mu \to 6n(\hbar c)^3/gT^2 \to 0^+$. For all μ and T the adiabatic index

$$\Gamma_1 = \left.\frac{d\ln P}{d\ln n}\right|_s = \left.\frac{d\ln P}{d\ln n}\right|_T + \frac{T}{P}\left(\frac{dP}{dT}\right)_n^2 \left(\frac{d\epsilon}{dT}\right)_n^{-1} = 4/3. \tag{2.6.5}$$

One may include the lowest order corrections for finite rest mass by expanding the integrands of Eq. (2.4.3) and using the recursion relations for the Fermi integrals:

$$\begin{aligned} n &= \frac{g}{6\pi^2}\left(\frac{\mu}{\hbar c}\right)^3 \left[1 + \mu^{-2}\left(\pi^2 T^2 - \frac{3}{2}m^2c^4\right)\right], \\ P &= \frac{g\mu}{24\pi^2}\left(\frac{\mu}{\hbar c}\right)^3 \left[1 + \mu^{-2}\left(2\pi^2 T^2 - 3m^2c^4\right) + \frac{\pi^2 T^2}{\mu^4}\left(\frac{7}{15}\pi^2 T^2 - m^2c^4\right)\right], \\ \epsilon &= \frac{g\mu}{8\pi^2}\left(\frac{\mu}{\hbar c}\right)^3 \left[1 + \mu^{-2}\left(2\pi^2 T^2 - m^2c^4\right) + \frac{\pi^2 T^2}{\mu^4}\left(\frac{7}{15}\pi^2 T^2 - \frac{1}{3}m^2c^4\right)\right], \\ s &= \frac{gT\mu^2}{6n\left(\hbar c\right)^3}\left[1 + \mu^{-2}\left(\frac{7}{15}\pi^2 T^2 - \frac{1}{2}m^2c^4\right)\right]. \end{aligned} \tag{2.6.6}$$

The relativistic relationship $\epsilon = 3P$ no longer holds. Interestingly, the cubic relationship between μ and n is preserved in this approximation, and the solution is still given by

Eq. (2.6.4) if we simply redefine $q = (\pi T)^2/3 - m^2c^4/2$. Including the finite rest mass terms lowers Γ_1 below 4/3:

$$\Gamma_1 = \frac{4}{3}\left(1 - \frac{5}{11}\left(\frac{mc^2}{\pi T}\right)^2\right) \tag{2.6.7}$$

when photons (see below) are also included.

2.6.2. Non-relativistic case:

In the degenerate case, $T \to 0$, $\mu \to (mc^2)^+$ and pairs are of negligible importance. We can use the non-relativistic, degenerate formulas already obtained for particles alone. At higher temperatures, μ reaches a maximum, and then decreases, eventually becoming less than mc^2, so that $\mu' < 0$. The gas is thus at most only partially degenerate when pairs are present and $n = n_+ - n_- > 0$. The non-degenerate expansion yields

$$n_\pm \simeq g\left(\frac{mT}{2\pi\hbar^2}\right)^{3/2} e^{\left[\pm\mu - mc^2\right]/T}. \tag{2.6.8}$$

Noting that $n = n_+ - n_-$ and

$$n_+ n_- = g^2\left(\frac{mT}{2\pi\hbar^2}\right)^3 e^{-2mc^2/T} \equiv n_1^2, \tag{2.6.9}$$

we can instead write

$$n_\pm = \mp\frac{n}{2} + \left[\left(\frac{n}{2}\right)^2 + n_1^2\right]^{1/2}. \tag{2.6.10}$$

$$P = (n_+ + n_-)\,T = \left(n^2 + 4n_1^2\right)^{1/2} T, \tag{2.6.11a}$$

$$\epsilon = (n_+ + n_-)\left(mc^2 + \frac{3}{2}T\right), \tag{2.6.11b}$$

$$s = \left(\frac{5}{2} + \frac{mc^2}{T}\right)\frac{(n_+ + n_-)}{n} - \frac{\mu}{T}, \tag{2.6.11c}$$

$$\mu = T\ln\left[\frac{n}{2n_1} + \left(\frac{n^2}{4n_1^2} + 1\right)^{1/2}\right]. \tag{2.6.11d}$$

Pairs are important in the non-relativistic case when $n \leq n_1$. Including photon pressure (see below), in the case when $n << n_1$, one has

$$\Gamma_1 \simeq \frac{4}{3}\left[1 - \frac{15}{32}\left(\frac{2mc^2}{\pi T}\right)^{7/2} e^{-mc^2/T}\right]. \tag{2.6.12}$$

Thus Γ_1 reaches a minimum value (1.02) when $T = \frac{2}{7}mc^2$, and is always less than $\frac{4}{3}$. The creation of a pair costs an energy of $2mc^2$ which is non-negligible in the non-relativistic case.

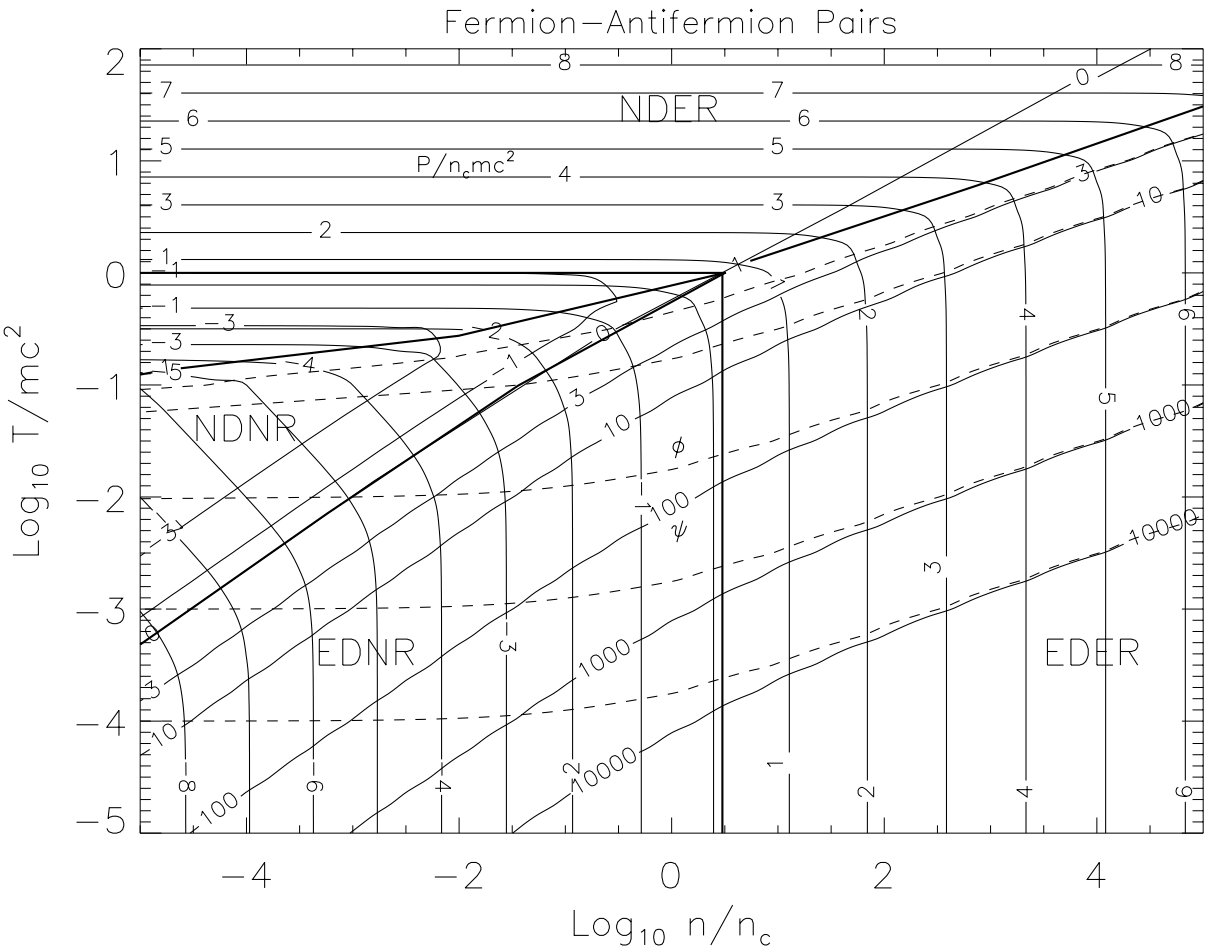

Figure 2.6.1: Thermodynamic quantities for a fermion-antifermion gas. See caption for Fig. 2.5.1.

2.6.3. Non-degenerate:

Consider the region for which $\cosh\phi - 1 << \cosh z$. Since $\mu = T\phi$ cannot be negative when pairs are included, the gas is at most partially degenerate in this non-degenerate limit. Expanding the $\cosh\phi$ in the denominator terms to lowest order in $\cosh\phi - \cosh z$,

$$\begin{aligned} n &= n_c z^{-3}\sinh\phi \int_0^\infty \frac{x^2 dx}{1+\cosh\sqrt{z^2+x^2}}, \\ P &= n_c T z^{-3}[(\cosh\phi - 1)\int_0^\infty \frac{x^2 dx}{1+\cosh\sqrt{z^2+x^2}} \\ &\quad + \frac{2}{3}\int_0^\infty \frac{x^4 dx}{\sqrt{x^2+z^2}}\frac{1}{1+e^{\sqrt{x^2+z^2}}}], \\ \epsilon &= n_c T z^{-3}[(\cosh\phi - 1)\int_0^\infty \frac{x\left(x^2+z^2\right)dx}{1+\cosh\sqrt{z^2+x^2}} \\ &\quad + 2\int_0^\infty \frac{x^2\sqrt{z^2+x^2}}{1+e^{\sqrt{z^2+x^2}}}dx], \end{aligned} \tag{2.6.13}$$

where $n_c = (g/2\pi^2)(mc/\hbar)^3 = 6 \times 10^6$ g cm^{-3} for $g = 2$. This is an interesting approximation because, given n and T, one can immediately evaluate μ or ϕ because they no longer appear within the integrals. The integrals can be easily evaluated by quadrature, with relatively few points, using Gauss-Laguerre for $z < 30$ and Gauss-Hermite for $z > 30$.

2.7. When are pairs important?

In the relativistic case, $n_- = 0.1 n_+$ is equivalent to $F_2(\phi) \simeq 10 F_2(-\phi)$ or $\phi \simeq 0.9$. In the non-relativistic case, we find $\phi \simeq \ln \sqrt{10}$ or $\phi \simeq 1.15$. $\phi \simeq 1$ is the effective boundary. The intrusion of this boundary into the NDNR region means that there are actually five limiting cases when pairs are considered, as opposed to four when pairs are ignored. This is an unfortunate complication.

2.8. Generalized Approximation for Fermion Gas

We explore here a technique invented by Eggleton, Faulkner and Flannery to bridge the limiting regions for a fermion gas. It is essential to maintain thermodynamic consistency in this approximation. To include pairs we simply apply the scheme separately to electrons and positrons. The scheme establishes an analytic formula for the thermodynamic potential (or pressure) as an explicit function of chemical potential and temperature. Then $n = T^{-1}\partial P/\partial\psi; ns = \partial P/\partial T - n\psi; \epsilon = T(\partial P/\partial T) - P + nmc^2$. Density and temperature are inputs, so iteration is necessary to determine the chemical potential. Johns, Ellis & Lattimer improved the accuracy of the scheme and fixed its entropy in the degenerate limit.

The four limiting cases we have discussed are:

$$\frac{P}{n_c mc^2} = \begin{cases} (\psi T)^4 \sum\sum a_{mn} \psi^{-2m} (\psi T)^{-n} & \text{ER, ED} : \psi T >> mc^2, \psi >> 1 \\ (\psi T)^{5/2} \sum\sum b_{mn} \psi^{-2m} (\psi T)^{n} & \text{NR, ED} : \psi T << mc^2, \psi >> 1 \\ T^4 e^{\psi} \sum\sum c_{mn} e^{m\psi} T^{-n} & \text{ER, ND} : \psi << -1, T >> mc^2 \\ T^{5/2} e^{\psi} \sum\sum d_{mn} e^{m\psi} T^{n} & \text{NR, ND} : \psi << -1, T << mc^2 \end{cases} \tag{2.8.1}$$

where $n_c = (g/2\pi^2)(mc/\hbar)^3$. The coefficients a_{mn}, b_{mn}, c_{mn} and d_{mn} $(m, n \in 0 \ldots \infty)$ can be determined from the limits. The key is to find functions $f(\psi), g(\psi, T)$ such that Eq. (2.8.1) can be rewritten as

$$\frac{P}{n_c mc^2} = \begin{cases} g^4 \sum\sum a'_{mn} f^{-m} g^{-n} & \text{ER, ED} : g >> 1, \quad f >> 1 \\ g^{5/2} \sum\sum b'_{mn} f^{-m} g^{n} & \text{NR, ED} : g << 1, \quad f >> 1 \\ f g^4 \sum\sum c'_{mn} f^{m} g^{-n} & \text{ER, ND} : g >> 1, \quad f << 1 \\ f g^{5/2} \sum\sum d'_{mn} f^{m} g^{n} & \text{NR, ND} : g << 1, \quad f << 1. \end{cases} \tag{2.8.2}$$

This is possible provided that

$$f(\psi) = \begin{cases} \psi^2 \sum r_m \psi^{-2m} & \text{ED}: \quad \psi >> 1 \\ e^{\psi} \sum s_m e^{m\psi} & \text{ND}: \quad \psi << -1 \end{cases} \tag{2.8.3}$$

and

$$g(\psi, T) = \begin{cases} \psi T \sum t_m \psi^{-2m} & \text{ED}: \quad \psi >> 1 \\ T \sum u_m e^{m\psi}. & \text{ND}: \quad \psi << -1 \end{cases} \tag{2.8.4}$$

r_{mn}, s_{mn}, t_{mn} and u_{mn} are additional coefficients. Then

$$\frac{P}{n_c mc^2} = \frac{f}{1+f} g^{5/2} (1+g)^{3/2} \frac{\sum_0^M \sum_0^N P_{mn} f^m g^n}{(1+f)^M (1+g)^N} \tag{2.8.5}$$

has the proper limits for any $M, N \geq 1$ when f and g are either large or small. P_{mn} are coefficients which are least squares fit to a numerical evaluation of P. From Eq. (2.8.4), $g \propto T$, and

$$g = \left(T/mc^2\right) \sqrt{1+f} \tag{2.8.6}$$

guarantees the right limiting behavior in Eq. (2.8.4).

On the other hand, it is also clear that $\partial f/\partial\psi$ is either $\sqrt{f}$ $(f \to \infty)$ or f $(f \to 0)$. We choose

$$\partial f/\partial\psi = f/\sqrt{1+f/a}, \tag{2.8.7}$$

where a is an adjustable parameter. Integrating this relation, we find the required relation between ψ and f:

$$\psi = 2\sqrt{1+f/a} + \ln \frac{\sqrt{1+f/a}-1}{\sqrt{1+f/a}+1}. \tag{2.8.8}$$

Explicitly evaluating the density, we find

$$n = \frac{1}{T} \frac{\partial P}{\partial \psi}\bigg|_T = \frac{1}{T} \frac{\partial f}{\partial \psi} \left(\frac{\partial P}{\partial f}\bigg|_g + \frac{\partial g}{\partial f}\bigg|_T \frac{\partial P}{\partial g}\bigg|_f \right); \tag{2.8.9}$$

$$\begin{aligned} \frac{n}{n_c} = {} & \frac{f g^{3/2} \sum_0^M \sum_0^N P_{mn} f^m g^n}{\sqrt{1+f/a}\,(1+f)^{M+1/2} (1+g)^{N-3/2}} \times \\ & \left[1 + m + \frac{f}{1+f} \left(\frac{1}{4} + \frac{n}{2} - M \right) + \frac{fg}{(1+f)(1+g)} \left(\frac{3}{4} - \frac{N}{2} \right) \right]. \end{aligned} \tag{2.8.10}$$

From $P + U = T(\partial P/\partial T)_\psi$, where $U = \epsilon - nmc^2$ is the internal energy density,

$$\begin{aligned} \frac{U}{n_c mc^2} = {} & f g^{5/2} (1+g)^{3/2} \frac{\sum_0^M \sum_0^N P_{mn} f^m g^n}{(1+f)^{M+1} (1+g)^N} \times \\ & \left[\frac{3}{2} + n + \frac{g}{1+g} \left(\frac{3}{2} - N \right) \right]. \end{aligned} \tag{2.8.11}$$

Given n and T, we invert Eq. (2.8.10) to determine f; g is trivially found. The pressure is given by Eq. (2.8.5), the chemical potential by Eq. (2.8.8), and the energy density by Eq. (2.8.11).

The entropy is found from $s = n^{-1}(\partial P/\partial T)_\psi - \psi$. A drawback of the Eggleton et al. scheme was that in the degenerate limit, although the entropy per particle has the correct asymptotic dependence $1/\sqrt{f}$, the coefficient is not exact:

$$s = \begin{cases} \sqrt{\dfrac{a}{f}}\left(2 + \dfrac{1}{a} - \dfrac{M}{a} + \dfrac{P_{M-1,N}}{aP_{M,N}}\right) \xrightarrow[M,N\to\infty]{} \dfrac{\pi^2}{2}\sqrt{\dfrac{a}{f}} & \text{ED, ER} \\ \dfrac{8}{5}\sqrt{\dfrac{a}{f}}\left(\dfrac{5}{4} + \dfrac{1}{4a} - \dfrac{M}{a} + \dfrac{P_{M-1,0}}{aP_{M,0}}\right) \xrightarrow[M,N\to\infty]{} \dfrac{\pi^2}{4}\sqrt{\dfrac{a}{f}}. & \text{ED, NR} \end{cases} \tag{2.8.12}$$

For $M, N = 2(3)$, Eqs. (2.8.12) have errors of 1.35 (0.0165)% and 0.254 (0.0637)%, respectively, for the ER and NR cases. The original Eggleton et al. errors for these cases (they assumed $a = 1$) are (2.4 (1.40)%, 1.0 (0.563)%), respectively.

From Eqs. (2.8.12), the corner values of P_{mn} should be:

P_{mn}	$n = 0$	$n = N$
$m = 0$	$e^2\sqrt{\pi/32}/a$	$e^2/(2a)$
$m = M - 1$	$\frac{5\pi^2-40+(32M-8)/a}{15a^{1/4}}$	$\frac{2\pi^2-8+4(M-1)/a}{3a}$
$m = M$	$32/(15a^{5/4})$	$4/(3a^2)$

We constrain the fit so that these corner values and the ED entropies in Eq. (2.8.12) are exactly fulfilled. For $M = N = 3$ we find an optimum fit for $a = 0.433$ with a root-mean-square error of $8.1 \cdot 10^{-5}$ and a maximum error of $3.0 \cdot 10^{-4}$ at the fitting points. The coefficients P_{mn} are:

P_{mn}	$n = 0$	$n = 1$	$n = 2$	$n = 3$
$m = 0$	5.34689	18.0517	21.3422	8.53240
$m = 1$	16.8441	55.7051	63.6901	24.6213
$m = 2$	17.4708	56.3902	62.1319	23.2602
$m = 3$	6.07364	18.9992	20.0285	7.11153

To extend this scheme to include pairs, let the subscript $+$ refer to particles and $-$ refer to antiparticles. Then

$$n = n_+(f_+, g_+) - n_-(f_-, g_-) \tag{2.8.13}$$

where $g_\pm = (T/mc^2)\sqrt{1 + f_\pm}$ and

$$\psi_\pm = 2\sqrt{1 + f_\pm/a} + \ln\frac{\sqrt{1 + f_\pm/a} - 1}{\sqrt{1 + f_\pm/a} + 1}. \tag{2.8.14}$$

One solves the simultaneous equations

$$\begin{aligned} A &= n - n_+(f_+, T) + n_-(f_-, T) = 0; \\ B &= \psi_+(f_+) + \psi_-(f_-) + 2mc^2/T = 0, \end{aligned} \tag{2.8.15}$$

where the second follows from $\mu_- = -\mu_+$. This is readily handled, since the derivatives are analytic:

$$\partial A/\partial f_\pm = \mp \partial n_\pm/\partial f_\pm; \qquad \partial B/\partial f_\pm = \sqrt{1 + f_\pm/a}/f_\pm. \tag{2.8.16}$$

2.9. Boson Gas

The boson pressure and energy density are obtained by employing the same equations as for fermions, but using the Bose distribution function

$$f_B = \left[\exp\left(\frac{E-\mu}{T}\right) - 1\right]^{-1}, \tag{2.9.1}$$

and a slightly different entropy formula

$$ns = -\frac{g}{h^3}\int \left[f_B \ln f_B - (1+f_B)\ln(1+f_B)\right] d^3p. \tag{2.9.2}$$

Since the occupation index cannot be negative, a free (non-interacting) Bose gas $\mu \leq mc^2$. If $\mu \to mc^2$, a "Bose condensate" appears and there will be a finite number of particles in a zero-momentum state. Some limiting cases:

2.9.1. Extremely Non-degenerate:

In the non-degenerate limit, $\mu/T \to -\infty$, the Bose and Fermion distributions become indistinguishable, so the limits for thermodynamic quantities evaluated previously for the Fermi gas apply.

2.9.2. Extremely Degenerate

For bosons, the "degenerate" limit is $\mu = mc^2$ or $\psi = 0$; the number density is

$$n = \frac{g}{2\pi^2\hbar^3}\int_0^\infty \frac{p^2}{e^{(E-mc^2)/T}-1} dp. \tag{2.9.3}$$

The integrals in this case can be written simply in terms of zero argument Fermi integrals:

$$\int_0^\infty \frac{x^i}{e^x - 1} dx = \left(1 - 2^{-i}\right)^{-1} F_i(0) = \Gamma(i+1)\,\zeta(i+1). \tag{2.9.4}$$

Therefore we have the following additional limits:

i. **Relativistic** $(T >> mc^2, \psi = 0)$

$$n = \frac{4g}{6\pi^2}\left(\frac{T}{\hbar c}\right)^3 F_2(0), \qquad \epsilon = 3P;$$

$$P = \frac{4gT}{21\pi^2}\left(\frac{T}{\hbar c}\right)^3 F_3(0) = \frac{g\pi^2 T}{90}\left(\frac{T}{\hbar c}\right)^3, \qquad s = \frac{\pi^4}{15F_2(0)} \simeq 3.601571.$$

ii. **Non-relativistic** ($T << mc^2, \psi = 0$)

$$n = \frac{g}{\pi^2}\frac{(mT)^{3/2}}{\hbar^3}\frac{F_{1/2}(0)}{\sqrt{2}-1}, \qquad \epsilon = nmc^2 + \frac{3}{2}P;$$
$$P = \frac{4gT}{3\pi^2}\frac{(mT)^{3/2}}{\hbar^3}\frac{F_{3/2}(0)}{2^{3/2}-1}, \qquad s = \frac{10}{3}\frac{F_{3/2}(0)}{F_{1/2}(0)}\frac{2^{1/2}-1}{2^{3/2}-1} \simeq 1.283781.$$

Note that in these limits the entropy per boson is constant. The location of the $\psi = 0$ trajectory in a boson density-temperature plot is not far from the same curve for fermions.

2.9.3. Extremely Relativistic

In this case, we take $m \to 0$, and we arrive at the simplest bose gas, the photon gas, for which $\mu_\gamma = 0$. With $g_\gamma = 2$, one obtains

$$\epsilon_\gamma = 3P_\gamma = \frac{3}{4}TS_\gamma = \frac{\pi^2 T}{15}\left(\frac{T}{\hbar c}\right)^3, \tag{2.9.5}$$

which is $(8/7g)$ times the value for a relativistic fermion gas. Here S is the entropy density. In any regime where electron-positron pairs are important, the photon pressure is also important. In the non-degenerate, relativistic domain, the total pressure from photons and electron-positron pairs is therefore $11P_\gamma/4$, Under situations when neutrino pairs of all three flavors are trapped in the matter, the total pressure increases to $43P_\gamma/8$. In the regime where electrons are degenerate, however, photon pressure is negligible.

2.9.4. Conclusion

In the regime where the electrons are non-degenerate and pairs are not important, the non-degenerate gas pressure of nuclei must be included, and photon pressure may or not be important. The pressure due to photons is important at lower temperatures than pair pressure, owing to the expense of creating electron-positron pairs. Since the photon pressure is $(8/7g)$ times the relativistic non-degenerate pair pressure, the boundary to the region in which photon pressure is significant is simply obtained by a continuation of the straight line relativistic boundary $\rho \propto T^3$ to low densities and is akin to the line $\phi = 1$ in the fermion-antifermion pair case.

Even excluding the contribution from electron-positron pairs, the adiabatic index of a non-relativistic gas changes from 5/3 to 4/3 as the temperature is increased and the contribution of radiation pressure increases. Denoting the fraction of the total pressure due to gas pressure (assuming complete ionization) by β,

$$\Gamma_1 = \frac{32 - 24\beta - 3\beta^2}{24 - 21\beta}. \tag{2.9.6}$$

This ultimately sets an upper limit to the mass of main sequence stars.

Chapter 3.
Stellar Structure

3.1. Hydrostatic Equilibrium

Spherically symmetric Newtonian equation of hydrostatics:

$$dP/dr = -Gm\rho/r^2, \qquad dm/dr = 4\pi\rho r^2. \tag{3.1.1}$$

$m(r)$ is mass enclosed within radius r.

Conditions at stellar centers $Q = P + Gm^2/8\pi r^4$:

$$\frac{dQ}{dr} = \frac{dP}{dr} + \frac{Gm}{4\pi r^4}\frac{dm}{dr} - \frac{Gm^2}{2\pi r^5} = -\frac{Gm^2}{2\pi r^5} < 0 \tag{3.1.2}$$

$$Q\,(r \to 0) \to P_c, \qquad Q\,(r \to R) \to GM^2/8\pi R^4.$$

M and R are total mass and radius.

3.1.1. Milne Inequality

Central pressure P_c

$$P_c > \frac{GM^2}{8\pi R^4} = 4 \times 10^{14} \left(\frac{M}{M_\odot}\right)^2 \left(\frac{R_\odot}{R}\right)^4 \text{dynes cm}^{-2}. \tag{3.1.3}$$

Average density is

$$\bar{\rho} = \frac{3M}{4\pi R^3} \simeq 1.4 \left(\frac{M}{M_\odot}\right) \left(\frac{R_\odot}{R}\right)^3 \text{g cm}^{-3}. \tag{3.1.4}$$

Estimate of T_c from perfect gas law:

$$T_c \simeq \frac{P_c \mu}{\bar{\rho} N_o} > 2.1 \times 10^6 \left(\frac{M}{M_\odot}\right) \left(\frac{R_\odot}{R}\right) \text{K}. \tag{3.1.5}$$

μ is mean molecular weight. T_c too low by factor of 7.

3.1.2. Better Estimate

$$\rho = \rho_c \left[1 - (r/R)^2\right], \qquad M = (8\pi/15)\,\rho_c R^3.$$

$$P = P_c - \frac{4\pi}{3} G\rho_c^2 R^2 \left[\frac{1}{2}\left(\frac{r}{R}\right)^2 - \frac{2}{5}\left(\frac{r}{R}\right)^4 + \frac{1}{10}\left(\frac{r}{R}\right)^6\right]. \tag{3.1.6}$$

$P(R) = 0$:

$$P_c = \frac{15GM^2}{16\pi R^4} = 3.5 \times 10^{15} \left(\frac{M}{M_\odot}\right)^2 \left(\frac{R_\odot}{R}\right)^4 \text{dynes cm}^{-2}, \tag{3.1.7}$$

$$P = P_c \left[1 - \left(\frac{r}{R}\right)^2\right]^2 \left[1 - \frac{1}{2}\left(\frac{r}{R}\right)^2\right] = \frac{P_c}{2}\left(\frac{\rho}{\rho_c}\right)^2 \left(1 + \frac{\rho}{\rho_c}\right). \tag{3.1.8}$$

The central density is

$$\rho_c = \frac{15M}{8\pi R^3} = \frac{5}{2}\bar{\rho} \simeq 3.6 \left(\frac{M}{M_\odot}\right)\left(\frac{R_\odot}{R}\right)^3 \text{ g cm}^{-3}, \tag{3.1.9}$$

and the central temperature becomes

$$T_c \simeq \frac{P_c \mu}{\rho_c N_o} \simeq 7.0 \times 10^6 \left(\frac{M}{M_\odot}\right)\left(\frac{R_\odot}{R}\right) \text{K}. \tag{3.1.10}$$

3.1.3. Mean molecular weight

Perfect ionized gas ($k_B = 1$)

$$P = T \sum_i (1 + Z_i)\, n_i \equiv \rho N_o T/\mu \equiv NT, \tag{3.1.11}$$

Z_i is charge of ith isotope. Abundance by mass of H, He and everything else denoted by X, Y, and $Z = \sum_{i>He} n_i A_i/(\rho N_o)$. Assuming $1 + Z_i \simeq A_i/2$ for $i >$He:

$$\mu = \left[2X + \frac{3}{4}Y + \sum_{i>He} \frac{n_i\,(1+Z_i)}{\rho N_o}\right]^{-1} \simeq \frac{4}{2 + 6X + Y} = \frac{4}{3 + 5X - Z}. \tag{3.1.12}$$

Solar gas ($X = 0.75, Y = 0.22, Z = 0.03$) has $\mu \simeq 0.6$.

Number of electrons per baryon for completely ionized gas $Z_{i>He} \simeq A_i/2$:

$$Y_e = X + \frac{Y}{2} + \sum_{i>He} \frac{n_i Z_i}{\rho N_o} \simeq X + \frac{Y}{2} + \frac{Z}{2} = \frac{1}{2}(1 + X). \tag{3.1.13}$$

3.2. The Virial Theorem

Position, momentum, mass of ith particle: $\vec{r}_i$, $\vec{p}_i$, m_i.

Newton's Law $\vec{F}_i = \dot{\vec{p}}_i$ with $\vec{p}_i = m_i \dot{\vec{r}}_i$:

$$\frac{d}{dt}\sum \vec{p}_i \cdot \vec{r}_i = \sum \left(\dot{\vec{p}}_i \cdot \vec{r}_i + \vec{p}_i \cdot \dot{\vec{r}}_i\right) = \frac{d}{dt}\sum m_i \dot{\vec{r}}_i \cdot \vec{r}_i = \frac{1}{2}\frac{d^2 I}{d^2 t}, \tag{3.2.1}$$

Moment of inertia: $I = \sum m_i \vec{r}_i^{\,2}$.

Static situation: $d^2 I/dt^2 = 0$.

Non-relativistic gas: $\sum m_i \dot{\vec{r}}_i^{\,2} = \sum \vec{p}_i \cdot \dot{\vec{r}}_i = 2K$.

Total kinetic energy:

$$K = \frac{1}{2}\sum \vec{p}_i \cdot \dot{\vec{r}}_i = -\frac{1}{2}\sum \dot{\vec{p}}_i \cdot \vec{r}_i = -\frac{1}{2}\sum \vec{F}_i \cdot \vec{r}_i = -\left(1/2\right)\Omega. \tag{3.2.2}$$

Sum is virial of Clausius. For perfect gas, only gravitational forces contribute, since forces involved in collisions cancel.

$$\sum \vec{F}_i^G \cdot \vec{r}_i = \sum_{pairs} \vec{F}_{ij}^G \cdot \left(\vec{r}_i - \vec{r}_j\right) = -\sum_{pairs} \frac{Gm_i m_j}{r_{ij}} \equiv \Omega. \tag{3.2.3}$$

Ω is gravitational potential energy, $r_{ij} = |\vec{r}_i - \vec{r}_j|$.

Perfect gas with constant ratio of specific heats, $\gamma = c_p/c_v$:

$$K = (3/2)\,NT, \qquad U = (\gamma - 1)^{-1}\,NT, \qquad E = U + \Omega = U - 2K.$$

U is internal energy, E is total energy.

$$E = U + \Omega = U\left(4 - 3\gamma\right) = \Omega\frac{3\gamma - 4}{3\left(\gamma - 1\right)}. \tag{3.2.4}$$

For $\gamma = 4/3$, $E = 0$. $\gamma < 4/3$, $E > 0$, configuration unstable. $\gamma > 4/3$, $E < 0$, configuration stable and bound by energy $-E$.

Application: contraction of self-gravitating mass $\Delta\Omega < 0$. If $\gamma > 4/3$, $\Delta E < 0$, so energy is radiated. However, $\Delta U > 0$, so star grows hotter.
Relativistic gas: $\sum \vec{p}_i \cdot \dot{\vec{r}}_i = c\sum \vec{p}_i = K = -\Omega$.

Another derivation:

$$VdP = -\frac{1}{3}\frac{Gm}{r}dm = -\frac{1}{3}d\Omega, \tag{3.2.5}$$

where $V = 4\pi r^3/3$. Its integral is

$$\int V\left(r\right)dP = PV\Big|_0^R - \int P\left(r\right)dV = -\frac{1}{3}\Omega \tag{3.2.6}$$

from Eq. (3.2.5). Thus $\Omega = -3\int P(r)dV$.
Non-relativistic case:

$$P = 2\epsilon/3, \qquad \Omega = -2K, \qquad E = \Omega + K = \Omega/2.$$

Relativistic case similar to non-relativistic case with $\gamma = 4/3$:

$$P = \epsilon/3, \qquad \Omega = -K, \qquad E = 0.$$

The critical nature of $\gamma = 4/3$ is important in stellar evolution. Regions of a star which, through ionization or pair production, maintain $\gamma < 4/3$ will be unstable, and will lead to instabilities or oscillations. Entire stars can become unstable if the average adiabatic index drops close to 4/3, and this actually sets an upper limit to the masses of stars. As we will see, the proportion of pressure contributed by radiation is a steeply increasing function of mass, and radiation has an effective γ of 4/3. We now turn our attention to obtaining more accurate estimates of the conditions inside stars.

3.3. Polytropic Equations of State

The polytropic equation of state, common in nature, satisfies

$$P = K\rho^{(n+1)/n} \equiv K\rho^{\gamma'}, \tag{3.3.1}$$

n is the polytropic index and γ' is the polytropic exponent.

1) Non-degenerate gas (nuclei + electrons) and radiation pressure. If $\beta = P_{gas}/P_{total}$ is fixed throughout a star

$$P = \frac{N_o}{\mu\beta}\left[\frac{3N_o}{\mu\beta a}(1-\beta)\right]^{1/3}\rho^{4/3} \tag{3.3.2a}$$

$$T = \left[\frac{3N_o}{\mu\beta a}(1-\beta)\right]^{1/3}\rho^{1/3} \tag{3.3.2b}$$

Here μ and a are the mean molecular weight of the gas and the radiation constant, respectively. Thus $n = 3$.

2) A star in convective equilibrium. Entropy is constant. If radiation pressure is ignored, then $n = 3/2$:

$$s = \frac{5}{2} - \ln\left[\left(\frac{\hbar^2}{2mT}\right)^{3/2}\rho N_o/\mu\right] = \text{constant} \tag{3.3.3a}$$

$$P = \frac{\hbar^2}{2m}\left(\frac{\rho N_o}{\mu}\right)^{5/3}\exp\left(\frac{2}{3}s - \frac{5}{3}\right) = K\rho^{5/3}. \tag{3.3.3b}$$

3) An isothermal, non-degenerate perfect gas, with pairs, radiation, and electrostatic interactions negligible: $n = \infty$. Could apply to a dense molecular cloud core in initial collapse and star formation.

4) An incompressible fluid: $n = 0$. This case can be roughly applicable to neutron stars.

5) Non-relativistic degenerate fermions: $n = 3/2$. Low-density white dwarfs, cores of evolved stars.

6) Relativistic degenerate fermions: $n = 3$. High-density white dwarfs.

7) Cold matter at very low densities, below 1 g cm^{-3}, with Coulomb interactions resulting in a pressure-density law of the form $P \propto \rho^{10/3}$, i.e., $n = 3/7$.

Don't confuse polytropic with adiabatic indices. A polytropic change has $c = dQ/dT$ is constant, where $dQ = TdS$. An adiabatic change is a specific case: $c = 0$.

$$\gamma' = \frac{\partial \ln P}{\partial \ln V} = \gamma\frac{c_v\,(c - c_p)}{c_p\,(c - c_v)},$$

where the adiabatic exponent $\gamma = (\partial \ln P/\partial \ln V)|_s$. If $\gamma = c_p/c_v$, as for a perfect gas, $\gamma' = (c - c_p)/(c - c_v)$. In the adiabatic case, $c = 0$ and $\gamma' = \gamma$ regardless of γ's value.

3.4. Polytropes

Self-gravitating fluid with a polytropic equation of state is a polytrope, with

$$\Omega = -\int \frac{Gm\,(r)\,dm\,(r)}{r} = -\frac{3}{5-n}\frac{GM^2}{R} = -3\int PdV. \tag{3.4.1}$$

For a perfect gas with constant specific heats,

$$E = -\frac{3\gamma-4}{\gamma-1}\frac{1}{5-n}\frac{GM^2}{R}. \tag{3.4.2}$$

For the adiabatic case $n = 1/(\gamma-1)$,

$$E = \frac{n-3}{5-n}\frac{GM^2}{R}. \tag{3.4.3}$$

For a mixture of a perfect gas and radiation,

$$U = \int \left[\frac{\beta}{\gamma-1} + 3\,(1-\beta)\right] PdV = \int \beta\frac{4-3\gamma}{\gamma-1}PdV - \Omega. \tag{3.4.4}$$

For $\beta =$ constant, Eq. (3.4.4) gives β times the result found in Eq. (3.4.2). A bound star has $E < 0$ and $\gamma > 4/3$. If $\gamma = 5/3$, $E = -(3\beta/7)(GM^2/R)$.

A nested polytrope has

$$\begin{aligned} P = K\rho^{1+1/n}; \quad & \epsilon = nP && \rho < \rho_t \\ P = K\rho_t^{1/n-1/n_1}\rho^{1+1/n_1}; \quad & \epsilon = n_1 P + (n-n_1)\,P_t && \rho > \rho_t. \end{aligned}$$

ρ_t and P_t are the transition density and pressure between indices n and n_1. ϵ is the energy density

$$\begin{aligned} E = \frac{n-3}{5-n}\left[\frac{Gm^2}{R} - \frac{GM_t^2}{R_t}\right] + \frac{n_1-3}{5-n_1}\frac{GM_t^2}{R_t^2} \\ + 3P_t\left[\frac{M_t}{\rho_t} - \frac{4\pi}{3}R_t^3\right]\left[\frac{n-1}{5-n} - \frac{n_1-1}{5-n_1}\right]. \end{aligned} \tag{3.4.5}$$

M_t and R_t are mass and radius interior to transition point. When $(n_1 \simeq 0)$ and $n \simeq 3$,

$$E = -\frac{3}{5}\frac{GM_t^2}{R_t}. \tag{3.4.6}$$

This could apply to a proto-neutron star with relativistic electron gas up to ρ_t, and relatively stiff matter beyond. The energy depends on inner core size only.

3.4.1. Structure of polytropes and Lane-Emden equation

$$r = A\xi, \quad \theta = \left(\frac{\rho}{\rho_c}\right)^{1/n}, \quad A = \left[(n+1)\,K\rho_c^{1/n-1}/\,(4\pi G)\right]^{1/2}. \tag{3.4.7}$$

$$\frac{1}{\xi^2}\frac{d}{d\xi}\left(\xi^2\frac{d\theta}{d\xi}\right) = -\theta^n. \tag{3.4.8}$$

Boundary conditions for are θ=1 and $\theta' = d\theta/d\xi = 0$ at ξ=0. The radius is found from ξ_1 where $\theta(\xi) = 0$.

n	γ'	θ	ξ_1	$-\xi_1^2\theta_1'$	$-\xi_1/3\theta_1'$	$[4\pi(n+1)\theta_1'^2]^{-1}$
0	∞	$1-\xi^2/6$	$\sqrt{6}$	$2\sqrt{6}$	1	$3/8\pi$
1	2	$\sin(\xi)/\xi$	π	π	$\pi^2/3$	$\pi/8$
3/2	5/3		3.654	2.714	5.992	0.7704
2	3/2		4.353	2.411	11.40	1.638
3	4/3		6.897	2.018	54.19	11.05
3.25	17/13		8.019	1.950	88.15	20.36
4	5/4		14.97	1.797	622.3	247.5
5	6/5	$1/\sqrt{1+\xi^2/3}$	∞	$\sqrt{3}$	∞	∞

Analytic solutions exist in the following cases:

$$\theta = 1-\xi^2/6; \quad \xi_1 = \sqrt{6} \quad n = 0, \gamma' = \infty; \tag{3.4.9a}$$

$$\theta = \sin\xi/\xi; \quad \xi_1 = \pi \quad n = 1, \gamma' = 2; \tag{3.4.9b}$$

$$\theta = 1/\sqrt{1+\xi^2/3}; \quad \xi_1 = \infty \quad n = 5, \gamma' = \frac{6}{5}. \tag{3.4.9c}$$

$$\text{Radius} : R = A\xi_1 \tag{3.4.10a}$$

$$\text{Mass} : M = -4\pi A^3\rho_c\xi_1^2\theta_1' \tag{3.4.10b}$$

$$\text{Density ratio} : \bar{\rho}/\rho_c = -3\theta_1'/\xi_1 \tag{3.4.10c}$$

$$\text{Central pressure} : P_c = GM/\left[4\pi\,(n+1)\,\theta_1'^2R^4\right] \tag{3.4.10d}$$

$$K = \frac{G}{n+1}\left[4\pi\left(\frac{M}{-\xi_1^2\theta_1'}\right)^{n-1}\left(\frac{R}{\xi_1}\right)^{3-n}\right]^{1/n}. \tag{3.4.11}$$

For $n \to \infty$, we have the *isothermal* Lane-Emden equation:

$$\frac{1}{\xi^2}\frac{d}{d\xi}\left(\xi^2\frac{d\phi}{d\xi}\right) = e^{-\phi} = \frac{\rho}{\rho_c}. \tag{3.4.12}$$

$$\rho = K/2\pi G r^2; R = \infty; m = 2Kr/G \quad n = \infty, \gamma' = 1. \tag{3.4.13}$$

For $n = 3$ mass does not depend on central density, but only on equation of state. For a relativistic degenerate electron gas,

$$P = \frac{\hbar c}{4} \left(3\pi^2\right)^{1/3} \left(nY_e\right)^{4/3}, \tag{3.4.14}$$

which implies a mass

$$M_{ch} = -4\pi \left(\frac{K}{G}\right)^{3/2} \times 2.018 = 5.76 Y_e^2 M_\odot. \tag{3.4.15}$$

This is the famous Chandrasekhar mass, the limiting mass of a white dwarf as $\rho_c \to \infty$. A degenerate mass larger than M_{ch} cannot be stabilized by electron pressure alone. For $T \neq 0$, the pressure has a small thermal component

$$P_{th} = \frac{T^2}{8\hbar c} \left(3\pi^2 \rho Y_e\right)^{2/3}. \tag{3.4.16}$$

For a massive stellar core just prior to collapse, $T \simeq 0.7$ MeV and $\rho \simeq 6 \times 10^9$ g cm^{-3}, and the $P_{th}/P \simeq 0.12$, and the effective M_{ch} is $(1.12)^{3/2} = 1.19$ times larger. The negative Coulomb lattice pressure, which is about 4% of the total, lowers this. At densities in excess of 10^6 g cm^{-3}, electron capture decreases Y_e. For a ^{56}Fe white dwarf, the zero-temperature Chandrasekhar mass is only 1.17 M$_\odot$.

As the cores of massive stars evolve, there is a general tendency for "core convergence" to occur, *i.e.*, the evolved cores of all massive stars, regardless of mass, tend to be nearly M_{ch}. We see that this is a result of the general requirement for stability. In fact, there is a slight trend for more massive stars to have larger cores, but this can be traced to the higher entropies in these stars (recall that Eq. (3.1.5) predicts that $T \sim M/R$) and their larger effective Chandrasekhar masses.

3.5. Standard Model Stars – The Main Sequence

Those stars converting H to He. Standard model assumes $\beta =$ constant.

$$K = \left(\frac{N_o}{\mu\beta}\right)^{4/3} \left(\frac{3}{a}\left(1-\beta\right)\right)^{1/3}. \tag{3.5.1}$$

$$\begin{aligned} R &= 11.18 \left[\frac{1-\beta}{\mu^4\beta^4\rho_c^2}\right]^{1/6} R_\odot \\ M &= 18\frac{\sqrt{1-\beta}}{\mu^2\beta^2} M_\odot \\ \rho_c/\bar{\rho} &= 54.2 \\ T_c &= 1.96\frac{\beta\mu M R_\odot}{M_\odot R} \times 10^7 \mathrm{K}. \end{aligned} \tag{3.5.2}$$

For $n = 3$ polytrope, mass is independent of ρ_c and for given composition μ, is parametrized by β.

For Sun, with $M = 1\mathrm{M}_\odot$ and $\mu \simeq 0.6$:

$$\beta \simeq 1 - \left(\frac{\mu^2}{18}\right)^2 = 0.9996; \quad \rho_c = \frac{11.18^3}{18} = 76.7 \text{ g cm}^{-3}, \tag{3.5.3}$$

$$T_c = 1.307 \times 10^7 \text{ K}.$$

But $\mu_c > \bar{\mu}$ since some H→He has occurred.

Luminosity will depend upon nuclear energy generation $\dot{\epsilon}$ and transport (opacity κ).

For $T > 8 \cdot 10^6 \rho^{1/3.5}$ electron scattering dominates:

$$\kappa \simeq 0.4 Y_e \text{ cm}^2 \text{ g}^{-1}. \tag{3.5.4}$$

Where $T > 10^4$ K, κ dominated by bound-bound and bound-free processes:

$$\kappa \simeq 2.5 \cdot 10^{25} Z Y_e \rho T^{-3.5} \text{ cm}^2 \text{ g}^{-1}. \tag{3.5.5}$$

For $Z < 10^{-4}$ have free-free opacity:

$$\kappa \simeq 8 \cdot 10^{22} (1 - Z) Y_e \rho T^{-3.5} \text{ cm}^2 \text{ g}^{-1}.$$

The dependence $\kappa \propto \rho T^{-3.5}$ is known as Kramer's opacity. For $T < 10^4 K$, matter barely ionized:

$$\kappa \simeq 10^{-32} (Z/.02) \rho T^{10} \text{ cm}^2 \text{ g}^{-1}. \tag{3.5.6}$$

Energy Transport:

$$L(r) = -4\pi r^2 \frac{4ac}{3\kappa_R \rho} T^3 \frac{dT}{dr}. \tag{3.5.7}$$

$L(r)$ is luminosity, κ_R is the "Rosseland mean" opacity, averaged over frequencies. $(\kappa\rho)^{-1}$ is photon mean free path, $d(acT^4/4)/dr$ is radiation energy density gradient. Multiplied together gives energy flux, and multiplied by area $4\pi r^2$ gives net energy flow. Use hydrostatic equilibrium:

$$\frac{dP_r}{dP} = \frac{\kappa L(r)}{4\pi c G m(r)}. \tag{3.5.8}$$

Luminosity function $\eta(r) = L(r)M/m(r)L$, with M and L totals. η is sharply peaked at origin.

$$d[(1 - \beta) P] = \frac{L}{4\pi c G M} \kappa(r) \eta(r) dP. \tag{3.5.9}$$

$$L = \frac{4\pi c G M}{\bar{\kappa\eta}} (1 - \beta_c) \tag{3.5.10}$$

$\bar{\kappa\eta}$ is a pressure average. (ssm: $\kappa\eta =$ cons.) With Eq. (3.5.5)

$$L_{ssm} = (4\pi)^3 \frac{4ac}{3\kappa_o \eta_c} \left(\frac{\mu_c \beta G}{4N_o}\right)^{7.5} \frac{M^{5.5}}{\left(-\xi_1^2 \theta_1'\right)^{4.5}} \left(\frac{\xi_1}{R}\right)^{0.5}$$

$$\simeq .667\frac{(\mu_c\beta_c)^{7.5}}{\eta_c Z Y_{e,c}}\left(\frac{M}{M_\odot}\right)^{5.5}\left(\frac{R_\odot}{R}\right)^{0.5} L_\odot. \tag{3.5.11}$$

With Eq. (3.5.4), appropriate instead for more massive stars,

$$L \simeq 97.5\frac{1}{\eta_c Y_{e,c}}(\beta\mu_c)^4\left(\frac{M}{M_\odot}\right)^3 L_\odot. \tag{3.5.12}$$

For Sun: $\mu_c = 0.73, Y_{e,c} = 0.75$ (i.e., $X \simeq 0.5$ and $Y \simeq 0.5$),

$$L \simeq (2.8/\eta_c)\, L_\odot.$$

Alternatively, use proton-proton rate ($T_6 = T/10^6$):

$$\eta = 2.0\times 10^6 \rho X^2 T_6^{-2/3}\exp\left(-33.8T_6^{-1/3}\right)\frac{M_\odot}{L_\odot}. \tag{3.5.13}$$

With $\rho_c = 76.7$ g cm^{-3}, $T_{c,6} = 13.07$ from ssm η_c=4.05. Try using knowledge of polytropic structure. Assume ideal gas and

$$\dot\epsilon = \dot\epsilon_c\left(\frac{\rho}{\rho_c}\right)^\lambda\left(\frac{T}{T_c}\right)^\nu. \tag{3.5.14}$$

For polytrope, $\rho = \rho_c\theta^n$ and $T = T_c\theta$:

$$L = 4\pi A^3\rho_c\dot\epsilon_c\int\xi^2\theta^{2n\lambda+\nu}d\xi \simeq 4\pi A^3\rho_c\dot\epsilon_c\sqrt{\frac{27\pi}{2}}\,(2n\lambda+\nu)^{-3/2}, \tag{3.5.15}$$

since $2n\lambda+\nu >> 1$. With $\theta \simeq \exp(-\xi^2/6), n = 3$,

$$\eta_c = \dot\epsilon_c\frac{M}{L} = -\left(\xi^2\theta'\right)_1\sqrt{\frac{2}{27\pi}}\,(2n\lambda+\nu)^{3/2} = 0.31\,(6\lambda+\nu)^{3/2}, \tag{3.5.16}$$

P-p cycle has $\lambda = 1, \nu \simeq 4$, so $\eta_c \simeq 9.8$.
CNO cycle has $\lambda = 1, \nu \simeq 20$, so $\eta_c \simeq 41$.

3.6. Scaling Relations for Standard Solar Model

For Kramer's opacity, $\kappa \propto Z(1+X)\rho T^{-3.5}$. For electron scattering, $\kappa \propto (1+X)$. Suggests

$$\kappa \propto (1+X)\, Z^u\rho^n T^{-s}, \tag{3.6.1}$$

with $u = 0, 1$. Similarly

$$\dot\epsilon \propto X^{2-m}Z^m\rho^\lambda T^\nu, \tag{3.6.2}$$

with $m = 0(1)$ for p-p (CNO) cycle. Using

$$L \propto RT^4/\kappa\rho \propto M\dot\epsilon, \qquad T \propto \mu\beta M/R, \qquad \rho \propto M/R^3, \tag{3.6.3}$$

we find

$$\begin{aligned} L &\propto M^{\alpha_M}\,(\mu\beta)^{\alpha_\mu}\,X^{\alpha_X}\,(1+X)^{\alpha_1}\,Z^{\alpha_Z}, \\ R &\propto M^{\beta_M}\,(\mu\beta)^{\beta_\mu}\,X^{\beta_X}\,(1+X)^{\beta_1}\,Z^{\beta_Z}, \\ T_{eff} \propto \left(L/R^2\right)^{1/4} &\propto M^{\gamma_M}\,(\mu\beta)^{\gamma_\mu}\,X^{\gamma_X}\,(1+X)^{\gamma_1}\,Z^{\gamma_Z}, \\ L &\propto T_{eff}^{\delta_T}\,(\mu\beta)^{\delta_\mu}\,X^{\delta_X}\,(1+X)^{\delta_1}\,Z^{\delta_Z}. \end{aligned} \tag{3.6.4}$$

With $i = (M, \mu, X, (1+X), Z, T)$, $\gamma_i = \alpha_i/4 - \beta_i/2$, $\delta_i = 2(\alpha_M\beta_i - \alpha_i\beta_M)/(\alpha_M - 2\beta_M)$, $D = \nu - s + 3(n+\lambda)$:

$i \rightarrow$	M	μ	T
$\alpha_i D$	$\nu(3+2n) + 9\lambda + 3n + s(2\lambda - 1)$	$7\nu + 3\lambda(4+s)$	0
$\beta_i D$	$\lambda + \nu + n - s - 2$	$\nu - 4 - s$	$2D$
$i \rightarrow$	X	1	Z
$\alpha_i D$	$m(3n-s) - u(3\lambda+s)$	$-(s+3\lambda)$	$(3n-s)(2-m)$
$\beta_i D$	$u+m$	1	$2-m$

	α_M	α_μ	α_X	α_1	α_Z	α_T
low	71/13	101/13	-2/13	-14/13	-16/13	0
high	3	4	0	-1	0	0
	β_M	β_μ	β_X	β_1	β_Z	β_T
low	1/13	-7/13	4/13	2/13	2/13	2
high	19/23	16/23	1/23	1/23	1/23	2
	γ_M	γ_μ	γ_X	γ_1	γ_Z	γ_T
low	69/52	87/52	-3/26	-9/26	-7/13	-2
high	31/92	15/23	-1/46	-25/92	-1/46	-2
	δ_M	δ_μ	δ_X	δ_1	δ_Z	δ_T
low	0	-4/3	44/69	8/23	68/69	284/69
high	0	-56/31	6/31	44/31	6/31	276/31

Values refer to low-mass ($\nu = 4, \lambda = 1, m = 0, u = 1, n = 1, s = 3.5$) or high-mass ($\nu = 20, \lambda = 1, m = 1, u = 0, n = 0, s = 0$) M-S stars.

1) As H consumed, X decreases and μ increases

$$\mu \simeq 4/\left(5X + 3\right)$$

and β is nearly constant. So L increases and T_{eff} increases; stars evolve *up* the main sequence. This explains why in globular clusters the M-S turnoff luminosity $>> L_\odot$ even though $M \leq \mathrm{M}_\odot$. Also, the early Sun was less luminous, and cooler, than present. If initial (present) $X = 0.75(0.7)$,

$$\frac{L_{today}}{L_{initial}} \simeq 1.4, \quad \frac{T_{eff,today}}{T_{eff,initial}} \simeq 1.11,$$

$$\frac{T_{c,today}}{T_{c,initial}} \simeq 1.09, \quad \frac{R_{today}}{R_{initial}} \simeq 0.96.$$

2) Stars on the p-p cycle ($\nu = 4$) have R nearly independent of M: $R \propto M^{1/13}$ for Kramer's opacity. For stars on the CNO cycle, however, $R \propto M^{11/15}$ for Kramer's opacity and $R \propto M^{19/23}$ for electron scattering opacity.

3) Population II stars are characterized by low metal compositions, $Z < 0.001$. For a given T_{eff}, $L \propto Z^{\delta Z}$ dominates the composition dependence. The Population II M-S is shifted to lower L than the Population I M-S. Also, for a given M, $T_{eff} \propto Z^{\gamma Z}$ implies a shift of the M-S to higher T_{eff}.

4) For a given M, $L \propto Z^{\alpha Z}$, which is larger for Population II than for Population I stars. Stellar lifetimes $\tau \propto M/L$ are nearly $\propto Z$ since $\kappa \propto Z(1+X)$. Thus, lifetimes of Population II stars are substantially less than Population I for a given mass. This is observed in H-R diagrams of globular clusters.

3.7. Idealized Stars

3.7.1. Radiative Zero Solution

Besides the standard model, we could consider an idealized star in which the energy generation is uniform throughout, *i.e.,* $\eta(r) = 1$, and the equation of state is that of an ideal gas alone. If such a star is in radiative equilibrium, we can write

$$\frac{d\ln T}{d\ln P} = \frac{3L\kappa P}{16\pi acGMT^4} = \frac{3\kappa_o L}{16\pi acGM}\left(\frac{\mu}{N_o}\right)^m \frac{P^{m+1}}{T^{4+t+m}} \tag{3.7.1}$$

where the opacity is assumed to scale as

$$\kappa = \kappa_o \rho^n T^{-s}. \tag{3.7.2}$$

The *radiative zero solution* is obtained if $d\ln T/d\ln P$ is constant. Eq. (3.7.1) then implies that $d\ln T/d\ln P = (n+1)/(n+s+4)$ and

$$P \propto T^{(4+s+n)/(n+1)}; \quad P \propto \rho^{(4+s+n)/(s+3)}. \tag{3.7.3}$$

For a Kramer's opacity law ($n = 1, s = 3.5$) we find the effective polytropic index to be 3.25, and, from Eq. (3.7.1),

$$L = (4\pi)^3 \frac{4ac}{3\kappa_o}\left(\frac{4\mu G}{17N_o}\right)^{7.5} \frac{M^{5.5}}{\left(-\xi_1^2\theta_1'\right)^{4.5}}\left(\frac{\xi_1}{R}\right)^{0.5} \simeq 0.8\eta_c \left(\frac{\mu}{\mu_c}\right)^{7.5}\left(\frac{Y_{e,c}}{Y_e}\right) L_{ssm}. \tag{3.7.4}$$

(Note that ξ_1 and θ_1' are evaluated for the $n = 3.25$ polytrope, and not the $n = 3$ polytrope as for the standard model). Had we used the Thomsen opacity ($n = s = 0$) instead, we would have just found Eq. (3.5.12) with β_c=1.

3.7.2. Completely Convective Stars

To conclude this section, we now consider the idealized completely convective star. This case is especially relevant to the pre-main sequence phase of stellar evolution. For a perfect gas, an $n = 3/2$ polytrope must result for constant entropy. We immediately find

$$\begin{aligned} \rho_c/\bar{\rho} &= 6, \\ T_c &= 1.2\frac{\mu M R_\odot}{M_\odot R} \times 10^7 \mathrm{K}, \\ P_c &= 8.7\frac{M^2 R_\odot^4}{M_\odot^2 R^4} \mathrm{erg\ cm^{-3}}. \end{aligned} \tag{3.7.5}$$

It is also clear that, dimensionally (*cf*. Eq. (3.4.10))

$$\begin{aligned} M &\propto K^{3/2}\rho_c^{1/2} \\ R &\propto K^{1/2}\rho_c^{-1/6} \propto KM^{-1/3} \propto e^{2s/3}\,(\text{for fixed } M) \\ E &= \frac{3}{14}\frac{GM^2}{R} \propto M^{7/3}K^{-1} \propto e^{-2s/3}\,(\text{for fixed } M) \end{aligned} \tag{3.7.6}$$

where K is given by Eq. (3.3.3). In the last two equations, s is the entropy per baryon, not the temperature dependence of the energy generation rate.

It is straightforward to show that both the heat flux and luminosity vary as the 3/2 power of the difference of the actual temperature gradient from the purely adiabatic one (*e.g.*, Ref. **@Ref.Clayton@**, p. 257). Typically, near the outside of a star, this difference is only 10^{-6} of the temperature gradient itself. Therefore it is impossible to determine the luminosity from the transport equation as we did in the radiative case. But because radiation eventually escapes, the transport must become radiative just below the surface. Using the photospheric condition for the optical depth $\tau = \int \kappa\rho dr \simeq 2/3$ one may determine the surface temperature and hence the luminosity. Hydrostatic equilibrium can be rewritten as

$$dP/d\tau = -g/\kappa \tag{3.7.7}$$

where $g = GM/r^2 \simeq GM/R^2$, the surface gravity, is nearly constant throughout the thin surface region. As a zeroth approximation, we may write

$$P_p \simeq \frac{2}{3}\frac{g_p}{\kappa_p} = \frac{2}{3}GMR_p^{-2}\kappa_o^{-1}\rho_p^{-n}T_p^s \tag{3.7.8}$$

where the subscript p indicates photospheric values. Only if κ varies rapidly in the surface region will this result be inaccurate. Combining Eqs. (3.7.8) and (3.4.11), using values for a $n = 3/2$ polytrope, and employing the perfect gas law, we can find the photospheric temperature:

$$T_p = \left[\left(\frac{2GM}{3\kappa_o R_p^2}\right)^2 \left(\frac{\mu}{N_o}\right)^{3n+5} K^{3+3n}\right]^{1/(5+3n-2s)} \propto \left(M^{3+n}R_p^{3n-1}\right)^{1/(5+3n-2s)}. \tag{3.7.9}$$

The luminosity follows immediately from $L = 4\pi R_p^2 \sigma T_p^4$:

$$\begin{aligned} L =& \sigma \left[(4\pi)^{-n-5} \left(\frac{3\kappa_o}{5}\right)^4 \left(\frac{5N_o}{2G\mu}\right)^{10+6n} \left(-\xi_1^5\theta_1'\right)^{2+2n} \frac{T_p^{6+18n-4s}}{M^{6+2n}} \right]^{1/(3n-1)} \\ =& \sigma \left[(4\pi)^{13+11n-2s} \left(\frac{5}{3\kappa_o}\right)^8 \left(\frac{2\mu G}{5N_o}\right)^{20+12n} \frac{M^{12+4n} R_p^{6+18n-4s}}{\left(-\xi^5\theta_1'\right)^{4+4n}} \right]^{1/(5+3n-2s)} . \end{aligned} \tag{3.7.10}$$

This relation shows the tremendous sensitivity of the luminosity to the photospheric temperature: typically in the low density surface regions, $s \approx -10$.

In general, a star is convective if its luminosity is large enough to force a superadiabatic temperature gradient. Thus, there must exist a minimum luminosity below which a star cannot be completely convective. A star in convective equilibrium has $d\ln T/d\ln P = 2/5 (n = 3/2)$, so from Eq. (3.4.11),

$$P_c = \left(\frac{N_o T_c}{\mu}\right)^{5/2} K^{-3/2}; \quad T_c = \frac{-2}{5\xi_1\theta_1'} \frac{\mu G M}{N_o R}. \tag{3.7.11}$$

On the other hand, a star in radiative equilibrium, from Eq. (3.7.4), satisfies, at the center,

$$\frac{d\ln T}{d\ln P} = \frac{3}{16\pi acG} \frac{\kappa_c P_c L \eta_c}{T_c^4 M}. \tag{3.7.12}$$

If the logarithmic temperature gradient at the center falls below 2/5, the star will cease to be completely convective. Therefore from the previous two equations, we find

$$\begin{aligned} L_{min} &= \frac{32\pi acGM}{15\eta_c} \frac{T_c^4}{\kappa_c P_c} \\ &= \frac{4ac}{3\eta_c\kappa_o} (4\pi)^{n+2} \left(\frac{2G\mu}{5N_o}\right)^{4+s} \frac{\xi_1^{s-3n}}{\left(-\xi_1^2\theta_1'\right)^{2+s-n}} \frac{M^{s-n+3}}{R^{s-3n}} \\ &= 271 \frac{\mu^{7.5} \left(M/M_\odot\right)^{5.5}}{\eta_c \left(R/R_\odot\right)^{.5}} L_\odot \end{aligned} \tag{3.7.13}$$

where the last equality holds for Kramer's opacity. This can be compared with the luminosity from the standard solar model (for 1 $M_\odot$ and 1 $R_\odot$), which behaves on the physical variables in a similar way:

$$\begin{aligned} L_{min}/L_{ssm} &= \left(\frac{8\mu}{5\beta\mu_{ssm}}\right)^{7.5} \left(\frac{\xi_{1,3}^2\theta_{1,3}'}{\xi_{1,3/2}^2\theta_{1,3/2}'}\right)^{4.5} \left(\frac{\xi_{1,3/2}R_{ssm}}{\xi_{1,3}R}\right)^{0.5} \frac{\eta_{ssm}Y_{e,ssm}}{\eta_c Y_e} \\ &\simeq 6.518 \left(\frac{\mu}{\mu_{ssm}}\right)^{7.5} \left(\frac{R_{ssm}}{R}\right)^{0.5} \frac{\eta_{ssm}Y_{e,ssm}}{\eta_c Y_e}. \end{aligned} \tag{3.7.14}$$

We expect that $\eta_{ssm}/\eta_c \approx 2$, and $\mu/\mu_{ssm} \simeq 0.82$, so with $R \simeq 3R_\odot$ we find that $L_{min} \simeq 1.6 L_{ssm}$ for a solar-type star. This is larger than the actual minimum luminosity reached along the Hayashi track, but the star overshoots this minimum luminosity as it gradually becomes more and more radiative.

We will further explore pre-main sequence stars in the next chapter.

3.8. Implicit Integration – Henyey Method

3.8.1. Non-relativistic case

In this exercise, you will solve for the structure of a star of mass M for a polytropic equation of state $P = K\rho^\gamma$. (However, for the case $\gamma = 4/3$, one must have $M = (3/\sqrt{2}\pi)(K/G)^{3/2}$ so that K and M cannot both be arbitrary.) It is convenient to reformulate the original equations as

$$\frac{d\ln r}{dm} = \frac{1}{4\pi\rho r^3}\,;$$

$$\frac{d\ln P}{dm} = -\frac{Gm}{4\pi P r^4}\,.$$

We substitute $x = \ln r$, $y = \ln P$ and $q = \ln\rho$ and input an equation of state $\rho(P)$ or equivalently $q(y)$. We rewrite these differential equations as finite-difference equations to be zeroed at each position i:

$$\phi_i = y_i - y_{i-1} + \frac{G}{8\pi}\left(m_i^2 - m_{i-1}^2\right)\mathrm{e}^{-\frac{1}{2}(y_i+y_{i-1})-2(x_i+x_{i-1})},$$

$$\psi_i = x_i - x_{i-1} - \frac{1}{4\pi}\left(m_i - m_{i-1}\right)\mathrm{e}^{-\frac{3}{2}(x_i+x_{i-1})-\frac{1}{2}(q_i+q_{i-1})}.$$

These equations are valid for $2 \le i \le N-1$, where i is the zone number and N is the number of (radial) zones into which we divide the star. Thus, m_i, y_i, x_i are the values of the respective variables at the outer edge of the ith zone. Note that the values of m_i are set in advance for the star and will not change during the iteration. Also note how the finite differencing is done so as to reduce errors:

$$mdm = \frac{1}{2}dm^2 \to \frac{1}{2}\left(m_i^2 - m_{i-1}^2\right), \quad \frac{1}{P} = \mathrm{e}^{-\ln P} \to \mathrm{e}^{-\frac{1}{2}(y_i+y_{i-1})}.$$

At the inner and outer boundaries, these equations must be rewritten since at $i = 0$, $x \to -\infty$, and at $i = N$, $y \to -\infty$. The inner boundary can be approximated using the incompressible fluid result

$$P(r) \simeq P_c - \frac{G}{2}\left(\frac{4\pi}{3}\rho_c^4 m(r)^2\right)^{1/3}; \qquad r \simeq \left(\frac{3m(r)}{4\pi\rho_c}\right)^{1/3},$$

which are valid near the origin. Thus, using the subscript $_0$ for the origin,

$$\phi_1 = y_1 - y_0 + \frac{G}{2}\left(\frac{4\pi}{3}\right)^{1/3} M_1^{2/3} e^{4q_0/3 - y_0}\,;$$

$$\psi_1 = x_1 - \frac{1}{3}\left(\ln\left[\frac{3M_1}{4\pi}\right] - q_0\right).$$

The surface can be approximated in several ways. For example, the polytropic index might be nearly constant there, with a value γ_R, and the mass in the outermost zone is negligible compared to the total mass M. (In fact, we are assuming $\gamma_R = \gamma$.) Then it is easy to show that two independent equations for the behavior of P and r near the surface are

$$P = \frac{GM\left(M - m\left(r\right)\right)}{4\pi r^4},$$
$$\frac{P}{\rho} = GM\left(1 - \gamma_R^{-1}\right)\left(\frac{1}{r} - \frac{1}{R}\right).$$

These lead to

$$\phi_N = y_{N-1} + 2\left(x_N + x_{N-1}\right) - \ln\frac{Gm_N\left(m_N - m_{N-1}\right)}{4\pi};$$
$$\psi_N = e^{y_{N-1}-q_{N-1}} - Gm_N\left(1 - \left.\frac{dq}{dy}\right|_{q\to 0}\right)\left(e^{-x_{N-1}} - e^{-x_N}\right).$$

Thus, in total, there are N values of x_i and y_i to solve for, and we have N equations each for ϕ and ψ to do it with.

Since we want to solve $\phi_i(x_i, x_{i-1}, y_i, y_{i-1}) = 0$ and $\psi_i(x_i, x_{i-1}, y_i, y_{i-1}) = 0$, we expand them in Taylor series:

$$\phi_i + a_i\Delta x_{i-1} + b_i\Delta y_{i-1} + c_i\Delta x_i + d_i\Delta y_i = 0;$$
$$\psi_i + a'_i\Delta x_{i-1} + b'_i\Delta y_{i-1} + c'_i\Delta x_i + d'_i\Delta y_i = 0,$$

where the notation Δx_i and Δy_i refers to the changes in the values of x_i and y_i that will zero the ϕ and ψ equations. That is, we need to solve the above equations for these Δ's in order to determine how much the x's and y's should be changed for each iteration. The quantities a, b, c and d are the derivatives

$$a_i = \frac{\partial\phi_i}{\partial x_{i-1}}, \qquad b_i = \frac{\partial\phi_i}{\partial y_{i-1}}, \qquad c_i = \frac{\partial\phi_i}{\partial x_i}, \qquad d_i = \frac{\partial\phi_i}{\partial y_i},$$
$$a'_i = \frac{\partial\psi_i}{\partial x_{i-1}}, \qquad b'_i = \frac{\partial\psi_i}{\partial y_{i-1}}, \qquad c'_i = \frac{\partial\psi_i}{\partial x_i}, \qquad d'_i = \frac{\partial\psi_i}{\partial y_i}.$$

These are functions of the x's and y's. These equations are linear in the Δ's, so we can assume

$$\Delta x_i = -\gamma_i - \alpha_i\Delta y_i; \qquad \Delta x_{i-1} = -\gamma_{i-1} - \alpha_{i-1}\Delta y_{i-1}.$$

By substitution and elimination into the equations for ϕ and ψ, we find

$$\gamma_i = \frac{\left(b'_i - a'_i\alpha_{i-1}\right)\left(\phi_i - a_i\gamma_{i-1}\right) - \left(b_i - a_i\alpha_{i-1}\right)\left(\psi_i - a'_i\gamma_{i-1}\right)}{c_i\left(b'_i - a'_i\alpha_{i-1}\right) - c'_i\left(b_i - a_i\alpha_{i-1}\right)};$$

$$\alpha_i = \frac{d_i\left(b'_i - a'_i\alpha_{i-1}\right) - d'_i\left(b_i - a_i\alpha_{i-1}\right)}{c_i\left(b'_i - a'_i\alpha_{i-1}\right) - c'_i\left(b_i - a_i\alpha_{i-1}\right)}.$$

We also can find

$$\Delta y_{i-1} = -\frac{\left(\psi_i - a'_i\gamma_{i-1} + c'_i\Delta x_i + d'_i\Delta y_i\right)}{b'_i - a'_i\alpha_{i-1}}.$$

Now we are in a position to determine new guesses from the original ones. Note that $r_0 = 0$ implies $\Delta x_0 = 0$ since the radius at the origin is always zero. Thus we must have $\gamma_0 = \alpha_0 = 0$. We can loop through the above equations for γ and α to now find α_i and γ_i from their values for $i-1$. From the fact that the pressure vanishes on the outer boundary, $\Delta y_N = 0$ which also implies $\Delta x_N = -\gamma_N$. We can find Δy_{N-1} in terms of $\Delta x_N, \Delta y_N$ and the coefficients $a'_{N-1}, b'_{N-1}, c'_{N-1}, d'_{N-1}$, and then employ $\Delta x_{N-1} = -\gamma_{N-1} - \alpha_{N-1}\Delta y_{N-1}$. In this way, one can loop back to find the remaining Δy's and Δx's. Note that this is a form of Gaussian elimination.

When the changes Δx_i and Δy_i become small enough, we have convergence. It is important to note that this is a Newton-Raphson technique, and therefore its success depends upon suitable initial guesses. I have found that an initial guess based upon the analytic solution for an incompressible gas works adequately. For the incompressible gas, we have

$$m\,(r) = \frac{4\pi\rho_c r^3}{3}\,; \qquad P\,(r) = P_c - \frac{2\pi}{3}G\rho^2 r^2\,.$$

These can be expressed also as

$$r\,(m) = \left(\frac{3m}{4\pi\rho_c}\right)^{1/3}\,; \qquad P\,(m) = P_c - G\frac{2\pi}{3}\left(\frac{3m\rho_c^2}{4\pi}\right)^{2/3}\,.$$

The values of P_c and ρ_c in this approximation are found from $P_c/\rho_c^{4/3} = (2\pi G/3)(.75M/\pi)^{2/3} = K^{4/3\gamma}P_c^{1-4/3\gamma}$, which follows from $P(M) = 0$:

$$P_c = K^{4/(4-3\gamma)}\left(\frac{2\pi G}{3}\right)^{3\gamma/(3\gamma-4)}\left(\frac{3M}{4\pi}\right)^{2\gamma/(3\gamma-4)}\,,$$

for any $\gamma \neq 4/3$. If $\gamma = 4/3$, then $K = (2\pi G/3)(.75M/\pi)^{2/3}$.

3.8.2. Henyey Technique for Relativistic Stars

To include the effects of General Relativity, one must distinguish between the gravitational mass $m(r)$ and the baryon mass $b(r)$, where $b(r)$ is the number of baryons within a radius r times the baryon mass (m_B). Because in GR the gravitational mass is dependent upon the local gravitational field, but the baryon number is an invariant quantity, we must use $b(r)$ as the independent variable instead of $m(r)$. The relevant equations become

$$\begin{aligned}
\frac{d\ln r}{db} &= \frac{\sqrt{1-2Gm/rc^2}}{4\pi n m_B r^3} \\
\frac{d\ln P}{db} &= -\frac{G\left(m + 4\pi r^3 P/c^2\right)\left(\rho + P/c^2\right)}{4\pi r^4 n m_B P\sqrt{1-2Gm/rc^2}} \\
\frac{dm}{db} &= \frac{\rho}{n m_B}\sqrt{1-2Gm/rc^2}.
\end{aligned} \tag{3.8.1}$$

Here, the total mass density is $\rho = n(m_B + e/c^2)$ where n is the baryon density and e is the internal energy per baryon. Employing $y = \ln(P/c^2), x = \ln r$ and $q = \ln\rho$, with, in addition, $z = \ln(nm_B)$, we find

$$\begin{aligned}
\phi_i =& y_i - y_{i-1} + \frac{G}{4\pi c^2}\frac{b_i - b_{i-1}}{\Lambda}\left[1 + e^{\frac{1}{2}(q_i+q_{i-1}-y_i-y_{i-1})}\right] \\
& \left(\frac{m_i + m_{i-1}}{2} + 4\pi e^{\frac{3}{2}(x_i+x_{i-1})+\frac{1}{2}(y_i+y_{i-1})}\right) e^{-\frac{1}{2}(z_i+z_{i-1})-2(x_i+x_{i-1})} \\
\psi_i =& x_i - x_{i-1} - \frac{1}{4\pi}\left(b_i - b_{i-1}\right) e^{-\frac{3}{2}(x_i+x_{i-1})-\frac{1}{2}(z_i+z_{i-1})}\Lambda, \\
\chi_i =& m_i - m_{i-1} - \left(b_i - b_{i-1}\right) e^{\frac{1}{2}(q_i+q_{i-1}-z_i-z_{i-1})}\Lambda,
\end{aligned} \tag{3.8.2}$$

where

$$\Lambda = \sqrt{1 - \frac{G}{c^2}\left(m_i + m_{i-1}\right) e^{-\frac{1}{2}(x_i+x_{i-1})}}.$$

At the inner and outer boundaries, the first two equations must be replaced by equations similar to before, but the third equation is well-behaved at these boundaries and does not have to be replaced. Thus, at the inner boundary,

$$\begin{aligned}
\phi_1 =& y_1 - y_0 + \frac{G}{c^2}\left(\frac{\pi m_1^2}{6}\right)^{1/3} e^{\frac{4}{3}q_0 - y_0}\left(1 + e^{y_0-q_0}\right)\left(1 + 3e^{y_0-q_0}\right), \\
\psi_1 =& x_1 - \frac{1}{3}\left[\ln\left(\frac{3m_1}{4\pi}\right) - q_0\right], \\
\chi_1 =& m_1 - b_1 e^{\frac{1}{2}(q_1+q_0-z_1-z_0)}\sqrt{1 - \frac{2G}{c^2}\left(\frac{\pi m_1^2}{3}\right)^{1/3} e^{q_0/3}},
\end{aligned} \tag{3.8.3}$$

and, at the outer boundary,

$$\begin{aligned}
\phi_N =& y_{N-1} + 2\left(x_N + x_{N-1}\right) - \ln\left[\frac{G\left(m_N + m_{N-1}\right)\left(b_N - b_{N-1}\right)}{8\pi\sqrt{1 - 2Gm_N e^{-x_N}/c^2}}\right], \\
\psi_N =& e^{y_{N-1}-z_{N-1}} + \frac{1}{2}\left(1 - \left.\frac{dz}{dy}\right|_{y\to 0}\right)\ln\left[\frac{1 - 2Gm_N e^{-x_{N-1}}/c^2}{1 - 2Gm_N e^{-x_N}/c^2}\right], \\
\chi_N =& m_N - m_{N-1} - \left(b_N - b_{N-1}\right)\sqrt{1 - 2Gm_N e^{-x_N}/c^2}.
\end{aligned} \tag{3.8.4}$$

To implement the boundary conditions, it is convenient to use the linear relation

$$\Delta y_i = -\gamma_i - \alpha_i \Delta x_i - \beta_i \Delta m_i, \tag{3.8.5}$$

and the corresponding expression for $i - 1$. At the inner boundary, we must have $\Delta x_0 = \Delta m_0 = 0$, so $\Delta y_0 = -\gamma_0$. Similarly, at the outer boundary, the condition $\Delta y_N = 0$ implies that $\gamma_N = \alpha_N = \beta_N = 0$. Therefore, we seek relations for $\gamma_{i-1}, \alpha_{i-1}$ and β_{i-1} in terms of γ_i, α_i and β_i. In addition, we need expressions for Δy_i, Δx_i and Δm_i in terms of $\Delta y_{i-1}, \Delta x_{i-1}$ and Δm_{i-1}. Therefore the recursions will proceed oppositely to the scheme we employed for the Newtonian calculations.

We expand the functions ϕ_i, ψ_i, χ_i in Taylor series in the variables $y_{i-1}, y_i,\ x_{i-1}, x_i,$ m_{i-1}, m_i, which will define the coefficients a_i, a_i', a_i'' and so forth for b, c, d, e and f:

$$\begin{aligned}
&\phi_i + a_i\Delta y_{i-1} + b_i\Delta x_{i-1} + c_i\Delta m_{i-1} + d_i\Delta y_i + e_i\Delta x_i + f_i\Delta m_i = 0,\\
&\psi_i + a_i'\Delta y_{i-1} + b_i'\Delta x_{i-1} + c_i'\Delta m_{i-1} + d_i'\Delta y_i + e_i'\Delta x_i + f_i'\Delta m_i = 0,\\
&\chi_i + a_i''\Delta y_{i-1} + b_i''\Delta x_{i-1} + c_i''\Delta m_{i-1} + d_i''\Delta y_i + e_i''\Delta x_i + f_i''\Delta m_i = 0.
\end{aligned} \tag{3.8.6}$$

We assume the linear relation Eq. (3.8.5) exists among the Δs. One finds the relations

$$\begin{aligned}
\gamma_{i-1} =& \frac{B'\Psi - B\Phi + B''X + \gamma_i\left[b_i''A'' + b_iA - b_i'A'\right]}{B'D' - BD + B''D''},\\
\alpha_{i-1} =& \frac{B'E' - BE + B''E''}{B'D' - BD + B''D''},\\
\beta_{i-1} =& \frac{B'F' - BF + B''F''}{B'D' - BD + B''D''},\\
\Delta x_i =& \frac{\gamma_i\left(A - \Phi\right) - \Delta y_{i-1}D - \Delta x_{i-1}E - \Delta m_{i-1}F}{C''B' - C'B''},\\
\Delta m_i =& \frac{\psi_iB - \phi_iB' + \gamma_i\left(a_ib_i' - a_i'b_i\right) - \Delta y_{i-1}G - \Delta x_{i-1}G' - \Delta m_{i-1}G''}{c_iB' - c_i'B + \beta_i\left(a_i'b_i - a_ib_i'\right)},
\end{aligned} \tag{3.8.7}$$

where

$$\begin{aligned}
\Phi =& \psi_iC'' - \chi_iC', \quad \Psi = \phi_iC'' - \chi_iC, \quad X = \psi_iC - \phi_iC',\\
A =& a_i'C'' - a_i''C', \quad A' = a_iC'' - Ca_i'', \quad A'' = a_iC' - a_i'C,\\
B =& b_i - \alpha_ia_i, \quad B' = b' - \alpha_ia_i', \quad B'' = b_i'' - \alpha_ia'',\\
C =& c_i - \beta_ia_i, \quad C' = c_i' - \beta_ia_i', \quad C'' = c_i'' - \beta_ia_i'',\\
D =& d_i'C'' - d_i''C', \quad D' = d_iC'' - d_i''C, \quad D'' = d_iC' - d_i'C,\\
E =& e_i'C'' - e_i''C', \quad E' = e_iC'' - e_i''C, \quad E'' = e_iC' - e_i'C,\\
F =& f_i'C'' - f_i''C', \quad F' = f_iC'' - f_i''C, \quad F'' = f_iC' - f_i'C.\\
G =& d_iB' - d_i'B, \quad G' = e_iB' - e_i'B, \quad G'' = f_iB' - f_i'B.
\end{aligned} \tag{3.8.8}$$

These are supplemented by Eq. (3.8.5).

The polytropic pressure law is usually taken to be

$$P = Kn^\gamma, \quad n = \left(\frac{P}{K}\right)^{1/\gamma}, \quad \rho = n\left(m_B + \frac{u_0}{c^2}\right) + \frac{P}{(\gamma-1)\,c^2}, \tag{3.8.9}$$

where u_0 is the energy per baryon of zero pressure matter, measured relative to the baryon mass m_B. Usually, we have $m_B = 939$ MeV$/c^2$ and $u_0 = -9$ MeV$/c^2$. One also finds

$$\frac{dq}{dy} = \frac{\rho c^2 + P}{\gamma P}, \qquad \frac{dz}{dy} = \frac{1}{\gamma}. \tag{3.8.10}$$

Chapter 4.
Radiative Transfer and Luminosity

$dE = I_\nu(\vec{x},\vec{k})dS\ d\omega\ d\nu\ dt$ is energy crossing dS perpendicular to $\vec{k}$ in $d\omega$ in $d\nu$ in dt. This defines I_ν. As radiation moves distance ds along $\vec{k}$, I_ν changes

1. Absorption: $dI_{abs} = -\kappa\rho I ds$.
2. Scattering: $dI_{scat} = -\sigma\rho I ds + \sigma\rho ds \int I(\vec{k}')p(\vec{k},\vec{k}')d\omega'$.
   Scattering is into and out of beam; p is probability function.
3. Emission: $dI_{em} = j\rho ds = (j_{spon} + j_{stim})\rho ds$ in near thermal equilibrium.
   Stimulated: $j_{stim} = \kappa I \exp(-h\nu/kT)$
   Spontaneous: $j' = j_{spon} = j - j_{stim}$
   With $\kappa' = \kappa[1 - \exp(-h\nu/kT)]$, j' and κ' are isotropic.

$$\frac{dI}{\rho ds} = j' - \kappa' I - \sigma I + \sigma \int I\left(\vec{k}'\right) p\left(\vec{k},\vec{k}'\right) d\omega'. \tag{4.1}$$

In thermal equilibrium, $I = B,\ \ j' = \kappa' B$.
Interior is close to thermal equilibrium:

$$I\left(\vec{x},\vec{k}\right) = B\left(\vec{x}\right) + \delta\left(\vec{x},\vec{k}\right) \tag{4.2}$$

$$j' = \kappa' B + \delta' \tag{4.3}$$

Substitute (B is isotropic, $\int p(\vec{k},\vec{k}')d\omega' = 1$):

$$\frac{dB}{\rho ds} = \delta' - \left(\kappa' + \sigma\right)\delta + \sigma \int \delta\left(\vec{k}'\right) p\left(\vec{k},\vec{k}'\right) d\omega'. \tag{4.4}$$

Most scattering processes are symmetric between forwards and backwards scattering: $p(\vec{k},\vec{k}') = p(\vec{k},-\vec{k}')$. If true, then

$$\delta = -\frac{1}{\left(\kappa' + \sigma\right)\rho}\frac{dB}{ds} + \frac{\delta'}{\kappa'}. \tag{4.5}$$

Note

$$\int \frac{dB}{ds} p\left(\vec{k},\vec{k}'\right) d\omega' = 0, \tag{4.6}$$

so that

$$I\left(\vec{k}\right) = B - \frac{1}{\left(\kappa' + \sigma\right)\rho}\frac{dB}{ds} + \frac{\delta'}{\kappa'}. \tag{4.7}$$

In spherical symmetry,

$$\frac{dB}{ds} = \cos\theta\frac{dB}{dr} = \cos\theta\frac{dB}{dT}\frac{dT}{dr}. \tag{4.8}$$

Luminosity:

$$L\left(r\right) = \int L_\nu\ d\nu = \int \left[4\pi r^2 \int I_\nu\left(\vec{k}\right)\cos\theta d\omega\right] d\nu. \tag{4.9}$$

With $d\omega = \sin\theta d\theta d\phi$ and $\int \cos^2\theta d\omega = 4\pi/3$,

$$L(r) = -\frac{16\pi^2 r^2}{3\rho}\frac{dT}{dr}\int \frac{dB}{dT}\frac{d\nu}{(\kappa' + \sigma)}. \tag{4.10}$$

Define

$$\frac{1}{\kappa_R} = \frac{\int (dB/dT)\,(\kappa' + \sigma)^{-1}\, d\nu}{\int (dB/dT)\, d\nu}, \tag{4.11}$$

so that

$$\frac{dT}{dr} = -\frac{3\kappa_R L\rho}{16\pi acr^2 T^3}. \tag{4.12}$$

Opacity κ_R related to thermal conductivity:

$$L = -4\pi r^2 \lambda_R \frac{dT}{dr}; \quad \kappa_R = \frac{4acT^3}{3\rho\lambda_R}. \tag{4.13}$$

4.1. Convective Energy Transport

4.1.1. Schwarzschild criterion for convective instability

Consider a rising bubble. Pressure equilibrium maintained if $v < v_{sound}$. If no energy exchange with surroundings (bubble is adiabatic). Bubble exands and cools. Upward motion will continue if $T_{bubble} > T$ at new position, since perfect gas law $P = N_o\rho T/\mu$ implies $\rho_{bubble} < \rho$ at new position (μ unchanged). If locally in radiative equilibrium, this occurs if

$$\left.\frac{dT}{dr}\right|_{ad} < \left.\frac{dT}{dr}\right|_{rad} \tag{4.1.1}$$

since gradients are negative. Convective instability occurs if

$$\nabla_{ad} = \left.\frac{d\ln T}{d\ln P}\right|_{ad} < \left.\frac{d\ln T}{d\ln P}\right|_{rad} = \nabla_{rad}. \tag{4.1.2}$$

Adiabatic temperature gradient:

$$dQ = dE + PdV, \quad C_V = \left.\frac{\partial E}{\partial T}\right|_V, \quad C_P = \left.\frac{\partial E}{\partial T}\right|_P. \tag{4.1.3}$$

With $PV = N_o T$ and $V = \mu/\rho$, find $C_P = C_V + N_o$ ($k_B = 1$). Define $\gamma = C_P/C_V$. For adiabatic change $dQ = 0$

$$\left.\frac{d\ln T}{d\ln P}\right|_{ad} = \nabla_{ad} = \frac{\gamma - 1}{\gamma}. \tag{4.1.4}$$

For monatomic gas, $C_V = (3/2)N_o, C_P = (5/2)N_o, \gamma = 5/3, \nabla_{ad} = 2/5$.

Convection can occur if either C_V becomes large (*e.g.*, ionization) or $|dT/dr|_{rad}$ becomes large (*e.g.*, intense nuclear energy generation).

Instability condition rewritten:

$$\left.\frac{dT}{dr}\right|_{rad} = -\frac{3\kappa_R\rho}{4acT^3}\frac{L\left(r\right)}{4\pi r^2} > \left(1-\gamma^{-1}\right)\frac{T}{P}\frac{dP}{dr}, \tag{4.1.5}$$

$$L\left(r\right) \geq \frac{16\pi acG}{3\kappa_R}\left(1-\gamma^{-1}\right)\frac{T^4}{P}m\left(r\right). \tag{4.1.6}$$

For ideal nondegenerate gas,

$$\eta\left(r\right) \geq 0.62\frac{\mu T_6^3}{\kappa_R\rho}\frac{M}{\mathrm{M}_\odot}\frac{\mathrm{L}_\odot}{L}. \tag{4.1.7}$$

This is, for the ssm using electron scattering for the opacity at the center, $\eta_c \geq 30.6(\frac{M}{\mathrm{M}_\odot})^3(\frac{\mathrm{L}_\odot}{L})$. For the Sun, η_c is much larger than the value for H burning, 9.8. For lower masses, electron scattering is not a good approximation. For higher mass stars, η_c is smaller, while η for CNO burning is 40. Thus, stars of greater than $1.5\mathrm{M}_\odot$ have convective cores.

With convection, energy flux carried by both radiation and convection:

$$L\left(r\right) = L_{rad} + L_{conv}, \quad L_{rad} = -4\pi r^2\frac{4ac}{3\kappa_R\rho}T^3\frac{dT}{dr}. \tag{4.1.8}$$

Convecting matter has upward and downward mass flows ($\mathrm{g/cm^2/s}$): $\rho_{u,d}v_{u,d}$. Heat contents per g: $e_{u,d} = c_P T_{u,d}$. For no net mass flow, and $\rho_u = \rho_d = \rho$, one has $v_u = v_d = \bar{v}$. Net energy transport is

$$L_{conv} = 4\pi r^2\rho\bar{v}c_P\left(T_u - T_d\right) = 4\pi r^2\rho\bar{v}c_P\Delta T. \tag{4.1.9}$$

4.1.2. Mixing Length Theory

$$\Delta T = -\left(\frac{dT}{dr} - \left.\frac{dT}{dr}\right|_{ad}\right)\ell = \ell\Delta\nabla T, \quad \Delta\rho = -\left(\frac{d\rho}{dr} - \left.\frac{d\rho}{dr}\right|_{ad}\right)\ell = \ell\Delta\nabla\rho. \tag{4.1.10}$$

For perfect monatomic nondegenerate gas, since $\Delta\nabla P = 0$,

$$\Delta\nabla\rho = \frac{\rho}{T}\left(1 - \frac{d\ln\mu}{d\ln T}\right)\Delta\nabla T = Q\Delta\nabla T. \tag{4.1.11}$$

Velocity determined by buoyancy force per unit volume: $F = g\Delta\rho$ with $g = Gm/r^2$ the local gravity. Net acceleration per gram is F/ρ.

$$\frac{v^2}{2} = \int_0^\ell \frac{F}{\rho}d\ell = gQ\frac{\Delta\nabla T}{T}\frac{\ell^2}{2}. \tag{4.1.12}$$

$$\bar{v} = \frac{v}{2} = \frac{\ell}{2}\sqrt{\frac{gQ\Delta\nabla T}{T}}. \tag{4.1.13}$$

$$L_{conv} = 4\pi r^2 \rho c_P \sqrt{\frac{gQ}{T}} \left(\Delta\nabla T\right)^{3/2} \frac{\ell^2}{2}. \tag{4.1.14}$$

Choice of ℓ:

$$\ell \approx \frac{dr}{d\ln P} = \frac{N_o T}{g\mu} \simeq \frac{T\left(r\right)}{\mathrm{T}_\odot} \frac{\mathrm{M}_\odot}{m\left(r\right)} \left(\frac{r}{\mathrm{R}_\odot}\right)^2 \mathrm{R}_\odot. \tag{4.1.15}$$

In interior, $\ell \approx \mathrm{R}_\odot/10$. The constraint that $L_{conv} < L$ implies

$$\Delta\nabla T < \left(\frac{4Gr}{15\ell^2 N_o k_B}\right)^{2/3} \left(\frac{T}{g}\right)^{1/3}. \tag{4.1.16}$$

For the interior of the ssm, this is

$$\Delta\nabla T < 4 \cdot 10^{-16} \ \mathrm{K\ cm^{-1}} << |dT/dr|; \tag{4.1.17}$$

when convection occurs, the temperature gradient is effectively adiabatic.

Chapter 5.
Nuclei and Nuclear Matter

5.1. Nuclear energies: The Liquid Drop Model

Nuclei have internal baryon densities $n \simeq n_s = 0.16$ fm^{-3}, corresponding to mass densities $\rho_s = n_s m_n \simeq 2.7 \cdot 10^{14}$ g cm^{-3}. They also have roughly equal numbers of neutrons and protons: $x = Z/A \simeq 1/2$.

$$E(Z,N) = E_{bulk}A + E_{surf}A^{2/3} + E_{Coul}A^{5/3} + \cdots$$

$$E_{bulk} \simeq -16 + \frac{K}{18}\left(1 - \frac{n}{n_s}\right)^2 + S_V(1-2x)^2 + \cdots$$

$K \approx 240$ MeV is incompressibility parameter, $S_V \approx 30n/n_s$ MeV is volume symmetry parameter.

$$E_{surf} \simeq 18 - S_S(1-2x)^2 \ \text{ MeV},$$

where $S_S \simeq 45$ MeV is the surface symmetry parameter.

$$E_{Coul} = \frac{3}{5}\frac{x^2e^2}{r_0} \simeq 0.75x^2 \ \text{ MeV},$$

where $r_0 = (4\pi n_s/3)^{-1/3} \simeq 1.12$ fm.

Consider an infinite nucleus. Saturation density is where energy per particle for a given composition is minimized:

$$\left.\frac{\partial E_{bulk}}{\partial n}\right|_x = \frac{P_{bulk}}{n^2} = 0.$$

This occurs where pressure vanishes, or $n = n_s$ if $x = 1/2$. If $x \neq 1/2$, then

$$\frac{P_{bulk}}{n^2} = -\frac{K}{9n_s}\left(1 - \frac{n}{n_s}\right) + \frac{\partial S_V}{\partial n}(1-2x)^2,$$

$$\frac{n}{n_s} \simeq 1 - \left.\frac{9nS_V'(1-2x)^2}{K}\right|_{n_s} \simeq 1 - 1.1(1-2x)^2.$$

Optimize energy per particle with respect to composition:

$$\left.\frac{\partial E_{bulk}}{\partial x}\right|_n = -(\mu_n - \mu_p) = -4S_V(1-2x) = 0,$$

that is, $x = 1/2$ for all n. However, we've neglected electrons. Optimum composition determined by:

$$\mu_n - \mu_p = \mu_e, \quad 4S_V(1-2x) = \hbar c\left(3\pi^2 n x\right)^{1/3}.$$

S_V is assumed to be $S_0 n/n_s$, so as $n \to 0$, $x \to 0$. But for $n \to \infty$,

$$n = \left(3\pi^2 x\right)^{2/3} \left(\frac{\hbar c n_s}{4S_0\left(1-2x\right)}\right)^{3/2}$$

where $S_0 = 30$ MeV. Thus $x \to 1/2$ in this limit. When $n = n_s, x \approx 0.04$.

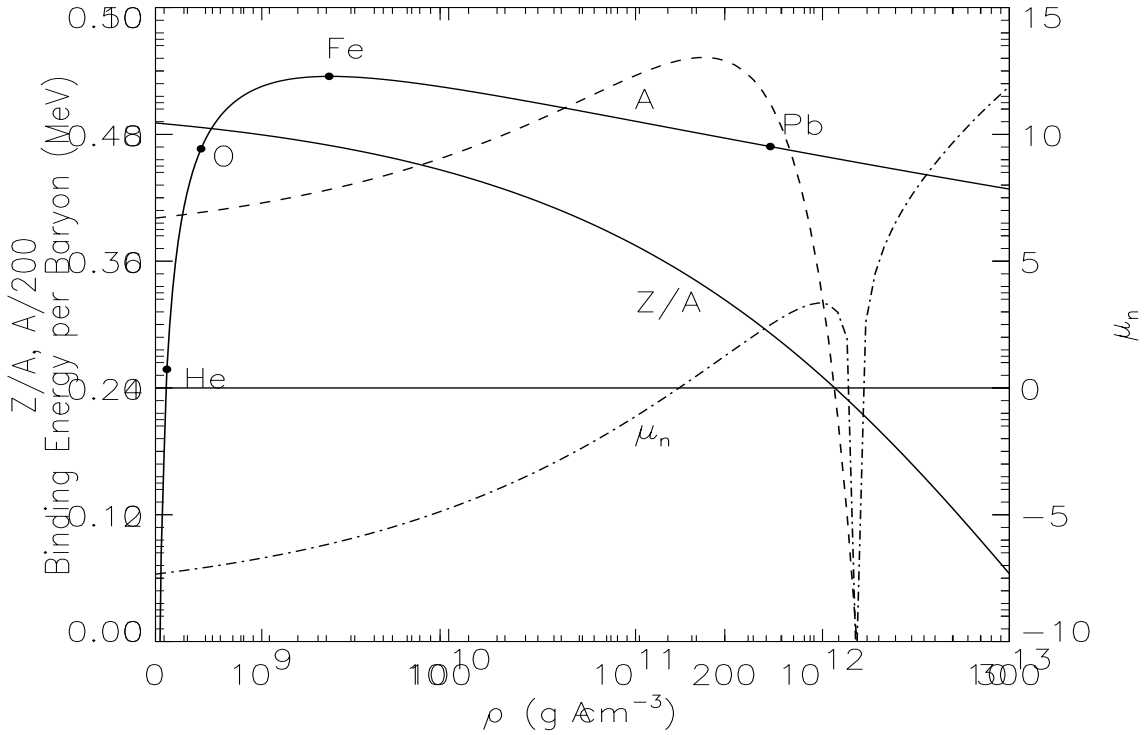

A finite nucleus has an optimum mass, for a given x:

$$\left.\frac{\partial E/A}{\partial A}\right|_x = -\frac{E_{surf}}{3A^{4/3}} + \frac{2E_{Coul}}{3A^{1/3}} = 0.$$

This becomes $E_{surf}A^{2/3} = 2E_{Coul}A^{5/3}$, the so-called *Nuclear Virial Theorem*. So

$$A_{opt} = E_{surf}/\left(2E_{Coul}\right). \tag{5.1.1}$$

This increases with decreasing x near $1/2$ roughly as x^{-2}. For $x = 1/2$, $A_{opt} = 18/.375 \simeq 48$. A nucleus also has an optimum charge, for a given A:

$$\left.\frac{\partial E/A}{\partial x}\right|_A = -4\left(S_V - S_S A^{-1/3}\right)\left(1-2x\right) + 2E_{Coul}A^{2/3}/x = 0,$$

$$x_{opt} = \left[2 + \frac{0.75A^{2/3}}{2\left(S_V - S_S A^{-1/3}\right)}\right]^{-1}. \tag{5.1.2}$$

This path represents the Valley of Beta Stability in the Chart of the Nuclides. If there was no Coulomb energy, or the mass is very small, then $x_{opt} = 1/2$. For larger masses,

x_{opt} decreases from 1/2. The simultaneous solution of Eqs. (5.1.1) and (5.1.2) yields $x_{opt} \simeq 0.432$, $A_{opt} \simeq 61$, $Z_{opt} \simeq 26$, or ^{61}Fe. Along the Valley of Beta Stability, the nuclear energy is

$$\begin{aligned} E/A &= -16 + 18A^{-1/3} + 0.375 x_{opt} A^{2/3} \\ &= -16 + 18A^{-1/3} + \left[\frac{16}{3A^{2/3}} + \frac{1}{S_V - S_S A^{-1/3}}\right]^{-1} . \end{aligned}$$

This rises steeply with A to the maximum, then decreases relatively slowly beyond the maximum.

The binding energies of ^{4}He and ^{56}Fe, per baryon, are about 7.1 and 8.9 MeV, respectively, relative to individual neutrons and protons. The nuclear energy release in H burning is far greater than the energy released in all subsequent burning stages, which end in Fe formation.

Behavior of Nuclei at High Density

We treated nuclei in isolation. By the end of stellar evolution in massive stars, $\rho \simeq 10^7$ g cm^{-3}. The filling factor of nuclei is $u \simeq \rho/\rho_s \simeq 3.7 \cdot 10^{-8}$, so the distance between nuclei is about $2u^{-1/3} \approx 600$ nuclear radii. This is large enough that the effective nuclear Coulomb energy is diminished because of electron screening. For uniformly distributed electrons, the Coulomb energy becomes:

$$E_{Coul} = \frac{3}{5}\frac{x^2 e^2}{r_0}\left(1 - \frac{3}{2}u^{1/3} + \frac{u}{2}\right).$$

Therefore, at high densities, the average nuclear size increases as $(1 - \frac{3}{2}u^{1/3} + u/2)^{-1/3}$. However, decreasing proton fractions in nuclei lead to:

5.2. Neutron Drip

The energies of the *last* neutron and proton in nuclei are μ_n and μ_p:

$$\mu_n = \left.\frac{\partial E_{nuc}}{\partial N}\right|_Z = \frac{E_{nuc}}{A} - \frac{Z}{A}\left.\frac{\partial\left(E_{nuc}/A\right)}{\partial\left(Z/A\right)}\right|_A$$

$$\mu_p = \left.\frac{\partial E_{nuc}}{\partial Z}\right|_N = \frac{E_{nuc}}{A} + \left(1 - \frac{Z}{A}\right)\left.\frac{\partial\left(E_{nuc}/A\right)}{\partial\left(Z/A\right)}\right|_A .$$

So

$$\begin{aligned} \mu_n &= -16 + 18A^{2/3} + \left(S_V - S_S A^{-1/3}\right)\left(1 - 4x^2\right) - E_{Coul}A^{2/3}, \\ \mu_p &= -16 + 18A^{2/3} + \left(S_V - S_S A^{-1/3}\right)(1-x)(2x-3) + \frac{(2-x)}{x}E_{Coul}A^{2/3}. \end{aligned}$$

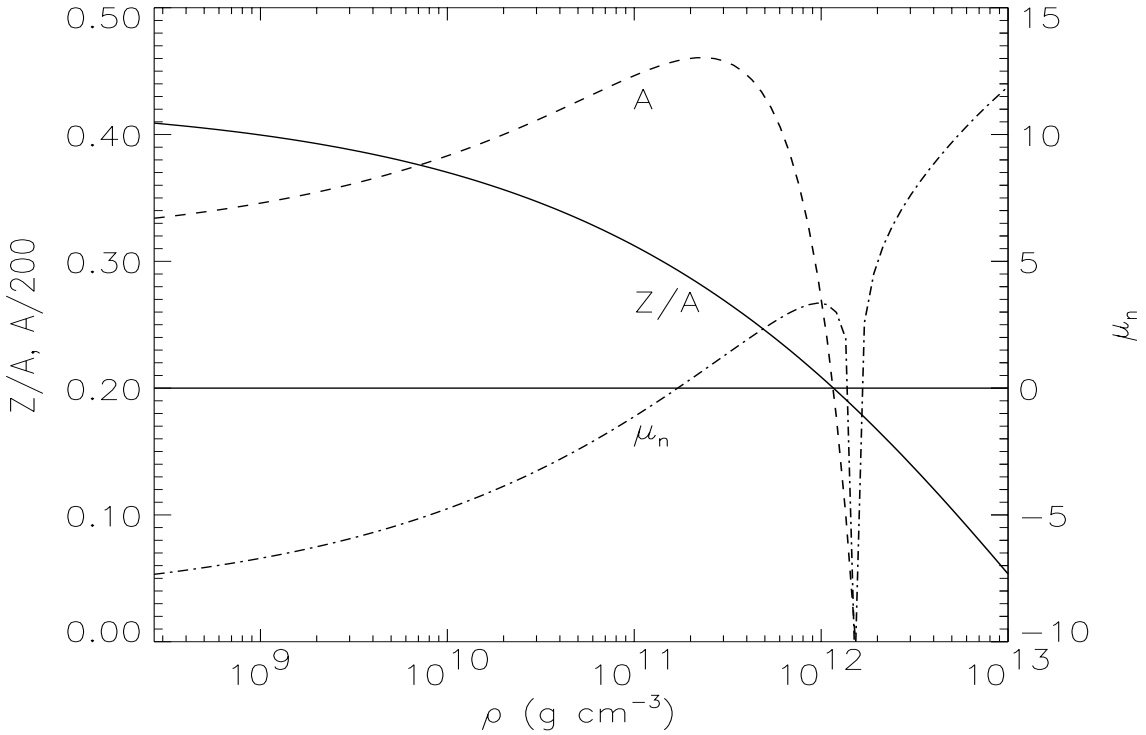

When μ_n is positive, neutrons exist outside the nuclei. In this case, the relation $u = n/n_s$ is modified to $u = (n - n_n)/n_s$. The curves in the figure have a singularity at $Z/A \simeq 0.18$ where E_{surf} vanishes, due to its oversimplified representation.

Chapter 6.
Thermonuclear Reactions

6.1. Non-resonant Reaction Rates

Schrödinger equation:

$$-\frac{\hbar^2}{2\mu}\nabla^2\Psi + V(r)\Psi = E\Psi.$$

$\mu = m_1 m_2/(m_1+m_2)$,

$$V(r) = \begin{array}{ll} Z_1 Z_2 e^2/r & r > R \\ -V_0 & r < R \end{array}$$

$$\Psi = \frac{\chi_\ell(r)}{r} Y_\ell^m(\theta,\phi)$$

Assume radial symmetry, ignore angular parts.

$$-\frac{\hbar^2}{2\mu}\chi_\ell'' + \left[\frac{\ell(\ell+1)\hbar^2}{2\mu r^2} + V(r) - E\right]\chi_\ell(r) = -\frac{\hbar^2}{2\mu}\chi_\ell'' + f(r)\chi_\ell(r) = 0.$$

$$f(r) \quad \begin{array}{ll} < 0 & r > R_0 \\ > 0 & r < R_0 \end{array},$$

$$E = \frac{Z_1 Z_2 e^2}{R_0} + \frac{\ell(\ell+1)\hbar^2}{2\mu R_0^2}.$$

$$\chi_\ell(r) = A\mathrm{e}^{i\phi(r)/\hbar},$$

$$i\hbar\phi'' - \left(\phi'\right)^2 + f = 0.$$

Lowest order approximation: Neglect ϕ'':

$$\phi(r) \simeq \pm\sqrt{2\mu}\int_R^r \sqrt{E - V(r')}dr',$$

which is valid for $r >> R_0$ or $r << R_0$. The integrand is real for $r > R_0$ and imaginary for $r < R_0$. The constant A is set by normalization, so $\chi^*(r)\chi(r)$ gives the probability per unit radial distance that incoming nucleus is at r. The penetration factor $P_\ell(E,r)$ is then

$$P_\ell(E,r) = \frac{\chi^*(R)\chi(R)}{\chi^*(r)\chi(r)} \propto \exp\left(-2\int_R^r \sqrt{-\frac{2\mu}{\hbar^2}f(r')}dr'\right).$$

Setting $R \approx 0$, $r \approx R_0$ (the solution oscillates for $r > R_0$), and for the case $\ell = 0$, the argument of the exponential is

$$-2\int_0^{R_0}\sqrt{-\frac{2\mu}{\hbar^2}f\left(r'\right)}dr' = \frac{\sqrt{2\mu E}}{\hbar}\frac{Z_1 Z_2 e^2}{E}\frac{\pi}{2} = \pi\frac{Z_1 Z_2 e^2}{\hbar v},$$

using $v^2 = 2E/\mu$. This forms the *Gamow factor*.

6.2. Cross Section and Reaction Rate

(Reactions/s)/(Incident Flux), units of area.

Number of reactions per unit volume per unit time at a given energy is

$$r = n_1 n_2 v\sigma\left(v\right)/\left(1+\delta_{1,2}\right).$$

But number densities of nuclei n_1, n_2 depend on energy (relative velocity v), so

$$r = \int n_1\left(v\right) n_2\left(v\right) v\sigma\left(v\right) d^3v.$$

Maxwellian distributions:

$$n_1\left(v_1\right) = n_1\left(\frac{m_1}{2\pi kT}\right)^{3/2}\mathrm{e}^{-\frac{m_1 v_1^2}{2kT}}d^3v_1.$$

Note that

$$\int_0^\infty n_1\left(v_1\right)d^3v_1 \equiv n_1.$$

The relative velocity v and the center-of-mass velocity V are:

$$v_1 = V - \frac{m_2}{m_1+m_2}v, \qquad v_2 = V + \frac{m_1}{m_1+m_2}v.$$

$$n_1\left(v_1\right)d^3v_1\ \ n_2\left(v_2\right)d^3v_2 =$$
$$n_1 n_2\left[\left(\frac{m_1+m_2}{2\pi kT}\right)^{3/2}\mathrm{e}^{-\frac{(m_1+m_2)V^2}{2kT}}d^3V\right]\left[\left(\frac{\mu}{2\pi kT}\right)^{3/2}\mathrm{e}^{-\frac{\mu v^2}{2kT}}d^3v\right].$$

First bracket is unity, and

$$\begin{aligned} r =& \frac{n_1 n_2}{1+\delta_{1,2}}\int_0^\infty v\sigma\left(v\right)\left(\frac{\mu}{2\pi kT}\right)^{3/2}\mathrm{e}^{-\frac{\mu v^2}{2kT}}d^3v \\ =& \frac{n_1 n_2}{1+\delta_{1,2}}\sqrt{\frac{8}{\mu\pi kT}}\int_0^\infty\frac{E\sigma\left(E\right)}{kT}\mathrm{e}^{-\frac{E}{kT}}dE. \end{aligned}$$

The Gamow factor is most significant part of nuclear cross sections. Also, since maximum quantum mechanical geometrical cross section $\propto \lambda^2 \propto 1/E$, it is convenient to write

$$\sigma\left(E\right) = \frac{S\left(E\right)}{E}\mathrm{e}^{-b/\sqrt{E}},$$

where $S(E)$ is slowly varying. For $\ell = 0$, $A = \mu/m_b$,

$$b = \frac{\pi\sqrt{2\mu}Z_1Z_2}{\hbar} = 31.3Z_1Z_2\sqrt{A}\ \text{keV}^{1/2}.$$

$$\begin{aligned} r =& \frac{n_1n_2}{1+\delta_{1,2}}\sqrt{\frac{8}{\mu\pi kT}}\frac{1}{kT}\int_0^\infty S\left(E\right)\mathrm{e}^{-E/kT-b/\sqrt{E}}dE \\ =& \frac{n_1n_2}{1+\delta_{1,2}}\sqrt{\frac{8}{\mu\pi kT}}\frac{1}{kT}\mathrm{e}^{-3E_0/kT}S\left(E_0\right)\int_0^\infty \exp\left(-\left[\frac{E-E_0}{\Delta/2}\right]^2\right)dE \\ =& \frac{n_1n_2}{1+\delta_{1,2}}\sqrt{\frac{2}{\mu\pi kT}}\frac{\Delta}{kT}\mathrm{e}^{-3E_0/kT}S\left(E_0\right). \end{aligned}$$

Here we approximated the integrand as a Gaussian with centroid

$$E_0 = \left(\frac{bkT}{2}\right)^{2/3} = 1.22\left(Z_1^2Z_2^2AT_6^2\right)^{1/3}\ \text{keV}$$

and width

$$\Delta = 4\sqrt{\frac{E_0kT}{3}} = 0.75\left(Z_1^2Z_2^2AT_6^5\right)^{1/6}\ \text{keV}.$$

Define

$$\tau = \frac{3E_0}{kT} = 42.5\left(\frac{Z_1^2Z_2^2A}{T_6}\right)^{1/3}$$

one has $\Delta = 4\sqrt{\tau}kT/3$ and

$$\begin{aligned} r =& \frac{n_1n_2}{1+\delta_{1,2}}\frac{2}{3\mu}\frac{\tau^2}{9b}S\left(E_0\right)\mathrm{e}^{-\tau} \\ =& 4.5\cdot10^{14}\frac{n_1n_2}{1+\delta_{1,2}}\frac{S\left(E_0\right)}{AZ_1Z_2}\tau^2\mathrm{e}^{-\tau}. \end{aligned}$$

6.3. Electron Screening

Modified Coulomb potential because of electron screening:

$$\frac{Z_1e}{r}\mathrm{e}^{-r/\lambda_D} \approx \frac{Z_1e}{r} - \frac{Z_1e}{\lambda_D}$$

with λ_D the Debye length

$$\lambda_D = \sqrt{\frac{kT}{4\pi\left(Z_1+1\right)e^2n_e}} \simeq 9.2\cdot10^{-9}\sqrt{\frac{T_6}{\rho Y_e\left(Z_1+1\right)}}\ \text{cm}.$$

Then reaction rate increased by

$$\exp\left(\frac{Z_1Z_2e^2}{kT\lambda_D}\right) \simeq \exp\left(0.17Z_1Z_2\sqrt{\frac{\rho Y_e\left(Z_1+1\right)}{T_6^3}}\right).$$

6.4. Effective Thermonuclear Rate

:

Near a temperature T_0, one can write $r = r_0(T/T_0)^n$, where

$$n = \left.\frac{d\ln r}{d\ln T}\right|_{T_0} = \left.\frac{d\ln\tau}{d\ln T}\frac{d\ln r}{d\ln\tau}\right|_{T_0} = \left.\frac{\tau-2}{3}\right|_{T_0}.$$

6.5. Nuclear Reactions and Resonances

Consider the reaction

$$a + X \to Z^* \to Y + b \qquad \text{or} \qquad (X\,(a,b)\,Y)$$

with a the projectile, X the target and b and Y the products. Z^* is an intermediary stage, the compound nucleus. Often there are many b, Y possibilities, and each has a probability of occuring, $\mathcal{P}_i = \tau/\tau_i$ where τ_i is the mean-life for reaction i and $\tau = [\sum \tau_i^{-1}]^{-1}$. Among the exit channels is the one in which b, Y=a, X which represents scattering.

Energy width Γ_i defined through the uncertainty principle,

$$\Gamma_i\tau_i = \hbar, \qquad \Gamma = \sum \Gamma_i.$$

The cross section can be written as

$$\sigma_{ab}\,(E) = \pi\left(\frac{\lambda}{2\pi}\right)^2 g\frac{\Gamma_a\Gamma_b}{\Gamma^2} f\,(E)$$

where

$$\pi\left(\frac{\lambda}{2\pi}\right)^2 = \frac{\pi\hbar^2}{2Em_b} = \frac{0.657\ \text{MeV}}{E}\frac{1}{\mu}\ \text{barns}$$

with 1 barn=10^{-24} cm^2. g is a spin-dependent factor. The so-called "maximum cross section" is geometrical. A particle a with linear momentum p approaching X with impact parameter b has a quantized angular momentum $bp = \ell\hbar$. Then the fractional cross section of the ring defined by ℓ and $\ell+1$ is $\pi(\lambda/2\pi)^2(2\ell+1)$ where $(\lambda/2\pi) = \hbar/p$.

The shape factor $f(E)$ is controlled by whether the reaction is resonant or non-resonant. For non-resonant reactions,

$$\sigma_{ab}\,(E) = \frac{S\,(E)}{E}e^{-b/\sqrt{E}}.$$

For resonant reactions, we have the Breit-Wigner formula

$$f\,(E) = \frac{\Gamma^2}{(E-E_r)^2 + (\Gamma/2)^2},$$

which is sharply peaked near the resonance energy E_r. Supposing that Γ doesn't vary much within the energy $\Gamma/2$ of E, and that f is sharply peaked, we can write the Maxwellian

average of the cross section and velocity as

$$\begin{aligned} < \sigma_{ab} v > &= \frac{\pi\hbar^2 g}{2m}\sqrt{\frac{8}{\mu m_b}}\,(kT)^{-3/2}\,e^{-E_r/kT}\int_0^\infty \frac{\Gamma_a\Gamma_b dE}{(E-E_r)^2+(\Gamma/2)^2} \\ &= \hbar^2\left(\frac{2\pi}{m_b kT}\right)^{3/2} g\frac{\Gamma_a\Gamma_b}{\Gamma}e^{-E_r/kT} \\ &= 2.56\times 10^{-13}\frac{(\omega\gamma)_r}{(\mu T_9)^{3/2}}e^{-11.605E_r/T_9}\ \text{cm}^3\ \text{s}^{-1}. \end{aligned}$$

Here we've used

$$\int_0^\infty \sigma_{ab}(E)\,dE = \frac{\hbar^2\pi^2}{mE_r}\left[g\frac{\Gamma_a\Gamma_b}{\Gamma}\right] = \frac{\hbar^2\pi^2}{mE_r}(\omega\gamma)_r\,.$$

This is useful since a poor resolution experiment only yields an integrated cross section. E_r and $(\omega\gamma)_r$ are in MeV. Note that near a temperature T_9 the effective temperature exponent for a resonant rate is

$$n = \frac{11.605E_r}{T_9} - \frac{3}{2}.$$

6.6. Weak Interaction Rates

Fermi's Golden Rule #2:

$$\Gamma = \frac{2\pi}{\hbar}|H_{mi}|^2\rho.$$

Here H_{mi} is the perturbed part of the time-dependent Hamiltonian and ρ is the density of final states. The Fermi theory of weak interactions for the reaction $n \to p + e + \bar{\nu}$ has

$$H_{mi} = G_F\int \psi_p^*\psi_e^*\psi_{\bar{\nu}}^*\psi_n d^3r.$$

The wave functions of the electron and antineutrino are plane waves with de Broglie wavlengths much greater than the nucleon dimension, so $\psi_e\psi_{\bar{\nu}} \approx 1$. We have

$$H_{pn} = G_F\int \psi_p^*\psi_n d^3r.$$

The overlap integral is nearly unity for nucleon decay, but can be much less than one for other weak interactions, and zero for one in which β decay is not allowed. Here $G_F \simeq 1.4\times 10^{-49}$ erg cm^3. The density of final states results in the transition rate

$$d\Gamma = \frac{2\pi}{\hbar}M^2\rho_e\rho_{\bar{\nu}}\delta\left(E_e + E_{\bar{\nu}} - E_n + E_p\right)dE_e dE_{\bar{\nu}},$$

where $M^2 = \sum_{spin}|H_{pn}|^2/2$. Integrating over $E_{\bar{\nu}}$,

$$d\Gamma = \frac{2\pi}{\hbar}M^2\rho_e\rho_{\bar{\nu}}dE_e.$$

Neglecting spin, the density of electron and antineutrino states:

$$\rho_e = \frac{4\pi p_e^2}{h^3}\frac{dp_e}{dE_e} = \frac{4\pi p_e E_e}{c^2 h^3}, \qquad \rho_{\bar{\nu}} = \frac{4\pi \left(E_n - E_p - E_e\right)^2}{h^3 c^3}.$$

Thus

$$d\Gamma = \frac{64\pi^4 G_F^2 M^2}{h^7} m_e^5 c^4 \sqrt{\epsilon^2 - 1}\epsilon \left(\epsilon_0 - \epsilon\right)^2 d\epsilon,$$

where

$$\epsilon = \frac{E_e}{m_e c^2}, \qquad \epsilon_0 = \frac{E_n - E_p}{m_e c^2}.$$

For neutron decay, $E_n - E_p \approx (m_n - m_p)c^2 = 1.297$ MeV and $\epsilon_0 \approx 2.53$. The integration over energy yields

$$\begin{aligned} f\left(\epsilon_0\right) =& \int_1^{\epsilon_0} \sqrt{\epsilon^2 - 1}\epsilon \left(\epsilon_0 - \epsilon\right)^2 d\epsilon \\ =& \sqrt{\epsilon_0^2 - 1}\left(\frac{\epsilon_0^4}{30} - \frac{3\epsilon_0^2}{20} - \frac{2}{15}\right) + \frac{\epsilon_0}{4}\ln\left[\epsilon_0 + \sqrt{\epsilon_0^2 - 1}\right], \end{aligned}$$

which is 1.64 for neutron decay. The cross section is $\sigma = \Gamma/v$.

For the proton-proton reaction, $\epsilon_0 = (2m_p - m_D)/m_e \simeq 2.33$. The cross section also involves the Coulomb barrier penetration, and M^2 is not unity:

$$\begin{aligned} \sigma_{pp} =& P\left(E\right)\sigma = \frac{2\pi e^2 \sigma}{\hbar v} e^{-2\pi e^2/\hbar v} \\ \sigma \simeq& 4 \times 10^{-49} \ \text{cm}^2. \end{aligned}$$

Chapter 7.
Advanced Evolutionary Stages

Beyond helium burning, stellar evolution becomes increasingly dominated by neutrino processes: thermal pair creation and electron captures on protons in nuclei:

$$\begin{aligned} e^+ + e^- &\rightarrow \nu_e + \bar{\nu}_e \\ e^- + A_Z^N &\rightarrow \nu_e + A_{Z-1}^{N+1}. \end{aligned} \tag{7.1}$$

Temperatures and lifetimes of burning stages are determined by equilibrium between nuclear and neutrino rates.

Neutrino pair energy generation rate:

$$\dot{\epsilon}_{\nu\bar{\nu}} = n_{e^+} n_{e^-} \langle \sigma v E \rangle \tag{7.2}$$

where E is the total energy of the pair and the average is with respect to the $e^- - e^+$ velocity distribution. The annihilation cross section σ is of order G_F^2, proportional to energy squared, and the relevant velocity is c:

$$\sigma v = 1.42 \times 10^{-45} c \left[\left(\frac{w}{m_e c^2} \right)^2 - 1 \right] \ \text{cm}^2, \tag{7.3}$$

where w is the center of momentum total energy. General result is complicated, but simplifies in NDNR and NDR limits.

NDNR ($T_9 < 1$). Recall that

$$n_{e^+} n_{e^-} = 2.3 \times 10^{58} T_9^3 e^{-11.9/T_9} \ \text{cm}^{-6}. \tag{7.4}$$

Also, in the non-relativistic case $w \simeq E \simeq 2 m_e c^2$. Thus

$$\dot{\epsilon}_{\nu\bar{\nu}} = 4.9 \times 10^{18} T_9^3 e^{-11.9/T_9} \ \text{erg cm}^{-3} \ \text{s}^{-1}. \tag{7.5}$$

NDER ($T_9 > 3$). $e^- - e^+$ pairs are slightly degenerate even at high T. For $\mu_e \rightarrow 0$,

$$n_+ n_- = \frac{1}{\pi^4} \left(\frac{T}{\hbar c} \right)^6 F_2^2 (0) \simeq 2.3 \times 10^{56} T_9^6 \ \text{cm}^{-6}. \tag{7.6}$$

The average energy is $w \simeq 2[F_3(0)/F_2(0)]T$.

$$\dot{\epsilon}_{\nu\bar{\nu}} = 8.74 \times 10^{15} T_9^9 \ \text{erg cm}^{-3} \ \text{s}^{-1}. \tag{7.7}$$

More accurate calculations gives 5.2 instead of 8.74.

7.1. Electron capture rates

Depend sensitively on the Q-value (capture on free protons $\propto \Delta^5$, on heavy nuclei $\propto \Delta^{3-4}$, where $\Delta = \mu_e - \mu_n + \mu_p$ is available energy. For C or Ne burning, $\mu_e \simeq \mu_n - \mu_p$ and the matter is in beta equilibrium. But for Si burning and beyond, beta equilibrium is not maintained, $\Delta > 0$, and electron capture increases. Although ^{56}Fe has $Z/A \simeq 0.464$, $\langle Z/A \rangle = Y_e \simeq 0.42$ after Si burning. Because of thermal excitations, inverse processes (positron capture) can also proceed on some nuclei:

$$\begin{aligned} e^- + A_Z^N &\rightarrow \nu_e + A_{Z-1}^{N+1}, \\ e^+ + A_{Z-1}^{N+1} &\rightarrow \bar{\nu}_e + A_Z^N. \end{aligned} \tag{7.1.1}$$

This cyclic process occurs in spite of the fact that the available energy for one of the reactions is formally negative, because some of those nuclei are in excited states at finite temperature. The neutrino production rate from these so-called URCA processes is proportional to T^5, but their importance has to be considered on a case-by-case basis. Gamow named these processes URCA from a casino in Rio: you always lose (it also seems the name is similar to a Russian word for thief). For our purposes, it is sufficient to ignore electron capture and URCA processes until gravitational collapse itself sets in.

In general, there is a well defined sequence of stellar burning stages leading to an "onionskin-like" layering. T and the duration of the burning are found by equilibrium between neutrino and nuclear rates.

7.2. C burning

$$\dot{\epsilon}_C \sim 7 \times 10^4 \left(\frac{X_C}{0.2}\right) \rho^2 T_9^{27} \text{ erg cm}^{-3}\text{s}^{-1} \tag{7.2.1}$$

near $T_9 \sim 1$, where X_C is the C mass fraction. (Note that this rate is still uncertain to perhaps a factor of 2 or 3.) Equating Eqs. (7.2.1) and (7.5):

$$\rho^2 \left(\frac{X_C}{0.2}\right) T_9^{24} e^{11.9/T_9} \simeq 7 \times 10^{13} \text{ g}^2\text{cm}^{-6}. \tag{7.2.2}$$

For $\rho \simeq 10^5$ g cm^{-3}, $T_9 \simeq 0.74$. This is an underestimate because of the extreme temperature sensitivity of the rates. Consider instead the total emission from a rate

$$\dot{\epsilon} = \dot{\epsilon}_o \left(\frac{\rho}{\rho_o}\right)^\lambda \left(\frac{T}{T_o}\right)^\nu \tag{7.2.3}$$

near ρ_o and T$_o$. In Lane-Emden variables, $\dot{\epsilon} = \dot{\epsilon}_o \theta^{n\lambda+\nu}$ and

$$\langle \dot{\epsilon} \rangle = \dot{\epsilon}_o \int_0^{\xi_1} \theta^{n\lambda+\nu} \xi^2 d\xi \Big/ \int_0^{\xi_1} \xi^2 d\xi. \tag{7.2.4}$$

n is the polytropic index. If $n\lambda + \nu >> 1$, the integrand is sharply peaked at the origin. Approximating $\theta \simeq e^{-\xi^2/6}$ (valid for all n) and extending the numerator's integral to ∞:

$$\langle \dot{\epsilon} \rangle = \frac{3\dot{\epsilon}_o}{\xi_1^2} \frac{\sqrt{27\pi/2}}{(n\lambda + \nu)^{3/2}}. \tag{7.2.5}$$

Assuming the core structure of massive stars is approximated by an $n = 3$ polytrope, the right hand side of Eq. (7.2.2) should be multiplied by $[(3\lambda + \nu)_C/(3\lambda + \nu)_\nu]^{3/2}$. We have $\lambda_C = 2, \nu_C = 27$, and for $T_9 \simeq 0.8$ $\lambda_\nu = 0, \nu_\nu = 3 + 11.9/.8 \simeq 18$. Thus the ratio is $(33/19)^{3/2} \simeq 2.5$ and the solution of Eq. (7.2.2) gives $T_9 = 0.82$.

The C burning duration is

$$\tau = \frac{\rho \Delta B}{\dot{\epsilon}_{nuc}} X_c \tag{7.2.6}$$

where $\Delta B = 4 \times 10^{17}$ erg g^{-1} is the specific energy released in C burning. Thus

$$\tau \simeq 10/T_9^{27} \text{ yr} \simeq 2100 \text{ yr}, \tag{7.2.7}$$

which is about 7 times too large compared to detailed calculations.

Following C burning are the Ne, O and Si burning stages. For the first two, $3 > T_9 > 1$ and neither the ER or NR limits apply. But the ER rate Eq. (7.7) is closer.

7.3. Ne burning

This is a nuclear rearrangement 2Ne$\rightarrow$ O + Mg. For $X_O = 0.7$

$$\begin{aligned} \dot{\epsilon} &\sim 2 \times 10^{24} \rho \left(\frac{X_{Ne}}{0.2} \right) T_9^{12} e^{-54.9/T_9} \text{ erg cm}^{-3} \text{ s}^{-1} \\ \Delta B &\simeq 1.1 \times 10^{17} \text{ erg g}^{-1}. \end{aligned} \tag{7.3.1}$$

Note the single power of density, since this is a photodisintegration reaction. From Eq. (7.7), $\lambda_\nu = 0, \nu_\nu = 9$, and $\lambda_{Ne} = 1, \nu_{Ne} = 54.9/T_9 + 12$. We thus find the implicit equation for T_9:

$$3.8 \times 10^8 \rho T_9^3 e^{-54.9/T_9} \left(\frac{15 + 54.9/T_9}{9} \right)^{3/2} = 1, \tag{7.3.2}$$

which gives $T_9 \simeq 1.4$ if $\rho = 2 \times 10^5$ g cm^{-3}. The neon burning duration is about 17 yr, but will be increased by convective mixing.

7.4. O burning

$2O^{16} \rightarrow {}^{28}Si + He$ or ^{32} S via a large number of secondary reactions. In this stage almost all nuclei heavier than Fe photodisintegrate into Fe peak nuclei, and a general increase of the neutron excess $(N-Z)/A \simeq 0.01$ occurs. A good approximation for the energy generation is 2O→S

$$\dot{\epsilon} \sim 10^{-5} X_O^2 \rho^2 T_9^{33} \text{ erg cm}^{-3} \text{ s}^{-1}, \quad \Delta B \simeq 5 \times 10^{17} \text{ erg g}^{-1}. \tag{7.4.1}$$

Using $X_O \simeq 0.7, \rho \simeq 2 \times 10^6$ g cm^{-3} we find

$$3.8 \times 10^{-9} T_9^{24} (39/9)^{3/2} = 1 \tag{7.4.2}$$

or $T_9 \simeq 2.0$. The indicated lifetime is about 2 months.

7.5. Si burning

Essentially photodisintegraton rearrangement into Fe-peak nuclei. Si fusions are prohibited by the high Coulomb barrier. α particles released by photodisintegrations are added to heavy nuclei, pushing the distribution toward the optimum binding state, or nuclear statistical equilibrium. Only the density, temperature and neutron excess or Y_e are needed to find nuclear abundances (if binding energies and partition functions are known). Energy generation is

$$\begin{aligned} \dot{\epsilon} \sim & 4 \times 10^{27} X_{Si} \rho T_9^{6.5} e^{-142.1/T_9} \\ \simeq & 3.2 \times 10^{13} X_{Si} \rho \left(\frac{T_9}{3.5}\right)^{47} \text{ erg cm}^{-3}\text{s}^{-1}, \\ \Delta B \simeq & 1.9 \times 10^{17} \text{ erg g}^{-1} \end{aligned} \tag{7.5.1}$$

near $T_9 = 3.5$. The implicit T equation is

$$7.8 \times 10^{-8} X_{Si} \rho \left(\frac{T_9}{3.5}\right)^{38} \left(\frac{50}{9}\right)^{3/2} = 1 \tag{7.5.2}$$

or $T_9 \simeq 3.3$ if $\rho \simeq 10^7$ g cm^{-3}. The indicated lifetime is about 1.5 days.

7.6. Nuclear Statistical Equilibrium

The free energy per baryon of a nucleus (Z, A) is

$$F(Z,A) = B(Z,A) + \frac{T}{A}\left(\ln\left[\left(\frac{2\pi\hbar^2}{mAT}\right)^{3/2} \frac{n(Z,A)}{G(Z,A)}\right] - 1\right) \tag{7.6.1}$$

where $B(Z,A)$, $G(Z,A)$, and $n(Z,A)$ are the binding energy per particle, partition function, and number density of the nucleus, respectively. Nuclei and nucleons are treated as non-degenerate and non- interacting. The baryon mass is m. The total free energy density is then

$$f = \sum_{Z,A} F\left(Z,A\right) n\left(Z,A\right). \tag{7.6.2}$$

Two constraints, mass and charge conservation:

$$\sum_{Z,A} An\left(Z,A\right) = n \qquad \sum_{Z,A} Zn\left(Z,A\right) = nY_e. \tag{7.6.3}$$

Minimizing f with respect to each $n(Z,A)$, subject to these constraints, gives

$$F\left(Z,A\right) + T/A - \lambda_1 A - \lambda_2 Z = 0. \tag{7.6.4}$$

The total free energy density is therefore

$$f = -P + \mu_n n\left(1 - Y_e\right) + \mu_p n Y_e = -\sum_{Z,A} \frac{n\left(Z,A\right)T}{A} + \lambda_1 n + \lambda_2 n Y_e. \tag{7.6.5}$$

Thus, $\lambda_1 = \mu_n$ and $\lambda_2 = -(\mu_n - \mu_p) \equiv -\hat{\mu}$. The number densities of each nucleus are then

$$n\left(Z,A\right) = G\left(Z,A\right)\left(\frac{mAT}{2\pi\hbar^2}\right)^{3/2} \exp\left[-\frac{AB\left(Z,A\right) + N\mu_n + Z\mu_p}{T}\right]. \tag{7.6.6}$$

Number densities of nucleons are

$$n_{n,p} = 2\left(\frac{mT}{2\pi\hbar^2}\right)^{3/2} e^{\mu_{n,p}/T}, \tag{7.6.7}$$

so

$$n\left(Z,A\right) = G\left(\frac{mT}{2\pi\hbar^2}\right)^{\frac{3(1-A)}{2}} \left(\frac{1}{2}\right)^A A^{3/2} n_n^{A-Z} n_p^Z e^{-\frac{AB(Z,A)}{T}}. \tag{7.6.8}$$

At low temperatures, $G(Z,A) \simeq 1$, but above a few MeV,

$$G \simeq \frac{\pi}{6aT} e^{aT} \tag{7.6.9}$$

where $a \simeq A/9$ MeV^{-1} is the usual level density parameter. The partition function will begin to dominate the composition when $aT > AB/T$, or when $T > \sqrt{9B} \simeq 9$ MeV. Nuclei are dissociated by such large T, except near nuclear density.

The optimum nucleus satisfies $\partial n/\partial Z\Big|_A = \partial n/\partial A\Big|_Z = 0$, or

$$\hat{\mu} = A\left(\frac{\partial B}{\partial N}\bigg|_Z - \frac{\partial B}{\partial Z}\bigg|_N\right) = -\frac{\partial B}{\partial\left(Z/A\right)}\bigg|_A \tag{7.6.10}$$

using Eq. (7.6.9). With electronic energy also minimized, we have $\hat{\mu} = \mu_e$, the usual condition for beta equilibrium. For densities above 10^6 g cm^{-3}, the electrons are relativistic.

In stellar cores, the electrons are degenerate as well. Eq. (7.6.2) should properly include the rest masses of the neutrons and protons, so an extra term $(m_n - m_p)c^2 Y_e$ appears:

$$\hat{\mu} + (m_n - m_p)\, c^2 = \mu_e.$$

Since $Y_e = \langle Z/A \rangle$, we see that the most abundant nucleus is the one that has the largest binding energy *for a given neutron excess*. Thus, although ^{62}Ni has a larger binding energy than ^{56}Ni (8.795 MeV compared to 8.790 MeV), ^{56}Ni is more abundant near the valley of beta stability.

Chapter 8.
Stellar Birth and Main Sequence Evolution

8.1. Jean's Mass

Criterion for stability – neglect magnetic fields. Critical mass is called the Jean's mass M_J, where a cloud's potential energy equals its kinetic energy. If spherical with uniform temperature,

$$\Omega = GM_J^2/R \simeq M_J v_s^2/2 \tag{8.1.1}$$

or

$$M_J \simeq \frac{v_s^2}{2G}R = \left(\frac{5v_s^2}{6G}\right)^{3/2}\left(\frac{3}{4\pi\bar{\rho}}\right)^{1/2}. \tag{8.1.2}$$

$v_s \simeq \sqrt{2N_0T}$ is the sound velocity, $v_s \simeq 1$ km/s for $T = 100$ K. For a mean density $\bar{\rho} = 10^{-24}$ g cm^{-3}, $M_J \simeq 2\cdot 10^4$ M$_\odot$. Eventual star formation must occur by fragmentation of more massive collapsing clouds.

Apply virial theorem to a cloud bounded by the ISM with pressure P_o.

$$\int_0^M \frac{Gm\,(r)}{r}dm = 3\int_0^M \frac{P}{\rho}dm - 4\pi R^3 P_o\,.$$

For an isothermal gas, using the fact that $m \propto r$, this is

$$\frac{GM^2}{R} = 3N_oTM - 4\pi R^3 P_o\,, \qquad P_o = \frac{3N_oTM}{4\pi R^3} - \frac{GM^2}{4\pi R^4}\,.$$

For small R, $P_o < 0$. For large R, $P_o > 0$ but tends to zero. There is a maximum of P_o, at R_m, which represents a stability limit. Reducing R from R_m lowers P_o and the ISM will force compression of the cloud, triggering collapse. This won't happen if $R > R_m$. From $(\partial P_o/\partial R)_M = 0$ one finds

$$R_m = \frac{4GM_J}{9N_oT}, \qquad M_J = \frac{9N_0T}{4G}R_m$$

where we identify the mass with the Jean's mass. Note that M_J is 4.5 times larger than the preceding estimate.

Clouds exceeding the Jeans mass are stabilized by magnetic fields.

$$\frac{B^2}{8\pi} \geq \frac{3GM^2}{4\pi R^4}, \tag{8.1.3}$$
$$M \leq BR^2/\sqrt{6G} \approx 50\,(R/\mathrm{pc})^2\,M_\odot,$$

if $B \approx 30$ μG. A solar mass originates from within a region of less than about 0.14 pc.

Another source of support is rotation. For an Oort constant of 16 km/s/kpc, the angular rotation rate is $2\cdot 10^{-16}$ s^{-1}. The Keplerian frequency is $\Omega_K = \sqrt{GM/R^3}$, implying a limit

$$M \geq \Omega_K^2 R^3/G = 0.8\,(R/\mathrm{pc})^3 \;\; \mathrm{M}_\odot\,.$$

This gives a limiting radius of about 0.9 pc for 1 solar mass.

8.2. Collapse

How does collapse occur? Rotation is removed by magnetic fields, and magnetic fields are dissipated by ambipolar diffusion over times of $10^4 - 10^5$ years, which is 10 times the dynamical time scale $1/\sqrt{G\rho}$. It is more likely that clouds are dissipated before collapse ensues, so star formation is essentially inefficient, and gas remains in the Galaxy today.

Hydrostatic equilibrium for an isothermal gas gives

$$\rho\left(r\right) = \frac{v_s^2}{2\pi G r^2}; \qquad m\left(r\right) = \frac{2v_s^2 r}{G}. \tag{8.2.1}$$

Ample observational evidence exists for this r^{-2} density dependence. "Jean's" mass is close to previous estimate.

The cloud initially collapses isothermally because photons freely escape. M_J decreases and smaller condensed regions of the cloud become unstable to collapse: it fragments. The free-fall timescale is $\tau_{ff} = \sqrt{3/(8\pi G\bar{\rho})}$. The total energy to be radiated is of order GM^2/R, giving an estimated luminosity

$$L \simeq \frac{GM^2}{R}\sqrt{\frac{8\pi G\bar{\rho}}{3}} = \sqrt{2}G^{3/2}\left(\frac{M}{R}\right)^{5/2}.$$

This can't be larger than the blackbody luminosity $4\pi R^2\sigma T_{eff}^4$, giving

$$M \leq \left(8\pi^2 R^9\sigma^2 T_{eff}^8/G^3\right)^{1/5}.$$

Fragmentation stops when $R < R_J = 4GM_J/(9N_oT_{eff})$. Thus

$$M_J > \frac{81N_o^2}{32G}\left(\frac{9N_oT_{eff}}{2\pi^2\sigma^2G^2}\right)^{1/4} \simeq 0.005T^{1/4}\ \mathrm{M}_\odot.$$

For a temperature of 100 K, we find $M_J > 0.03\ \mathrm{M}_\odot$, greater than planetary masses, but of order of smallest stellar mass.

8.3. Self-Similar Description of Collapse

The Euler equations of hydrodynamics:

$$\frac{\partial\rho}{\partial t} + \frac{1}{r^2}\frac{\partial r^2\rho v}{\partial r} = 0,$$

$$\frac{\partial v}{\partial t} + v\frac{\partial v}{\partial r} = -\frac{1}{\rho}\frac{\partial P}{\partial r} - \frac{Gm\left(r\right)}{r^2},$$

where $m(r) = \int 4\pi\rho r^2 dr$ is the mass contained within the radius r. Applied to a polytropic equation of state $P = K\rho^\gamma$, these coupled partial differential equations can be replaced by ordinary differential equations. Define the self-similar variable

$$X\left(r,t\right) = K^{-1/2}G^{(\gamma-1)/2}r\left(\mp t\right)^{\gamma-2}. \tag{8.3.1}$$

The convention is that the collapse begins at $t = -\infty$ and the central density reaches infinite values when $t = 0$. The collapse continues through positive values of t.

The hydrodynamical variables ρ, v and m can be written as dimensionless functions of X, with scale factors depending on K, G, γ and $(\mp t)$. Thus

$$\begin{aligned} \rho(r,t) &= G^{-1}(\mp t)^{-2} D(X), \\ v(r,t) &= K^{1/2} G^{(1-\gamma)/2} (\mp t)^{1-\gamma} V(X), \\ m(r,t) &= \int 4\pi\rho r^2 dr = K^{3/2} G^{(1-3\gamma)/2} (\mp t)^{4-3\gamma} M(X). \end{aligned} \tag{8.3.2}$$

Thus, a solution in terms of X tells us the behavior of a quantity *at all times at a given place* or *at all places at a given time.*

In dimensionless variables the Euler equations are:

$$\frac{D'}{D}[V \pm X(2-\gamma)] + V' = \mp 2 - 2\frac{V}{X}, \tag{8.3.3}$$

$$\gamma D^{\gamma-2} D' + V'[V \pm X(2-\gamma)] = -\frac{M}{X^2} \mp (\gamma - 1) V. \tag{8.3.4}$$

The upper (lower) sign refers to $t < 0$ ($t > 0$).

In spherical symmetry, mass can only move radially. The equation of continuity is

$$\frac{dm(r,t)}{dt} = \frac{\partial m(r,t)}{\partial t} + v\frac{\partial m(r,t)}{\partial r} = 0.$$

This equation is easily integrated:

$$M(X) = \int 4\pi D X^2 dX = \frac{4\pi X^2 D[X(2-\gamma) \pm V]}{4 - 3\gamma}.$$

If $\gamma = 4/3$, however, we must have either $V = \mp 2X/3$ or $D = 0$.

The dimensionless Euler equations possess a singularity analogous to the one encountered in steady-state accretion and stellar winds. The physicaly acceptable solution is the one which is regular at the *critical point* where the determinant of the coupled equations Eq. (8.3.4) is zero,

$$[V(X_c) \pm X_c(2-\gamma)]^2 = \gamma D^{\gamma-1}(X_c), \tag{8.3.5}$$

and which has the correct behavior as $X \to 0$ and $X \to \infty$.

In the limit $(\mp t) \to 0$, or $r \to \infty$ for $t \neq 0$, in order to ensure that all variables are non-singular, one must have the asymptotic behavior

$$\left.\begin{array}{c} D \propto X^{-2/(2-\gamma)}; \quad V \propto X^{(1-\gamma)/(2-\gamma)} \\ M \propto X^{(4-3\gamma)/(2-\gamma)} \end{array}\right\} \quad X \to \infty \tag{8.3.6}$$

For $\gamma = 4/3$, the mass becomes constant at large radii and tends to infinity for $\gamma < 4/3$. This is no problem since the solution can be terminated at large X. In the case $\gamma > 4/3$, the mass tends to zero in the large X limit which seems unphysical. For $1 < \gamma < 2$ both D

and V tend to 0, and also $V \propto \sqrt{M/X}$ as $X \to \infty$, so $V \propto V_{ff} = \sqrt{2M/X}$, the free-fall velocity.

In the limit $X \to 0$, which is $r \to 0$ for $t \neq 0$, or $(-t) \to \infty$ for finite r (i.e., the initial system), one can show

$$\left.\begin{aligned} D &= D_o; \quad V = -(2/3)\,X \\ M &= (4\pi/3)\,D_o X^3 \end{aligned}\right\} X \to 0, \quad t < 0. \tag{8.3.7}$$

D_o is an integration constant which depends only on γ. The central collapsing regions are *homologous*, *i.e.*, v varies linearly with r. A boundary separates the two asymptotic behaviors for V, and the inner core from the outer core. (For $\gamma = 4/3$, there is no outer core; D falls to zero by the value $X = X_c = 2.77$.) The boundary is near the maximum velocity point, $|dV/dX| = 0$, and where the velocity equals the sound speed,

$$v = v_s = \sqrt{\partial P/\partial \rho}\,; \qquad V = A = \gamma^{1/2} D^{(\gamma-1)/2}\,. \tag{8.3.8}$$

The dimensionless sound speed is A. Homology breaks down at larger radii because information travels at a slower rate than that of the collapsing matter.

At $t = 0$ the asymptotic power-law relations Eq. (8.3.6) hold everywhere, and form initial conditions for a self-similar solution valid for $t > 0$ (lower sign of t in Eqs. (8.3.3) and (8.3.4). There is no singular point, the initial conditions determine the solution. The asymptotic relations Eq. (8.3.6) for $X \to \infty$ are still valid, but for $X \to 0$ a new set of asymptotic relations applies:

$$\left.\begin{aligned} M &= M_o; \quad V = -\sqrt{2M/X} \\ D &= \frac{\sqrt{M_o/2}}{4\pi X^{3/2}} \end{aligned}\right\} X \to 0, \quad t > 0 \tag{8.3.9}$$

The constant M_o is determined by integration. This limit corresponds, for a given r, to a sufficiently long time after the center has collapsed to infinite density. For $t < 0$, the outer core cannot go into free-fall because the inner core is collapsing too slowly. This obstacle is removed at $t = 0$, after which the outer core builds up momentum, and approaches free-fall as $X \to 0$. The free-fall collapse of the outer core is made possible by a reduction in the pressure gradient relative to gravity due to a substantial reduction in density.

The case $\gamma = 4/3$ is special in that there is no finite solution for the case $t > 0$. The solution for $t < 0$ ended at $X_c = 2.77$, with $D = 0$ for $X > X_c$. This cannot be matched to the asymptotic behavior unless $D = 0$ for $X > 0$ when $t > 0$. The hydrodynamics equation for $t < 0$ can be written as

$$\frac{4}{3} D^{-2/3} D' = -\frac{M}{X^2} \pm \frac{2X}{9}.$$

Taking a derivative after multiplying by X^2, and substituting $M' = 4\pi D X^2$, one finds

$$\frac{1}{X^2}\frac{d}{dX}\left(X^2 \frac{dD^{1/3}}{dX}\right) = -\pi D + \frac{1}{6}.$$

Letting $\theta = (D/D_o)^{1/3}, \xi = X\sqrt{\pi D_o}$, we have

$$\frac{1}{\xi^2}\frac{d}{d\xi}\left(\xi^2\frac{d\theta}{d\xi}\right) = -\theta^3 + \frac{1}{6\pi D_o}.$$

The constant $D_o = 8.11$ from numerical integration. This is the just the Lane-Emden equation for $\gamma = 4/3$ except for the constant term. The first zero of θ now occurs at $\xi_1 = X_c\sqrt{\pi D_o} = 9.99$ as opposed to 6.854 when this term is absent. It is interesting that the value of the constant term, $(6\pi D_o)^{-1}$, is the largest value that will still produce a zero of θ; thus, when $\xi = \xi_1$, we have $\theta_1 = \theta_1' = 0$ and $\theta_1'' = (6\pi D_o)^{-1}$. Near the origin, the density dependence is nearly identical to that of a static $\gamma = 4/3$ polytrope, but deviates from this for $X \to X_c$. Thus a collapsing $\gamma = 4/3$ polytrope has a finite extent, which is not the case for other polytropic exponents.

Now examine the behavior of the dimensionless energy

$$\begin{aligned} e(r,t) &= \int 4\pi\rho r^2\left[\frac{1}{2}v^2 + \frac{K}{\gamma-1}\rho^{\gamma-1} - \frac{Gm(r)}{r}\right]dr \\ &= K^{5/2}G^{(3-5\gamma)/2}(\mp t)^{6-5\gamma}E(X). \end{aligned}$$

As $X \to \infty$, the behavior of E satisfies $E \propto X^{(6-5\gamma)/(2-\gamma)}$, which results in finite total energy for $X < \infty$ if $2 > \gamma > 6/5$. The effective range for physical collapse solutions is then $6/5 < \gamma < 4/3$.

8.3.1. Isothermal Case

However, a physical solution for the isothermal case, $\gamma = 1$, exists also for $t > 0$. We have $K = v_s^2$, so $X = v_s^{-1}r/t$. A solution can be found that has the steady state solution Eq. (8.2.1) as an initial condition for $t \to 0^+$ or $X \to \infty$,

$$D = K\left(2\pi X^2\right)^{-1}, \qquad V = 0, \qquad M = 2KX. \tag{8.3.10}$$

Near $X = 0$, Eq. (8.3.9) gives

$$\begin{aligned} m(r,t) &= \frac{v_s^3}{G}m_o t; \quad v(r,t) = \sqrt{\frac{2m_o v_s^3 t}{r}} = \sqrt{\frac{2Gm}{r}}; \\ \rho(r,t) &= \frac{1}{4\pi G}\sqrt{\frac{m_o v_s^3}{2tr^3}} = \frac{1}{4\pi}\sqrt{\frac{Gm}{tr^3}}. \end{aligned} \tag{8.3.11}$$

The parameter $m_o = 0.975$, determined by numerical integration, represents the mass that accumulates at the origin (where the density is infinite). It grows linearly with time, i.e., a constant accretion rate $\dot{m} = v_s^3 m_o/G$ exists.

In this case, a singular point is reached for $V - X = -1$, seen from Eq. (8.3.5). Since for $X > 1$, the solution is the steady state solution itself, Eq. (8.3.10), for which $V = 0$. Therefore we have that $X_c = 1$. A physical interpretation of these results is that the collapsing region begins at the center and expands linearly with the sound speed. The bottom falls out of the cloud and the collapse is inside-out. The total infalling mass, the

mass within $X = 1$, is $m_{in} = 2v_s^3 t/G$, just over twice the mass accumulated at the origin, $m_{core} = m_o v_s^3 t/G$.

While the infall will be radial near the origin, at some point the centrifugal barrier becomes appreciable. With angular momentum conservation, the angular velocity $\Omega = \Omega_o (r_o/r)^2$ of each mass unit increases during infall (o refers to initial values). Ω reaches Keplerian magnitude, where centrifugal barrier balances gravity, when $r = R_C = (GM)^{1/3}/\Omega^{2/3} = \Omega_o^2 r_o^4/GM$. For 1 $M_\odot$, $\Omega_o = 2 \cdot 10^{-16}$ s^{-1}, and $r_o = 0.33$ pc, one finds $R_C \simeq 20$ AU. The formation of an extensive disc, of the order the size of planetary system, is inevitable. A protostar forms at the center, with a central density that increases in a runaway that is halted only when the core becomes optically thick.

The opacity in the collapsing cloud core, while small, nevertheless is large enough to ensure optical thickness when

$$\kappa \sim (R\rho)^{-1} \sim 5 \times 10^{-7} \left(\frac{R}{1\text{AU}}\right)^2 \text{cm}^2 \ \text{g}^{-1}. \tag{8.3.12}$$

For a core mass $M = m_o v_s^3/G$, this occurs for $R \simeq 1$ AU if $T \simeq 15$ K. Beyond this point, the collapse will be nearly adiabatic since the surface temperature is so small. The abrupt halt of the central collapse unleashes a shock, which runs out through the infalling matter, raising its temperature and ionizing it.

With the Virial Theorem, $n = 3/2$, and assuming complete ionization (kinetic energy equals ionization energy),

$$K = -\frac{1}{2}\Omega = \frac{3}{7}\frac{GM^2}{R} = I = MN_o \left(\chi_H X + \chi_{He} Y\right), \tag{8.3.13}$$

where the ionization potentials $\chi_H(\chi_{He}) = 15.8(19.8)$ eV. For a solar composition, $I/MN_o \simeq 17$ eV. Inverting, we find $R \simeq 50\ \text{R}_\odot = 0.23$ AU, close to the above value. From the relation $K \simeq 3MN_o\bar{T}/(2\mu)$, with $\mu = 0.6$, we find $\bar{T} \sim 9 \times 10^4$ K.

8.4. Convective Protostar: Hayashi Track

Consider slow contraction of a convective protostar. For $T_p < 5000$ K, where ionization is incomplete and $s \simeq -10$, T_p is extremely insensitive to L and M. With the correct constants

$$\begin{aligned} L &\simeq 0.024 \left(\frac{M}{\text{M}_\odot}\right)^{4/7} \left(\frac{R}{\text{R}_\odot}\right)^{16/7} \text{L}_\odot \\ &\simeq 1.64 \cdot 10^4 \left(\frac{\text{M}_\odot}{M}\right)^4 \left(\frac{T_p}{3500\ \text{K}}\right)^{32} \text{L}_\odot. \end{aligned} \tag{8.4.1}$$

Therefore, in an Hertzsprung-Russell diagram, a collapsing protostar moves vertically along a line of nearly fixed temperature, the so-called *Hayashi track*. The luminosity $L \propto M^{4/7} R^{16/7}$ decreases with contraction. For fixed M, an $n = 3/2$ polytrope has $R \propto \sqrt{K} \propto e^{s/3}$: the star contracts only if the entropy per particle falls. The contraction timescale is easily found from

$$\tau_{cont} \simeq -\frac{E}{L} \simeq 5.3 \times 10^8 \left(\frac{M}{M_\odot}\right)^{10/7} \left(\frac{R}{R_\odot}\right)^{-23/7} \text{yr}, \tag{8.4.2}$$

which increases rapidly as the star shrinks. It also decreases rapidly with mass, since for a given value of I/M, $R \propto M$: thus $\tau_{cont} \propto M^{-13/7}$. At the beginning of the Hayashi track, when $R \sim 50 R_\odot$ for a $1 M_\odot$ protostar, $\tau_{cont} \simeq 1400$ yr, but much greater than the free fall time.

For very massive protostars, accretion occurs all the way to the main sequence. For less massive stars, accretion ceases during protostar collapse. How does a star know when to stop accretion? Essentially, this happens when the central temperature rises to the value needed to ignite deuterium, about 10^6 K. Thus, using the perfect gas law with the $n = 3/2$ polytrope relations, we find the "stellar birthline" $R/R_\odot \simeq 8.3 M/\mathrm{M}_\odot$ and $L \simeq 3 (M/\mathrm{M}_\odot)^{20/7}$ $\mathrm{L}_\odot$. Deuterium ignition drives stellar winds that effectively halt further accretion.

The protostar leaves the Hayashi track when L falls below the minimum for a fully convective star. With $\mu = 0.6$

$$L_{min} = \frac{5.8}{\eta_c} \left(\frac{M}{M_\odot} \right)^{5.5} \left(\frac{R_\odot}{R} \right)^{.5} L_\odot. \tag{8.4.3}$$

A fully convective star does not quite have a uniform energy generation, but one that is proportional to the temperature. For a perfect gas law, $T = P\mu/N_o\rho \propto \rho^{1/n} \propto \theta$, where θ is the Lane-Emden variable. Therefore

$$\eta_c = \frac{T_c M}{\int T dM} = \frac{\xi_1^2 \theta_1'}{\int \theta d\left(\xi^2 \theta'\right)} = -\frac{\xi_1^2 \theta_1'}{\int \xi^2 \theta^{n+1} d\xi} \tag{8.4.4}$$

which is approximately 2 for all polytropes. (Direct integration gives 5/2, 2 and $16/3\pi$ for the cases n=0, 1, and 5, respectively). Using $\eta_c \simeq 2.5$ and equating Eqs. (8.4.1) and (8.4.3),

$$L_{min} \simeq 1.0 \left(\frac{M}{\mathrm{M}_\odot} \right)^{60/13} \mathrm{L}_\odot; \quad R_{min} \simeq 5.1 \left(\frac{M}{M_\odot} \right)^{23/13} \mathrm{R}_\odot. \tag{8.4.5}$$

Although this luminosity is about 50% too large, the minimum radius too large by an even greater factor, compared to more detailed calculations, probably owing to poor assumptions about the opacity. Also

$$T_{c,min} = \frac{G\mu M}{N_o \left(n+1\right) R_{min} \left(-\xi_1 \theta_1'\right)} \simeq 1.4 \cdot 10^6 \left(\frac{M_\odot}{M} \right)^{10/13} \mathrm{K}, \tag{8.4.6}$$

which is comfortably above the temperature where deuterium burning occurs. From Eq. (8.4.2), the time needed to collapse from infinity to a given radius is $(7/23)\tau_{cont}$, so the time needed to collapse to R_{min} is

$$t_{min} \simeq 7.6 \times 10^5 \left(\frac{M_\odot}{M} \right)^{399/91} \mathrm{yr}. \tag{8.4.7}$$

8.5. From the Hayashi Track to the Main Sequence: the Henyey Track

During collapse, the Virial Theorem says that half the energy goes into radiation and the other half into heat (if n fixed):

$$L = -\frac{1}{2}\frac{dE}{dt} = \frac{n-3}{5-n}\frac{GM^2}{2R^2}\frac{dR}{dt};$$
$$\frac{dL}{dt} = -\frac{1}{2}\frac{d^2E}{dt^2} = \frac{n-3}{5-n}\frac{GM^2}{2R^2}\left[-\frac{2}{R}\left(\frac{dR}{dt}\right)^2 + \frac{d^2R}{dt^2}\right].$$

Constancy of T_{eff} with $L = 4\pi\sigma R^2 T_{eff}^4$ implies $dL/L = 2dR/R$ and $d^2R/dt^2 = 4(dR/dt)^2/R$. This leads to a solution

$$R = R_o\left(1 + \frac{6L_oR_ot}{GM^2}\right)^{-1/3},$$

where R_o and L_o refer to the initial radius and luminosity.

Continued collapse to the main sequence involves a change in the polytropic structure from $n = 3/2$ to $n = 3$ (the standard model). If we neglect this, however, and use the hydrostatic condition $d^2I/dt^2 = 0$ where $I \propto MR^2$ is the moment of inertia, one finds that $Rd^2R/dt^2 = -(dR/dt)^2$. This implies that $dL/L = -3dR/R$, which is now positive, and to a solution

$$R = R_o\sqrt{1 - \frac{4R_oL_ot}{GM^2}}.$$

This also implies that $d\ln T_{eff}/d\ln R = -5/4$ and $d\ln L/d\ln T_{eff} = 12/5$. This phase of collapse is known as the *Henyey* phase, and results in an increase in L and T_{eff} with stellar shrinkage. The stellar radius, for a one solar mass star, must shrink from R_{min} to $R_\odot$, the effective temperature rises from about 3500 K to 5500 K, so $L_{min} \simeq (3500/5500)^{12/5} \simeq 3$ $L_\odot$ and $R_{min} \simeq (5500/3500)^{4/5} \simeq 0.7$ $R_\odot$. The slope in the H-R diagram of the Henyey track is 2.4, smaller than that of the main sequence, so the Henyey trajectory will eventually intersect it.

Note from the above that L_{min} varies with mass less steeply than does L_{ssm}. Since we expect that for solar mass stars that $L_{min}/L_{ssm} < 1$ (although we didn't get this result in the above), in principle as mass is decreased there will be a point at which $L_{min} = L_{ssm}$. For small enough masses, the Henyey phase essentially disappears, and a lower limit to stellar masses occurs.

8.6. Main Sequence Structure

The main sequence is defined as those stars that burn hydrogen to helium in their cores. Lower mass stars do this via the pp cycle, and higher mass stars via the CNO cycle. The latter is much more temperature sensitive, and leads to convective cores in massive stars. The adiabatic temperature gradient is

$$\left.\frac{dT}{dr}\right|_{ad} = -\frac{2}{5}\frac{T}{P}\frac{dP}{dr} = -\frac{8\pi}{15}\frac{\mu G\rho_o r}{N_o} \qquad (8.6.1)$$

for a perfect gas near the center. Diffusive transport leads to

$$\left.\frac{dT}{dr}\right|_{rad} = -\frac{3}{4ac}\frac{\kappa\rho}{T^3}\frac{L}{4\pi r^2} \simeq -\frac{\kappa_o\rho_c^2\epsilon_c r}{acT_c^3}, \tag{8.6.2}$$

where we used the Thomsen opacity (valid at high temperatures) and approximated $L(r) \simeq (4\pi/3)\rho_c\epsilon_c r^3$. The condition for convective instability is simply $|dT/dr|_{rad} > |dT/dr|_{ad}$, or

$$\epsilon_c > \frac{8\pi}{15}\frac{\mu GacT_c^3}{N_o\kappa_o\rho_c} \simeq 1.2\times10^4\left(\frac{T_{c,6}}{14}\right)^3\left(\frac{150\ \mathrm{g\ cm^{-3}}}{\rho_c}\right)\mathrm{erg\ g^{-1}s^{-1}}. \tag{8.6.3}$$

For comparison, the pp cycle has an energy generation rate of

$$\epsilon_{pp} \simeq 17\left(\frac{T_6}{14}\right)^4\left(\frac{\rho}{150\ \mathrm{g\ cm^{-3}}}\right)\mathrm{erg\ g^{-1}s^{-1}}, \tag{8.6.4}$$

so the Sun's core must be radiative. In a massive star, for CNO, we have

$$\epsilon_{CNO} \simeq 4\times10^5\left(\frac{T_6}{25}\right)^{17}\left(\frac{\rho}{150\ \mathrm{g\ cm^{-3}}}\right)\mathrm{erg\ g^{-1}s^{-1}}; \tag{8.6.5}$$

these stars have convective cores.

If energy generation is very temperature sensitive, approximate the core as having a point-like energy source. Thus, for $r > 0$, we have $L(r) = L$. We look for a power-law solution for T outside the convective core: $T = br^m$. With the radiative transport equation,

$$m = -\frac{1}{4} \qquad b^4 = \frac{3\kappa_o\rho_c L}{16\pi ac} \tag{8.6.6}$$

if ρ is constant. The convective core's radius will be determined by $|dT/dr|_{rad} = |dT/dr|_{ad}$:

$$r_{core} = \left(\frac{3\kappa_o L}{16\pi ac}\right)^{1/9}\left(\frac{15N_o}{32\pi\mu G}\right)^{4/9}\rho_c^{-1/3}. \tag{8.6.7}$$

Using the relation $\rho_c \propto M/R^3$ we have

$$r_{core}/R \propto L^{1/9}/M^{1/3} \propto M^{5/18} \tag{8.6.8}$$

using the standard solar model for $L(M)$. Convective cores increase with stellar mass.

8.7. Red Giant Structure

The large expansion of the outer layers is attributed to the abrupt change in the mean molecular weight and entropy and the large energy production at a hydrogen-burning shell exterior to the helium core. A red giant has two basic components–a core and an extended envelope. If the envelope/core mass ratio is negligible, and envelope transport is diffusive,

the radiative zero solution is valid for the envelope ($n = 3.25$). If transport in the envelope is convective, $n = 3/2$. In either case

$$\frac{dP}{dr} = -\frac{GM\rho}{r^2} = (n+1)\,\frac{P}{T}\frac{dT}{dr}. \tag{8.7.1}$$

Using the perfect gas law $P = N_o T\rho/\mu$ we find

$$\frac{dT}{dr} = -\frac{\mu GM}{N_o r^2\,(n+1)} \tag{8.7.2}$$

since M varies little in the envelope. Also

$$T\,(r) = \frac{\mu GM}{N_o\,(n+1)}\left[\frac{1}{r} - \frac{1}{R}\right]. \tag{8.7.3}$$

The diffusion equation implies that

$$\rho\,(r) = \left(\frac{4\mu GM}{17N_o}\right)^{15/4}\left(\frac{16\pi ac}{3\kappa_o L}\right)^{1/2}\left[\frac{1}{r} - \frac{1}{R}\right]^{13/4}. \tag{8.7.4}$$

As L increases, ρ decreases rapidly, meaning a large expansion of the envelope occurs. Estimating the core-envelope interface density $\rho_i = \alpha(3M/4\pi R^3)$, where $\alpha \leq 1/10$, we find

$$L = \frac{256\pi^3 ac}{2\alpha^2\kappa_o}\left(\frac{4\mu G}{17N_o}\right)^{15/2}\frac{M^{11/2}}{R^{1/2}} = \frac{266}{\alpha^2}\left(\frac{M}{M_\odot}\right)^{11/2}\left(\frac{R_\odot}{R}\right)^{1/2} L_\odot. \tag{8.7.5}$$

A huge L is needed to sesure this expansion. To check that the envelope has negligible mass, integrate Eq. (8.7.4) from R_i to R:

$$M_e/M \simeq 12\alpha\left(1 + \frac{13}{3}\frac{R_i}{R}\right). \tag{8.7.6}$$

Another approach is to posit power law solutions to the diffusion and hydrostatic equilibrium equations in the envelope:

$$P = P_s\left(\frac{r}{R_s}\right)^{-a} \qquad T = T_s\left(\frac{r}{R_s}\right)^{-b} \tag{8.7.7a}$$

$$\rho = \rho_s\left(\frac{r}{R_s}\right)^{-c} \qquad M = M_s\left(\frac{r}{R_s}\right)^{d} \tag{8.7.7b}$$

With Kramer's opacity, $a = 43/11, b = 10/11, c = 32/11, d = 1/11$, so the polytropic index is $n = c/b = 3.2$. We find

$$\rho_s = \frac{1}{44\pi}\frac{M_s}{R_s^3} \qquad T_s = \frac{11}{42}\frac{\mu GM_s}{N_o R_s} \tag{8.7.8}$$

so the value of α from above is $1/33$. Utilizing the diffusion equation to solve for the luminosity, we find

$$L = \frac{16\pi ac}{3\kappa_o}\frac{10}{11}\frac{R_s T_s^{7.5}}{\rho_s^2} = 2490\left(\frac{M_s}{M_\odot}\right)^{11/2}\left(\frac{R_\odot}{R_s}\right)^{1/2} L_\odot. \tag{8.7.9}$$

With $T_s \simeq 10^7$ K, $M_s \simeq M_\odot$ we find $R_s \simeq 0.4R_\odot$. Substituting into Eq. (8.7.7*a*) we find ($T_p \sim 5000$ K) $R = 1711\mathrm{R}_\odot = 8$ AU, very large indeed. This model has flaws. We find the total mass is $M = 2.1\mathrm{M}_\odot$, so the envelope mass exceeds the core mass. Nevertheless, it illustrates how large L and R are inevitable.

Discontinuities in the mean molecular weight and entropy exists also. Because of P and T continuity, an abrupt decrease in μ is accompanied by a corresponding decrease in ρ and $|dP/dr|$. An abrupt increase in s also results in a decrease in ρ. Both result in expansions of the outer layers and L in a kind of runaway. The core of a star with a molecular weight or entropy discontinuity is denser than the core of a star withut one, since ρ must increase. The virial theorem

$$3N_o\bar{T}M/\bar{\mu} + \Omega = 0 \tag{8.7.10}$$

where $\bar{T}$ and $\bar{\mu}$ are global averages. As the core contracts, T_c and Ω barely change for a given L. Core shrinkage means expansion of the envelope.

Expansion factors of red giant envelopes are 100-500 times, but μ gradients or core shrinkage produce only 50–100% change. This large factor can be traced to isothermality of the core.

Assume T, M and R obey power law relations just outside the core and well into the envelope as in Eq. (8.7.7). Then

$$T_s = \frac{\mu G M_s}{N_o\,(n+1)\,R_s}. \tag{8.7.11}$$

Since T_s is fixed by nuclear requirements during shell burning, this suggests that $R_s \propto M_s$. However, M_s increases as the shell slowly burns outward in mass, and the core's center contracts due to the higher gravity. Nevertheless, R_s slowly increases. The quantity

$$U = \frac{d\ln M}{d\ln r} = \frac{3\rho\,(r)}{\bar{\rho}} = \frac{4\pi r^3\rho\,(r)}{M\,(r)} \tag{8.7.12}$$

is very small just beyond the shell. Expanding $\rho(r)$ and $M(r)$ about the origin in an isothermal core,

$$\rho = \rho_c\left(1 - \frac{2\pi G\rho_c\mu}{3N_oT_c}R_s^2\right) \qquad M = \frac{4\pi}{3}\rho_c R_s^3\left(1 - \frac{2\pi\rho_c\mu}{5N_oT_c}R_s^2\right) \tag{8.7.13}$$

we find

$$U = 3\left(1 - \frac{4\pi\mu G\rho_c}{15N_oT_c}R_s^2\right) \simeq 3\left[1 - 0.07\rho_c\frac{3\times10^7\mathrm{K}}{\mathrm{T_c}}\left(\frac{R_s}{R_\odot}\right)^2\right] \tag{8.7.14}$$

which rapidly decreases as ρ_c increases and R_s increases. For comparison, for an $n = 3$ polytrope, the factor of 0.07 will be reduced a factor of 4 for the same conditions. The radius of the star swells as a result, since $\ln R \propto \int U^{-1}d\ln M$.

An isothermal core develops in stars whose mass is less than about 6 $M_\odot$. For larger stars, the core mass fraction, when hydrogen shell burning begins, exceeds the so-called *Chandrasekhar-Schönberg limit*

$$M_{cs} = 0.37\left(\frac{\mu_e}{\mu_c}\right)^2 M, \tag{8.7.15}$$

for which an isothermal core is unable to support the envelope's weight. Here μ_e and μ_c are the mean molecular weight of the envelope and core, respectively. These stars do not expand as dramatically as less massive stars.

The relation Eq. (8.7.15) can be motivated from a dimensional analysis of the core and the virial theorem. Apply the virial theorem to the core alone:

$$\frac{3N_oTM_c}{n\mu_c} + \frac{3}{5-n}\frac{GM_c}{R_c} = 4\pi R_c^3 P_c \tag{8.7.16}$$

The term on the right-hand side stems from the pressure P_c at the edge of the isothermal core (with temperature T, mass M_c, molecular weight μ_c and radius is R_c) does not vanish. Solving for P_c yields:

$$P_c = \frac{3}{4\pi R_c^3}\left[\frac{N_oTM_c}{n\mu_c} - \frac{GM_c^2}{(5-n)\,R_c}\right].$$

The maximum core radius that can be supported is found by maximizing P_c with respect to R_c, which gives

$$R_c = \frac{n\mu_c GM_c}{(5-n)\,N_oT}; \qquad P_{c,max} = \frac{3}{4\pi M_c^2}\left(\frac{5-n}{G}\right)^3\left(\frac{N_oT}{n\mu_c}\right)^4.$$

Since $T \propto \mu M/R$, and $P_c \propto M^2/R^4$, where M and R are for the whole star, one finds that

$$q_c = \frac{M_c}{M} \propto \left(\frac{\mu}{\mu_c}\right)^2.$$

An isothermal core supports at most 37% of the stellar mass, but if the core is mostly He, this is reduced to about 10%.

Stars less than about 15 $M_\odot$ develop degenerate cores, which leads to the well-known *Helium flash* behavior at the tip of the red giant branch. Partially degenerate cores don't obey the Chandrasekhar- Schönberg limit and support larger masses. As red giants expand, and T_p cools, they approach the Hayashi track and are nearly completely convective.

Chapter 9.
Compact Stars – White Dwarfs, Planets, Neutron Stars

White dwarf structure dominated by $P(\rho)$ for degenerate electron gas.

$$\begin{aligned} R &= \left[\frac{(n+1)\,K}{4\pi G}\right]^{1/2} \rho_c^{(1-n)/(2n)} \xi_1 \\ M &= 4\pi R^{(3-n)/(1-n)} \left[\frac{(n+1)\,K}{4\pi G}\right]^{n/(n-1)} \xi_1^{(3-n)/(n-1)} \left(-\xi_1^2\theta_1'\right) \\ &= 4\pi \left[\frac{(n+1)\,K}{4\pi G}\right]^{3/2} \rho_c^{(3-n)/(2n)} \left(-\xi_1^2\theta_1'\right). \end{aligned}$$

Non-relativistic $\gamma = 5/3$:

$$\begin{aligned} K &= \frac{\left(3\pi^2\right)^{2/3}}{5}\frac{\hbar^2}{m_e}\left(N_o Y_e\right)^{5/3} = 10^{13} Y_e^{5/3} \ \text{ cgs} \\ R &= 1.121\times 10^4 \rho_{c,6}^{-1/6}\left(2Y_e\right)^{5/6} \ \text{ km} \\ M &= 0.496\rho_{c,6}^{1/2}\left(2Y_e\right)^{5/2} \ \text{ M}_\odot \\ &= 0.701\left(\frac{R}{10^4 \ \text{km}}\right)^{-3}\left(2Y_e\right)^5 \ \text{ M}_\odot. \end{aligned} \tag{9.1}$$

Relativistic $\gamma = 4/3$:

$$\begin{aligned} K &= \frac{\left(3\pi^2\right)^{1/3}}{4}\hbar c\left(N_o Y_e\right)^{4/3} = 1.24\times 10^{15} Y_e^{4/3} \ \text{ cgs} \\ R &= 3.35\times 10^4 \rho_{c,6}^{-1/3}\left(2Y_e\right)^{2/3} \ \text{ km} \\ M &= 1.457\left(2Y_e\right)^2 \ \text{ M}_\odot. \end{aligned} \tag{9.2}$$

Very low density (Thomas-Fermi regime $\gamma = 10/3$):

$$\begin{aligned} K &= \frac{\pi^3 e^2}{10} 3^{1/3}\left(\frac{4\pi N_o}{A}\right)^{10/3}\left(3\frac{\hbar c}{m_e c^2}\frac{\hbar c}{e^2}\right)^6 = 1.05\times 10^{13}\left(\frac{12}{A}\right)^{10/3} \ \text{ cgs} \\ R &= 1.18\times 10^5\left(\frac{12}{A}\right)^{5/3}\rho_c^{2/3} \ \text{ km} \\ M &= 0.001915\left(\frac{12}{A}\right)^5 \rho_c^3 \ \text{ M}_\odot \\ &= 2.88\times 10^{-8}\left(\frac{A}{12}\right)^{5/2}\left(\frac{R}{10^4 \ \text{km}}\right)^{9/2} \ \text{ M}_\odot. \end{aligned} \tag{9.3}$$

9.1. Physical reasoning behind the Chandrasekhar mass

Consider N degenerate fermions in a star of radius R, so that number density $n \propto NR^{-3}$. Momentum of a fermion is $\sim \hbar n^{1/3}$ and Fermi energy is $E_F \sim \hbar c N^{1/3} R^{-1}$. The gravitational energy per fermion is $\sim -GMm_B R^{-1}$ if $M = Nm_B$. The total energy is

$$E = E_F + E_G = \hbar c N^{1/3}/R - GNm_b^2/R.$$

Equilibrium is reached when this is minimized. Both terms scale as $1/R$.

When E is positive, E can be decreased by increasing R. This decreases E_F so that eventually the fermions become non-relativistic: then $E_F \sim p_F^2 \sim R^{-2}$. This then decreases faster than E_G, so E becomes negative. However, as $R \to \infty$, $E \to 0$. This implies there is a minimum of E at a finite value of R.

When E is negative, E can be decreased without bound by decreasing R so that no equilibrium state is possible and a black hole forms.

The maximum baryon number for equilibrium is determined by setting $E = 0$:

$$N_{max} \sim \left(\frac{\hbar c}{Gm_b^2}\right)^{3/2} \sim 2 \times 10^{57}$$
$$M_{max} \sim N_{max} m_B \sim 1.5\ \mathrm{M}_\odot.$$

Note that the mass is independent of the fermion's mass.

The radius at equilibrium is set by the condition $E_F \geq mc^2$, so

$$R \leq \frac{\hbar c}{mc^2}\left(\frac{\hbar c}{Gm_B^2}\right)^{1/2} \sim \begin{cases} 5 \times 10^3\ \mathrm{km}, & m = m_e \\ 3\ \mathrm{km}, & m = m_n\,. \end{cases}$$

At sufficiently high density, neutronization and pyconuclear reactions can occur. Thus, both A and $N-Z$ will increase with density. The neutronization threshold for ^{56}Fe is about 10^9 g cm^{-3}. At this density, the Fermi energy of an electron is about $m_e c^2 + 3.695$ MeV, the threshold for the inverse beta-decay $^{56}\mathrm{Fe} + e^- \to {}^{56}\mathrm{Mn} + \nu_e$. The Mn immediately electron captures: $^{56}\mathrm{Mn} + e^- \to {}^{56}\mathrm{Cr} + \nu_e$. The Cr is stable until densities above 10^{10} g cm^{-3} are reached.

Lighter nuclei have other thresholds: ^{4}He is at 20.6 MeV, ^{12}C is at 13.4 MeV, ^{16}O is at 10.4 MeV and ^{20}Ne is at 7.0 MeV. The loss of electrons softens the EOS: the Chandrasekhar mass decreases. A white dwarf at these densities will begin to gravitationally collapse. Thus the maximum density $\lesssim 10^{10}$ g cm^{-3}, with a minimum radius $\gtrsim 1500$ km.

9.2. Electrostatic corrections and the Low-Density Equation of State

In a degenerate system in which the nuclei are ordered in either a solid or liquid, there is Coulomb energy associated with the ordering. If the nuclei are equally spaced and surrounded by a uniform density electron gas, we proved that the interaction energy per electron is

$$E_c/Z = -\frac{9}{10}\frac{Ze^2}{R_c} = -\frac{9}{10}\left(\frac{4\pi}{3}\right)^{1/3} Z^{2/3} e^2 n_e^{1/3}$$

where $n_e = 3Z/(4\pi R_c^3)$. The corresponding pressure is

$$P_c = n_e^2 \frac{\partial E_c/Z}{\partial n_e} = -\frac{3}{10}\left(\frac{4\pi}{3}\right)^{1/3} Z^{2/3} e^2 n_e^{4/3}.$$

In the extreme relativistic limit this is just a constant fraction (a few percent) of the degeneracy pressure:

$$\frac{P_c}{P_d} = -\frac{2^{5/3}}{5}\left(\frac{3}{\pi}\right)^{1/3} \frac{e^2}{\hbar c} Z^{2/3}.$$

In the non-relativistic limit, P_c becomes more important at lower and lower densities:

$$\frac{P_c}{P_d} = -\frac{m_e e^2 Z^{2/3}}{(2n_e)^{1/3}\,\pi\hbar^2}.$$

At low enough density, $P_c = -P_d$:

$$n_{e,c} = \frac{Z^2\left(m_e e^2\right)^3}{2\pi^3\hbar^6} \qquad \left(\rho_c \simeq 0.4 Z^2 \text{ g cm}^{-3}\right),$$

and the total pressure vanishes. For iron this is about 250 g cm^{-3}, which is not the laboratory value of 7.86 g cm^{-3} because it is incorrect to treat the e^- gas as uniform.

The Fermi energy of the electrons is modified by the Coulomb potential:

$$E_F = -eV(r) + \frac{p_F^2}{2m_e}$$

and is constant in space, otherwise electrons would move to a lower E_F. The electron density is

$$n_e = \frac{8\pi}{3h^3} p_F^3 = \frac{8\pi}{3h^3}\left[2m_e\left(E_F + eV(r)\right)\right]^{3/2}.$$

The potential is determined by Poisson's equation

$$\nabla^2 V = 4\pi e n_e + \text{ nuclear contribution}$$

where the last term is effectively a delta function at the origin. Omitting it for $r > 0$, we have the boundary condition: $rV(r) \to Ze$ as $r \to 0$. The electric field should vanish at the outer boundary, since this volume must be overall neutral: $dV/dr|_{R_c} = 0$. Poisson's equation in spherical geometry becomes

$$\frac{d^2\phi}{dx^2} = \frac{\phi^{3/2}}{x^{1/2}}, \tag{9.2.1}$$

where

$$E_F + eV(r) = \frac{Ze^2\phi(r)}{r}, \quad x = r\left(\frac{128Z}{9\pi^2}\right)^{1/3} \frac{m_e e^2}{\hbar^2}.$$

Eq. (9.2.1) has boundary conditions

$$\phi(0) = 1, \qquad \phi(x_o)' \equiv \left.\frac{d\phi}{dx}\right|_{x_o} = \frac{\phi(x_o)}{x_o},$$

where x_o corresponds to $r = R_c$. The latter condition can be seen by evaluation of $Z = 4\pi \int n_e r^2 dr$ over the entire volume. The equation Eq. (9.2.1) has a unique solution, when $\phi'(0) = -1.588071$, in that as $x_o \to \infty$, $\phi(x_o) \to 144 x_o^{-3} \to 0$. Otherwise, for larger values of $\phi'(x_o)$, ϕ doesn't vanish anywhere and diverges as $x \to \infty$. At some point, the second boundary condition will be satisfied.

The pressure at the outer boundary is the free particle expression

$$P = \frac{8\pi}{15h^3 m_e} p_F^5 (R_c) = \frac{1}{10\pi} Z^2 e^2 \left(\frac{128Z}{9\pi^2}\right)^{4/3} \left(\frac{m_e e^2}{\hbar^2}\right)^4 \left[\frac{\phi(x_o)}{x_o}\right]^{5/2} .$$

The density is the total mass in the volume divided by the volume:

$$\rho = \frac{3Am_B}{4\pi} \frac{128Z}{9\pi^2} \left(\frac{m_e e^2}{\hbar^2 x_o}\right)^3 = \frac{4Am_B Z}{3} \left(\frac{2m_e e^2}{\pi\hbar^2 x_o}\right)^3 .$$

For low densities, the solution approaches the unique solution with $\phi(x_o) \to 144 x_o^{-3}$. Thus, we have that $P \propto \rho^{10/3}$, with a constant K given by Eq. (9.3).

9.3. Mass-Radius Relation for Degenerate Objects

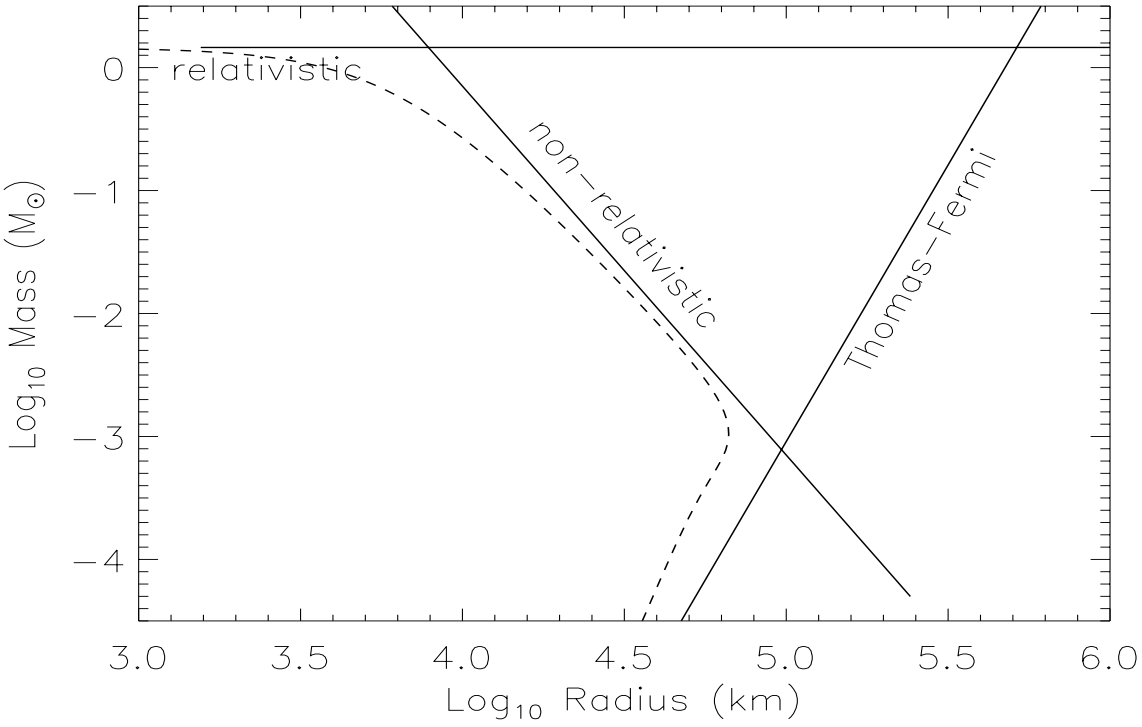

Figure 9.3.1: The mass-radius diagram for cold compact objects. The solid lines are the limiting expressions; the dashed line is the full result for a composition of pure ^{12}C.

The maximum radius configuration has the properties, approximately, of the planet Jupiter.

In the relativistic limit, for radii much smaller than 5000 km, the equation of state will deviate from that of a $\gamma = 4/3$ gas. Electron capture will reduce Y_e and the value of the Chandrasekhar mass. Therefore, a regime where $dM/d\rho_c < 0$ will exist. Such a regime is dynamically unstable. At sufficiently high density, where nuclear forces become important, the effective value of γ will increase, the mass will reach a minimum value ($M_{min} \simeq 0.01$ $M_\odot$, where $R \simeq 300$ km), and stability is restored. As the central density increases further, $dM/d\rho_c > 0$. This is the neutron star regime. As the mass increases, and the radius shrinks, general relativity, which we have heretofore ignored, becomes important. The most important feature that general relativity introduces is that at densities well in excess of the nuclear saturation density, $\rho_s = 2.7 \cdot 10^{14}$ g cm^{-3}, the mass reaches a maximum value, in the range 1.5-3 $M_\odot$. Larger density configurations are once again dynamically unstable. The maximum mass is discussed in a subsequent lecture.

9.4. Cooling of white dwarfs

The interior of a white dwarf has energy transport dominated by conduction. The electrons are extremely degenerate, nowever, so they must have very large mean free paths. The thermal conductivity is very high. The temperature gradient must be rather small. The interior is roughly isothermal. Near the surface, isothermality breaks down as the opacity increases. The surface regions are diffusive, with a temperature gradient

$$\frac{dT}{dr} = -\frac{3}{4ac}\frac{\kappa\rho}{T^3}\frac{L}{4\pi r^2}.$$

At the high densities, Kramer's opacity is dominant: $\kappa = \kappa_o \rho T^{-3.5}$, with $\kappa_o \simeq 4.3 \times 10^{24} Z(1+X)$ cm^2 g^{-1}. With hydrostatic equilibrium,

$$\frac{dP}{dT} = \frac{4ac}{3}\frac{4\pi G m\,(r)}{\kappa_o L}\frac{T^{6/5}}{\rho}.$$

The surface layer is thin, so $m(r) = M$. Using the nondegenerate pressure $P = N_o \rho k T/\mu$, and eliminating ρ, we have

$$PdP = \frac{4ac}{3}\frac{4\pi GM}{\kappa_o L}\frac{kN_o}{\mu}T^{7.5}dT.$$

This can be integrated from $P = 0$ at $T = 0$ to the interior, which gives

$$\rho = \sqrt{\frac{2}{8.5}\frac{4ac}{3}\frac{4\pi GM}{\kappa_o L}\frac{\mu}{kN_o}}T^{3.25}.$$

The surface approximation breaks down in the interior when matter becomes degenerate. This occurs when the non-degenerate pressure equals the degenerate pressure at radius r_* where one has ρ_* and T_*. This results in

$$\rho_* = 2/4 \times 10^{-8} T_*^{3/2} Y_e^{-1} \text{ g cm}^{-3},$$

or

$$L = 5.7 \times 10^5 \frac{\mu Y_e^2}{Z\,(1+X)} \frac{M}{\mathrm{M}_\odot} T_*^{3.5} \ \mathrm{ergs}^{-1}.$$

This is similar to the blackbody law $L = 4\pi R^2 \sigma T_{eff}^4$, but involves the interior temperature, not the visible temperature of the surface. It suggests a relation like $T_e ff \propto T_*^{7/8}$ exists. From L and M, and the composition, one can deduce T_*, the interior temperature. L of $10^{-2} - 10^{-5}$ $\mathrm{L}_\odot$ imply $T_* = 10^6 - 10^7$ K and $\rho_* < 10^3$ g cm^{-3}. One can find also that

$$\frac{R - r_*}{R} \simeq 4.25 \frac{R N_o k T_*}{G M \mu} \lesssim 10^{-2}.$$

The energy that is radiated as thermal energy by the white dwarf is the residual ion thermal energy, since the electrons are degenerate and the star can't release any gravitational energy. For a monatomic non-degenerate ion gas, with $c_v = 3k/2$ the total thermal energy is (with $T_* = T$)

$$U = \frac{3}{2} \frac{N_o k}{A} T M.$$

The cooling rate is $L = -dU/dt$. Using $L = CMT^{7/2}$, one finds

$$t = t_o + \frac{3}{5} \frac{k N_o}{AC} \left(T^{-5/2} - T_o^{-5/2} \right).$$

Taking $T << T_o$, the cooling time is

$$\tau = \frac{3}{5} \frac{N_o k T}{A} \frac{M}{L} = \frac{3}{5} \frac{N_o k}{CA} \frac{CM}{L}^{5/7}.$$

For $L \sim 10^{-3}$ $\mathrm{L}_\odot$, we obtain $\tau \sim 10^9$ yr.

It is interesting to compare the cooling theory with observations. Like cars on a highway, the slower they go, the more congested the freeway (or vice versa). The number of white dwarfs of a given luminosity should relate to their relative abundance, especially if the birth rate of white dwarfs has been roughly constant in time. The luminosity function is $\phi(L)$ which is the space density of white dwarfs per unit interval of $\log L$. Thus, with a uniform production rate,

$$\phi\,(L) \propto \left[\frac{d \log\,(L)}{dt} \right]^{-1}.$$

If $\tau \propto L^{-\alpha}$, where our theory suggests $\alpha \simeq 5/7$, one finds

$$\log \phi = -\alpha \log L + \ \text{constant}.$$

It turns out this is approximately matched by observations, until $L \lesssim 10^{-4}$ $\mathrm{L}_\odot$. Theoretical corrections to the specific heat of very cold white dwarfs imply that $\alpha \to 0$ below this luminosity, but observations actually reveal that $\alpha << 0$ when $L \lesssim 10^{-4.5}$. This deficit of white dwarfs of low luminosity is due to the finite age of the galactic disc. The cooling time of the white dwarfs where the sudden drop in α occurs then yields an estimate of the age of the galactic disc, about 10 billion years.

Chapter 10.
Stellar Atmospheres

10.1. Basic Assumptions for Stellar Atmospheres

A stellar atmosphere is by definition a boundary, one in which photons decouple from matter. Deep in an atmosphere, photons and matter are in strict thermodynamic equilibrium. Near the surface, however, the photon mean free path becomes comparable to the length scale (temperature scale height or pressure scale height) and the photons decouple, eventually becoming freely streaming. Nevertheless, the matter itself is maintained in local thermodynamic equilibrium nearly up to the physical surface itself, by which point the photons are nearly completely decoupled.

It is often useful to discriminate between the continuum and lines in the emergent spectrum, although the continuum is in reality the sum of many weak lines.

The thickness of the atmosphere will generally be very small compared to the radius of the star. Then the geometry will be that of a semi-infinite slab, in which the gravity is constant: $g = GM/R^2$. The equation of hydrostatic equilibrium is then

$$dP/dz = g\rho,$$

where $z = (R - r)$ is the depth. In addition, no appreciable sources or sinks of energy exist in a normal atmosphere, so the conservation of energy is

$$\nabla \cdot \vec{F} = 0 = dF/dz, \qquad F = \text{ constant} = \sigma T_e^4 = L/\left(4\pi R^2\right),$$

where F is the flux and T_e is the effective temperature.

10.2. Equation of Radiative Transfer

The flow equation for photons is derived from the Boltzmann transport equation. In general, if f represents the density in phase space (both spatial and momentum), we can write

$$\frac{\partial f}{\partial t} + \sum_i^3 \left(\dot{x}_i \frac{\partial f}{\partial x_i} + \dot{p}_i \frac{\partial f}{\partial p_i} \right) = S, \tag{10.2.1}$$

where S is the source function which governs the creation and destruction, locally, of photons.

The specific intensity describes the flow of energy in a particular direction ($\vec{n}$), through a differential area (dA), into a differential solid angle ($d\Omega$), at a specific point:

$$I_\nu\left(p, \vec{n}\right) = \frac{dE_\nu}{dA \cos\theta d\Omega d\nu dt}.$$

The momentum p is related to the frequency ν by $p = h\nu/c$. The number of photons travelling in direction $\vec{n}$ and crossing dA in a time dt comes from the volume $dV = cdAdt$, while the number of photons occupying that volume is

$$dN = f\left(4\pi p^2 dp\right)(cdAdt).$$

Therefore the energy contained in those "travelling" photons, moving in the direction $\vec{n}$, is

$$dE_\nu = h\nu\cos\theta dN d\Omega/4\pi.$$

Therefore

$$I_\nu(p,\vec{n}) = \frac{h^4\nu^3}{c^3}f, \qquad f = \frac{c^3}{h^4\nu^3}I_\nu(p,\vec{n}).$$

Eq. (10.2.1) can be written

$$\frac{\partial f}{\partial t} + \dot{\vec{r}}\cdot\nabla f + \dot{\vec{p}}\cdot\nabla_p f = S,$$

which can be simplified because we will be assuming no time dependence for our atmosphere, and that there are no strong potentials influencing the photons, so that $\dot{\vec{p}} = 0$. Using $\dot{\vec{r}} = c\vec{n}$, and $\vec{n}\cdot\nabla = \cos\theta d/dr$

$$\cos\theta\frac{dI_\nu}{dr} = \frac{h^4\nu^3}{c^3}S.$$

Photons are lost from the flow due to absorption and to scattering, but are added to the flow due to emission and to scattering. This can be summarized by

$$\begin{aligned}\frac{h^4\nu^3}{c^2}S =& \rho j_\nu - (\kappa_\nu + \sigma_\nu)\rho I_\nu(\Omega) + \\ & \frac{\rho\sigma_\nu}{4\pi}\int_0^\infty\int_{4\pi} R_{\nu,\nu'}\left(\Omega,\Omega'\right)I_{\nu'}\left(\Omega'\right)d\Omega' d\nu'.\end{aligned} \tag{10.2.2}$$

Here, $R = \frac{h}{c}(\frac{\nu}{\nu'})^3\mathcal{R}$, where R is the scattering redistribution function, normalized so

$$\int_0^\infty\int_0^\infty\int_{4\pi}\int_{4\pi}\mathcal{R}_{\nu',\nu}\left(\Omega',\Omega\right)d\Omega' d\Omega d\nu' d\nu = 1.$$

Also, j_ν is the volume emissivity, κ_ν is the opacity (mass absorption coefficient), and σ_ν is the scattering opacity (mass scattering coefficient). In thermal equilibrium, Kirchoff's law stipulates that

$$j_\nu = \kappa_\nu B_\nu(T)$$

where $B_\nu(T)$ is Planck's function. The optical depth is defined

$$d\tau_\nu = -(\kappa_\nu + \sigma_\nu)\rho dr = (\kappa_\nu + \sigma_\nu)dz$$

(note it is frequency dependent) and we may now write the equation of radiative transfer

$$\mu\frac{dI_\nu(\mu,\tau_\nu)}{d\tau_\nu} = I_\nu(\mu,\tau_\nu) - S_\nu(\mu,\tau_\nu). \tag{10.2.3}$$

The source function S_ν is the ratio of the total emissivity to the total opacity

$$S_\nu = \frac{\kappa_\nu B_\nu}{\kappa_\nu + \sigma_\nu} + \frac{\sigma_\nu}{4\pi\left(\kappa_\nu + \sigma_\nu\right)} \int_0^\infty \int_{4\pi} R_{\nu',\nu} I_{\nu'}\left(\Omega'\right) d\Omega' d\nu'.$$

To appreciate the meaning of the source function, note that if scattering is unimportant, $S_\nu = B_\nu$ since all photons locally contributed to the radiation field are thermal. If pure absorption processes are negligible, then the source function depends only on the incident radiation field, and is just an average of the specific intensity over angle and energy. In this case, the source function is not dependent on local conditions (i.e., ρ and T). This is the situation in a fog: the light transmitted through the fog carries no information about the physical conditions in the fog. But the transfer equation can be solved without knowing anything about the fog.

The redistribution function can have the following limits:

- Coherent scattering: no energy change, but a directional change. Then R contains $\delta(\nu - \nu')$.
- Noncoherent scattering: frequency of scattered photon is uncorrelated with that of the incident photon. Then R is independent of both ν' and ν.
- Isotropic scattering: direction of scattered photon is uncorrelated with that of incident photon. Then R is independent of both Ω' and Ω.
- Coherent isotropic scattering: $R = \delta(\nu - \nu')$. This is the situation prevailing in normal stellar atmospheres, and one has

$$S_\nu = \frac{\kappa_\nu B_\nu}{\kappa_\nu + \sigma_\nu} + \frac{\sigma_\nu}{4\pi\left(\kappa_\nu + \sigma_\nu\right)} \int_{4\pi} I_\nu\left(\Omega'\right) d\Omega'.$$

10.3. Moments of the Radiation Field

Mean Intensity (Zeroth Moment)

$$\begin{aligned} J_\nu\left(\tau_\nu\right) &= \frac{\int_{4\pi} I_\nu\left(\mu,\tau_\nu\right) d\Omega}{\int_{4\pi} d\Omega} = \frac{1}{4\pi}\int_{4\pi} I_\nu\left(\mu,\tau_\nu\right) d\Omega \\ &= \frac{1}{2}\int_{-1}^{1} I_\nu\left(\mu,\tau_\nu\right) d\mu, \end{aligned} \tag{10.3.1}$$

where the last holds in a plane-parallel atmosphere.

Flux (First Moment)

$$\begin{aligned} \vec{H}_\nu\left(\tau_\nu\right) &= \frac{\int_{4\pi} I_\nu\left(\mu,\tau_\nu\right)\vec{n} d\Omega}{\int_{4\pi} d\Omega} = \frac{1}{4\pi}\int_{4\pi} I_\nu\left(\mu,\tau_\nu\right)\vec{n} d\Omega \\ &= \frac{\vec{n}}{2}\int_{-1}^{1} I_\nu\left(\mu,\tau_\nu\right)\mu d\mu \end{aligned} \tag{10.3.2}$$

We will use the radiative flux, defined by

$$F_\nu(\tau_\nu) = 2\int_{-1}^{1} I_\nu(\mu,\tau_\nu)\,\mu d\mu. \tag{10.3.3}$$

Pressure (Second Moment)

In the plane-parallel case, one can define

$$K_\nu(\tau_\nu) = \frac{1}{2}\int_{-1}^{1} I_\nu(\mu,\tau_\nu)\,\mu^2 d\mu = \frac{c}{4\pi}P_\nu(\tau_\nu). \tag{10.3.4}$$

10.4. Radiative Equilibrium

Integrate the radiative transfer equation over all ν and Ω:

$$\frac{1}{\rho}\frac{d}{dz}\int d\nu\int_{4\pi} I_\nu\mu d\Omega = \int d\nu\int_{4\pi}(\kappa_\nu+\sigma_\nu)\,I_\nu d\Omega - \int_{4\pi} d\Omega\int(\kappa_\nu+\sigma_\nu)\,S_\nu d\nu = 0. \tag{10.4.1}$$

This vanishes because in local equilibrium the energy gained from the beam must balance the energy lost. This means both

$$\int(\kappa_\nu+\sigma_\nu)\,J_\nu d\nu = \int(\kappa_\nu+\sigma_\nu)\,S_\nu d\nu, \qquad \frac{d}{dz}\int F_\nu d\nu = \frac{dF}{dz} = 0. \tag{10.4.2}$$

10.5. Moments of the Radiative Transfer Equation

In turn, we multiply the transfer equation by powers of μ, then integrate over μ. Assume coherent isotropic scattering, for which

$$S_\nu = \frac{\kappa_\nu}{\kappa_\nu+\sigma_\nu}B_\nu + \frac{\sigma_\nu}{\kappa_\nu+\sigma_\nu}J_\nu.$$

Now integrating the transfer equation over μ yields

$$\frac{1}{4}\frac{dF_\nu(\tau_\nu)}{d\tau_\nu} = \frac{\kappa_\nu}{\kappa_\nu+\sigma_\nu}\left[B_\nu(\tau_\nu) - J_\nu(\tau_\nu)\right].$$

Scattering contributions have disappeared. Multiply by μ and integrate to obtain the first moment equation:

$$2\frac{dK(\tau_\nu)}{d\tau_\nu} = \frac{1}{2}F_\nu(\tau_\nu), \tag{10.5.1}$$

as the integral of μS_ν vanishes.

Note that if we integrate the zeroth moment equation over all frequencies, the right-hand side must vanish since no energy is gained or lost in the atmosphere. Then we have

$$\frac{dF(\tau)}{d\tau} = 0, \qquad F(\tau) = \text{ constant}. \tag{10.5.2}$$

10.6. Boundary Conditions

Imagine that one can expand the radiation field:

$$I_\nu(\mu,\tau_\nu)=\sum_i I_i(\tau_\nu)\,\mu^i,$$

which is especially useful when I_0 dominates (isotropy of radiation field). Then, $J_\nu\simeq I_0$, $F_\nu\simeq(4/3)I_1$, $K_\nu\simeq I_0/3$, which will apply deep in the interior. Thus in conditions of near isotropy we have that

$$K_\nu(\tau_\nu)\simeq\frac{1}{3}J_\nu(\tau_\nu),\qquad \tau_\nu\to\infty \tag{10.6.1}$$

which is known as the diffusion approximation. It can be used to close the moment equations:

$$\frac{dF_\nu(\tau_\nu)}{d\tau_\nu}=\frac{4\kappa_\nu}{\kappa_\nu+\sigma_\nu}\left[B_\nu(\tau_\nu)-J_\nu(\tau_\nu)\right],\quad \frac{dJ(\tau_\nu)}{d\tau_\nu}=\frac{3}{4}F_\nu(\tau_\nu). \tag{10.6.2}$$

Consider instead conditions near the surface. Generally, there is no incident radiation field. Assuming the emergent intensity nevertheless to be nearly isotropic in the forward direction, we have

$$J_\nu(0)=\frac{1}{2}\int_0^1 I_\nu(\mu,0)\,d\mu=\frac{1}{2}\sum_i\frac{I_i(0)}{i+1}\simeq\frac{I_0(0)}{2},$$
$$F_\nu(0)=2\int_0^1 I_\nu(\mu,0)\,\mu d\mu=2\sum_i\frac{I_i(0)}{i+2}\simeq I_0(0).$$

Therefore,

$$J_\nu(0)=F_\nu(0)/2,\qquad \tau_\nu\to 0 \tag{10.6.3}$$

which is the Eddington approximation.

10.7. Solutions of the Radiative Transfer Equation

10.7.1. Classical Solution

For simplicity, we will drop the ν subscript (but remeber that it is there!).

$$\mu\frac{dI(\mu,\tau)}{d\tau}=I(\mu,\tau)-S(\mu,\tau) \tag{10.7.1}$$

This equation has an integrating factor $e^{-\tau/\mu}$:

$$\mu\frac{d}{d\tau}\left[I(\mu,\tau)\,e^{-\tau/\mu}\right]=-S(\tau)\,e^{-\tau/\mu}.$$

Integrating:

$$I(\mu,\tau)\,e^{-\tau/\mu} = -\int S(t)\,e^{-t/\mu}\frac{dt}{\mu}, \tag{10.7.2}$$

to within a constant. Suppose we evaluate this between two optical depth points, τ_1 and τ_2. Then

$$I(\mu,\tau_1) = I(\mu,\tau_2)\,e^{(\tau_1-\tau_2)/\mu} + \int_{\tau_1}^{\tau_2} S(t)\,e^{(\tau_1-t)/\mu}\frac{dt}{\mu}. \tag{10.7.3}$$

The emergent intensity of a semi-infinite slab can be found if we take $\tau_1 = 0$ and $\tau_2 = \infty$:

$$I(\mu,0) = \int_0^{\infty} S(t)\,e^{-t/\mu}\frac{dt}{\mu}, \tag{10.7.4}$$

which is a weighted mean of the source function, the weighting function being the fraction of energy that can penetrate from depth t to the surface. If S is a linear function of depth $S(t) = a + bt$ then $I(\mu,0)$ is the Laplace transform of S, $I(0,\mu) = a + b\mu$.

Now suppose that we have a finite atmosphere of thickness T within which S is constant. Then the emergent intensity is

$$\begin{aligned} I(\mu,0) &= I(\mu,T)\,e^{-T/\mu} + S\int_0^T e^{-t/\mu}\frac{dt}{\mu} \\ &= I(\mu,T)\,e^{-T/\mu} + S\left(1 - e^{-T/\mu}\right). \end{aligned} \tag{10.7.5}$$

If $T >> 1$ we have $I(\mu,0) = S$: the intensity saturates and is independent of angle.

It is most convenient to discuss this equation at an arbitray point when we impose one of two boundary conditions, either at $\tau = 0$ or $\tau = \infty$. If $\tau_1 = 0$ we have

$$I(\mu,0) = I(\mu,\tau)\,e^{-\tau/\mu} + \int_0^{\tau} S(t)\,e^{-t/\mu}\frac{dt}{\mu},$$

or

$$I(\mu,\tau) = I(\mu,0)\,e^{\tau/\mu} - \int_0^{\tau} S(t)\,e^{(\tau-t)/\mu}\frac{dt}{\mu}.$$

In particular, for $\mu < 0$ when there is no incident radiation ($I(\mu,0) = 0$),

$$I(\mu,\tau) = -\int_0^{\tau} S(t)\,e^{(\tau-t)/\mu}\frac{dt}{\mu}. \qquad -1 < \mu < 0 \tag{10.7.6}$$

For $\mu > 0$ we can take $\tau_1 = \infty$, on the other hand, and using $\tau_2 = \tau$

$$I(\mu,\tau) = \int_{\tau}^{\infty} S(t)\,e^{(\tau-t)/\mu}\frac{dt}{\mu}. \qquad 1 > \mu > 0 \tag{10.7.7}$$

10.7.2. Schwarzschild-Milne Integral Equations

Consider the mean intensity

$$J(\tau) = \frac{1}{2}\int_{-1}^{+1} I(\mu,\tau)\,d\mu$$
$$= \frac{1}{2}\int_0^1 d\mu \int_\tau^\infty S(t)\,e^{(\tau-t)/\mu}\frac{dt}{\mu} - \frac{1}{2}\int_{-1}^0 d\mu \int_0^\tau S(t)\,e^{(\tau-t)/\mu}\frac{dt}{\mu}.$$

Interchange the order of integration:

$$J(\tau) = \frac{1}{2}\int_\tau^\infty S(t)\,dt \int_1^\infty e^{-w(t-\tau)}\frac{dw}{w} + \frac{1}{2}\int_0^\tau S(t)\,dt \int_1^\infty e^{-w(\tau-t)}\frac{dw}{w},$$

where we used $w = 1/\mu$ in the first term and $w = -1/\mu$ in the second. The w integrals are called exponential integrals:

$$E_n(x) = \int_1^\infty t^{-n}e^{-xt}dt = x^{n-1}\int_x^\infty t^{-n}e^{-t}dt. \tag{10.7.8}$$

Note that

$$E_n'(x) = -E_{n-1}(x) \tag{10.7.9}$$

and

$$E_n(x) = \frac{1}{n-1}\left[e^{-x} - xE_{n-1}(x)\right], \qquad n > 1. \tag{10.7.10}$$

For large arguments, an asymptotic expansion exists:

$$E_1(x) = \frac{e^{-x}}{x}\left[1 - \frac{1}{x} + \frac{2!}{x^2} - \frac{3!}{x^3} + \cdots\right]. \tag{10.7.11}$$

For small x, we can use

$$E_1(x) = -\gamma - \ln x + \sum_{k=1}^\infty (-1)^{k-1}\frac{x^k}{kk!}, \qquad x > 0, \tag{10.7.12}$$

where $\gamma = 0.5572156\ldots$. Obviously, $E_1(x)$ is singular at the origin, but $E_n(0) = (n-1)^{-1}$ is finite for $n > 1$. However, $E_2(x)$ has a singularity in its first derivative at the origin: $E_2'(0) = -E_1(0)$.

It is useful to collect also these results for the integrals of elementary functions with E_1:

$$\frac{1}{2}\int_0^\infty E_1|t-\tau|t^p dt = \frac{p!}{2}\left[\sum_{k=0}^p \frac{\tau^k}{k!}\delta_\alpha + (-1)^{p+1}E_{p+2}(\tau)\right], \tag{10.7.13}$$

where $\delta_\alpha = 0$ if $\alpha = p+1-k$ is even, and $\delta_alpha = 2/\alpha$ if α is odd. For $p = 0$ [1] (2), the right-hand side of Eq. (10.7.13) is $1 - E_2(\tau)/2$ $[\tau + E_3(\tau)/2]$ $(2/3 - E_4(\tau) + \tau^2)$. Finally, for $a > 0$ and $a \neq 1$,

$$\frac{1}{2}\int_0^\infty E_1|t-\tau|e^{-at}dt = \frac{e^{-a\tau}}{2a}\left[\ln\left|\frac{a+1}{a-1}\right| - E_1(\tau - a\tau)\right] + \frac{E_1(\tau)}{2a}.$$

The mean flux can be written now as

$$\begin{aligned} J(\tau) &= \frac{1}{2}\int_{\tau}^{\infty} S(t)\, E_1(t-\tau)\, dt + \frac{1}{2}\int_{0}^{\tau} S(t)\, E_1(\tau - t)\, dt \\ &= \frac{1}{2}\int_{0}^{\infty} S(t)\, E_1|t-\tau| dt. \end{aligned} \tag{10.7.14}$$

Similarly, we can find

$$F(\tau) = 2\int_{\tau}^{\infty} S(t)\, E_2(t-\tau)\, dt - 2\int_{0}^{\tau} S(t)\, E_2(\tau - t)\, dt, \tag{10.7.15}$$

and

$$K(\tau) = \frac{1}{2}\int_{0}^{\infty} S(t)\, E_3|t-\tau| dt. \tag{10.7.16}$$

Recall that the source function, in the case of coherent isotropic scattering, can be written as

$$S = \frac{\kappa}{\kappa+\sigma}B + \frac{\sigma}{\kappa+\sigma}J \equiv J + \epsilon(B-J), \tag{10.7.17}$$

so we can find an integral equation for the source function itself:

$$S(\tau) = \epsilon B(\tau) + \frac{1-\epsilon}{2}\int_{0}^{\infty} S(t)\, E_1|\tau - t| dt. \tag{10.7.18}$$

The Planck function makes this equation inhomogeneous. This equation is more general than the assumptions indicate. As long as the angular dependence of the redistribution function is known, it is possible to do the solid angle integrals and express the source function as moments of the radiation field. The moments can be generated from the classical solution, which yields an integral equation like the above.

Since S can be written in terms of J, we also have

$$J(\tau) = \int_{0}^{\infty} \frac{\epsilon}{2} B(t)\, E_1|\tau - t| dt + \int_{0}^{\infty} \frac{1-\epsilon}{2} J(t)\, E_1|\tau - t| dt. \tag{10.7.19}$$

Remember that ϵ is a function of τ and has to be inside the integrals.

10.7.3. Asymptotic Form of the Transfer Equation

The condition of radiative equilibrium demands that at each point

$$\int_{0}^{\infty} (\kappa_\nu + \sigma_\nu) J_\nu(\tau_\nu)\, d\nu = \int_{0}^{\infty} (\kappa_\nu + \sigma_\nu) S_\nu(\tau_\nu)\, d\nu.$$

For isotropic coherent scattering, we have

$$\int_{0}^{\infty} (\kappa_\nu + \sigma_\nu) J_\nu(\tau_\nu)\, d\nu = \int_{0}^{\infty} \kappa_\nu B_\nu(\tau_\nu)\, d\nu + \int_{0}^{\infty} \sigma_\nu J_\nu(\tau_\nu)\, d\nu,$$

or simply

$$\int_{0}^{\infty} \kappa_\nu J_\nu(\tau_\nu)\, d\nu = \int_{0}^{\infty} \kappa_\nu B_\nu(\tau_\nu)\, d\nu. \tag{10.7.20}$$

The scattering has cancelled out. This suggests that at large optical depth, the source function is nearly the Planck function. Also, the thermal emission is set by the local radiation field.

Now consider great depths in a semi-infinite atmosphere, where we expect that $S_\nu \approx B_\nu$. Making a Taylor expansion:

$$S_\nu(t) = \sum_{n=0}^{\infty} \frac{(t-\tau)^n}{n!} \frac{d^n B_\nu(\tau)}{d\tau^n}. \tag{10.7.21}$$

Substituting into the classical solution Eq. (10.7.2) we find for $\mu > 0$

$$\begin{aligned} I_\nu(\mu,\tau) &= \sum_{n=0}^{\infty} \frac{1}{n!} \frac{d^n B_\nu}{d\tau^n} \int_\tau^\infty (t-\tau)^n e^{(\tau-t)/\mu} \frac{dt}{\mu} = \sum_{n=0}^{\infty} \frac{d^n B_\nu}{d\tau^n} \frac{1}{n!} \int_0^\infty x^n e^{-x/\mu} \frac{dx}{\mu} \\ &= \sum_{n=0}^{\infty} \mu^n \frac{d^n B_\nu}{d\tau^n} = B_\nu(\tau) + \mu \frac{dB_\nu}{d\tau} + \mu^2 \frac{d^2 B_\nu}{d\tau^2} + \cdots. \end{aligned} \tag{10.7.22}$$

For $\mu < 1$, to within terms of $e^{-\tau/\mu} << 1$, the same result for $I_\nu(\mu,\tau)$ exists. Therefore

$$J_\nu(\tau) = \frac{1}{2} \sum_{n=0}^{\infty} \frac{d^n B_\nu}{d\tau^n} \int_{-1}^{1} \mu^n d\mu = \sum_{n=0}^{\infty} \frac{1}{2n+1} \frac{d^{2n} B_\nu}{d\tau^{2n}} = B_\nu(\tau) + \frac{1}{3} \frac{d^2 B_\nu}{d\tau^2} + \cdots, \tag{10.7.23}$$

$$F_\nu(\tau) = \sum_{n=0}^{\infty} \frac{4}{2n+3} \frac{d^{2n+1} B_\nu}{d\tau^{2n+1}} = \frac{1}{3} \frac{dB_\nu}{d\tau} + \frac{1}{5} \frac{d^3 B_\nu}{d\tau^3} + \cdots, \tag{10.7.24}$$

and

$$K_\nu(\tau) = \sum_{n-0}^{\infty} \frac{1}{2n+3} \frac{d^{2n} B_\nu}{d\tau^{2n}} = \frac{1}{3} B_\nu(\tau) + \frac{1}{5} \frac{d^2 B_\nu}{d\tau^2} + \cdots. \tag{10.7.25}$$

Note the relation to the diffusion approximation Eq. (10.6.1) established earlier. We can write

$$F_\nu = -\frac{4}{3} \left(\frac{1}{\kappa_\nu \rho} \frac{dB_\nu}{dT} \right) \frac{dT}{dr}, \tag{10.7.26}$$

where the coefficient of dT/dr is the *radiative conductivity*. This equation is simply the stellar structure luminosity equation established earlier.

It turns out to be conceptually simplifying to keep μ positive for *all* rays. Thus, where $\mu < 0$ in the above, we will write $-\mu$ henceforth. The classical solution, using $\tau_1 = 0, \tau_2 = \tau$ and $I_\nu(-\mu, 0) = 0$ for $\mu < 0$, and $\tau_1 = \tau, \tau_2 = \infty$ for $\mu > 0$ is then

$$\begin{aligned} I_\nu(+\mu,\tau) &= \int_\tau^\infty \frac{S_\nu(t)}{\mu} e^{(\tau-t)/\mu} dt \qquad \mu > 0 \\ I_\nu(-\mu,\tau) &= \int_0^\tau \frac{S_\nu(t)}{\mu} e^{-(\tau-t)/\mu} dt. \qquad \mu < 0 \end{aligned} \tag{10.7.27}$$

10.8. Mean Opacities

For each a given atmospheric equation, it is possible to write the general frequency-dependent equation in a gray form by defining a different mean opacity. For example, if we wanted a correspondance for the fluxes

$$\int_0^\infty \kappa_\nu F_\nu d\nu \equiv \kappa_F F,$$

we could define a flux-weighted mean:

$$\bar{\kappa}_F = \int_0^\infty \kappa_\nu \left(F_\nu / F\right) d\nu. \tag{10.8.1}$$

However, a practical difficulty is that we don't know F_ν a priori.

A correspondance for the integrated flux

$$\int_0^\infty F_\nu d\nu = F$$

would instead imply the mean $\bar{\kappa}$:

$$\frac{1}{\rho\bar{\kappa}}\frac{dK}{dz} = \frac{F}{4} = \int_0^\infty \frac{F_\nu}{4} d\nu = \int_0^\infty \frac{1}{\rho\kappa_\nu}\frac{dK_\nu}{dz} d\nu. \tag{10.8.2}$$

Obviously, we don't know K_ν a priori either, but at great depth, where $3K_\nu \to J_\nu \to B_\nu$, we can define the Rosseland mean opacity

$$\frac{1}{\bar{\kappa}_R} = \frac{\int_0^\infty \frac{1}{\kappa_\nu}\frac{dB_\nu}{dz}}{\int_0^\infty \frac{dB_\nu}{dz} d\nu} = \frac{\int_0^\infty \frac{1}{\kappa_\nu}\frac{dB_\nu}{dT} d\nu}{\frac{dB}{dT}}. \tag{10.8.3}$$

This choice is especially useful, since the frequency-integrated form of the structure equation Eq. (10.7.26) would involve precisely this mean.

10.9. Gray Atmospheres

In a gray atmosphere, there is by definition no frequency dependence. The condition of radiative equilibrium then states simply that

$$S\left(\tau\right) = J\left(\tau\right) = B\left(\tau\right) = \frac{\sigma T^4}{\pi}, \tag{10.9.1}$$

illustrating that the individual roles of scattering and absorption are irrelevant. The integral equations for the source function and the moments of the radiation field become:

$$B\left(\tau\right) = \frac{1}{2}\int_0^\infty B\left(t\right) E_1|t-\tau| dt, \qquad J\left(\tau\right) = \frac{1}{2}\int_0^\infty J\left(t\right) E_1|t-\tau| dt,$$

$$F(\tau) = 2\int_{\tau}^{\infty} B(t)\, E_2(t-\tau)\, dt - 2\int_{0}^{\tau} B(t)\, E_2(\tau - t)\, dt,$$

$$K(\tau) = \frac{1}{2}\int_{0}^{\infty} B(t)\, E_3|t-\tau| dt. \tag{10.9.2}$$

The zeroth moment of the transfer equation is now

$$\frac{1}{4}\frac{dF}{d\tau} = J - J = 0 \tag{10.9.3}$$

and the first moment equation is

$$\frac{dK}{d\tau} = \frac{F}{4}. \tag{10.9.4}$$

These are integrable:

$$K(\tau) = \frac{1}{4}F\tau + \text{ constant}. \tag{10.9.5}$$

At very large depth, the diffusion approximation gives $J(\tau) \to 3K(\tau) \to 3F\tau/4$, and at the surface the Eddington approximation gives $J(0) = F(0)/2$. Therefore, a general expression for J is

$$J(\tau) = \frac{3}{4}F[\tau + q(\tau)]. \tag{10.9.6}$$

From Eq. (10.9.2) one sees that then

$$\tau + q(\tau) = \frac{1}{2}\int_{0}^{\infty} [t + q(t)]\, E_1|t-\tau| dt.$$

In addition, the constant in Eq. (10.9.5) must be $q(\infty)$ since $K = 3J$ as $\tau \to \infty$. A general solution of the gray atmosphere is equivalent to solving for $q(\tau)$. We will look at some approximate solutions.

10.9.1. Approximate Solutions

Evaluating the expression Eq. (10.9.6) at the surface, we find

$$J(0) = \frac{3F}{4}q(0) \simeq \frac{F}{2},$$

or $q(0) \simeq 2/3$. The simplest solution to the gray atmosphere problem is simply to choose $q(\tau) = 2/3$.

Formally, the Eddington approximation consists of assuming $K = J/3$ everywhere. This has already shown to be true at great depths, but in fact is true in a wider variety of situations also. Consider:

a) $I(\mu)$ expandable in odd powers of μ only (except for I_0 which is still dominate). Therefore only the I_0 term contributes to J or K and we generally obtain $J = 3K$.

b) $I(\mu) = I_0$ for $\mu > 0$ and 0 for $\mu < 0$. Then

$$J = \frac{I_0}{2}\int_{0}^{1} d\mu = \frac{I_0}{2}, \qquad K = \frac{I_0}{2}\int_{0}^{1} \mu^2 d\mu = \frac{I_0}{6}.$$

c) Two-stream model. $I(\mu) = I_+$ for $\mu > 0$ and I_- for $\mu < 0$. Then

$$J = \frac{I_+}{2}\int_0^1 d\mu + \frac{I_-}{2}\int_{-1}^0 d\mu = \frac{I_+ + I_1}{2}, \quad K = \frac{I_+}{2}\int_0^1 \mu^2 d\mu + \frac{I_-}{2}\int_{-1}^0 \mu^2 d\mu = \frac{I_+ + I_-}{6}.$$

An exception is provided by a beam, in which $I(\mu) = \delta(\mu - \mu_0)$, for which $J = I_0$ and $K = I_0\mu_0^2$.

When $J = 3K$, we can write the result $K_E = F\tau/4 + C$ as

$$J_E(\tau) = B(\tau) = 3F\tau/4 + C'. \tag{10.9.7}$$

Using Eq. (10.9.2) for the flux at the surface, we have

$$F(0) = 2\int_0^\infty \left(\frac{3}{4}Ft + C'\right) E_2(t)\, dt = 2C'E_3(0) + \frac{3}{4}F\left[\frac{4}{3} - 2E_4(0)\right] = F.$$

With $E_n(0) = (n-1)^{-1}$, we find $C' = F/2$ and

$$J_E(\tau) = \frac{3}{4}F\left(\tau + \frac{2}{3}\right).$$

Since $B(\tau) = \sigma T^4/\pi$, we also have

$$T^4 = \frac{3}{4}T_{eff}^4\left(\tau + \frac{2}{3}\right),$$

so $T(0) = 2^{-1/4}T_{eff}$. Also note that when $\tau = 2/3$ that $T = T_{eff}$, so the effective depth of the continuum is often taken to be at optical depth 2/3.

10.9.2. Limb Darkening

From the gray result for the mean flux in the Eddington approximation, Eq. (10.9.7), we can immediately calculate the angular dependence of the emergent intensity using the classical solution's properties of Laplace transforms:

$$I_E(\mu, 0) = \frac{3}{4}F\int_0^\infty \left(\tau + \frac{2}{3}\right) e^{-\tau/\mu}\frac{d\tau}{\mu} = \frac{3}{4}F\left(\mu + \frac{2}{3}\right).$$

Applied to the Sun, the center of its disc is at $\mu = 1$. The relative intensity as one traverses the Sun's disc is therefore

$$\frac{I_E(\mu, 0)}{I_E(1, 0)} = \frac{3}{5}\left(\mu + \frac{2}{3}\right),$$

with an intensity of the Sun's limb only 40% of its center. This is not in serious disagreement with observations.

Since the source function is determined by T, the depth dependence of T can be determined by measuring the angular dependence of limb darkening. Measurements of this limb darkening therefore yields information on the temperature gradient underneath the surface.

10.9.3. Improvements to Eddington Approximation

Note that in the Eddington approximation $J_E(0) = F/2$ and $I_E(0,0) = F/2$ so that

$$J_E(0) = I_E(0,0).$$

Actually, this result is true in general.

A check on the accuracy of the Eddington approximation is to evaluate

$$J(0) = \frac{1}{2}\int_0^1 I_E(\mu,0)\,d\mu = \frac{1}{2}\int_0^1\int_0^\infty J_E(t)\,e^{-t/\mu}\frac{dt}{\mu}d\mu = \frac{7}{16}F.$$

Thus, the Eddington approximation is internally not self-consistent.

We can improve upon the Eddington approximation by using Eq. (10.9.2): on the right-hand side of the second equation, use the Eddington approximation. Thus

$$J_{E'}(\tau) \simeq \frac{3}{4}F\left[\tau + \frac{1}{2}E_3(\tau) + \frac{2}{3} - \frac{1}{3}E_2(\tau)\right].$$

Asymptotically, this approaches J_E at large depth. The biggest difference between this and J_E occurs at the surface: $J_{E'}(0)/J_E(0) = 7/8$. The new estimate of $T(0)/T_{eff} = (7/16)^{1/4}$, while $q(\infty)$ remains 2/3, but $q(0) = 7/12$ instead of 2/3. (The exact value is $1/\sqrt{3}$, only 1% different). This new estimate for J can be used for an improved estimate of limb darkening:

$$\begin{aligned} I_{E'}(\mu,0) &= \frac{3}{4}F\int_0^\infty e^{-t/\mu}\left[t + \frac{2}{3} + \frac{1}{2}E_3(t) - \frac{1}{3}E_2(t)\right]\frac{dt}{\mu} \\ &= \frac{3}{4}F\left[\frac{7}{12} + \frac{\mu}{2} + \left(\frac{\mu}{3} + \frac{\mu^2}{2}\right)\ln\left(\frac{1+\mu}{\mu}\right)\right]. \end{aligned}$$

We now have $I_{E'}(0,0) = J_{E'}(0) = 7F/16$, and $I_{E'}(0,0)/I_{E'}(0,1) = 0.351$ (the exact value is 0.344). Note that the Eddingon approximation establishes J_E from the assumption that F is constant. Using the third of Eq. (10.9.2), one can show that

$$F_E(\tau) = \frac{3}{4}F\left[\frac{4}{3} - 2E_4(\tau) + \frac{4}{3}E_3(\tau)\right],$$

which is only approximately constant (to within 3%). The result for $F_{E'}$ by using the improvement $J_{E'}$ is about 10 times better.

Another way of solving the gray atmosphere involves the Milne integral relations Eq. (10.9.2) themselves. The solution of these equations is not analytic, and care must be taken because of the bad behavior of $E_1(x)$ as $x \to 0$. Some gain is made by adding and subtracting $B(\tau)$ to the right-hand side of the first of Eq. (10.9.2):

$$B(\tau) = \frac{1}{2}\int_0^\infty [B(t) - B(\tau)]\,E_1|t-\tau|dt + \frac{B(\tau)}{2}\int_0^\infty E_1|t-\tau|dt.$$

The integrand of the first of these is well behaved since $B(t) - B(\tau)$ goes to zero faster than the logarithmic divergence of E_1. The second integral follows from the properties of exponential integrals:

$$\int_0^x E_1(x)\,dx = E_2(0) - E_2(x), \qquad E_2(0) = 1, \tag{10.9.8}$$

Table 10.9.1: Points and Weights for Gauss-Laguerre Quadrature

n	x_i	W_i	n	x_i	W_i
2	0.585786	0.853553	3	0.415775	0.711093
	3.41421	0.146447		2.29428	0.278518
				6.28995	0.0103893
4	0.322548	0.603154	5	0.26356	0.521756
	1.74576	0.357419		1.4134	0.398667
	4.53662	0.0388879		3.59643	0.0759424
	9.39507	0.000539295		7.08581	0.00361176
				12.6408	0.00002337

so that we find the well-behaved result

$$B(\tau) = E_2^{-1}(\tau) \int_0^\infty [B(t) - B(\tau)] E_1|t-\tau| d\tau. \tag{10.9.9}$$

These integrals are efficiently performed using Gauss-Laguerre quadrature

$$B(\tau) = E_2^{-1}(\tau) \sum_{i=0}^{n} [B(t_i) - B(\tau)] E_1|t_i-\tau| W_i, \tag{10.9.10}$$

where t_i and W_i are the points and weights of the quadrature (see Table 10.9.1).

Evaluating Eq. (10.9.10) at the quadrature points t_i, then rearranging,

$$\sum_{k=1}^{m} B(t_k) \left[\sum_{i=1}^{n} \frac{(\delta_{ik} - \delta_{jk}) W_i E_1|t_i - t_j|}{E_2(t_j)} - \delta_{kj} \right] = 0. \tag{10.9.11}$$

These represent n linear homogeneous algebraic equations, an eigenvalue problem. The eigenvalue is the total radiative flux, which is a constant.

10.10. Method of Discrete Ordinates

For a gray atmosphere

$$\mu \frac{dI}{d\tau} = I - \frac{1}{2} \int_{-1}^{1} I(\mu, \tau) d\mu = I - \frac{1}{2} \sum_{j=-n}^{n} a_j I_j. \tag{10.10.1}$$

$$\mu_i \frac{dI_i}{d\tau} = I_i - \frac{1}{2} \sum_{j=-n}^{n} a_j I_j. \tag{10.10.2}$$

Here, i, j are $\pm 1, \ldots, \pm n$, and $I_i(\tau) = I(\mu_i, \tau)$. The a_i are the Gauss-Legendre weights for the points μ_i (see Table 10.10.1, for n even). We will not use schemes with points where

Table 10.10.1: Points and Weights for Gauss-Legendre Quadrature

n even	μ_i	a_i	n odd	μ_i	a_i
1	$\pm\frac{1}{\sqrt{3}}$	1	1	0	$\frac{8}{9}$
				$\pm\sqrt{\frac{3}{5}}$	$\frac{5}{9}$
2	$\pm\sqrt{\frac{3}{7}-\frac{2}{7}\sqrt{\frac{6}{5}}}$	$\frac{1}{2}+\frac{1}{6}\sqrt{\frac{5}{6}}$	2	0	$\frac{128}{225}$
	$\pm\sqrt{\frac{3}{7}+\frac{2}{7}\sqrt{\frac{6}{5}}}$	$\frac{1}{2}-\frac{1}{6}\sqrt{\frac{5}{6}}$		$\pm\frac{1}{3}\sqrt{5-2\sqrt{\frac{10}{7}}}$	$\frac{322+13\sqrt{70}}{900}$
				$\pm\frac{1}{3}\sqrt{5+2\sqrt{\frac{10}{7}}}$	$\frac{322-13\sqrt{70}}{900}$

$\mu_i = 0$, see below. We've replaced the continuous radiation field by a finite set of pencil beams. This should become exact in the limit $n \to \infty$. Eq. (10.10.2) is a first-order, linear equation. Use a trial function $I_i = g_i e^{-k\tau}$: then we must have

$$g_i = \frac{C}{1+k\mu_i}, \qquad 1 = \sum_{j=-n}^{n} \frac{a_j}{1+k\mu_j}. \tag{10.10.3}$$

The latter is called the characteristic equation for k. Since $a_{-j} = a_j$ and $\mu_{-j} = -\mu_j$, we can write this as

$$1 = \sum_{j=1}^{n} \frac{a_j}{1-k^2\mu_j^2}.$$

Since $\int_{-1}^{1} d\mu = 2$, we have $\sum_{j=-n}^{n} a_j = 2$ and $\sum_{j=1}^{n} a_j = 1$. Thus $k^2 = 0$ is a solution, and there are $n-1$ additional solutions. These solutions satisfy

$$\frac{1}{\mu_1^2} < k_1^2 < \frac{1}{\mu_2^2} < \cdots < k_{n-1}^2 < \frac{1}{\mu_n^2}.$$

The general solution is then

$$I_i(\tau) = \sum_{\alpha=1}^{n-1} \frac{L_\alpha e^{-k_\alpha \tau}}{1+k_\alpha \mu_i} + \sum_{\alpha=1}^{n-1} \frac{L_{-\alpha} e^{k_\alpha \tau}}{1-k_\alpha \mu_i}.$$

There is also a particular solution corresponding to the case $k^2 = 0$: Substituting $I_i = b(\tau + q_i)$ into the original differential equation Eq. (10.10.2),

$$I_i(\tau) = b(\tau + Q + \mu_i).$$

Thus the complete solution is

$$I_i(\tau) = b(\tau + Q + \mu_i) + \sum_{\alpha=1}^{n-1} \frac{L_\alpha e^{-k_\alpha \tau}}{1+k_\alpha \mu_i} + \sum_{\alpha=1}^{n-1} \frac{L_{-\alpha} e^{k_\alpha \tau}}{1-k_\alpha \mu_i}.$$

There are still $2n$ unknown coefficients (Q, b and $L_{\pm\alpha}$) to be determined. Use the boundary conditions to do this. In the case of a semi-infinite atmosphere, we have the boundary condition that $I_{-i}(0) = 0$ and also that $I(\tau)$ should remain finite in the limit $\tau \to \infty$. The latter constraint immediately implies that $L_{-\alpha} = 0$. The former constraint means that

$$Q + \sum_{\alpha=1}^{n-1} \frac{L_\alpha}{1 - k_\alpha \mu_i} - \mu_i = 0.$$

Finally, we must demand that the flux equals the flux F, or

$$F = 2\int_{-1}^{1} \mu I(\mu, \tau)\, d\mu = 2\sum_{j=-n}^{n} a_j \mu_j I_j(\tau).$$

Using the complete solution above, we have

$$F = 2b\left[(\tau + Q)\sum_{j=-n}^{n} a_j\mu_j + \sum_{j=-n}^{n} a_j\mu_j^2 + \sum_{n=1}^{n-1} L_\alpha e^{-k_\alpha\tau} \sum_{j=-n}^{n} \frac{a_j\mu_j}{1 + k_\alpha\mu_j}\right].$$

Now the first sum is zero, the second sum is $2/3$, and the third sum is

$$\frac{1}{k_\alpha}\sum_{j=-n}^{n} a_j\left(1 - \frac{1}{1 + k_\alpha\mu_j}\right) = \frac{2}{k_\alpha}\left(1 - \frac{1}{2}\sum_{j=-n}^{n}\frac{a_j}{1 + k_\alpha\mu_j}\right) = 0,$$

because of the characteristic equation Eq. (10.10.3). So we have that $b = 3F/4$, and a constant flux is then automatic. The final result is

$$I_i(\tau) = \frac{3}{4}F\left(\tau + Q + \mu_i + \sum_{\alpha=1}^{n-1}\frac{L_\alpha e^{-k_\alpha\tau}}{1 + k_\alpha\mu_i}\right). \tag{10.10.4}$$

The mean intensity is

$$\begin{aligned} J(\tau) &= \frac{1}{2}\sum_{j=-n}^{n} a_j I_j \\ &= \frac{3}{4}F\left[(\tau + Q)\frac{1}{2}\sum_{j=-n}^{n} a_j + \frac{1}{2}\sum_{j=-n}^{n} a_j\mu_j + \sum_{\alpha=1}^{n-1} L_\alpha e^{-k_\alpha\tau}\frac{1}{2}\sum_{j=-n}^{n}\frac{a_j}{1 + k_\alpha\mu_j}\right]. \end{aligned}$$

With the characteristic equation, this becomes

$$B(\tau) = J(\tau) = \frac{3}{4}F\left[\tau + Q + \sum_{\alpha=1}^{n-1} L_\alpha e^{-k_\alpha\tau}\right].$$

The Hopf function is then

$$q(\tau) = Q + \sum_{\alpha=1}^{n-1} L_\alpha e^{-k_\alpha\tau}, \qquad q(\infty) = Q. \tag{10.10.5}$$

Table 10.10.2: Points and Weights for Double-Gauss Quadrature

n	μ_i	a_i
2	$\pm\frac{1}{2}(1 \pm \frac{1}{\sqrt{3}})$	$\frac{1}{2}$
4	$\pm\frac{1}{2}(1 \pm \sqrt{\frac{3}{7} - \frac{2}{7}\sqrt{\frac{6}{5}}})$	$\frac{1}{4} + \frac{1}{12}\sqrt{\frac{5}{6}}$
	$\pm\frac{1}{2}(1 \pm \sqrt{\frac{3}{7} + \frac{2}{7}\sqrt{\frac{6}{5}}})$	$\frac{1}{4} - \frac{1}{12}\sqrt{\frac{5}{6}}$

For the cases of small n, the solutions for $q(\tau)$ are straightforward:

$$
\begin{aligned}
n = 1: &\quad q(\tau) = 1/\sqrt{3} \\
n = 2: &\quad = 0.694025 - 0.116675e^{-1.97203\tau} \\
n = 3: &\quad = 0.703899 - 0.101245e^{-3.20295\tau} - 0.02530e^{-1.22521\tau} \\
n = 4: &\quad = 0.70692 - 0.08392e^{-4.45808\tau} - 0.03619e^{-1.59178\tau} - 0.00946e^{-1.10319\tau}.
\end{aligned}
$$

The exact result for $q(0)$ is $1/\sqrt{3}$; only the case $n = 1$ yields this value. The exact result for Q is 0.710446, and the case $n = 1$ gives a value 25% too small. For $n = 4$ the maximum error in J compared to the exact result is about 4%.

One can greatly improve the accuracy of this scheme by recognizing that with no incident radiation, the solution for I has a discontinuity for $\mu = 0, \tau = 0$. Splitting the integral of Eq. (10.10.1), which has the discontinuous integrand, into two parts that avoid the discontinuity, and then performing each integral by Gauss-Legendre quadrature, accomplishes this. We have

$$
\mu\frac{dI}{d\tau} - I = -\frac{1}{2}\left[\int_{-1}^{0} I(\mu)\,d\mu + \int_{0}^{1} I(\mu)\,d\mu\right] = -\frac{1}{4}\left[\int_{-1}^{1} I(\nu)\,d\nu + \int_{-1}^{1} I(\omega)\,d\omega\right], \tag{10.10.6}
$$

where

$$
\nu = 2\mu + 1, \qquad \omega = 2\mu - 1. \tag{10.10.7}
$$

Thus

$$
\mu_i\frac{dI_i}{d\tau} = I_i - \frac{1}{4}\sum_{j=-n}^{n} a_j\left[I_{\nu_j} + I_{\omega_j}\right]. \tag{10.10.8}
$$

Formally, this looks identical to Eq. (10.10.2) (for an even number of points) if $n \to 2n$, $a_j \to a_j/2$, and the points are accordingly redefined as in Eq. (10.10.7). In short, we use the points and weight in Table 10.10.2. The double-Gauss quadrature formula achieves

0.6% accuracy even for $n = 4$. For $n = 2$, one can show that

$$\begin{aligned} I_i(\tau) &= \frac{3}{4}F\left[\tau + Q + \mu_i + \frac{Le^{-k\tau}}{1+k\mu_i}\right] \\ B(\tau) = J(\tau) &= \frac{3}{4}F\left[\tau + Q + Le^{-k\tau}\right] \\ k &= \sqrt{\frac{1-a_2}{\mu_2^2} + \frac{1-a_1}{\mu_1^2}} = 2\sqrt{3} \\ Q &= \mu_1 + \mu_2 - \frac{1}{k} = 1 - \frac{1}{2\sqrt{3}} \\ L &= \frac{(1-k\mu_1)(1-k\mu_2)}{k} = \frac{\sqrt{3}}{2} - 1. \end{aligned} \tag{10.10.9}$$

Note that this gives an exact result for $q(0)$, and a result for $q(\infty) = Q$ in error by only 0.1%. The discrete ordinate method can be generalized to yield the exact solution, but we won't work it out here.

10.11. The Emergent Flux from a Gray Atmosphere

Although in a gray atmosphere the opacity is independent of frequency, the flux dependence on frequency still varies with depth. We have

$$B(\tau) = \frac{\sigma T(\tau)^4}{\pi} = J(\tau), \qquad T(\tau)^4 = \frac{3}{4}T_{eff}^4\left[\tau + q(\tau)\right].$$

From the frequency dependence of the source function, Eq. (10.9.2) yields

$$F_\nu(\tau) = 2\int_\tau^\infty B_\nu\left[T(t)\right]E_2(t-\tau)\,dt - 2\int_0^\tau B_\nu\left[T(t)\right]E_2(\tau-t)\,dt,$$

where the Planck function is

$$B_\nu(T) = \frac{2h\nu^3}{c^2}\left(e^{h\nu/kT} - 1\right)^{-1}.$$

Using the parameter $\alpha = h\nu/kT_{eff}$, where $T_{eff}/T = (3[t+q(t)]/4)^{-1/4}$, the flux is $F_\alpha(\tau) = F_\nu(\tau)\frac{d\nu}{d\alpha}$:

$$\frac{F_\alpha(\tau)}{F} = \frac{30\alpha^3}{\pi^4}\left[\int_\tau^\infty \frac{E_2(t-\tau)\,dt}{e^{\alpha T_{eff}/T} - 1} - \int_0^\tau \frac{E_2(\tau-t)\,dt}{e^{\alpha T_{eff}/T} - 1}\right].$$

As the figure shows, for $\tau = 0(2)$, this peaks near $\alpha = 3(5)$, and the peak value for $\tau = 2$ is 25% smaller than for $\tau = 0$. The mean photon energy is degraded as they are transferred from the interior to the surface. The Planck function (B_α/F) for $T = T_{eff}$ is shown for comparison: the emergent spectra ($\tau = 0$) is slightly harder.

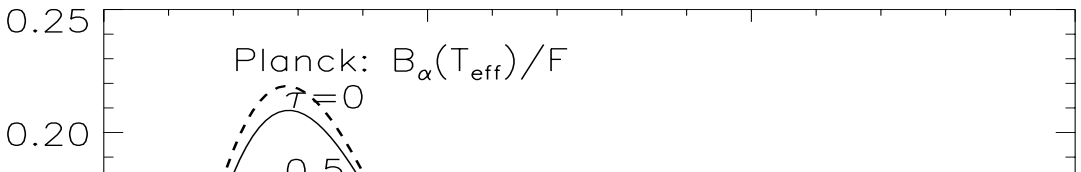

10.11.1. Correction for Stimulated Emission

In general, there are 3 types of transitions:

- Spontaneous Emission: $N_{i\to j} = N_i A_{ij} dt$
- (Stimulated) Absorption $N_{j\to i} = N_j B_{ji} I_{\nu_{ij}} dt$
- Stimulated Emission (enhanced in the presence of a photon of the same energy as the spontaneous transition) $N_{i\to j} = N_i B_{ij} I_{\nu_{ij}} dt$

Note the symmetric process of spontaneous absorption cannot occur. In strict thermal equilibrium, detailed balance occurs, and the photon distribution is the Planck function, so

$$N_j B_{ji} B_{\nu_{ij}}(T) = N_i \left[A_{ij} + B_{ij} B_{\nu_{ij}}(T)\right].$$

The Boltzmann formula must hold for the relative abundances of the two states:

$$\frac{N_i}{N_j} = \frac{g_i}{g_j} e^{-h\nu_{ij}/kT}.$$

Writing out the Planck function:

$$A_{ij}\frac{g_i}{g_j} = \frac{2h\nu^3}{c^2} B_{ji} \frac{e^{h\nu_{ij}/kT} - \frac{B_{ij}g_i}{B_{ji}g_j}}{e^{h\nu_{ij}/kT} - 1}.$$

The Einstein coefficients are independent of temperature (properties of atoms), which can only happen if

$$\frac{B_{ij}g_i}{B_{ji}g_j} = 1, \qquad A_{ij} = B_{ji}\left(\frac{2h\nu^3}{c^2}\frac{g_j}{g_i}\right).$$

Now recall from an early discussion that the source function, in the absence of scattering, is the ratio of the emissivity j_ν to the opacity k_ν. The total energy produced per unit volume and flowing through a solid angle $d\Omega$ is

$$j_\nu \rho d\nu d\Omega = h\nu N_i \left(A_{ij} + B_{ij} I_\nu\right) = N_i A_{ij} h\nu \left(1 + \frac{I_\nu c^2}{2h\nu^3}\right)$$

and the total absorbed energy is

$$I_\nu \kappa_\nu \rho d\nu d\Omega = N_j B_{ji} I_\nu h\nu.$$

Then

$$S_\nu = \frac{j_\nu}{\kappa_\nu} = \frac{N_i A_{ij}\left(1 + \frac{c^2 I_\nu}{2h\nu^3}\right)}{N_j B_{ji}} = \frac{N_i g_j}{N_j g_i}\left(\frac{2h\nu^3}{c^2} + I_\nu\right).$$

$$S_\nu = e^{-h\nu/kT}\left(\frac{2h\nu^3}{c^2} + I_\nu\right) = B_\nu\left(1 - e^{-h\nu/kT}\right) + I_\nu e^{-h\nu/kT}.$$

In the equation of radiative transfer, we have

$$\mu\frac{dI_\nu}{d\tau} = I_\nu - S_\nu = (I_\nu - B_\nu)\left(1 - e^{-h\nu/kT}\right),$$

which can be turned into

$$\mu \frac{dI_\nu}{d\tau} = I_\nu - B_\nu$$

if the opacity κ_ν is redefined as $\kappa_\nu(1 - e^{-h\nu/kT})$.

10.12. Formation of Spectral Lines

Definitions:

$$f_\nu(\mu) = \frac{I_\nu(\mu, 0)}{I_c(\mu, 0)}: \quad \text{residual intensity}$$

$$r_\nu = \frac{F_\nu(0)}{F_c(0)}: \quad \text{residual flux}$$

$$W_\lambda = \int_0^\infty (1 - r_\lambda)\, d\lambda: \quad \text{equivalent width}$$

The subscript ν refers to the line, and the subscript c refers to the continuum. The equivalent width is the width of a completely black line that absorbs the same number of photons as the spectral line of interest. The integrals range of 0 and ∞ just means "far from the line center". Note that $W_\nu \approx (\nu/\lambda) W_\lambda$.

Spectral lines are of two types: pure absorption where the absorbed energy is fully shared with the gas, and resonance lines in which it is not. In the former, the emission of photons is completely uncorrelated with previous absorption. In resonance scattering, the emitted photon is completely correlated with the absorbed photon (coherent scattering). Treating the line and continuum processes separately, the radiative transfer equation is

$$\mu \frac{dI_\nu(\mu, \tau_\nu)}{d\tau_\nu} = I_\nu(\mu, \tau_\nu) - \frac{(\kappa + \kappa_\nu) B_\nu + (\sigma + \sigma_\nu) J_\nu}{\kappa + \kappa_\nu + \sigma + \sigma_\nu},$$

where the optical depth in the line is $d\tau_\nu = (\kappa + \kappa_\nu + \sigma + \sigma_\nu)\rho dz$.

10.12.1. Schuster-Schwarzschild Model

Suppose we have strong resonance lines formed in a thin layer overlying the photosphere. Then $\kappa << \sigma$ and $\sigma_\nu >> \sigma$. Then

$$\mu \frac{dI_\nu}{d\tau_\nu} = I_\nu - J_\nu, \qquad d\tau_\nu = -\sigma_\nu \rho dx.$$

This looks like the transfer equation for a gray atmosphere, and we must have from radiative equilibrium $F_\nu(\tau_\nu) =$ constant for each frequency. From the results for a gray atmosphere, using $n = 1$,

$$I_+(\tau_\nu) = \frac{3F_\nu\left(\tau_\nu + 1/\sqrt{3} + Q\right)}{4}, \qquad I_-(\tau_\nu) = \frac{3F_\nu\left(\tau_\nu - 1/\sqrt{3} + Q\right)}{4}.$$

The boundary condition $I_-(0) = 0$ implies that $Q = 1/\sqrt{3}$ and

$$I_+(\tau_\nu) = \frac{3F_\nu\left(\tau_\nu + 2/\sqrt{3}\right)}{4}, \qquad I_-(\tau_\nu) = \frac{3F_\nu\tau_\nu}{4}.$$

If we require that the line intensity on the base of the thin cool gas layer be the same as the emergent intensity of the continuum,

$$I_+(\tau_o) = \frac{3F_c\left(0 + 2/\sqrt{3}\right)}{4} = \frac{3F_\nu\left(\tau_o + 2/\sqrt{3}\right)}{4}.$$

The residual flux is just

$$r_\nu = \frac{F_\nu}{F_c} = \left(1 + \frac{\sqrt{3}\tau_o}{2}\right)^{-1}.$$

The angular dependence can be found from the classical solution

$$I_\nu(\mu, 0) = \int_0^\infty \frac{J_\nu(t_\nu)\, e^{-t_\nu/\mu} dt_\nu}{\mu} + I_c(\mu, 0)\, e^{-\tau_o/\mu}.$$

The mean intensity can be approximated as

$$J_\nu(\tau_\nu) = \frac{1}{2}\left[I_+(\tau_\nu) + I_-(\tau_\nu)\right] = \frac{3F_\nu\left(\tau_\nu + 1/\sqrt{3}\right)}{4}.$$

Using this relations, one finds

$$f_\nu(\mu) = \frac{3F_c}{4I_c(\mu, 0)\left(1 + \sqrt{3}\tau_o/2\right)}\left[\mu + \frac{1}{\sqrt{3}} - \left(\mu + \tau_o + \frac{1}{\sqrt{3}}\right)e^{-\tau_o/\mu}\right] + e^{-\tau_o/\mu}.$$

In the limit of weak lines, $\tau_o << 1$, we find

$$f_\nu(\mu) \simeq 1 - \frac{3F_c}{4I_c(\mu, 0)}\tau_o.$$

There is no angular dependence except what arises due to limb-darkening of the continuum. Thus scattering lines are visible at all point on the stellar disk with roughly equal strength. In the limit of strong lines, $\tau_o >> 1$,

$$f_\nu(\mu) \simeq \frac{\sqrt{3}F_c}{2I_c(\mu, 0)\,\tau_o}\left(\mu + 1/\sqrt{3}\right).$$

The range in line strength between the center of the disk and the edge is about 2. This will contrast with that to be found from pure absorption lines, discussed next.

10.12.2. Milne-Eddington Model

In the case of pure absorption, we have to specify something about the depth dependence of the opacity and source function, which was unecessary in the scattering case. Define

$$\epsilon_\nu = \frac{\kappa_\nu}{\kappa_\nu + \sigma_\nu}, \qquad \eta_\nu = \frac{\kappa_\nu + \sigma_\nu}{\kappa}, \qquad \mathcal{L}_\nu = \frac{\kappa_\nu + \kappa}{\kappa + \kappa_\nu + \sigma_\nu} = \frac{1 + \eta_\nu \epsilon_\nu}{1 + \eta_\nu}.$$

ϵ_ν measures the importance of absorption to total extinction in the line; η_ν measures the line strength; $\mathcal{L}_\nu$ measures net effect of absorption in line and continuum. The line transfer equation is

$$\mu \frac{dI_\nu}{d\tau_\nu} = I_\nu - \mathcal{L}_\nu B_\nu - (1 - \mathcal{L}_\nu) J_\nu, \qquad d\tau_\nu = (\kappa + \kappa_\nu + \sigma_\nu) \rho dz. \tag{10.12.1}$$

Note in the continuum,

$$d\tau = \kappa \rho dz = \frac{\kappa d\tau_\nu}{\kappa + \kappa_\nu + \sigma_\nu} = \frac{d\tau_\nu}{1 + \eta_\nu},$$

so $\tau = \tau_\nu/(1 + \eta_\nu)$. In the Eddington approximation, $B(\tau) = a + b\tau$, or

$$B_\nu(\tau_\nu) = a + b\tau_\nu/(1 + \eta_\nu). \tag{10.12.2}$$

Attempt to solve Eq. (10.12.1) by taking moments:

$$\frac{dF_\nu}{d\tau_\nu} = 4\mathcal{L}_\nu (J_\nu - B_\nu), \qquad \frac{dK_\nu}{d\tau_\nu} = \frac{F_\nu}{4}.$$

With $K_\nu \approx J_\nu/3$,

$$\frac{d^2 J_\nu}{d\tau_\nu^2} = \frac{3}{4}\frac{dF_\nu}{d\tau_\nu} = 3\mathcal{L}_\nu (J_\nu - B_\nu).$$

Using the linear relation in Eq. (10.12.2), we must have

$$J_\nu(\tau_\nu) - B_\nu(\tau_\nu) = ce^{-3\mathcal{L}_\nu \tau_\nu},$$

where the positive exponent term vanishes since $J_\nu \to B_\nu$ as $\tau_\nu \to \infty$. At the surface, the Eddington approximation leads to $J_\nu(0) \approx F_\nu(0)/2$, or

$$\left.\frac{dJ_\nu}{d\tau_\nu}\right|_0 = \frac{3}{4}F_\nu(0) = \frac{3}{2}J_\nu(0) = \frac{3}{2}(a + c) = -c\sqrt{3\mathcal{L}_\nu} + \frac{b}{1 + \eta_\nu}.$$

Therefore

$$c = \left[\frac{b}{1 + \eta_\nu} - \frac{3}{2}a\right]\left(\sqrt{3\mathcal{L}_\nu} + \frac{3}{2}\right)^{-1},$$

$$J_\nu(\tau_\nu) = a + \frac{b\tau_\nu}{1 + \eta_\nu} + \frac{\frac{b}{1+\eta_\nu} - \frac{3}{2}a}{\sqrt{3\mathcal{L}_\nu} + \frac{3}{2}} e^{-\sqrt{3\mathcal{L}_\nu}\tau_\nu}.$$

In the continuum, $\eta_\nu = 0, \mathcal{L}_\nu = 1$. The residual flux is then

$$r_\nu = \frac{F_\nu(0)}{F_c(0)} = \frac{J_\nu(0)}{J_c(0)} = \frac{\left(\frac{b}{1+\eta_\nu} + a\sqrt{3\mathcal{L}_\nu}\right)\left(\sqrt{3}+\frac{3}{2}\right)}{\left(b+a\sqrt{3}\right)\left(\sqrt{3\mathcal{L}_\nu}+\frac{3}{2}\right)}.$$

The residual intensity requires a specification of the source function,

$$S_\nu(\tau_\nu) = \mathcal{L}_\nu B_\nu(\tau_\nu) + (1-\mathcal{L}_\nu) J_\nu(\tau_\nu).$$

In the continuum $\mathcal{L} = 0$, so $S(\tau) = B_\nu(\tau)$.

$$\begin{aligned} f_\nu(\mu) = \frac{I_\nu(\mu,0)}{I_c(\mu,0)} = \frac{\int_0^\infty \frac{S_\nu(t_\nu)e^{-t_\nu/\mu}dt_\nu}{\mu}}{\int_0^\infty \frac{S_c(t)e^{-t/\mu}dt}{\mu}} = \\ \frac{a+\frac{b\mu}{1+\eta_\nu}}{a+b\mu} - \frac{(1-\mathcal{L}_\nu)\left[\frac{3}{2}a - \frac{b}{3(1+\eta_\nu)}\right]}{(a+b\mu)\left(1+\mu\sqrt{3\mathcal{L}_\nu}\right)\left(\frac{3}{2}+\sqrt{3\mathcal{L}_\nu}\right)}. \end{aligned} \tag{10.12.3}$$

Note that the second term will vanish in the case of pure absorption ($\mathcal{L} \to 1$). In this case

$$r_\nu = \frac{a\sqrt{3}+\frac{b}{1+\eta_\nu}}{a\sqrt{3}+b}, \qquad f_\nu(\mu) = \frac{a+\frac{b\mu}{1+\eta_\nu}}{a+b\mu}. \tag{10.12.4}$$

In an isothermal atmosphere, $b = 0$ and $r_\nu = f_\nu(\mu) = 1$, and the line disappears. In the absence of temperature gradients, there can be no spectral absoprtion lines. Thus, the stronger the source function gradient, the stronger the line. Therefore, late-type stars have stronger features than early-type stars. Late-type stars have visible features at wavelengths shorter than the peak energies, where the spectrum is decaying exponentially. Early-type stars have features at wavelengths longer than the peak energies, on the Rayleigh-Jeans tail where the source function varies more slowly with temperature.

For strong absorption, $\eta_\nu >> 1$, we have

$$r_\nu = \frac{a\sqrt{3}}{a\sqrt{3}+b}, \qquad f_\nu(\mu) = \frac{a}{a+b\mu}. \qquad \eta_\nu >> 1$$

Even the strongest line vanishes as $\mu \to 0$ at the limb. For this line of sight, grazing the limb, the effects of temperature gradients are minimized. For weak absorption, $\eta_\nu << 1$, we have

$$r_\nu = 1 - \frac{b\eta_\nu}{a\sqrt{3}+b}, \qquad f_\nu(\mu) = 1 - \frac{b\mu\eta_\nu}{a+b\mu}. \qquad \eta_\nu << 1$$

The line strength is proportional to η_ν and to κ_ν, and thus to the number of absorbers.

Now consider the case of pure scattering, $\epsilon_\nu = 0$, which requires $\mathcal{L}_\nu = (1+\eta_\nu)^{-1}$ as $\kappa_\nu = 0$.

For strong scattering,

$$r_\nu = \frac{\left(\sqrt{3}+2\right)\sqrt{\mathcal{L}_\nu}}{a\sqrt{3}+b}, \qquad f_\nu(\mu) = \frac{a\sqrt{3\mathcal{L}_\nu}\left(\mu+\frac{2}{3}\right)}{a+b\mu}. \qquad \eta_\nu >> 1 \tag{10.12.5}$$

Now, even if the atmosphere is isothermal, lines will persist to the edge of the limb, where the residual intensity is still about 1/2 of the residual flux. These lines do not depend upon the thermodynamic property of the gas, but upon the existence of a boundary, which permits the selective escape of photons.

For weak scattering, $\eta_\nu \to 0$ and $\mathcal{L}_\nu \to 1$:

$$\begin{aligned} r_\nu &= 1 - \frac{b\eta_\nu}{a\sqrt{3}+b} \\ f_\nu(\mu) &= 1 - \frac{b\mu\eta_\nu}{a+b\mu} - \frac{\eta_\nu\left(\frac{3}{2}a-b\right)}{(a+b\mu)\left(1+\mu\sqrt{3}\right)\left(\sqrt{3}+\frac{1}{2}\right)}. \end{aligned} \qquad \eta_\nu << 1 \qquad (10.12.6)$$

The residual flux has the same form as for weak pure absorption, but the residual intensity is diffferent: even for an isothermal atmosphere, a weak scattering line will be visible at the limb.

10.13. The Curve of Growth of the Equivalent Width

Spectral lines are broadened from the transition frequency for a number of reasons. Thermal motions and turbulence introduce Doppler shifts between atoms and the radiation field. The probability that an atom will have a velocity v is

$$\frac{dN}{N} = \frac{e^{-(v/v_0)^2}}{\sqrt{\pi}v_0}dv,$$

where v_0 is the mean velocity (of the combined thermal and turbulent motions). The frequency ν' at which an atom will absorb in terms of the rest frequency ν_0 is

$$\nu' = \nu_0 + \frac{\nu_0 v}{c}.$$

In addition, viewed either classicaly or quantum mechanically, each transition has a damping profile or Lorentz profile, such that the atomic absorption coefficient will be proportional to

$$S_\omega \propto \frac{\Gamma_{ik}}{(\omega-\omega_0)^2 + (\Gamma_{ik}/2)^2}.$$

Here Γ_{ik} is related to the Einstein coefficient or strength of spontaneous emission, and ω_0 is the difference in energy of the states. The source of broadening in this case is due to the Heisenberg uncertainty principle. The combined effects in the atomic absorption coefficient are

$$S_\nu(v) \propto \frac{\Gamma_{ik}}{[\nu_0(1+v/c)-\nu]^2 + (\Gamma_{ik}/4\pi)^2}.$$

Multiplying this by the probability for the velocity and integrating over all velocities results in

$$S_\nu \propto \Gamma_{ik}\int_{-\infty}^{\infty} \frac{1}{\sqrt{\pi}\nu_0}\frac{e^{-(v/v_0)^2}dv}{[\nu_0(1+v/c)-\nu]^2 + (\Gamma_{ik}/4\pi)^2}.$$

Define the dimensionless variables

$$u = \frac{c\left(\nu - \nu_0\right)}{\nu_0 v_0}, \qquad y = \frac{v}{v_0}, \qquad a = \frac{c\Gamma_{ik}}{4\pi\nu_0 v_0}.$$

$$S_\nu\left(u\right) \propto \frac{a}{\nu_0 v_0}\int_{-\infty}^{\infty}\frac{e^{-y^2}dy}{a^2+\left(u-y\right)^2} = \frac{\sqrt{\pi}}{\nu_0 v_0}H\left(a,u\right).$$

Here the Voigt function is

$$H\left(a,u\right) = \frac{a}{\pi}\int_{-\infty}^{\infty}\frac{e^{-y^2}dy}{a^2+\left(u-y\right)^2}.$$

Now we can relate the size and shape of the spectral line to the abundance of the species responsible for it. Consider the Schuster-Schwarzschild model, that of a gas layer above the normal atmosphere. In this model, we have

$$r_\nu = \frac{F_\nu}{F_c} = \left(1+\frac{\sqrt{3}\tau_0}{2}\right)^{-1},$$

where

$$\tau_0 = \int_0^{\tau_0} dt_\nu = \int_0^{z_0}\kappa_\nu\rho dz = \int_0^{z_0} n_i S_\nu dz =< S_\nu > \int_0^{z_0} n_i dz = N_i < S_\nu > .$$

N_i is the column density of the atom giving rise to the line, and $< S_\nu >$ is the line absorption coefficient averaged over depth. In this model, we neglect depth dependences, and we write $< S_\nu >= S_0 H(a,u)$. Thus the line profile is

$$r_\nu = \left(1+\frac{\sqrt{3}\tau_0}{2}\right)^{-1} = \left(1+\frac{\sqrt{3}S_0 H\left(a,u\right)N_i}{2}\right)^{-1}.$$

Now we can write the equivalent width

$$W_\lambda = 2\int_0^\infty \frac{\sqrt{3}\tau_0/2}{1+\sqrt{3}\tau_0/2}d\lambda = 2\Delta\lambda_d\int_0^\infty \frac{\sqrt{3}S_0 H\left(a,u\right)N_i du/2}{1+\sqrt{3}S_0 H\left(a,u\right)N_i/2},$$

where $du = d\lambda/\Delta\lambda_d$. Now write $\eta_0 = \sqrt{3}S_0 N_i/2$ so

$$W_\lambda = 2\Delta\lambda_d\int_0^\infty \frac{\eta_0 H\left(a,u\right)du}{1+\eta_0 H\left(a,u\right)}.$$

There are two limiting cases. First, for small a and small u, the Voigt function behaves as $H(a,u)\to e^{-u^2}$ since the integrand peaks at $y=u$. Then we have

$$\frac{W_\lambda}{2\Delta\lambda_d} = \int_0^\infty \frac{\eta_0 e^{-u^2}du}{1+\eta_0 e^{-u^2}} = \int_0^\infty \frac{dx x^{-1/2}}{e^{x-\ln\eta_0}+1} = \frac{1}{2}F_{-1/2}\left(\ln\eta_0\right), \tag{10.13.1}$$

with F the usual Fermi integral. In the limit that $\eta_0 \to 0$, this becomes

$$\frac{W_\lambda}{2\Delta\lambda_d} \simeq \eta_0 + \ldots \qquad \eta_0 << 1, \quad a < 1.$$

The equivalent width is proportional to N_i, the column density of absorbers. When η_0 is large, the opposite expansion of $F_{-1/2}$ yields

$$\frac{W_\lambda}{2\Delta\lambda_d} \simeq \sqrt{\ln \eta_0} + \ldots \qquad \eta_0 > 1, \quad a < 1$$

and the line saturates, increasing only as $\sqrt{\ln N_i}$.

As the number of absorbers grows still further, however, absorption in the wings becomes important. The relevant case is to take the $u \to \infty$ limit of the Voigt function:

$$H(a,u) \to \frac{a}{\pi}\int_{-\infty}^{\infty} u^{-2} e^{-y^2} dy = \frac{a u^{-2}}{\sqrt{\pi}} \qquad u \to \infty.$$

Note that this result is valid for any a. W_λ will thus grow faster again:

$$\frac{W_\lambda}{2\Delta\lambda_d} \simeq \int_0^\infty \frac{du}{\frac{\sqrt{\pi}}{a\eta_0}u^2 + 1} = \frac{\sqrt{\pi a \eta_0}}{2}, \qquad \eta_0 >> 1.$$

which depends on $\sqrt{N_i}$.

These results are valid for scattering lines, but in fact most applications require a more sophisticated treatment.

10.14. Feautrier's Method for Radiative Transfer

This project is to use Feautrier's method to solve the Gray Atmosphere problem for a plane-parallel atmosphere. In a gray atmosphere, there is no frequency dependence. The problem is to find the intensity as a function of depth and angle; in particular, to find the outgoing intensity as a function of angle. The equation of transfer is

$$\mu \frac{dI(\tau,\mu)}{d\tau} = I(\tau,\mu) - S(\tau) = I(\tau,\mu) - B(\tau),$$

where we can use the gray relation $S = B$. We have to assume that $B(\tau)$ is known. For this problem, assume it is given by

$$B(\tau) = \frac{3}{4}F\left(\tau + \frac{2}{3}\right)$$

where F is the (constant) flux. At the end of this project, you will compute F to determine how accurate this approximation is. In the real world, you would then have to alter the above approximation to ensure that F remains constant through the atmosphere. By such iterations, the full atmosphere model is then found. Also, in the real world, $S \neq B$

and one has to make use of opacity information, which is also a function of density. To determine the density, the equation of hydrostatic equilibrium has to be used. However, in this project, we will neither consider this complication, nor do this iteration.

It is customary to divide the intensity into outgoing and ingoing streams, so that the variable μ is now a positive quantity:

$$\begin{aligned}\mu\frac{dI(\tau,+\mu)}{d\tau} =& I(\tau,+\mu) - B(\tau)\\ -\mu\frac{dI(\tau,-\mu)}{d\tau} =& I(\tau,-\mu) - B(\tau).\end{aligned}$$

In this method, one defines

$$\begin{aligned}u(\tau,\mu) =& \frac{1}{2}\left[I(\tau,+\mu) + I(\tau,-\mu)\right]\\ v(\tau,\mu) =& \frac{1}{2}\left[I(\tau,+\mu) - I(\tau,-\mu)\right].\end{aligned}$$

Thus,

$$\begin{aligned}\mu\frac{dv(\tau,\mu)}{d\tau} =& u(\tau,\mu) - B(\tau)\\ \mu\frac{du(\tau,\mu)}{d\tau} =& v(\tau,\mu).\end{aligned}$$

We can combine them to eliminate v:

$$\mu^2\frac{d^2u(\tau,\mu)}{d\tau^2} = u(\tau,\mu) - B(\tau)$$

The boundary conditions on I are taken to be that of no incoming flux at the surface, and the diffusion approximation at the atmosphere's base:

$$\begin{aligned}I(0,-\mu) =& 0\\ I(\tau\to\infty,+\mu) =& \left[B(\tau) + \mu\frac{dB(\tau)}{d\tau} + \mu^2\frac{d^2B(\tau)}{d^2\tau} + \cdots\right]_{\tau\to\infty}.\end{aligned}$$

The second and higher derivatives of B are zero for our assumptions. These translate to

$$\begin{aligned}\mu\frac{du(\tau\to 0,\mu)}{d\tau} =& u(0,\mu)\\ \left[u(\tau,\mu) + v(\tau,\mu)\right]_{\tau\to\infty} =& \left[u(\tau,\mu) + \mu\frac{du(\tau,\mu)}{d\tau}\right]_{\tau\to\infty} = \left[B(\tau) + \mu\frac{dB(\tau)}{d\tau}\right]_{\tau\to\infty}.\end{aligned} \tag{10.14.1}$$

To solve these equations, we must discretize them. Choose angles based upon Gauss-Legendre quadrature (for ease, choose 3 positive and 3 negative values for μ_j). Choose optical depths ranging from 0 to, say, 10, with a fixed interval of $\Delta = 0.1$. Thus $\tau_{i+1} - \tau_i \equiv \Delta$. It would be better in general to choose $\ln\tau$ for the independent variable for accuracy's sake, but this complicates the algebra and a linear grid is sufficient here. We can write the system of equations for $1 < i < N$) as

$$-A_{i,j}u_{i-1,j} + D_{i,j}u_{i,j} - C_{i,j}u_{i+1,j} = E_i. \tag{10.14.2}$$

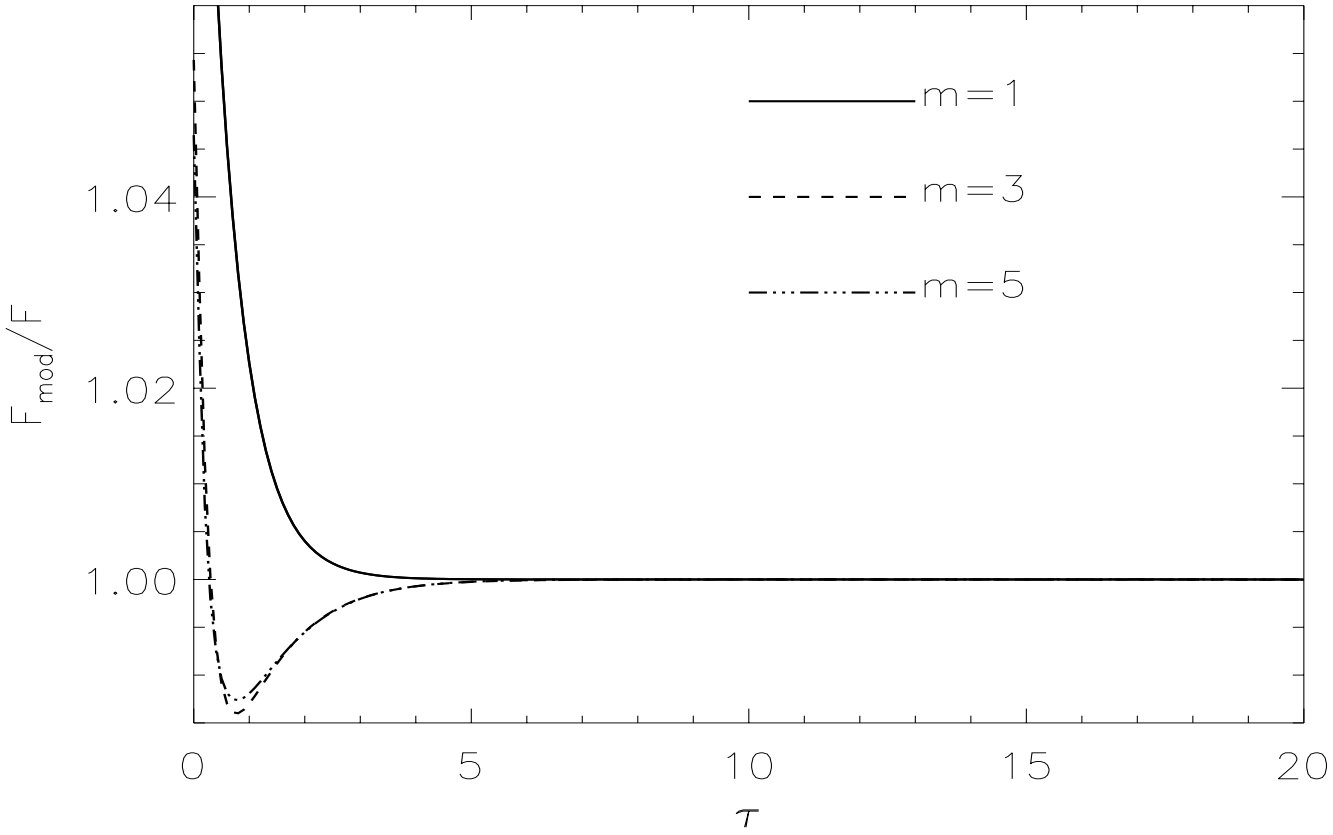

Figure 10.14.1: Flux conservation test for Feautrier's method with the approximation $B = (3F/4)(\tau + 2/3)$.

For $2 \leq i \leq N-1$ one has, using central differencing,

$$A_{i,j} = \mu_j^2/\Delta^2, \qquad D_{i,j} = 1 + 2\mu_j^2/\Delta^2, \qquad C_{i,j} = \mu_j^2/\Delta^2, \qquad E_i = B_i \equiv B\left(\tau_i\right).$$

At the boundaries, coupling adjacent zones only, we may write

$$A_{1,j} = 0, \qquad D_{1,j} = 1 + \mu_j/\Delta, \qquad C_{1,j} = \mu_j/\Delta, \qquad E_1 = 0$$

and

$$A_{N,j} = \mu_j/\Delta - 1/2, \qquad D_{N,j} = 1/2 + \mu_j/\Delta, \qquad C_{N,j} = 0,$$
$$E_N = B_N\left(1/2 + \mu_j/\Delta\right) + B_{N-1}\left(1/2 - \mu_j/\Delta\right).$$

Eq. (10.14.2) is linear, and we can use a substitution scheme similar to that of the Henyey technique. Assume for each j, using the shorthand $u_i = u_{i,j}$,

$$u_i = \alpha_{i+1} + \beta_{i+1} u_{i+1}. \tag{10.14.3}$$

By substitution, one finds

$$\alpha_i = \frac{E_{i-1} + \alpha_{i-1} A_{i-1}}{D_{i-1} - \beta_{i-1} A_{i-1}},$$
$$\beta_i = \frac{C_{i-1}}{D_{i-1} - \beta_{i-1} A_{i-1}}. \tag{10.14.4}$$

Beginning at the surface, $\beta_2 = C_1/D_1$ since $A_1 = 0$. Now one can determine all α_is and β_is up to $i = N+1$. In turn, one uses Eq. (10.14.3) to obtain each u_i from $i = N$ to $i = 1$.

After the u_is are determined, one reconstructs the flux:

$$\begin{aligned} F(\tau_i) =& 2\int_{-1}^{+1} \mu I(\tau_i,\mu)\, d\mu = 2\sum_j w_j\mu_j \left[I(\tau_i,+\mu_j) - I(\tau_i,-\mu_j)\right] \\ =& 4\sum_j w_j\mu_j v_{i,j} = 4\sum_j w_j\mu_j^2 u'_{i,j}\,. \end{aligned}$$

Here, w_j are the Gauss-Legendre weights, and the sums are only over postive values of j. To find $u'_{i,j} = (du/d\tau)_{i,j}$, use the discretized relation

$$u'_{i,j} = \frac{u_{i+1,j} - u_{i-1,j}}{2\Delta},$$

which is valid for $2 \le i \le N-1$. For the boundary values $F(\tau_0)$ and $F(\tau_N)$, Taylor-series expansions yield

$$u'_{0,j} = \frac{4u_{1,j} - 3u_{0,j} - u_{2,j}}{2\Delta}, \qquad u'_{N,j} = \frac{3u_{N,j} + u_{N-2,j} - 4u_{N-1,j}}{2\Delta}.$$

How constant is F as a function of depth? The figure shows that near the surface, the flux is especially poorly determined. To ensure that F remains constant as a function of depth, it is necessary to alter the approximation $B = (3F/4)(\tau + 2/3)$. This procedure is commonly known as Λ-iteration, since Λ is the operator that yields S.

In the gray atmosphere case, the constancy of the flux implies $B = J$, so one procedure would be to update B by using

$$\begin{aligned} B(\tau) =& J(\tau) = \frac{1}{2}\int_{-1}^{+1} I d\mu = \frac{1}{2}\sum_j w_j \left[I(\tau,+\mu_j) + I(\tau,-\mu_j)\right] \\ =& \sum_j w_j u(\tau,\mu_j)\,. \end{aligned}$$

Once this value for B is used in the Feautrier scheme, new values for $u_{i,j}$ are determined. This iteration must be repeated until convergence. Unfortunately, typically thousands of iterations are necessary. (In the figure, each curve represents 10 iterations.) This happens because at large optical depth, we will always find $J \to B$ no matter what, and the changes in B are exponentially small. Note that the flux was not used in the computation of the correction of B.

A better approach is the so-called Unsöld-Lucy procedure. Begin with the transfer equation and its first two moments, in the gray case with no scattering in which $S = B$:

$$\mu\frac{dI}{d\tau} = I - B, \quad \frac{1}{4}\frac{dF}{d\tau} = J - B, \quad \frac{dK}{d\tau} = \frac{1}{4}F.$$

Since B is not the correct source function, F will not be constant. Integrate the last of the above relations, and use the Eddington approximation $J = 3K$:

$$K(\tau) = \frac{1}{4}\int_0^\tau F\left(\tau'\right) d\tau' + \frac{1}{3}C,$$

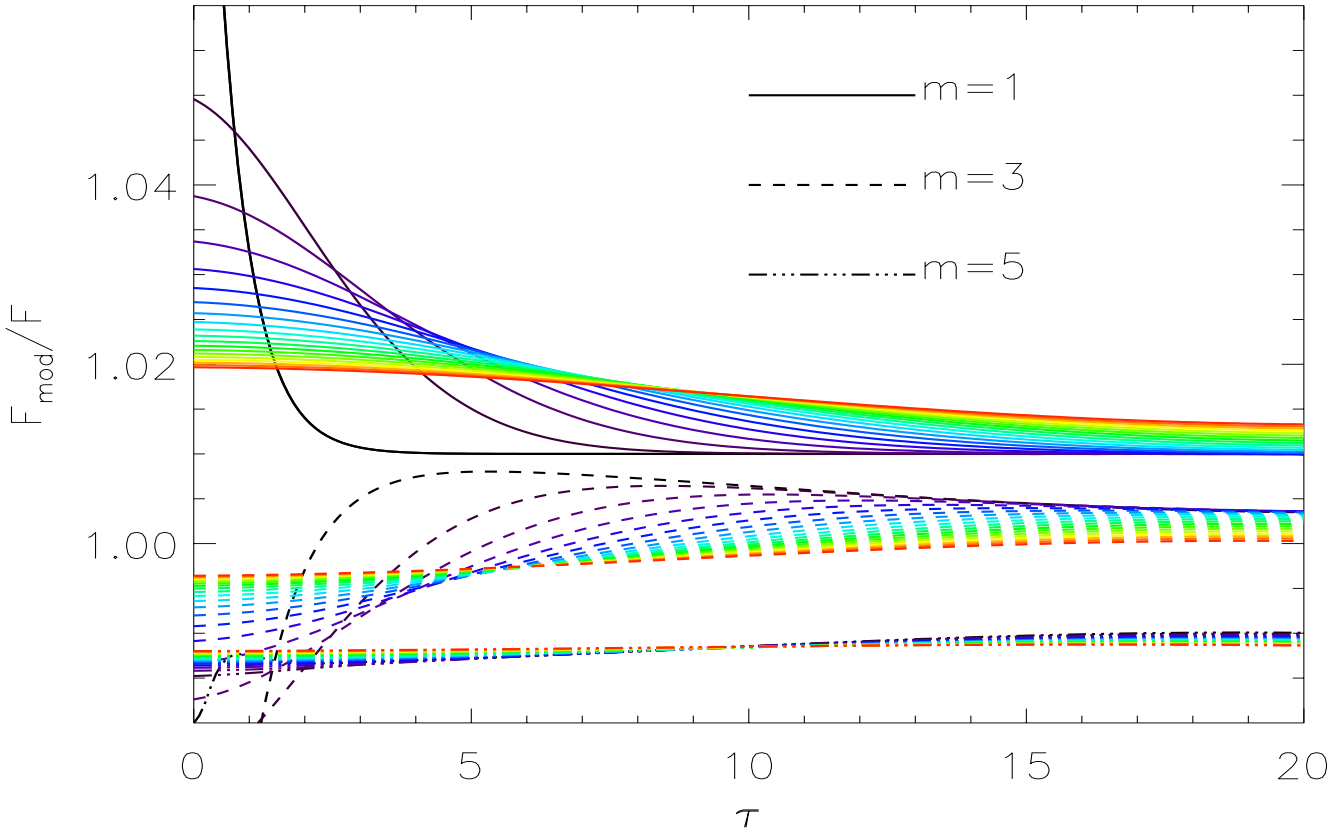

Figure 10.14.2: Convergence for lambda iteration. Different angular rays are offset for clarity.

where C is a constant. C can be found if we further approximate $J(0) = F(0)/2$, so

$$J \simeq \frac{3}{4}\int_0^\tau F\left(\tau'\right)d\tau' + \frac{1}{2}F\left(0\right).$$

The first moment equation becomes

$$B\left(\tau\right) = J\left(\tau\right) - \frac{1}{4}\frac{dF\left(\tau\right)}{d\tau} \simeq \frac{3}{4}\int_0^\tau F\left(\tau'\right)d\tau' + \frac{1}{2}F\left(0\right) - \frac{1}{4}\frac{dF\left(\tau\right)}{d\tau}.$$

Now, the correction $\Delta B(\tau)$ should be that which makes F constant:

$$B\left(\tau\right) \simeq \frac{3}{4}\int_0^\tau F^* d\tau' + \frac{1}{2}F^* + \Delta B\left(\tau\right),$$

where F^* is the correct, constant, flux. So,

$$\Delta B\left(\tau\right) = \frac{3}{4}\int_0^\tau \left[F\left(\tau'\right) - F^*\right]d\tau' + \frac{1}{2}\left[F\left(\tau\right) - F^*\right] - \frac{1}{4}\frac{d\left[F\left(\tau\right) - F^*\right]}{d\tau}.$$

Even though we used a number of approximations, the correction term uses only flux information, so that convergence to the proper solution is guaranteed. Fig. **@Fg.lucy@** shows how well this works. Typically, only 5 or 6 iterations are adequate.

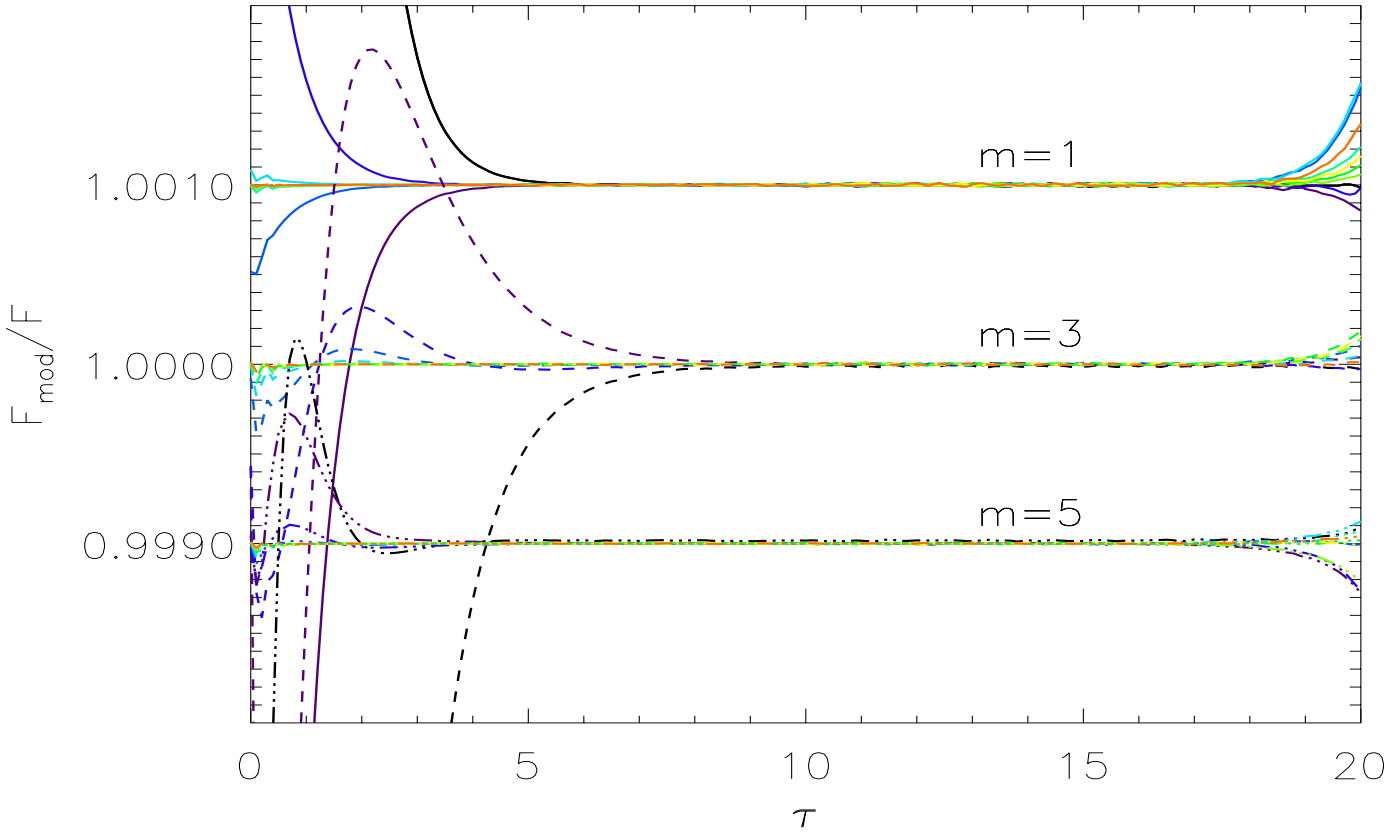

Figure 10.14.3: Convergence for the Lucy-Unsöld iterations. Results for the different m rays are offset for distinguishability.

Chapter 11.
Binary Stars

Consider a binary composed of two stars of masses M_1 and M_2. We define $M = M_1 + M_2$ and $\mu = M_1 M_2/M$. If a_1 and a_2 are the mean distances of the stars from the center of mass, then $M_1 a_1 = M_2 a_2$. The mean separation of the stars is $a = a_1 + a_2$. If the orbit is elliptical with eccentricity e, then the separation at periastron is $a(1-e)$ and at apastron it is $a(1+e)$. The total energy and angular momentum of the binary are

$$E = -\frac{1}{2}\frac{GM_1M_2}{a} \qquad J = \mu\sqrt{GaM\left(1-e^2\right)} = \mu\Omega a^2\sqrt{1-e^2}.$$

Kepler's Law is

$$\Omega^2 = \left(\frac{2\pi}{P}\right)^2 = \frac{GM}{a^3}.$$

The projected orbital velocity of star 1 is

$$v_1 = \Omega a_1 \sin i.$$

The quantity

$$f_1\left(M_1, M_2, i\right) = \frac{\left(M_2 \sin i\right)^3}{M^2} = \frac{v_1^3}{G\Omega}$$

is known as the mass function since it depends only on observables v_1, P. If Doppler shifts from star 2 are measured, then

$$f_2\left(M_1, M_2, i\right) = \frac{\left(M_1 \sin i\right)^3}{M^2} = \frac{v_2^3}{G\Omega}$$

can also be found. Then

$$\frac{M_2}{M_1} = \frac{v_1}{v_2}$$

independent of i. If the binary is eclipsing, the angle i can be determined and the masses individually determined as well.

11.1. The Roche Lobe

The total potential of a binary is

$$-\Phi = \frac{GM_1}{r_1} + \frac{GM_2}{r_2} + \frac{1}{2}d^2\Omega^2,$$

where r_1 and r_2 are the distances to stars 1 and 2 and d is the distance to the rotation axis. Restricting ourselves to the orbital plane, with the origin at the center of mass,

$$-\Phi\left(x, y\right) = \frac{GM_1}{\sqrt{\left(x-a_1\right)^2 + y^2}} + \frac{GM_2}{\sqrt{\left(x+a_2\right)^2 + y^2}} + \frac{1}{2}\left(x^2+y^2\right)\frac{GM}{a^3}.$$

In dimensionless coordinates $\bar{x} = x/a$, $\bar{y} = y/a$, $m_1 = M_1/M$, $m_2 = M_2/M$:

$$-\Phi(\bar{x},\bar{y}) = \frac{GM}{a}\left[\frac{m_1}{\sqrt{(\bar{x}-m_2)^2+\bar{y}^2}} + \frac{m_2}{\sqrt{(\bar{x}+m_1)^2+\bar{y}^2}} + \frac{1}{2}\left(\bar{x}^2+\bar{y}^2\right)\right].$$

Contours of constant Φ are shown in the figure. There are deep minima at the stellar centers, and maxima at five so-called Lagrangian points. The L_1 point between the stars is significant because if a star expands and reaches the potential surface passing through it, mass can be transferred to its companion.

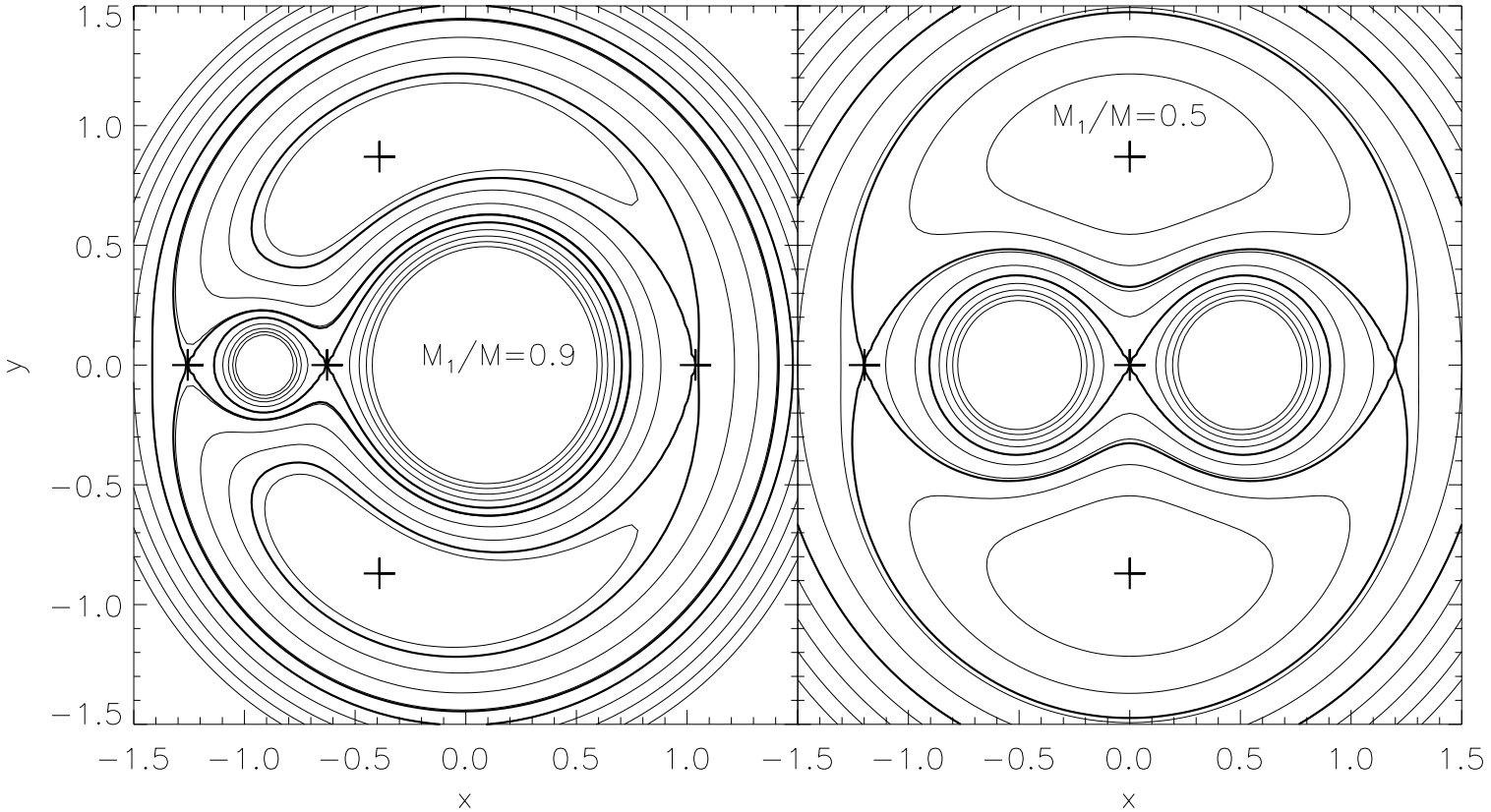

Figure 11.1.1: Contours of constant potential for a binary star. Lagrangian points are indicated, as is the Roche lobe (thick contour).

The equipotential surface that passes through L_1 is called the Roche lobe, and its size depends upon the mass ratio of the binary. Kopal (1959) gives for the radius R_R with nearly the same volume as the Roche lobe:

$$\frac{R_R}{a} = 0.46\left(\frac{M_1}{M}\right)^{1/3}. \tag{11.1.1}$$

A better fit is by Eggleton:

$$R_R/a = 0.49\left[.6 + \left(\frac{M_1}{M_2}\right)^{-2/3}\ln\left(1+\left(\frac{M_1}{M_2}\right)^{1/3}\right)\right]^{-1}. \tag{11.1.2}$$

11.2. Mass Transfer

Assume the binary is circular. Then

$$a = \frac{MJ^2}{GM_1^2\left(M - M_1\right)^2}, \qquad da = \left(\frac{2a}{M_1}\right)\left(\frac{2M_1 - M}{M - M_1}\right) dM_1, \tag{11.2.1}$$

if $dM = dJ = 0$. This shows that if $M_2 < M_1$, transferring mass from M_1 to M_2 results in a shrinkage of the orbit. Am episode of *conservative* mass transfer in a binary results in

$$a_{final} = a_{initial}\left(\frac{M_{1,initial}M_{2,initial}}{M_{1,final}M_{2,final}}\right)^2.$$

Eq. (11.2.1) implies that in terms of the mass ratio of the binary, $q = M_2/M_1$,

$$da = \frac{2a}{q}\left(\frac{q-1}{1+q}\right) dq, \tag{11.2.2}$$

or $a \propto (1+q)^4 q^{-2}$. Expressing Eq. (11.1.1) in terms of q, then taking the derivative and combining with Eq. (11.2.2),

$$dR_L = R_L\frac{da}{a} - \frac{R_L}{3}\frac{dq}{1+q} = R_L\left[\frac{2}{q}\left(\frac{q-1}{1+q}\right) - \frac{1}{3\left(1+q\right)}\right] dq.$$

This implies that the Roche lobe size reaches its minimum value when $q = 6/5$, or $M_1 = 5M/11$.

On the other hand, suppose that mass is lost from one star in the form of a wind and is not accreted onto the companion. Then we might expect that

$$a_{final} = a_{initial}\frac{M}{M - \Delta M},$$

and mass loss will cause an increase in a binary's separation.

Now consider mass transfer when star 1 fills its Roche lobe. Stable mass transfer occurs when the change in radius of star 1 after transferring an increment of mass through the inner Lagrangian point is not offset by a corresponding change in the Roche radius, triggered by the new mass ratio of the binary. This requires that the logarithmic change of radius with mass for star 1 satisfies

$$\frac{d\ln R}{d\ln M_1} \equiv \alpha \geq \frac{d\ln R_R}{d\ln M_1} = \frac{d\ln a}{d\ln M_1} + \frac{1}{3} = 2\left(\frac{2M_1 - M}{M - M_1}\right) + \frac{1}{3}.$$

In an equal mass binary, the first term vanishes. Generally, we can expect that this condition is generally satisfied. It is not, however, for a star with a convective envelope, for which $\gamma = 5/3$ and $R \propto M^{-1/3}$.

In some situations, mass transfer will be driven by losses of orbital angular momentum. The primary sources of angular momentum loss are magnetic braking and gravitational radiation. We have

$$\frac{\dot{a}}{a} = 2\frac{\dot{J}}{J} - 2\left(1 - \frac{M_2}{M_1}\right)\frac{\dot{M}_2}{M_2},$$

where the donor star is taken to be 2, so that $\dot{M}_2 < 0$. Using the simple Roche lobe formula,

$$\frac{\dot{R}_R}{R_R} = 2\frac{\dot{J}}{J} - 2\left(1 - \frac{M_2}{M_1}\right)\frac{\dot{M}_2}{M_2} + \frac{1}{3}\frac{\dot{M}_2}{M_2}.$$

Assume that $\dot{R}_2/R_2 = \alpha(\dot{M}_2/M_2$, where $\alpha = -1/3$ for a non-relativistic degenerate, or convective, star, and $\alpha = 1$ for a main sequence star. For stable mass transfer, R_2 should remain equal to R_R. Then we have

$$\frac{\dot{J}}{J} = \left(\frac{5}{6} + \frac{\alpha}{2} - \frac{M_2}{M_1}\right)\frac{\dot{M}_2}{M_2}.$$

Since both sides of this equation must be negative, we find

$$\frac{M_2}{M_1} \leq \frac{5}{6} + \frac{\alpha}{2}.$$

When $\alpha = -1/3(1)$, $M_2/M_1 \leq 2/3(4/3)$. Gravitational radiation leads to

$$\frac{\dot{J}}{J} = -\frac{32G^3}{5c^5}\frac{M_1 M_2 (M_1 + M_2)}{a^4} \ \mathrm{s}^{-1}. \tag{11.2.3}$$

11.3. Catastrophic Mass Loss and Binary Disruption

Another case of mass transferral occurs after a supernova explosion, but here the mass loss is catastrophic and the companion does not accept the mass. If too much mass is lost from the system, the binary will be disrupted. At the moment of explosion, the stars have instantaneous velocities relative to the center of mass (in a circular orbit) of

$$v_1 = \Omega a_1 = M_2\sqrt{\frac{G}{aM}}, \qquad v_2 = \Omega a_2 = M_1\sqrt{\frac{G}{aM}}.$$

Immediately after the supernova explosion, in which star 1 loses the mass ΔM, the velocities of the stars are

$$v_1' = \Omega a_1' = M_2\sqrt{\frac{G}{a\,(M - \Delta M)}}, \qquad v_2' = \Omega a_2' = (M_1 - \Delta M)\sqrt{\frac{G}{a\,(M - \Delta M)}}.$$

The energy of the binary is now

$$\begin{aligned} E &= \frac{1}{2}(M_1 - \Delta M)\, v_1'^2 + M_2 v_2'^2 - \frac{G\,(M_1 - \Delta M)\, M_2}{a} \\ &= \frac{G\,(M_1 - \Delta M)\, M_2}{2a}\left[\frac{M M_2}{(M - \Delta M)^2} + \frac{M\,(M_1 - \Delta M)}{(M - \Delta M)^2} - 2\right] \\ &= \frac{G\,(M_1 - \Delta M)\, M_2}{2a\,(M - \Delta M)}\left[M - 2\,(M - \Delta M)\right]. \end{aligned}$$

Therefore, the condition for the binary to survive the explosion is $E < 0$ or $\Delta M < M/2$. In practice, two important effects modify this result. First, the remnant of a supernova receives a substantial "kick" in the explosion. Pulsars are moving with average velocities of 200-500 km s^{-1}, far too large to explain by the velocity received from a disrupted binary. Depending upon the direction of the kick relative to the orbital motion, a larger mass loss might be tolerated without disrupting the binary. Second, we have ignored the possibility that the initial binary had substantial eccentricity.

Chapter 12.
Stellar Explosions

12.1. Approximate Model

Three assumptions make modeling tractable analytically. First, the pressure of the expanding remnant is dominated by radiation pressure. Second, the energy radiated from the surface and by gamma emission from radioactivity in the interior are small compared to the total energy. Third, spherical symmetry is valid to zeroth order.

The first law of thermodynamics $dE + PdV = TdS = dQ$ is

$$\dot{E} + P\dot{V} = -\frac{\partial L}{\partial M} + \dot{\epsilon} \tag{12.1.1}$$

where $E = aT^4V$ and $P = aT^4/3$ are the energy per gram and the pressure. Dots represent time derivatives. The volume per gram is $V = 1/\rho$, $\dot{\epsilon}$ is the energy input per gram per second from radioactivity, $L(r,t)$ is the luminosity, and $M(r,t)$ is the mass. Define $x = r(M,t)/R(t)$ as a dimensionless Lagrangian radius containing mass M at time t and radius r. $R(t)$ is the surface (defined below). The density at a given enclosed mass scales in time with $R(t)^{-3}$ since

$$M(x) = 4\pi R(t)^3 \int_0^x \rho(r,t)\, x^2 dx \tag{12.1.2}$$

is independent of time. We define a dimensionless density $\eta(x)$ by

$$\rho(r,t) \equiv 1/V = \rho_o \eta(x) \left(\frac{R_o}{R(t)}\right)^3, \tag{12.1.3}$$

where $\rho_o \equiv \rho(0,0)$ and $R_o \equiv R(0)$. Thus $\dot{V}/V = 3\dot{R}/R$.

If the right-hand side of Eq. (12.1.1) was neglected, adiabaticity applies and $\dot{T}/T = -\dot{R}/R$. This is the major time dependence of T. Now define

$$T^4(r,t) = \Psi(x)\,\phi(t)\,T_o^4 R_o^4/R^4(t) \tag{12.1.4}$$

so $\dot{T}/T = -\dot{R}/R + \dot{\phi}/4\phi$. Here, $T_o \equiv T(0,0)$. The luminosity becomes

$$L(r,t) = -\frac{4\pi r^2}{3}\frac{ac}{\kappa\rho}\frac{\partial T^4}{\partial r} = -\frac{4\pi x^2}{3}\frac{ac}{\kappa\rho_o\eta}\phi T_o^4 R_o \frac{d\Psi}{dx}, \tag{12.1.5}$$

where κ is the opacity. The equation of energy, Eq. (12.1.1) becomes

$$-\frac{3\dot{\epsilon}\rho_o^2 R_o^2}{acT_o^4}\left(\frac{\eta}{\phi\Psi}\right) + \frac{3R_o^3\rho_o}{c}\frac{\dot{\phi}}{\phi R} = \frac{1}{\Psi x^2}\frac{d}{dx}\left(\frac{x^2}{\eta\kappa}\frac{d\Psi}{dx}\right). \tag{12.1.6}$$

For the moment, ignore the radioactive contributions. The opacity is dominated by electron scattering, for which κ=constant, except very near the surface where the temperature is low. There, a Kramer's opacity ;with $\kappa \propto \rho; T^{-3.5} \propto \eta(\Psi\phi)^{-7/8} R^{1/2}$ would be appropriate. For simplicity, we take $\kappa = \kappa_o$. The differential equation (12.1.6) is now separable. It becomes

$$\frac{3\rho_o \kappa_o R_o^3}{c} \frac{\dot{\phi}}{\phi R} = -\alpha = \frac{1}{\Psi x^2} \frac{d}{dx}\left(\frac{x^2}{\eta}\frac{d\Psi}{dx}\right). \tag{12.1.7}$$

The time dependence is easily solved for:

$$\phi(t) = \exp\left[-\frac{\alpha c}{6\rho_o \kappa_o R_o^3}\int_0^t R(t)\,dt\right] = \exp\left[-\frac{1}{2R_o\tau_o}\int_0^t R(t)\,dt\right] \tag{12.1.8}$$

where the usual diffusion timescale is

$$\tau_o = \frac{3R_o^2 \rho_o \kappa_o}{\alpha c}. \tag{12.1.9}$$

The explicit time behavior depends upon $R(t)$ (see below).

12.2. Spatial Solutions

We next examine the spatial solution, which permits us to evaluate the eigenvalue α. The boundary conditions on Ψ are easily given. First, at the origin, $\Psi(0) = 1$ and $\Psi'(0) = 0$. At the surface we use the Eddington boundary condition

$$\left(\frac{T}{T_e}\right)^4 = \frac{\Psi}{\Psi_e} = \frac{3}{4}\left(\tau + \frac{2}{3}\right) \tag{12.2.1}$$

where $\tau(r) = -\int_r^R \kappa\rho dr$ is the optical depth and the subscript e refers to the effective radiating surface where $\tau = 2/3$ and $r = R$. From Eq. (12.2.1) we have that

$$\Psi(1) \equiv \Psi(\tau = 0) = \frac{1}{2}\Psi_e \tag{12.2.2}$$

and by differentiation, using $\Psi' = d\Psi/dx$,

$$\Psi'(1) = -\frac{3}{4}\Psi_e (\kappa\rho)_{x=1} R. \tag{12.2.3}$$

Combining these two, we have

$$\Psi(1) = -\frac{2}{3}\frac{\Psi'}{\kappa\rho R}\bigg|_{x=1}. \tag{12.2.4}$$

With $\eta\kappa$ constant, the solution of Eq. (12.1.7) is a polytrope of index 1:

$$\Psi(x) = \frac{\sin\sqrt{\alpha}x}{\sqrt{\alpha}x}. \tag{12.2.5}$$

The boundary condition Eq. (12.2.4) implies

$$\frac{\sin\sqrt{\alpha}}{\sqrt{\alpha}} = -\frac{2}{3}\frac{1}{\kappa_o \rho R}\left(\cos\sqrt{\alpha} - \frac{\sin\sqrt{\alpha}}{\sqrt{\alpha}}\right), \tag{12.2.6}$$

or

$$\sqrt{\alpha} \simeq \pi\left(1 - \frac{2}{3}\frac{1}{\kappa_o \rho R}\right). \tag{12.2.7}$$

Note that $\kappa_o \rho R$ is the total optical depth in the case of uniform density. For $\kappa_o \rho R \to \infty$, we have $\Psi(1) = 0$ and $\alpha = \pi^2$. Only if the total optical depth is less than about 10 is there significant deviation from this result, and this generally occurs only after several months. The leading correction is $\Psi(1) \simeq 2/(3\kappa_o \rho R)$. In what follows, we will simply impose the outer boundary condition as $\Psi(1) = 0$.

Suppose the density η is not constant. For $\eta = \Psi^m$ the solution is related to the polytropic Lane-Emden solution θ_n for the index n:

$$\Psi = \theta_n^n, \quad \eta = \theta_n^{n-1}, \quad x = \xi\sqrt{n/\alpha}, \quad n = 1/(1-m). \tag{12.2.8}$$

With the boundary condition $\Psi(1) = 0$, some cases are shown in Table 1. Note that $m = 1/3(2/3)[4/5]$ is the $n = 3/2(3)[5]$ polytrope, and the eigenvalue α is $\alpha = n\xi_1^2$. The case $m = 4/5$ has $\alpha = \infty$; a density spike in the center with a zero density mantle – not physically very relevant.

The polytropic solutions all have η (density) decreasing with distance from the center. A shell-like behavior can also be modelled:

$$\eta = \frac{1}{1-\beta x^2}; \qquad \Psi = 1 + \gamma x^2 + \delta x^4. \tag{12.2.9}$$

The boundary condition on the outside becomes $\gamma + \delta = -1$. Physical solutions are possible for two cases:

a) $\alpha = (140/9)(1 - \sqrt{8/35}) \simeq 8.119, \beta = \alpha/28, \gamma = -\alpha/6, \delta = -1 + \alpha/6$.

b) $\alpha = 6, \beta = 3/5, \gamma = -1, \delta = 0$.

The ratios of densities of the surface and center are $\eta(1)/\eta(0) = 1/(1-\beta) = 2.5$ (1.41).

Table 12.2.1: Spatial solutions to Eq. (12.1.7)

η	α	I_M	I_K	I_T	αI_M	I_M/I_K
$\eta = \theta_3^2$	142.7	0.0132	0.0024	0.00615	1.882	5.42
$\eta = \theta_{3/2}^{1/2}$	20.03	0.151	0.071	0.0556	3.028	2.15
$\eta = \eta_o$	π^2	1/3	1/5	0.101	3.290	5/3
a: $\eta = (1-\beta x^2)^{-1}$	8.119	0.409	0.260	0.113	3.303	1.572
b: $\eta = (1-\beta x^2)^{-1}$	6	0.553	0.366	0.133	3.319	1.510

12.3. Temporal Evolution

The temporal evolution will yield the light curves. When the shock emerges at the surface R_o at time $t = 0$, the energy is nearly evenly divided between thermal and kinetic energies:

$$E_T(t) = \int_0^R aT^4 4\pi r^2 dr = 4\pi R_o^3 a T_o^4 \frac{R_o}{R}\phi(t) I_T = E_T(0)\,\phi(t)\,\frac{R_o}{R}, \tag{12.3.1}$$

$$E_K(t) = \frac{1}{2}\int_0^R \rho v^2 4\pi r^2 dr = 2\pi\rho_o R_o^3 \dot{R}^2 I_K = E_K(0)\,\frac{\dot{R}_o^2}{\dot{R}^2}, \tag{12.3.2}$$

where $I_T = \int_0^1 \Psi x^2 dx$, $I_K = \int_0^1 \eta x^4 dx$, $v = dr/dt = x\dot{R}$ and $\dot{R}_o$ is its initial value. The total energy E_{SN} is a constant of the motion if the energy lost in radiation or gained from radioactivity is negligible, and is given by its initial value:

$$E_{SN} = E_T(0) + E_K(0) \simeq 2E_T(0). \tag{12.3.3}$$

Reference to Eq. (12.1.5) allows us to now write the luminosity as

$$L(t) = -\frac{4\pi}{3}\frac{ac}{\kappa_o\rho_o} R_o T_o^4 \left(\frac{\Psi'}{\eta}\right)_{x=1}\phi(t) = -\frac{4\pi c I_M R_o E_T(0)}{3\kappa_o M I_T}\left(\frac{\Psi'}{\eta}\right)_{x=1}. \tag{12.3.4}$$

The total ejected mass is $M = \int_0^R 4\pi\rho r^2 dr = 4\pi\rho_o R_o^3 I_M$, where $I_M = \int_0^1 \eta x^2 dx$. From Eq. (12.1.7) we have the identity

$$-\alpha I_T = \left(\frac{x^2\Psi'}{\eta}\right)_{x=1} = \left(\frac{\Psi'}{\eta}\right)_{x=1}, \tag{12.3.5}$$

so, with Eq. (12.3.4), we find

$$L(t) = \frac{2\pi c}{3\kappa_o}\frac{E_{SN}}{M}\alpha I_M R_o \phi(t) = \frac{E_{SN}\phi(t)}{2\tau_o}. \tag{12.3.6}$$

Conservation of energy $E_{SN} = E_T(t) + E_K(t)$ yields

$$\dot{R}^2 = \dot{R}_o^2\,(2 - \phi R_o/R). \tag{12.3.7}$$

At $t = 0$, $\phi(t)R_o/R(t) \simeq 1, R$ increases linearly with time: $R \simeq R_o + \dot{R}_o t$. The expansion timescale initially is

$$\tau_h = \frac{R_o}{\dot{R}_o} = 2.5\times 10^5 \left(\frac{R_o}{10^{14}\ \text{cm}}\right)\left(\frac{4\times 10^8\ \text{cm s}^{-1}}{\dot{R}_o}\right)\ \text{s}. \tag{12.3.8}$$

However, after a time of several τ_h, *i.e.*, at most days, the term $\phi R_o/R << 1$. The expansion is still linear in time, but $\sqrt{2}$ times faster than it was initially: the thermal energy has been converted into kinetic energy of expansion. A reasonable approximation is

$$R(t) = R_o + \sqrt{2}\dot{R}_o t. \tag{12.3.9}$$

We are finally able to solve for the function $\phi(t)$: using Eq. (12.1.8) we have

$$\phi\,(t) = \exp\left[-\frac{t}{\tau_o} - \frac{t^2}{\sqrt{2}\tau_o\tau_h}\right]. \tag{12.3.10}$$

Since $\tau_o >> \tau_h$, ϕ initially decreases exponentially, but before much decay has occurred, the decrease steepens into a Gaussian with time constant

$$\tau_{decay} = \sqrt{\sqrt{2}\tau_o\tau_h}. \tag{12.3.11}$$

12.4. The Light Curve

It is useful to now express things in terms of the quantities M, R_o and E_{SN} which we can hope to extract from a supernova's light curve. For example, the diffusion time becomes, using Eqs. (12.1.9),

$$\tau_o = 1.6\times10^7\frac{\kappa_o\pi^2}{\alpha I_M \mathrm{cm^2 g^{-1}}}\left(\frac{M}{\mathrm{M}_\odot}\right)\left(\frac{10^{14}\ \mathrm{cm}}{R_o}\right)\ \ \mathrm{s}. \tag{12.4.1}$$

The maximum observed velocities in the ejecta's spectra are, using Eqs. (12.3.2) and (12.3.3),

$$v_{max} \simeq \sqrt{2}\dot{R}_o = \sqrt{\frac{2E_{SN}I_M}{MI_K}} \simeq 10^9\sqrt{\frac{E_{SN}}{10^{51}\ \mathrm{ergs}}\frac{\mathrm{M}_\odot}{M}\frac{I_M}{I_K}}\ \ \mathrm{cm\ s^{-1}}. \tag{12.4.2}$$

Thus, the decay time, given by Eq. (12.3.11), becomes

$$\tau_{decay} = 1.7\times10^6\sqrt{\frac{\kappa_o\pi^2}{\alpha I_M\ \mathrm{cm^2 g^{-1}}}}\left(\frac{M}{\mathrm{M}_\odot}\right)^{3/4}\left(\frac{10^{51}\mathrm{ergs}}{E_{SN}}\right)^{1/4}\left(\frac{I_K}{I_M}\right)^{1/4}\ \ \mathrm{s}. \tag{12.4.3}$$

Additionally, we may write the luminosity, Eq. (12.3.6), as

$$L = 3.1\times10^{43}\frac{\alpha I_M\ \mathrm{cm^2 g^{-1}}}{\kappa_o\pi^2}\frac{E_{SN}}{10^{51}\mathrm{ergs}}\frac{\mathrm{M}_\odot}{M}\frac{R_o}{10^{14}\mathrm{cm}}\phi\ \ \mathrm{erg\ s^{-1}}, \tag{12.4.4}$$

and the effective temperature, $T_e = (L/4\pi\sigma R^2)^{1/4}$, as

$$T_e = 4.6\times10^4\left(\frac{\alpha I_M\ \mathrm{cm^2 g^{-1}}}{\kappa_o\pi^2}\right)^{1/4}\left(\frac{E_{SN}\ \mathrm{M}_\odot}{M\ 10^{51}\mathrm{ergs}}\right)^{1/4}\left(\frac{10^{14}\mathrm{cm}}{R_o}\right)^{1/4}\left(\frac{R_o}{R}\right)^{1/2}\phi^{1/4}\ \ \mathrm{K}, \tag{12.4.5}$$

The largest time dependence in the effective temperature is due to the expansion. The density and opacity dependences in the ejecta have a relatively small effect on observables, through $\sqrt{\alpha I_M}$ and $(I_M/I_K)^{1/4}$, which are insensitive to assumptions about η (Table I). For the last two cases shown, $I_M = \beta^{-3/2}(\tanh^{-1}(\sqrt{\beta}) - \sqrt{\beta})$ and $I_K = (I_M - 1/3)/\beta$.

For a Population I composition, $\kappa_o \simeq 0.33$ cm^2 g^{-1}, and the combination $\kappa_o \pi^2/\alpha I_M \simeq 1$. Similarly, $I_M/I_K \simeq 1.7$.

Summarizing: measurement of the largest velocities in the spectrum gives the ratio E_{SN}/M from Eq. (12.4.2). The effective temperature gives the initial radius, by Eq. (12.4.5). The peak luminosity, through Eq. (12.4.4) then can give the distance to the supernova. Finally, measurement of the decay timescale provide an estimate of the ejected mass, through Eq. (12.4.3).

12.5. Radioactive Heating

Typical Type 2 light curves do not show the effects of radioactive energy input until a year or more after peak light, but in Type 1s, it dominates the light curve from the first few days. Much more radioactive nickel is produced, and the ejecta mass and initial radius are much smaller.

Choose a simple parametrization of the radioactivity:

$$\dot{\epsilon} = \dot{\epsilon}_o \xi(x)\, e^{-t/\tau_r} \tag{12.5.1}$$

where ϵ_o is the energy released per gram of radioactive nuclei per second, ξ is the density distribution of the radioactive nuclei, and τ_r is the radioactive decay timescale. For ^{56}Ni$\rightarrow^{56}$Co, $\epsilon_o = 4.78\times10^{10}$ erg g^{-1} s^{-1} and $\tau_r = 7.6\times10^5$ s. For ^{56}Co$\rightarrow^{56}$Fe, $\epsilon_o = 7.97\times10^9$ erg g^{-1} s^{-1}, and $\tau_r = 9.82\times10^6$ s. In Type 1 events, however, the exploding envelope is transparent to much of the cobalt decay gamma rays and positrons, making a simple characterization of $\dot{\epsilon}$ difficult. This might have contributed to a mistaken identification with the decay time of Cf in some supernovae. For Ni-Co-Fe decay,

$$\dot{\epsilon} = \xi(x)\left[\dot{\epsilon}_o^{Ni} e^{-t/\tau_r^{Ni}} + \dot{\epsilon}_o^{Co}\left(1 - e^{-t/\tau_r^{Ni}}\right) e^{-t/\tau_r^{Co}}\right]. \tag{12.5.2}$$

The energy input from Co exceeds that from Ni when

$$\frac{t}{\tau_{Ni}} \simeq \frac{\ln\left(\dot{\epsilon}_o^{Ni}/\dot{\epsilon}_o^{Co}\right) + e^{-t/\tau_{Ni}}}{1 - \tau_{Ni}/\tau_{Co}} \simeq 2.08 \tag{12.5.3}$$

or about 18 days. After $4\tau_{Ni}$, the Ni decay is only producing 1/8 of the total energy, and Eq. (12.5.1) becomes a good approximation. The decay (^{56}Ni$\rightarrow^{56}$Fe) liberates 0.12 MeV/nucleon or about 2×10^{50} ergs per solar mass of radioactive material, which does not destroy the homologous expansion, since it is such a small fraction of E_{SN}.

Using

$$\dot{\epsilon} = \dot{\epsilon}_o \xi(x)\, f(t), \tag{12.5.4}$$

one notes that if the function $\dot{\epsilon}\eta/\phi\Psi$ is approximately independent of x, we can separate Eq. (12.1.6) as before. Taking $\xi(x)\eta(x)/\Psi(x) \equiv b$, a constant, is tantamount to concentrating radioactive nuclei in the center, not an obviously bad assumption. The initial mass of radioactive nuclei becomes

$$M_r = 4\pi R_o^3 \rho_o \int_0^1 \xi(x)\,\eta(x)\, x^2 dx = b\frac{I_T}{I_M} M. \tag{12.5.5}$$

We may now rewrite Eq. (12.1.6) as

$$\dot{\phi} + \phi \frac{R\left(t\right)}{\tau_o R_o} = f\left(t\right) \frac{R\left(t\right)}{R_o} \frac{2\dot{\epsilon}_o M_r}{E_{SN}}. \tag{12.5.6}$$

Define

$$\dot{u} = R\left(t\right) / \left(R_o \tau_o\right), \qquad u = t/\tau_o + t^2/\tau_{decay}^2.$$

The second follows from $R(t)$ (Eq. (12.3.9)). The solution of Eq. (12.5.6) is

$$\phi = \bar{\epsilon} e^{-u} \int_0^u e^u f du + e^{-u} \tag{12.5.7}$$

where

$$\bar{\epsilon} = \frac{2\dot{\epsilon}_o M_r \tau_o}{E_{SN}} = \frac{M_r \dot{\epsilon}_o}{L\left(0\right)} = 3.1 \frac{M_r M}{\mathrm{M}_\odot^2} \frac{10^{14}\ \mathrm{cm}}{R_o} \frac{10^{51}\ \mathrm{ergs}}{E_{SN}}, \tag{12.5.8}$$

evaluated for nickel decay. This quantity measures the importance of radioactivity to the light curve, especially at early times. For times $t < \tau_{Ni}$, we have $f \propto e^{-t/\tau_{Ni}}$, and for $t > 3\tau_{Ni}$, we have $f \propto e^{-t/\tau_{Co}}$. For extremely early times, $u << 1$, we may use the fact that $\tau_{Ni}, \tau_{decay} << \tau_o$ to find

$$\phi = 1 + \left(\bar{\epsilon} - 1\right) u \qquad u << 1. \tag{12.5.9}$$

For Type 1 supernovae, the initial radius is very small. For the envelope of the presupernova to be in hydrostatic equilibrium, the presupernova luminosity must be less than the Eddington limit $4\pi c G M_{core}/\kappa$. This implies that the envelope radius is limited to

$$R_o < \sqrt{\frac{cGM_{core}}{\sigma\kappa}} \frac{1}{T_e^2} = 2.1 \times 10^{13} \left(\frac{M_{core}}{1.4\mathrm{M}_\odot}\right)^{1/2} \left(\frac{6000\mathrm{K}}{\mathrm{T_e}}\right)^2 \mathrm{cm}. \tag{12.5.10}$$

Eq. (12.5.8) thus shows that $\bar{\epsilon} >> 1$, and we expect the bolometric luminosity to initially increase after the shock reaches the photosphere. For Type 2 supernovae with a red supergiant progenitor (we note the important exception of SN1987A!), $R_o \sim 10^{14}$ cm, $M_r < 0.1\mathrm{M}_\odot$, and so $\bar{\epsilon} \leq 1$ and the luminosity will begin to fall almost immediately.

Over very long times, Eq. (12.5.7) becomes

$$\phi \simeq e^{-u} + \bar{\epsilon}\left(f - e^{-u}\right). \qquad u >> 1 \tag{12.5.11}$$

Even for $\bar{\epsilon} < 1$ the radioactive term is important. For $t >> \tau_{decay}$, $u \propto t^2$ and $f \propto \exp(-t/\tau_{Co})$. The $f\bar{\epsilon}$ term will eventually dominate.

The luminosity function Eq. (12.5.7) has the property that it reaches a maximum when $\phi = f\bar{\epsilon}$, *i.e.*, the light curve peaks when it has the same value as the radioactive term, at least when $\bar{\epsilon} > 1$. If $\bar{\epsilon} < 1$, the maximum is at $t = 0$. The width of the maximum in the light curve, which may of course be measured, can be estimated from

$$\Delta_{peak} \simeq \left(\frac{d^2\phi}{dt^2}\right)_{t_{max}}^{-1/2} = \tau_{decay} \sqrt{\frac{\tau_{Co}}{2\phi_{max} t_{max}}} \tag{12.5.12}$$

where t_{max} is the time when the luminosity is maximum. Thus, the larger the decay time, the broader the peak of the light curve.

In summary, the luminosity, when radioactive input is considered, is

$$\begin{aligned} L &= 3.1\times 10^{43}\frac{E_{SN}}{10^{51}\ \text{ergs}}\frac{\mathrm{M}_\odot}{M}\frac{R_o}{10^{14}\ \text{cm}}\left[1+\bar{\epsilon}\int_0^u e^u f du\right]e^{-u}\ \text{ergs} \\ &= 3.1\times 10^{43}\left[\binom{3.1}{.5}\frac{M_r}{\mathrm{M}_\odot}\int_0^u e^u f du+\frac{E_{SN}}{10^{51}\ \text{ergs}}\frac{\mathrm{M}_\odot}{M}\frac{R_o}{10^{14}\ \text{cm}}\right]e^{-u}\ \text{ergs}. \end{aligned} \tag{12.5.13}$$

The upper (lower) number in the second equation corresponds to Ni (Co) decay. We have used representative values for the opacity and the spatial part of the solution. The more massive the ejecta, and the more compact the envelope, the more important radioactivity is. For consistency, the maximum amount of energy input by radioactivity ($\sum \dot{\epsilon}_o^r \tau_r$) should be small compared to E_{SN}. In the case of the Type 2 supernovae, with massive and extended envelopes, radioactivity becomes important at late enough times. From Eq. (12.5.11) this occurs when $e^{-u} \approx \bar{\epsilon} f$ or

$$\left(\frac{t}{\tau_{decay}}\right)^2-\frac{t}{\tau_{Co}}\simeq \ln\left[1+40\frac{E_{SN}}{10^{51}\ \text{erg}}\frac{\mathrm{M}_\odot}{M}\frac{0.1\mathrm{M}_\odot}{M_r}\frac{R_o}{10^{14}\ \text{cm}}\right], \tag{12.5.14}$$

which is generally $t \simeq (1-2)\tau_{decay} \simeq 100-200$ days.

12.6. Application to SN 1987A

SN 1987A appeared to be subluminous for a Type 2. Eq. (12.4.4) immediately suggests that the presupernova envelope must have been smaller than usual; in fact, from photographic identification, the progenitor was a blue, not a red, supergiant. Neutrinos being observed less than 4 hours before the optical display is corroborative evidence: the time necessary for the shock wave with a velocity equal to the largest velocities initially observed in the spectrum, about 5×10^8 cm s^{-1}, to traverse the envelope is equal to two hours (it takes 2 hours after shock breakout for the optical emission to occur) if $R_o \simeq 3\times10^{12}$ cm. The bolometric luminosity remained nearly constant for the first few weeks and then increased. The shape of the initial light curve thus cannot completely determine the envelope properties.

The initial luminosity, based on the assumed distance to the Large Magellanic Cloud of 50 kpc, was about 1.8×10^{41} ergs s^{-1}. Coupled with Eq. (12.5.13), evaluated at $t=0$, $R_o \simeq 2.5\times10^{12}$ cm gives an energy to mass ratio of $E_{SN}/M \simeq .18\times10^{51}$ ergs/$M_\odot$. Eq. (12.4.1) says that the diffusion time was about $\tau_o \simeq 20.2(M/M_\odot)$ yrs, and the decay time $\tau_{decay} \simeq 26.6\sqrt{M/M_\odot}$ days, for nominal values of the opacity, α, I_M and I_K.

After several months, the light curve became exponential decay with a halflife equal to that of Co decay. The total mass of radioactive nuclei may be found from the absolute position of the light curve's tail:

$$L\,(t\to\infty) \simeq 1.55\times10^{43}\left(\frac{M_r}{M_\odot}\right)e^{-t/\tau_{Co}}, \tag{12.6.1}$$

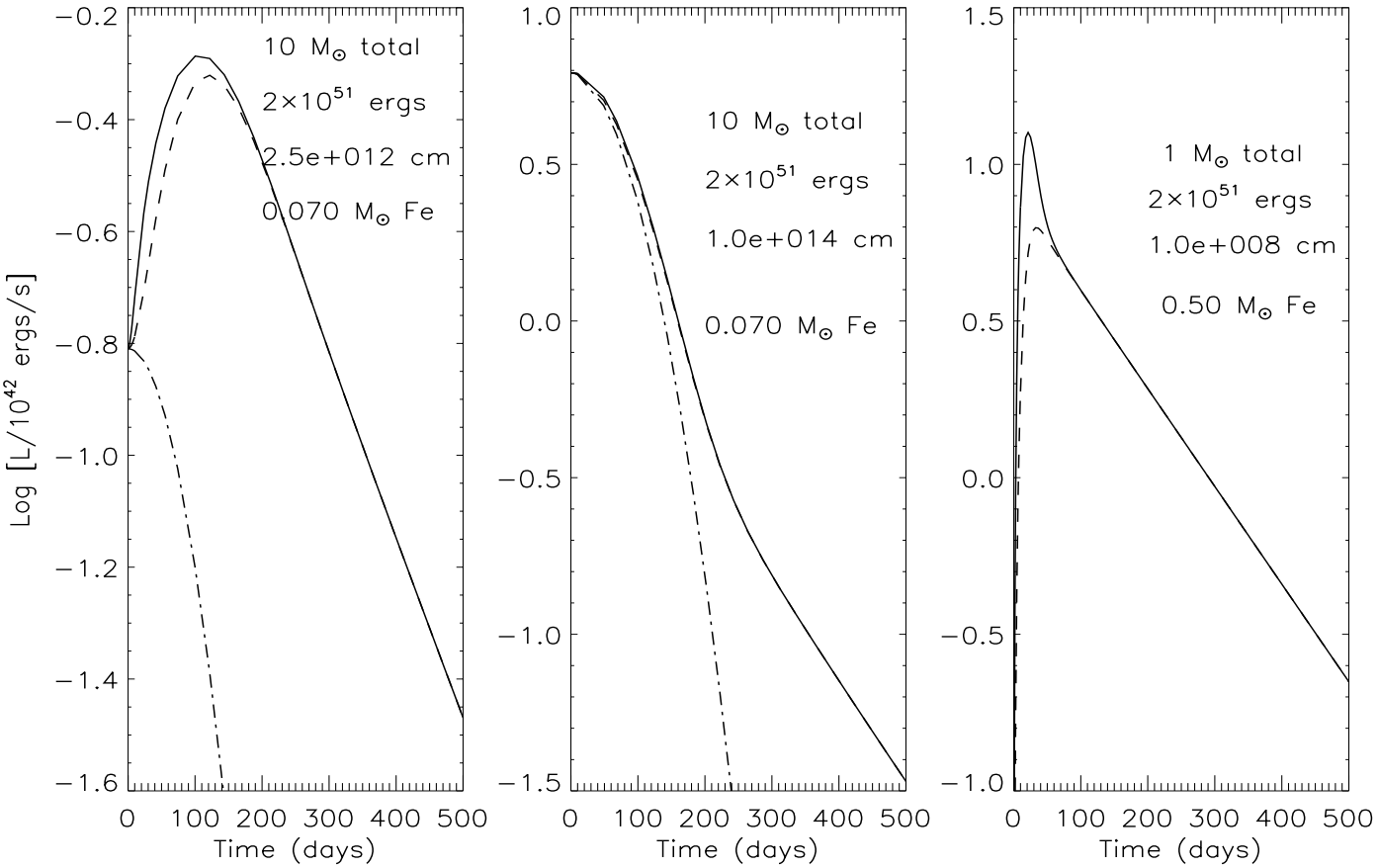

Figure 12.5.1: Light Curves for three typical cases of supernovae. Left panel: Type 2 supernova like SN 1987A. Middle panel: A more typical 'red giant' Type 2 supernova. Right panel: a Type 1a supernova. Solid lines are the full solutions with both Fe and Co radioactivity, dashed lines assume only Co radioactivity, and dash-dot lines assume no radioactive energy input.

which gives $M_r \simeq 0.075 M_\odot$. Therefore, for cobalt decay, one finds

$$\bar{\epsilon} = \frac{2\dot{\epsilon}_{Co} M_r \tau_o}{E_{SN}} = \frac{\dot{\epsilon}_{Co} M_r}{L\,(0)} \simeq 8.5, \tag{12.6.2}$$

and for nickel, $\bar{\epsilon} \simeq 40$. However, Eq. (12.5.9) demonstrates that until $\bar{\epsilon} u \simeq 1$, or $t \simeq \tau_{decay}/\sqrt{\bar{\epsilon}}$, the radioactive heating will have little effect. In the case of SN1987A, this occurs (for nickel) $32\sqrt{M/41 M_\odot}$ days after the explosion. The fact that the light curve began to increase due to radioactive heating after about 1 1/2 weeks is already an indication that the ejecta mass is in the range of 5–10 $M_\odot$.

The intermediate times are more complicated to describe analytically, but if we have simple radioactive decay of one species, so that $f = \exp(-t/\tau_{Co})$, one can describe the peak conditions according to:

$$u_{peak} + y \approx 1.8 - 2.0; \qquad \phi_{peak} \approx 0.17\bar{\epsilon}/y. \tag{12.6.3}$$

This approximation is valid when $\bar{\epsilon} >> 1$ and $0.3 < y < 1.5$ with

$$y = \frac{\tau_{decay}}{2\tau_{Co}} = 0.15 \left(\frac{M}{M_\odot}\right)^{3/4} \left(\frac{10^{51}\text{ergs}}{E_{SN}}\right)^{1/4}. \tag{12.6.4}$$

Thus, $t/\tau_{Co} \simeq 2y\sqrt{u}$. From the observation that the light curve peaked around $t_{peak} = 90$ days after the explosion, and the relations

$$u_{peak} = \left(t_{peak}/\tau_{decay}\right)^2 \simeq 12.3\,(M_\odot/M)\,; \qquad y = 0.23\sqrt{M/M_\odot},$$

we deduce that $M \approx 9 - 11 M_\odot$. We used the energy to mass ratio described above. The mass scales as the square root of the energy to mass ratio, and is inversely proportional to the opacity, whose value was taken to be equal to that for a solar composition gas (=0.33). For metal-rich ejecta the opacity is greater than for a solar gas, making our estimate of the mass too high.

It is worth noting that the light curve for SN 1987A, although agreeing with the general behavior of the solutions we have discussed, differs from them in some important respects. First, the observed peak value of the luminosity was about 5 times the initial luminosity (excluding transient effects due to the ultraviolet burst) compared to about $\phi_{peak} \simeq 0.17\bar{\epsilon}/y \simeq 2$ times in the analytic solution. Second, the peak of the observed light curve does not lie exactly on the asymptotic radioactive decay line, and it lacks the symmetry and breadth of the analytic solutions. This behavior implies the existence of additional energy sources or uneven distribution of radioactive components. One additional energy source is due to recombination in to the cooling wave that eats inward into the ejecta. This contribution cannot be easily included in the analytic solution.

12.7. Application to Type 1 Supernovae

In the case of Type 1 supernovae, involving the explosion of white dwarfs, the radius is of order 1000 km. The explosion energy is again of order 2×10^{51} ergs. Using Eq. (12.5.8), we find for Ni that $\bar{\epsilon} \approx 4 \times 10^5$ if the ejecta mass is 1 $M_\odot$ and 1/2 is Ni. We also note that the parameter

$$y = \tau_{decay}/2\tau_{Ni} = 1.3 \left(\frac{M}{M_\odot}\right)^{3/4} \left(\frac{10^{51}\ \text{erg s}^{-1}}{E_{SN}}\right)^{1/4} \approx 1.1 \tag{12.7.1}$$

for Ni decay. Eq. (12.6.3) then suggests that the peak in the light curve is reached when $u_{peak} \approx 0.6$ and $\phi_{peak} \approx 0.16\bar{\epsilon}$. The maximum luminosity is therefore about $0.16 M_r \dot{\epsilon}_{Ni} = 8 \times 10^{42}$ ergs/s, which is completely independent of R and is also insensitive to the explosion energy and the ejected mass. This is what makes Type 1 SN so valuable as distance indicators. Note that the light curve peak is noticeably shifted from the explosion time by a few weeks:

$$t_{peak} = \sqrt{u_{peak}}\tau_{decay} \approx 17 \text{ days}.$$

Chapter 13.
Supernovae and Neutrinos

The photonic and kinetic energies of a Type 2 supernovae are only a fraction of the total energy released. The optical energy is about 10^{43} erg/s for a month, or 10^{49} erg. The kinetic energy is about 10 $M_\odot$ at velocities 0.01 c^2, or 10^{51} erg. But the total energy released is the binding energy of the neutron star that's formed: $3GM^2/5R$ or $3 \cdot 10^{53}$ ergs. This energy emerges mostly in the form of neutrinos.

13.1. Neutrino Trapping

The discovery of neutral currents in the early 1970's led to the modern picture in which stellar collapse produces to a lepton-rich (electrons and neutrinos) remnant plus an ejected mantle powered by a shock and heat from neutrinos leaking out of the core. Electron capture, which otherwise would change the matter from $Y_e = Z/A \simeq 0.42$ before collapse to $Y_e \leq 0.1$ in cold, catalyzed neutron star matter, is suppressed because neutrino trapping occurs shortly after the collapse begins. We use $g_A = 1.253$,

$$\sigma_o = (4/\pi)\,(m_e c/\hbar)^4 \left(G_F/m_e c^2\right)^2 = 1.76 \times 10^{-44}\ \text{cm}^2.$$

1. Neutral current scattering by free nucleons,

$$\nu + n \stackrel{Z}{\rightarrow} \nu + n, \qquad \nu + p \stackrel{Z}{\rightarrow} \nu + p, \tag{13.1.1}$$

$$\sigma_n = \frac{\sigma_o}{4}\left(\frac{E_\nu}{m_e c^2}\right)^2 = 1.7 \times 10^{-44} E_\nu^2\ \text{cm}^2 \qquad ND,$$

$$\sigma_n = \frac{\pi^2 \sigma_o}{64}\left(1 + 2g_A^2\right)\left(\frac{T}{m_e c^2}\right)^2 \left(\frac{E_\nu}{p_F c}\right)\left(\frac{m_n c^2}{\epsilon_F}\right) = 2.1 \times 10^{-45} T^2 E_\nu \frac{\rho_s}{\rho}\ \text{cm}^2 \quad D.$$

2. Neutral current coherent scattering by heavy nuclei,

$$\nu + (Z, A) \stackrel{Z}{\rightarrow} \nu + (Z, A)\,, \tag{13.1.2}$$

$$\sigma_A = \frac{\sigma_o}{16}\left(\frac{E_\nu}{m_e c^2}\right)^2 \left[A + Z\left(4\sin^2\theta_W - 2\right)\right]^2 \simeq 4.2 \times 10^{-45} N^2 E_\nu^2\ \text{cm}^{-2}.$$

3. Charged current nucleon absorption,

$$\nu_e + n \stackrel{W}{\rightarrow} p + e^- \tag{13.1.3}$$

$$\sigma_a = \frac{\sigma_o}{2}\left(1 + 3g_A^2\right) Y_e \left(\frac{E_\nu}{m_e c^2}\right)^2 = 1.9 \times 10^{-43} Y_e E_\nu^2\ \text{cm}^2 \qquad ND,$$

$$\sigma_a = \frac{3\pi^2 \sigma_o}{128}\left(1 + 3g_A^2\right)\left(\frac{T}{m_e c^2}\right)^2 \left(\frac{m_n c^2}{\epsilon_F}\right)\left(\frac{Y_e}{1 - Y_e}\right)^{1/3} =$$

$$1.43 \times 10^{-42}\left(\frac{Y_e}{1 - Y_e}\right)^{1/3} T^2 \left(\frac{\rho_s}{\rho}\right)^{2/3}\ \text{cm}^2. \qquad D$$

4. Charged and neutral current electron-neutrino scattering,

$$\nu + e^- \overset{W,Z}{\rightarrow} \nu + e^-. \tag{13.1.4}$$

$$\sigma_e = 0.1\sigma_o \left(\frac{E_\nu}{m_e c^2}\right)^2 \frac{E_\nu}{\mu_e}. \tag{13.1.5}$$

The largest opacity is due to coherent scattering, and the neutrino mean free path ($\lambda_\nu = 1/ < \sigma\rho >$) is

$$\lambda_\nu \simeq \frac{60}{\rho_{12}} \left(6X_n + 5X_p + A\left(1 - x_N\right)^2 X_A\right)^{-1} \left(\frac{10 \text{ MeV}}{E_\nu}\right)^2 \text{km}. \tag{13.1.6}$$

We used a simple form for σ_α and $X_\alpha = 1 - X_n - X_p - X_H$. We find $\lambda_\nu = R \simeq (3M/4\pi\rho)^{1/3}$ when $\rho \simeq 3 \times 10^{10}$ g cm^{-3}. The actual trapping density occurs when the ν diffusion time is smaller than the collapse timescale:

$$\tau_d = \frac{3R^2}{\pi^2 c \lambda_\nu} \simeq .03\rho_{12} \text{ s} = \tau_c = \sqrt{33}\left(\frac{3}{8\pi G\rho}\right)^{1/2} \simeq 7.5 \times 10^{-3}\rho_{12}^{-1/2} \text{ s}.$$

The factor $\sqrt{33}$ follows from self similar models. Thus $\rho \simeq 4 \times 10^{11}$ g cm^{-3}.

$Y_L = Y_e + Y_\nu$ is frozen at values near 0.4, and the collapse is essentially adiabatic (no loss of neutrinos, no change in electron fraction). The adiabat has a rather low entropy, $s \simeq 1$ per nucleon, because of extensive neutrino cooling during the post-carbon burning stages of the precollapse iron core. At the beginning of collapse, $T \approx 0.7$ MeV, $\rho \approx 4 \times 10^9$ g cm^{-3}, and $Y_e \simeq 0.42$. The translational entropy of nuclei per *Fe nucleus* is

$$S_{nuc} = \frac{5}{2} + \log\left[\left(\frac{56mT}{2\pi\hbar^2}\right)^{3/2} \frac{1}{n_{56}}\right] \simeq 17.$$

Excited nuclear states will contribute an entropy per *nucleus* of

$$S_{ex} = 56\left(\frac{\pi^2}{2}\right)\left(\frac{T}{T_F}\right) \simeq 4.8,$$

where $T_F \simeq 35$ MeV is the fermi energy of nuclear matter. The entropy of electrons per *electron* is

$$S_e = \pi^2 \frac{T}{\mu_e} \simeq 1.1.$$

There is a dilute vapor of neutrons also, with an entropy per *nucleon* of

$$S_{vapor} = \frac{5}{2} + \log\left[\left(\frac{mT}{2\pi\hbar^2}\right)^{3/2} \frac{2}{n_n}\right] \simeq 12.9.$$

Summing these contributions, we find per baryon

$$s = X_H \frac{S_{nuc} + S_{ex}}{56} + S_e Y_e + S_{vapor} X_n \simeq 0.92.$$

(The solar center has an entropy per baryon in nuclei alone of 16.5).

13.2. Collapse

Consider a *one-zone* collapse model using $R \simeq (3M/4\pi\rho)^{1/3}$ to understand the evolution of Y_e and Y_L. Take

$$\frac{\partial \ln \rho}{\partial t} = \frac{1}{\tau_c}. \tag{13.2.1}$$

The first law of thermodynamics is

$$\dot{q} = T\dot{s} + \sum_i \mu_i \dot{Y}_i = < E_{\nu,esc} > \left(\dot{Y}_e + \dot{Y}_\nu\right), \tag{13.2.2}$$

where i refers to nucleons, nuclei and leptons. The heat change $\dot{q}$ is due to the escape of neutrinos with average energy $< E_{\nu,esc} >$. In nuclear statistical equilibrium, the sum is ($\hat{\mu} = \mu_n - \mu_p$)

$$\sum_i \mu_i \dot{Y}_i = \dot{Y}_e \left(\mu_e - \hat{\mu}\right) + \dot{Y}_\nu \mu_\nu. \tag{13.2.3}$$

$$T\dot{s} = -\dot{Y}_e \left(\mu_e - \hat{\mu} - \mu_\nu\right) - \left(\dot{Y}_e + \dot{Y}_\nu\right)\left(\mu_\nu - < E_{\nu,esc} >\right).$$

The first term is the entropy generation from being out of beta equilibrium while the second is due to losing νs. If νs freely escape, $\mu_\nu = 0$, and then

$$T\dot{s} = -\dot{Y}_e \left(\mu_e - \hat{\mu} - < E_{\nu,esc} >\right) \qquad \text{free escape.}$$

When νs are fully trapped, $< E_{\nu,esc} > = \mu_\nu$ because only νs at the top of the Fermi sea will escape. μ_ν increases until beta equilibrium is established and reverse reactions balance forward ones: entropy generation is halted.

For changes in Y_e, it is sufficient to consider only ν capture on free protons, which in the case of degenerate e^-s and freely escaping νs, is

$$\dot{Y}_e = -\frac{3}{5}\left(\frac{\mu_e}{m_e c^2}\right)^2 \mathcal{R} n Y_e X_p \sigma_o c = 488 \rho_{12} Y_e X_p \mu_e^2 \mathcal{R} \ \text{s}^{-1}, \tag{13.2.4}$$

where $\mathcal{R} = 1 - e^{(\mu_e - \hat{\mu} - \mu_\nu)/T}$ accounts for reverse processes that force the rates to 0 in $\beta-$equilibrium. Y_L changes due to neutrino loss. Early, νs freely stream out; later they leak out via diffusion. We can approximate

$$\dot{Y}_L \approx \frac{-Y_L}{\tau_\nu}; \qquad \tau_\nu = \frac{R}{c}\sqrt{1 + \left(\frac{3R}{\lambda_\nu}\right)^2}.$$

There is great sensitivity of Y_e on X_p and T. For non-interacting protons, $X_p \propto \exp(\mu_p/T)$. $\partial\mu_p/\partial Y_e \simeq 90$ MeV, when the sum of bulk, surface and Coulomb energies is considered. The entropy change is closely coupled to Y_e such that T will increase with ρ. Thus the system is highly self-regulating: as Y_e decreases, μ_p also decreases, which reduces X_p, turning off the electron captures. The net result is that full $\beta-$equilibrium is established by $\rho_{12} = 1$, and Y_L is marginally less than the initial Y_e.

13.3. Rebound and Shock Formation

Nuclei are not dissociated during the collapse due to the low entropy and high Y_e. When the central density approaches ρ_s, the nuclei merge into a nucleon fluid that is relatively incompressible. Only above this density is stability restored and the collapse halted. The pressure is dominated by relativistic electrons and neutrinos, with an effective adiabatic index constant at about 1.30. We've seen that a self-similar solution exists in this case. The collapsing core thus separates into an inner, homologous ($v \propto r$) part, and an outer, supersonically infalling part that is left behind. The mass of the inner core is somewhat larger than the equivalent Chandrasekhar mass $\propto Y_L^2$. When the collapse is halted, a shock wave is produced at the boundary between the inner and outer parts of the core, because outside of this point, sound travels more slowly than the matter is moving. Due to energy conservation, the initial energy of the shock is well approximated by the binding energy of the inner core $\propto GM^{5/3} \propto Y_L^{10/3}$.

For the shock to be successful, it must propagate through the outer core, and eject the envelope. The shock's energy is dissipated by dissociation of nuclei in its path, which takes about 9 MeV/nucleon, or $18{\times}10^{51}$ ergs/$M_\odot$. The mass of the outer core is that of the initial iron core minus the mass of the inner core. The success of the shock depends strongly on Y_L and the initial iron core mass. If the shock stalls, neutrino heating of matter behind the shock may eventually resuscitate it. Otherwise, the shock is forced back by ram pressure of infalling material, and a black hole would form.

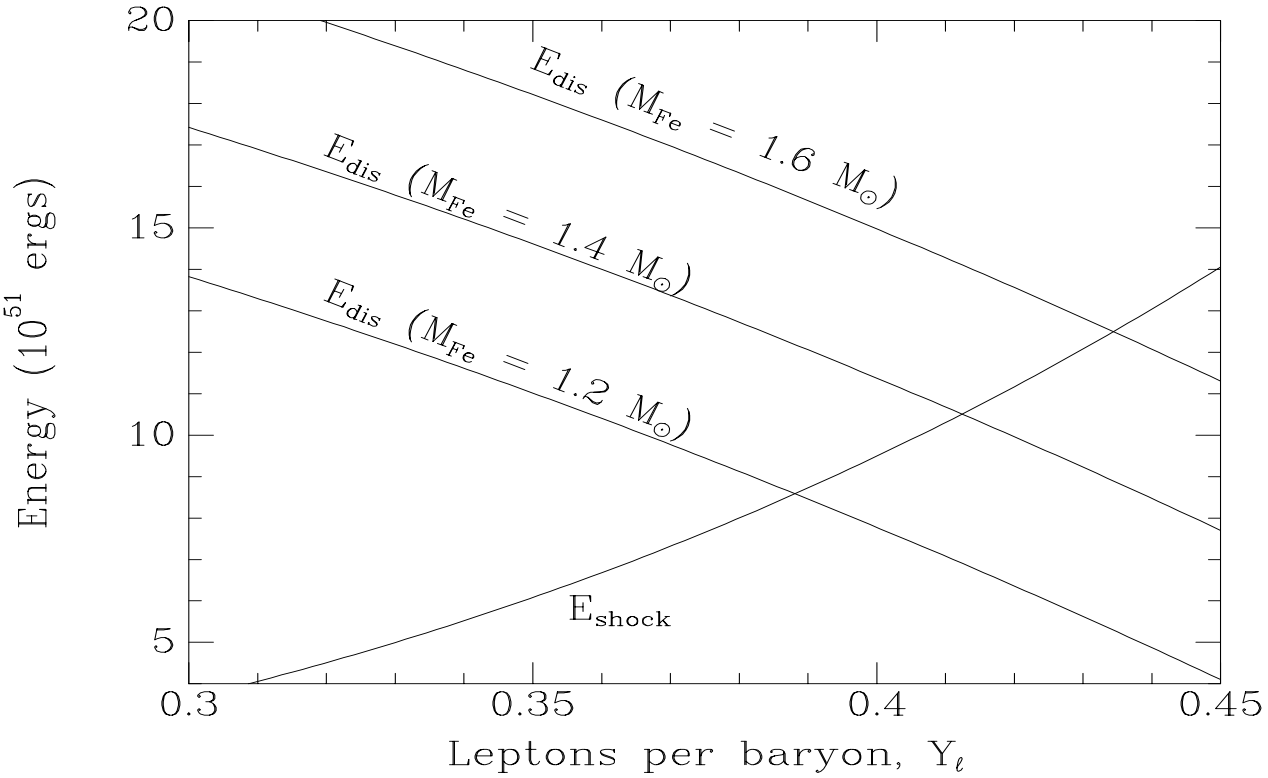

Figure 13.3.1: Competition of core size and dissociation in supernova energetics.

Can the shock succeed? The mass traversed and dissociated by the shock dissociate it, are both proportional to $\propto (Y_{Fe}^2 - Y_L^2)$, where $Y_{Fe} \simeq 0.41 - 0.43$ is the effective lepton fraction in the precollapse iron core, and Y_L is the trapped lepton fraction. On the other hand, the available energy scales as $Y_L^{10/3}$, showing the importance of Y_L (see the figure). It is essential that M_{Fe} be relatively small. Calculations show that $Y_L \leq 0.36 - 0.38$, so the shock alone appears to fail to eject the mantle and envelope of the star.

13.4. Neutrino Winds

Hundreds of milliseconds after bounce, $L_\nu = L_{\bar{\nu}} \approx 10^{52}$ ergs s^{-1}. This is smaller than the peak flux after bounce (10^{54} ergs/sec) and also the Eddington flux that would promptly lift off the outer envelope:

$$L_{edd} = \frac{4\pi cGM}{\kappa} \simeq 8.6 \times 10^{54} \frac{M}{M_\odot} \left(\frac{10 \text{ MeV}}{E_\nu} \right)^2 \text{ erg s}^{-1}.$$

Still, the flux heats the material behind the shock. The ν cross section is about $\kappa = \kappa_o E_\nu^2$, where $\kappa_o = 5.8 \times 10^{-20}$ cm^2 g^{-1} MeV^{-2}. The inverse processes of electron and positron capture cool the matter, with rates proportional to T^6. The fluxes are small and the mantle is transparent, so the net energy deposited is small. No more than about 0.1% of the total neutrino energy can be absorbed, but this may be sufficient.

The neutrino spectrum is thermal with T_ν and average energy

$$< E_\nu^2 >= \frac{F_5(0)}{F_3(0)} T_\nu^2 = \frac{310\pi^2}{147} T_\nu^2 = 20.8 T_\nu^2.$$

The net heating rate per gram, assuming $n_{e^-} = n_{e^+}$ and $F_\nu = F_{\bar{\nu}}$, is

$$\dot{q} = \frac{7}{16} \kappa_o a c T_\nu^6 \left[\frac{f}{4} \left(\frac{R_\nu}{R} \right)^2 - \left(\frac{T}{T_\nu} \right)^6 \right] \frac{F_5(0)}{F_3(0)}.$$

The factor of 7/16 is due to Fermi statistics; $a = \pi^2/[15(\hbar c)^3]$. Here T refers to an irradiated parcel at radius R, while the temperature and radius of the "neutrinosphere", from which the νs effectively emerge, are R_ν and T_ν. f is an anisotropy factor due to the spherical geometry that varies between 1, in the radial free streaming limit, to 4 in the opaque limit.

If T is small, $\dot{q} > 0$ and $\dot{T} > 0$. As T increases, $\dot{q} \to 0$ where the maximum temperature (*kinetic equilibrium*) occurs:

$$T_{max} = T_\nu \left(\frac{R_\nu}{2R} \right)^{1/3} \simeq 0.5 T_\nu / R_7^{1/3}, \tag{13.4.1}$$

if $f \simeq 1$, $R_\nu \simeq 30$ km and $R_7 = R/10^7$ cm. T_{max} is proportional to T_ν and depends inversely on radius. But $\dot{q} \propto T_\nu^6$. Hence, this mechanism thrives if T_ν is high. This requires careful transport and hydrodynamics.

In diffusion from a star with constant density, the neutrinosphere temperature T_ν decreases with time. But due to compressional heating as the mantle settles (the *negative specific heat effect*), and joule heating during transport, one finds that T_ν increases with time, until compression ceases. Suppose,initially, the stellar radius is R_1 with density and temperature profiles $\rho \propto r^{-n}$ and $T \propto r^{-n/3}$. The neutrinosphere is located at $R_{\nu 1} \sim R_1 - \ell_1$, where the mean free path of neutrinos is $\ell \propto (T^2\rho)^{-1} \propto r^{5n/3}$. Now compress the star by a factor α such that $R_1 = \alpha R_2$. The density and temperature at a given radius will scale to $\alpha^m\rho$ and $\alpha^{m/3}T$, respectively, where m might be about 3. The relation $R_{\nu 2} = R_2 - \ell_2$ now gives us the new radial position of the neutrinosphere and its temperature. Assuming that $\alpha - 1$ is small, we can see that

$$\begin{aligned} \frac{R_{\nu 2}}{R_{\nu 1}} &\simeq 1 + (\alpha - 1)\,\frac{5m - 3 - 3q}{3q + 5n}, \\ \frac{T_{\nu 2}}{T_{\nu 1}} &\simeq 1 + (\alpha - 1)\,\frac{n + q\,(n + m)}{3q + 5n}, \end{aligned} \tag{13.4.2}$$

where $q = R_{\nu 1}/\ell_1 \geq 1$. No matter what value q has, $T_{\nu 2} > T_{\nu 1}$, because $m > 0$ and $n > 0$. The question of whether or not the neutrinosphere moves in or out in space is more problematical, but is irrelevant.

Even if there is a net cooling near the neutrinosphere, since $\kappa \propto T^2$, a decrease in T will move the neutrinosphere deeper, to *higher* T. Paradoxically, the hotter interior core is revealed due to the cooling.

Early on, about 20 ms after bounce, just after the bounce-shock might have failed, the matter accreted through the shock has a density near 10^{10} g cm^{-3} and is electron-rich. At these electron densities, electron capture loss is swift, with a characteristic capture time

$$\tau_{cap} \simeq 5\,(2\rho_{10}Y_e)^{-5/3} \ \text{ ms.} \tag{13.4.3}$$

The mantle loses pressure support and sinks, falling onto the proto-neutron star. However, self-similar arguments show the pre-shock matter is thinning out with time roughtly as

$$\rho_{pre} \propto \rho_{post} \propto r^{-3/2}t^{1-3\gamma/2} \propto r^{-3/2}t^{-1},$$

since $\gamma \simeq 4/3$. It will only be a matter of time before the accreted matter has a low density and cools much less quickly.

The rarefaction of the accreted matter means it eventually beomes radiation dominated, when

$$\rho \simeq \rho_{rd} = 4 \times 10^9 \left(\frac{T}{2.5\ \text{MeV}}\right)^3 \ \text{g cm}^{-3} \simeq 4 \times 10^9 \left(\frac{T_\nu}{5\ \text{MeV}}\right)^3 \frac{1}{R_7} \ \text{g cm}^{-3}.$$

For matter-pressure dominated material, the specific internal energy $\propto T \simeq T_{max} \simeq$ constant. The gravitational specific energy

$$-E_g = \frac{GM}{R} \simeq 2 \times 10^{19} \frac{M}{1.5M_\odot}\frac{1}{R_7} \ \text{erg g}^{-1}$$

is independent of ρ, as is $E_{int} + E_g < 0$. However, the specific internal energy of radiation dominated matter increases with decreasing density. The density where $E_{int} = |E_g|$ is

$$\rho_{crit} = 7.4 \times 10^8 \left(\frac{T_\nu}{5 \text{ MeV}}\right)^4 \left(\frac{1}{R_7}\right)^{1/3} \text{ g cm}^{-3}. \tag{13.4.4}$$

When $\rho < \rho_{crit}$, the matter becomes unbound and explodes!

One must remember that this argument assumes that the heating to T_{max} is instantaneous, which is certainly unrealistic. A crude estimate of the heating time can be made by dividing $|E_g|$ by $\dot{q}$. We get

$$\tau_H \simeq \frac{10^{54} \text{ ergs s}^{-1}}{L_\nu} \frac{M}{1.5 M_\odot} \left(\frac{5 \text{ MeV}}{T_\nu}\right)^2 R_7 \text{ ms} \simeq 10 - 100 \text{ ms}, \tag{13.4.5}$$

where the neutrino luminosity is $L_\nu = 4\pi R_\nu^2 (7/64) a c T_\nu^4$. Thus, while the heating is certainly not instantaneous, it appears to be faster than some of the other relevant time scales, and fast enough to keep the post-shock matter near T_{max}.

Another point is that the binding energy of the mantle is constantly being buried through accretion in the proto-neutron star. Therefore, the binding energy that must be overcome to eject the envelope exterior to a given radius is constantly decreasing with time.

The time scales for T_ν increase, post-shock density decrease, binding energy decrease, capture turn-off, ram pressure increase, specific energy increase, etc., are all of the order of a few hundred milliseconds, while the heating is easily able to keep pace with all these changes. Time is on the supernova's side. If the neutrino fluxes are maintained and T_ν is reasonably high, all we have to do is wait a while for the shock to be revived by the core neutrinos.

13.5. The Birth of a Neutron Star

1. Following core bounce and shock passage, the star contains an unshocked, low entropy core of 0.5–0.7 $M_\odot$ with trapped neutrinos. This is surrounded by a low density, high entropy mantle accreting matter falling through the shock and rapidly losing energy due to electron captures and neutrino emission. The shock is momentarily stalled prior to an eventual explosion.
2. After about 0.5 s, accretion becomes much less important as the supernova becomes successful and the shock lifts off the stellar envelope. ν losses and deleptonization lead to pressure loss and mantle collapse. If enough accretion occurs, the star's mass could exceed M_{max} for hot, lepton-rich matter: if so a black hole forms and ν emission immediately halts.
3. This stage is dominated by neutrino diffusion causing deleptonization and heating of the core. $\nu-$nucleon absorption reactions set the diffusion timescale to 5–10 s. The maximum entropy reached in the core is about 2. As the core deleptonizes, strangeness, in the form of hyperons, a Bose condensate,

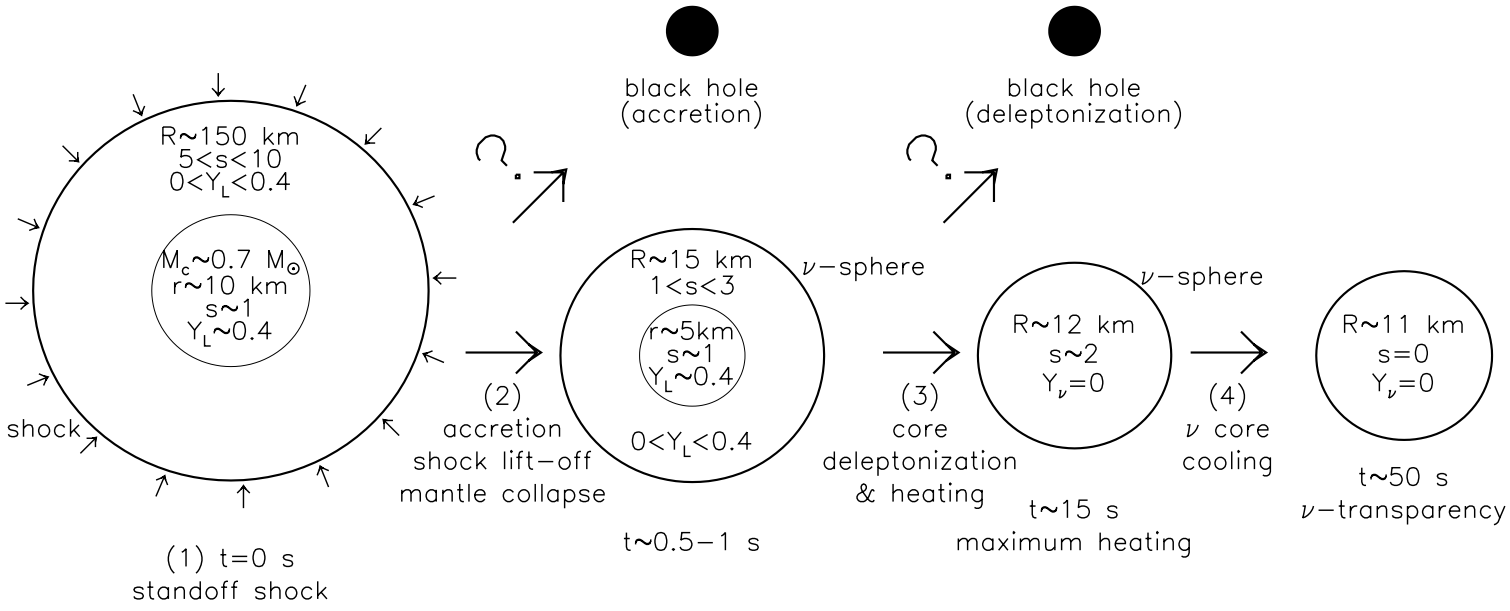

Figure 13.5.1: The main stages of the life of a protoneutron star.

or quarks, might apear. This could soften the equation of state and decrease M_{max} enough to form a black hole.

4. Following deleptonization is the long-term cooling phase. Although $\nu-$poor, thermally produced $\nu-\bar{\nu}$ pairs of all flavors are produced. The cooling timescale is determined by baryon and electron scattering of ν_μ and ν_τ, since ν_es remain more tightly coupled through absorption reactions. In approximately 50 s, as E_ν decreases, the star becomes essentially transparent to νs, and cools more rapidly.
5. (not shown) Following ν transparency, the core continues to cool by ν emission, but the star's crust cools less due to its low ν emissivity. The crust forms an insulating blanket preventing the star from coming to thermal equilibrium and keeps the surface relatively warm ($T \approx 3 \times 10^6$ K) for up to 100 years. This timescale is primarily sensitive to the neutron star's radius and the thermal conductivity of the mantle.
6. (not shown) Ultimately, the star achieves thermal equilibrium, a state of near isothermality, when the heat stored in the crust is depleted. The surface temperature T_{surf} is set by ν-rates in the star's core. If large (*rapid cooling*), T_{surf} becomes relatively small and the star is invisible. This could occur from direct Urca cooling from nucleons, hyperons, a Bose condensate or quarks. In *standard* cooling, relatively warm surfaces are maintained. Intermediate cases can occur if superfluids exist that suppress direct Urca cooling but don't eliminate it completely.

13.6. Analytic Models for Proto-Neutron Stars

We can examine some analytic models for proto-neutron star evolution. Let M be the gravitational mass, N the enclosed baryon mass, and F_ν and L_ν the number flux and luminosity of neutrinos. In GR, a term $e^\phi = \sqrt{-g_{00}}$ relates time at infinity τ with the coordinate time t. U is the internal energy per baryon.

$$\begin{aligned}
\frac{dP}{dr} &= -\frac{G\left(M + 4\pi r^3 P\right)\left(\rho + P/c^2\right)}{r\left(r - 2GM/c^2\right)} \\
\frac{dM}{dr} &= 4\pi r^2 \rho \\
\frac{dN}{dr} &= \frac{4\pi r^2 n}{\sqrt{1 - 2GM/rc^2}} \\
\frac{d\phi}{dP} &= -\frac{1}{P + \rho c^2} \\
\frac{dY_\nu}{d\tau} &= -e^{-\phi}\frac{\partial\left(4\pi r^2 F_\nu e^\phi\right)}{\partial N} + S_\nu \\
\frac{dY_e}{d\tau} &= -S_\nu \\
\frac{dU}{d\tau} &= -P\frac{d\left(1/n\right)}{d\tau} - e^{-2\phi}\frac{\partial L_\nu e^{2\phi}}{\partial N}
\end{aligned} \tag{13.6.1}$$

In the diffusion approximation, fluxes are driven by density gradients:

$$\begin{aligned}
F_\nu &= -\int_0^\infty \frac{c\lambda_\nu}{3}\frac{\partial n_\nu\left(E_\nu\right)}{\partial r} dE_\nu, \\
L_\nu &= -\int_0^\infty 4\pi r^2 \sum_i \frac{c\lambda_E^i}{3}\frac{\partial \epsilon_i\left(E_\nu\right)}{\partial r} dE_\nu.
\end{aligned} \tag{13.6.2}$$

The λ_ν and λ_E^i's are mean free paths for number and energy transport, respectively, and are functions of neutrino energy E_ν. $n_\nu(E_\nu)$ and $\epsilon_i(E_\nu)$ are the number and energy density of species $i = e, \mu$ at neutrino energy E_ν. GR corrections have been dropped for clarity.

We can combine Eq. (13.6.1) with the first law of thermodynamics to obtain the rate of change of the total lepton number and the entropy:

$$\begin{aligned}
n\frac{dY_L}{dt} = n\frac{dY_e}{dt} + \frac{dY_\nu}{dt} &= \frac{1}{r^2}\frac{\partial}{\partial r} r^2 F_\nu \\
nT\frac{ds}{dt} &= -\frac{1}{4\pi r^2}\frac{\partial L_\nu}{\partial r} - n\sum_{n,p,e,\nu} \mu_i \frac{dY_i}{dt}.
\end{aligned} \tag{13.6.3}$$

There are three main sources of opacity:

1. ν-nucleon absorption. Affects only $e-$types.

$$\lambda_{abs} \simeq 1.5\left(\frac{4\rho_s}{\rho}\right)^{5/3} f_{FL}\left(\frac{E_{\nu o}}{E_\nu}\right)^2 s^{-2} \text{ cm}$$

s is the entropy per baryon, $f_{FL} \simeq 2-3$ is a "Fermi-liquid" factor that corrects for interactions, and $E_{\nu o} \simeq 260$ MeV is typical at the beginning of deleptonization.

2. Neutrino-nucleon scattering. This elastic scattering affects all ν-types. $\lambda^e_{scn}/\lambda_{abs} \simeq 4(E_{\nu o}/E_\nu)$ for ν_e's. For ν_μ and ν_τ we have $\lambda^\mu_{scn} \simeq 2\lambda^e_{scn}$.
3. Neutrino-electron scattering. This inelastic scattering affects all types of neutrinos. The ratio $\lambda_{sce}/\lambda_{scn} \simeq 3s^2/f_{FL}$ in the degenerate limit and $19/f_{FL}$ when the neutrinos are nondegenerate.

Mean free paths for these processes are approximately:

1. $\lambda_{abs} \simeq 5$ cm, $\lambda_{abs} \propto E_\nu^{-2}$;
2. $\lambda_{scn} \simeq 20$ cm, $\lambda_{scn} \propto E_\nu^{-3}$;
3. $\lambda_{sce} \simeq 100$ cm, $\lambda_{sce} \propto E_\nu^{-3}$.

The opacities imply three kinds of fluxes:

1. a number flux F_ν of ν_es, dominated by absorption. With $\lambda_{abs} = \lambda_{abso}(E_{\nu o}/E_\nu)^2$, we have

$$F_\nu = \int_0^\infty \frac{c\lambda_{abs}}{3}\frac{\partial n_\nu\left(E_\nu\right)}{\partial r}dE_\nu = \frac{c\lambda_{abso}E^2_{\nu o}}{6\pi^2\left(\hbar c\right)^3}\frac{\partial \mu_\nu}{\partial r} \equiv a\frac{\partial \mu_\nu}{\partial r}. \tag{13.6.4}$$

2. an energy flux L^e_ν of ν_es, dominated by absorption:

$$L^e_\nu = \int_0^\infty 4\pi r^2\frac{c\lambda_{abs}}{3}\frac{\partial \epsilon_\nu\left(E_\nu\right)}{\partial r}dE_\nu = 4\pi r^2 a\frac{\partial}{\partial r}\left(\frac{\pi^2T^2}{6}+\mu^2_\nu\right). \tag{13.6.5}$$

3. an energy flux L^μ_ν of ν_μs and ν_τs, dominated by scattering. Since $\lambda_{scn} >> \lambda_{sce}$, but only electron scattering is effective in transferring energy, we have $\lambda_{eff} = \sqrt{\lambda_{scn}\lambda_{sce}} = \lambda_{effo}(E_{\nu o}/E_\nu)^3$.

$$L^\mu_\nu = 16\ln 2\pi r^2\frac{c\lambda_{effo}E^3_{\nu o}}{6\pi^2\left(\hbar c\right)^3}\frac{\partial T}{\partial r} \equiv 4\pi r^2 b\frac{\partial T}{\partial r}, \tag{13.6.6}$$

where we used the fact that $\mu_\nu = 0$ for ν_μs and ν_τs. Note also that $b >> aT$ since $\lambda_{eff} >> \lambda_{abs}$.

13.6.1. Deleptonization Era

Deleptonization is dominated by number transport:

$$n\frac{dY_L}{dt} = n\frac{\partial Y_L}{\partial Y_\nu}\frac{dY_\nu}{dt} = \frac{a}{r^2}\frac{\partial}{\partial r}\left(r^2\frac{\partial \mu_\nu}{\partial r}\right). \tag{13.6.7}$$

With the relations $nY_\nu \propto \mu^3_\nu$ and $\partial Y_L/\partial Y_\nu \propto \mu^{-1}_\nu$, valid for a degenerate neutrino gas, we establish

$$\mu_\nu\frac{\partial \mu_\nu}{\partial t} = \frac{a'}{r^2}\frac{\partial}{\partial r}\left(r^2\frac{\partial \mu_\nu}{\partial r}\right). \tag{13.6.8}$$

We seek separable solutions of the form $\mu_\nu = E_{\nu o}\phi(t)\psi(r)$.

$$\frac{E_{\nu o}}{a'}\frac{\partial\phi}{\partial t} = \frac{1}{r^2\psi^2}\frac{\partial}{\partial r}\left(r^2\frac{\partial\psi}{\partial r}\right) = -\alpha, \tag{13.6.9}$$

where α is a separation constant. One sees that

$$\phi = 1 - t/\tau_d; \qquad \tau_d = \frac{3}{c\lambda_{abso}\alpha}\left(\frac{\partial Y_L}{\partial Y_\nu}\right)_o. \tag{13.6.10}$$

The factor $(\partial Y_L/Y_\nu)_o \simeq 3$ for $Y_{\nu o} \simeq 0.06$. The radial dependence is

$$-\alpha R^2\psi^2 = \frac{1}{x^2}\frac{\partial}{\partial x}\left(x^2\frac{\partial\psi}{\partial x}\right), \tag{13.6.11}$$

i.e., a Lane-Emden polytope of index 2. Thus $\alpha R^2 \simeq 19$ and

$$\tau_d \simeq \frac{R^2}{2c\lambda_{abso}} \simeq 7.5 < s^2 > \left(\frac{R}{15\ \text{km}}\right)^2\ \text{s} \simeq 15\ \text{s}. \tag{13.6.12}$$

The deleptonization is accompanied by heating in the core, up to a maximum of about 2 in entropy per baryon. Cooling is delayed.

$$nT\frac{ds}{dt} = a\left[\frac{1}{r^2}\frac{\partial}{\partial r}\left(r^2\frac{\partial\left(\pi^2T^2/6\right)}{\partial r}\right) + \left(\frac{\partial\mu_\nu}{\partial r}\right)^2\right] + \frac{b}{r^2}\frac{\partial}{\partial r}\left(r^2\frac{\partial T}{\partial r}\right). \tag{13.6.13}$$

The first term is due to electrons, the second to the other neutrinos. There is heating or cooling depending on the sign of the T gradient, but the μ_ν gradients always lead to heating. When $\mu_\nu > T$, the first term dominates and we have net heating. When $\mu_\nu \simeq 0$, cooling dominates.

13.6.2. Thermal Cooling Era

The entropy is dominated by baryons for temperatures less than about 100 MeV. Thus, we may write

$$s \approx 2aT; \qquad a = \frac{1}{15}\frac{m^*}{m}\left(\frac{\rho_s}{\rho}\right)^{2/3}\ \text{MeV}^{-1} = a_o\left(\frac{\rho_c}{\rho_s}\right)^{-2/3}, \tag{13.6.14}$$

where m^* is the effective nucleon mass and ρ_c is the central density. Thus

$$T_{max} = \frac{s_{max}}{2a_c} \simeq 37.8s\left(\frac{m}{2m^*}\right)\left(\frac{n_c}{4n_s}\right)^{2/3}\ \text{MeV},$$

where a_o is the value of a at ρ_c at the beginning of cooling. Neglect the density dependence of m^* and use $m^* \simeq 0.5m$. Assuming separation of the time and radial dependence of the temperature $T = T_c\psi(r)\phi(t)$, and neglecting the first (electronic) term ($b >> aT$) in Eq. (13.6.13):

$$2anT_{max}\frac{d\phi}{dt} = \frac{b}{\psi r^2}\frac{\partial}{\partial r}\left(r^2\frac{\partial\psi}{\partial r}\right) = -\alpha. \tag{13.6.15}$$

Thus the spatial solution is an $n = 1$ polytrope with $\alpha = \pi^2$, and

$$\phi = 1 - (t - \tau_d)/\tau_c, \tag{13.6.16}$$

where

$$\tau_c = \frac{n s_o}{4 \ln 2} \frac{R^2}{\alpha} \frac{6\pi^2 (\hbar c)^3}{c \lambda_{eff o} E_{\nu o}^3} < s^3 > \simeq 7.5 \left(\frac{R}{12 \text{ km}} \right)^2 < s^3 > \text{ s} \simeq 25 \text{ s}. \tag{13.6.17}$$

This result agrees with numerical calculations. Thus, in spite of the fact that the mean free paths that dominate cooling are much larger than those that dominate deleptonization, the higher initial entropy and more compact remnant force the cooling timescale to be longer than the deleptonization timescale. Note that the temperature during cooling decreases linearly with time, which also agrees with numerical calculations show.

Chapter 14.
General Relativity and Compact Objects – Neutron Stars and Black Holes

14.1. Einstein's Equations

We confine attention to spherically symmetric configurations. The metric for the static case can generally be written

$$ds^2 = e^{\lambda(r)}dr^2 + r^2\left(d\theta^2 + \sin^2\theta d\phi^2\right) - e^{\nu(r)}dt^2. \tag{14.1.1}$$

Einstein's equations for this metric are:

$$\begin{aligned} 8\pi\rho\left(r\right) &= \frac{1}{r^2}\left(1 - e^{-\lambda}\right) + e^{-\lambda}\frac{\lambda'\left(r\right)}{r}, \\ 8\pi p\left(r\right) &= -\frac{1}{r^2}\left(1 - e^{-\lambda}\right) + e^{-\lambda}\frac{\nu'\left(r\right)}{r}, \\ p'\left(r\right) &= -\frac{p\left(r\right) + \rho\left(r\right)}{2}\nu'\left(r\right). \end{aligned} \tag{14.1.2}$$

Derivatives with respect to the radius are denoted by $'$. We employ units in which $G = c = 1$, so that 1 $M_\odot$ is equivalent to 1.475 km. The first of Eq. (14.1.2) can be exactly integrated. Defining the constant of integration so obtained as $m(r)$, the enclosed gravitational mass, one finds

$$e^{-\lambda} = 1 - 2m\left(r\right)/r, \qquad m\left(r\right) = 4\pi\int_0^r \rho r'^2 dr'. \tag{14.1.3}$$

The second and third of Einstein's equations form the equation of hydrostatic equilibrium, also known as the Tolman-Oppenheimer-Volkov (TOV) equation in GR:

$$\frac{-p'\left(r\right)}{\rho\left(r\right) + p\left(r\right)} = \frac{\nu'\left(r\right)}{2} = \frac{m\left(r\right) + 4\pi r^3 p\left(r\right)}{r\left(r - 2m\left(r\right)\right)}. \qquad r \le R \tag{14.1.4}$$

Near the origin, one has $\rho'(r) = p'(r) = m(r) = 0$. Outside the distribution of mass, which terminates at the radius R, there is vacuum with $p(r) = \rho(r) = 0$, and Einstein's equations give

$$m\left(r\right) = m\left(R\right) = M, \quad e^{\nu} = e^{-\lambda} = 1 - \frac{2M}{r}, \qquad r \ge R \tag{14.1.5}$$

the Schwarzschild solution. The black hole limit is seen to be $R = 2M$, which is 2.95 km for 1 $M_\odot$.

From thermodynamics, if there is uniform entropy per nucleon, the first law gives

$$0 = d\left(\frac{\rho}{n}\right) + pd\left(\frac{1}{n}\right)$$

where n is the number density. If e is the internal energy per nucleon, we have $\rho = n(m+e)$. From the above, $p = n^2 de/dn$, so that

$$d(\log n) = \frac{d\rho}{\rho + p} = -\frac{1}{2}\frac{d\rho}{dP}d\nu, \qquad dn = \frac{d\rho}{h},$$

where $h = (\rho + p)/n$ is the enthalpy per nucleon or the chemical potential. The constant of integration for the number density can be established from conditions at the surface of the star, where the pressure vanishes (it is not necessary that the energy density or the number density also vanish there). If $n = n_o, \rho = \rho_o$ and $e = e_o$ when $P = 0$, one finds $\rho_o - mn_o = n_o e_o$ and

$$mn(r) = (\rho(r) + p(r))\, e^{(\nu(r)-\nu(R))/2} - n_o e_o. \tag{14.1.6}$$

Another quantity of interest is the total number of nucleons in the star, N. This is not just M/m (m being the nucleon mass) since in GR the binding energy represents a decrease of the gravitational mass. The nucleon number is

$$N = \int_0^R 4\pi r^2 e^{\lambda/2} n(r)\, dr = \int_0^R 4\pi r^2 n(r) \left[1 - \frac{2m(r)}{r}\right]^{-1/2} dr, \tag{14.1.7}$$

and the total binding energy is

$$BE = Nm - M. \tag{14.1.8}$$

14.2. Analytic Solutions to Einstein's Equations

It turns out there are hundreds of analytic solutions to Einstein's equations. However, there are only 3 that satisfy the criteria that the pressure and energy density vanish on the boundary R, and that the pressure and energy density decrease monotonically with increasing radius. Three others are known that have vanishing pressure, but not energy density, at R.

14.2.1. Incompressible Fluid

Among the simplest analytic solutions is the so-called Schwarzschild interior solution for an incompressible fluid, $\rho(r) =$ constant. In this case,

$$\begin{aligned} m(r) &= \frac{4\pi}{3}\rho r^3, \qquad e^{-\lambda} = 1 - 2\beta(r/R)^2, \\ e^{\nu} &= \left[\frac{3}{2}\sqrt{1-2\beta} - \frac{1}{2}\sqrt{1-2\beta(r/R)^2}\right]^2, \\ p(r) &= \frac{3\beta}{4\pi R^2}\frac{\sqrt{1-2\beta} - \sqrt{1-2\beta(r/R)^2}}{\sqrt{1-2\beta(r/R)^2} - 3\sqrt{1-2\beta}}, \\ \rho &= n(m+e) = \text{ constant}, \qquad n = \text{ constant}. \end{aligned} \tag{14.2.1}$$

Here, $\beta \equiv M/R$. Clearly, $\beta < 4/9$ or else the central pressure will become infinite. It can be shown that this limit to β holds for *any* star. This solution is technically unphysical for the reasons that the energy density does not vanish on the surface, and that the speed of sound, $c_s = \sqrt{\partial p/\partial \rho}$ is infinite. The binding energy for the incompressible fluid is analytic (taking $e = 0$):

$$\frac{BE}{M} = \frac{3}{4\beta}\left(\frac{\sin^{-1}\sqrt{2\beta}}{\sqrt{2\beta}} - \sqrt{1-2\beta}\right) - 1 \simeq \frac{3\beta}{5} + \frac{9\beta^2}{14} + \cdots \tag{14.2.2}$$

In the case that e/m is finite, the expansion becomes

$$\frac{BE}{M} \simeq \left(1 + \frac{e}{m}\right)^{-1}\left[-\frac{e}{m} + \frac{3\beta}{5} + \frac{9\beta^2}{14} + \cdots\right]. \tag{14.2.3}$$

14.2.2. Buchdahl's Solution

In 1967, Buchdahl discovered an extension of the Newtonian $n = 1$ polytrope into GR that has an analytic solution. He assumed an equation of state

$$\rho = 12\sqrt{p_* p} - 5p \tag{14.2.4}$$

and found

$$\begin{aligned}
e^{\nu} &= (1-2\beta)\,(1-\beta-u)\,(1-\beta+u)^{-1}\,;\\
e^{\lambda} &= (1-2\beta)\,(1-\beta+u)\,(1-\beta-u)^{-1}\left(1-\beta+\beta\cos Ar'\right)^{-2}\,;\\
8\pi p &= A^2u^2\,(1-2\beta)\,(1-\beta+u)^{-2}\,;\\
8\pi\rho &= 2A^2u\,(1-2\beta)\,(1-\beta-3u/2)\,(1-\beta+u)^{-2}\,;\\
mn &= 12\sqrt{pp_*}\left(1-\frac{1}{3}\sqrt{\frac{p}{p_*}}\right)^{3/2}\,; \qquad c_s^2 = \left(6\sqrt{\frac{p_*}{p}} - 5\right)^{-1}\,.
\end{aligned} \tag{14.2.5}$$

Here, p_* is a parameter, and r' is, with u, a radial-like variable

$$\begin{aligned}
u &= \beta\left(Ar'\right)^{-1}\sin Ar';\\
r' &= r\,(1-\beta+u)^{-1}\,(1-2\beta)\,;\\
A^2 &= 288\pi p_*\,(1-2\beta)^{-1}\,.
\end{aligned} \tag{14.2.6}$$

For this solution, the radius, central pressure, energy and number densities, and binding energy are

$$\begin{aligned}
R &= (1-\beta)\sqrt{\frac{\pi}{288p_*\,(1-2\beta)}};\\
p_c &= 36p_*\beta^2\,; \quad \rho_c = 72p_*\beta\,(1-5\beta/2)\,; \quad n_c m_n c^2 = 72\beta p_*\,(1-2\beta)^{3/2}\,;\\
\frac{BE}{M} &= (1-1.5\beta)\,(1-2\beta)^{-1/2}\,(1-\beta)^{-1} - 1 \approx \frac{\beta}{2} + \frac{\beta^2}{2} + \frac{3\beta^3}{4} + \cdots.
\end{aligned} \tag{14.2.7}$$

This solution is limited to values of $\beta < 1/5$ for $c_{s,c} < 1$.

14.2.3. Tolman's Solution

In 1939, Tolman discovered that the simple density function $\rho = \rho_c[1-(r/R)^2]$ has an analytic solution. It is known as the Tolman 7 solution:

$$\begin{aligned} e^{-\lambda} &= 1-\beta x\,(5-3x)\,, \qquad e^{\nu} = (1-5\beta/3)\cos^2\phi, \\ P &= \frac{1}{4\pi R^2}\left[\sqrt{3\beta e^{-\lambda}}\tan\phi - \frac{\beta}{2}\,(5-3x)\right], \qquad n = \frac{(\rho+P)}{m}\frac{\cos\phi}{\cos\phi_1}, \\ \phi &= (w_1-w)\,/2+\phi_1, \qquad \phi_c = \phi\,(x=0)\,, \\ \phi_1 &= \phi\,(x=1) = \tan^{-1}\sqrt{\beta/\left[3\,(1-2\beta)\right]}, \\ w &= \log\left[x-5/6+\sqrt{e^{-\lambda}/\,(3\beta)}\right], \qquad w_1 = w\,(x=1)\,. \end{aligned} \tag{14.2.8}$$

In the above, $x=(r/R)^2$. The central values of P/ρ and the sound speed square $c_{s,c}^2$ are

$$\left.\frac{P}{\rho}\right|_c = \frac{2c_{s.c}^2}{15}\sqrt{\frac{3}{\beta}}, \qquad c_{s,c}^2 = \tan\phi_c\left(\tan\phi_c+\sqrt{\frac{\beta}{3}}\right). \tag{14.2.9}$$

There is no analytic result for the binding energy, but in expansion

$$\frac{BE}{M} \approx \frac{11\beta}{21}+\frac{7187\beta^2}{18018}+\frac{68371\beta^3}{306306}+\cdots\,. \tag{14.2.10}$$

This solution is limited to $\phi_c < \pi/2$, or $\beta < 0.3862$, or else P_c becomes infinite. For causality $c_{s,c} < 1$ if $\beta < 0.2698$.

14.2.4. Nariai's Solution

In 1950, Nariai discovered yet another analytic solution. It is known as the Nariai 4 solution, and is expressed in terms of a parametric variable r':

$$\begin{aligned} e^{-\lambda} &= \left(1-\sqrt{3\beta}\left(\frac{r'}{R'}\right)^2\tan f\left(r'\right)\right)^2, \quad e^{\nu} = (1-2\beta)\,\frac{e^2}{c^2}\left(\frac{\cos g\left(r'\right)}{\cos f\left(r'\right)}\right)^2, \\ f\left(r'\right) &= \cos^{-1}e+\sqrt{\frac{3\beta}{4}}\left[1-\left(\frac{r'}{R'}\right)^2\right], \quad g\left(r'\right) = \cos^{-1}c+\sqrt{\frac{3\beta}{2}}\left[1-\left(\frac{r'}{R'}\right)^2\right], \\ r &= \frac{e}{c}\frac{r'}{\cos f\left(r'\right)}\sqrt{1-2\beta}. \end{aligned} \tag{14.2.11}$$

The thermodynamic quantities are

$$\begin{aligned}
p\left(r'\right) &= \frac{\cos f\left(r'\right)}{4\pi R'^2}\frac{c^2}{e^2}\sqrt{3\beta}\Bigg[\sqrt{2}\cos f\left(r'\right)\tan g\left(r'\right) \\
&\quad \left[1-\sqrt{3\beta}\left(\frac{r'}{R'}\right)^2\tan f\left(r'\right)\right]-\sin f\left(r'\right)\left[2-\frac{3}{2}\sqrt{3\beta}\left(\frac{r'}{R'}\right)^2\tan f\left(r'\right)\right]\Bigg], \\
\rho\left(r'\right) &= \frac{\sqrt{3\beta}}{4\pi R'^2\sqrt{1-2\beta}}\frac{c^2}{e^2} \\
&\quad \left[3\sin f\left(r'\right)\cos f\left(r'\right)-\sqrt{\frac{3\beta}{4}}\left(\frac{r'}{R'}\right)^2\left(3-\cos^2 f\left(r'\right)\right)\right], \\
m\left(r'\right) &= \frac{r'^3}{R'^2}\frac{e}{c}\frac{\tan f\left(r'\right)}{\cos f\left(r'\right)}\sqrt{3\beta\left(1-2\beta\right)}\left[1-\sqrt{\frac{3\beta}{4}}\left(\frac{r'}{R'}\right)^2\tan f\left(r'\right)\right].
\end{aligned} \tag{14.2.12}$$

The quantities e and c are

$$\begin{aligned}
e^2 &= \cos^2 f\left(R'\right) = \frac{2+\beta+2\sqrt{1-2\beta}}{4+\beta/3} \\
c^2 &= \cos^2 g\left(R'\right) = \frac{2e^2}{2e^2+\left(1-e^2\right)\left(7e^2-3\right)\left(5e^2-3\right)^{-1}}.
\end{aligned}$$

The pressure-density ratio and sound speed at the center are

$$\begin{aligned}
\frac{P_c}{\rho_c} &= \frac{1}{3}\left(\sqrt{2}\cot f\left(0\right)\tan g\left(0\right)-2\right), \\
c_{s,c}^2 &= \frac{1}{3}\left(2\tan^2 g\left(0\right)-\tan^2 f\left(0\right)\right).
\end{aligned}$$

The central pressure and sound speed become infinite when $\cos g(0) = 0$ or when $\beta = 0.4126$, and the causality limit is $\beta = 0.223$. This solution is quite similar to Tolman 7.

14.3. The Neutron Star Maximum Mass

The TOV equation can be scaled by introducing dimensionless variables:

$$\begin{aligned}
&p = q\rho_o, \quad \rho = d\rho_o, \quad m = z/\sqrt{\rho_o}, \quad r = x/\sqrt{\rho_o}, \\
&\frac{dq}{dx} = -\frac{\left(q+d\right)\left(z+4\pi dx^3\right)}{x\left(x-2z\right)}, \qquad \frac{dz}{dx} = 4\pi dx^2 dx.
\end{aligned} \tag{14.3.1}$$

Rhoades and Ruffini showed that the causally limiting equation of state

$$p = p_o + \rho - \rho_o \qquad\qquad \rho > \rho_o \tag{14.3.2}$$

results in a neutron star maximum mass that is practically independent of the equation of state for $\rho < \rho_o$, and is

$$M_{max} = 4.2\sqrt{\rho_s/\rho_o}\ \mathrm{M}_\odot. \tag{14.3.3}$$

Here $\rho_s = 2.7 \cdot 10^{14}$ g cm^{-3} is the nuclear saturation density. One also finds for this equation of state that

$$R_{max} = 18.5\sqrt{\rho_s/\rho_o} \text{ km}, \qquad \beta_{max} \simeq 0.33\,. \tag{14.3.4}$$

Since the most compact configuration is achieved at the maximum mass, this represents the limiting value of β for causality.

Some analytic motivation for the above results was given by Nauenberg and Chapline. They assumed that in the interior of a star both n and ρ were constant, so P is also because of the first law. The TOV equation is not satisfied for this assumption, however, so the results of this analysis are very approximate. The baryon number for fixed n and ρ is

$$\begin{aligned} N &= 4\pi \int_0^R \frac{nr^2 dr}{\sqrt{1-8\pi\rho r^2/3}} = 4\pi n \left(\frac{3}{8\pi\rho}\right)^{3/2} \int_0^\chi \sin^2\theta d\theta \\ &= 2\pi n \left(\frac{3}{8\pi\rho}\right)^{3/2} (\chi - \sin\chi\cos\chi)\,, \end{aligned} \tag{14.3.5}$$

where $\sin\theta = \sqrt{2m(r)/r}$ and $\sin\chi = \sqrt{2\beta}$. In terms of χ, we can write the gravitational mass as

$$M = \sqrt{\frac{3}{32\pi\rho}} \sin^3\chi.$$

As χ increases, n, ρ and p in the star increase, and the mass M reaches a maximum for $\chi < \pi/2$. To guarantee stability, the total nucleon number N must also be maximized, which is equivalent to the equation

$$\left.\frac{\partial M}{\partial \chi}\right|_N = 0.$$

This results in a pair of equations:

$$\frac{d\rho}{\rho} = 6\frac{\cos\chi}{\sin\chi}d\chi, \qquad 4\sin^2\chi d\chi = (\chi - \sin\chi\cos\chi)\left(3\frac{d\rho}{\rho} - 2\frac{dn}{n}\right).$$

Combining this with the first law $d\rho/dn = (\rho + p)/n$, we obtain

$$\frac{p}{\rho} = \frac{6\cos\chi\,(\chi - \sin\chi\cos\chi)}{9\chi\cos\chi - 9\sin + 7\sin^3\chi}.$$

The condition that $p/\rho < \infty$ limits $\sin\chi < 0.985$, and $p/\rho < 1$ limits $\sin\chi < 0.956$. The further condition $dp/d\rho < 1$ limits $\sin\chi < 0.90$, which is equivalent to $\beta < 0.405$. Note this value is significantly larger than the limit obtained above, because of the less restrictive conditions. Nevertheless, we can now derive a maximum mass by employing the maximal equation of state Eq. (14.3.2). Rewriting this equation as

$$\rho > \frac{\rho_o - P_o}{1 - P/\rho},$$

and applying it to the mean density of the star $\rho = 3M/(4\pi R^3)$, using $\beta = M/R$, we find

$$M = \sqrt{\frac{3\beta^3}{4\pi\rho}} < \sqrt{\frac{3\beta^3}{4\pi\rho_o}\,(1 - p/\rho)}.$$

It is valid to have taken $p_o << \rho_o$. In geometrized units, the nuclear saturation density $\rho_s = 2.7 \cdot 10^{14}$ g cm^{-3} has the equivalence $\rho_s^{-1/2} = 70$ km or 45.5 $\mathrm{M}_\odot$. Therefore,

$$M < 45.5\sqrt{\frac{3\beta^3}{4\pi}\frac{\rho_s}{\rho_o}\,(1 - p/\rho)}\ \mathrm{M}_\odot.$$

With $\beta = 0.405$ and $p/\rho = 0.364$, the limiting mass is $M < 4.57\sqrt{\rho_s/\rho_o}\ \mathrm{M}_\odot$.

For the Buchdahl solution at the causal limit, $\beta = 1/6$ and $p/\rho = \beta/(2 - 5\beta)$, which lead to

$$M = (1 - \beta)\sqrt{\frac{\pi\beta^3\,(1 - 5\beta/2)}{4\,(1 - 2\beta)\,\rho_c}} < 2.14\sqrt{\rho_s/\rho_c}\ \mathrm{M}_\odot.$$

For the Tolman 7 solution at the causal limit, $\beta \simeq 0.27$ and $p/\rho = 2/(\sqrt{75\beta}) \simeq 0.44$, which lead to

$$M = \sqrt{\frac{15\beta^3}{8\pi\rho_c}} < 4.9\sqrt{\rho_s/\rho_c}\ \mathrm{M}_\odot.$$

Finally, for the Nariai 4 solution at the causal limit, $\beta \simeq 0.228$ and $p/\rho \simeq 0.246$, which lead to

$$M = \frac{\beta}{\cos f\,(R')}\sqrt{\frac{3^{3/2}\beta^{1/2}\sin f\,(0)\cos f\,(0)}{4\pi\rho_c}} < 3.4\sqrt{\rho_s/\rho_c}\ \mathrm{M}_\odot.$$

14.4. Maximal Rotation Rates for Neutron Stars

The absolute maximum rotation rate is set by the "mass-shedding" limit, when the rotational velocity at the equatorial radius (R) equals the Keplerian orbital velocity $\Omega = \sqrt{GM/R^3}$, or

$$P_{min} = 0.55\left(\frac{10\ \mathrm{km}}{R}\right)^{3/2}\left(\frac{M}{\mathrm{M}_\odot}\right)^{1/2}\ \mathrm{ms}. \qquad (14.4.1)$$

However, the actual limit on the period is larger because rotation induces an increase in the equatorial radius. In the so-called Roche model, one treats the rotating star as being highly centrally compressed. For an $n = 3$ polytrope, $\rho_c/\bar{\rho} \simeq 54$, so this would be a good approximation. In more realistic models, such as $\rho = \rho_c[1 - (r/R)^2]$, for which $\rho_c/\bar{\rho} = 5/2$, and an $n = 1$ polytrope, for which $\rho_c/\bar{\rho} = \pi^2/3$, this approximation is not as good. Using it anyway, the gravitationl potential near the surface is $\Phi_G = -GM/r$ and the centrifugal potential is $\Phi_c = -(1/2)\Omega^2 r^2 \sin^2\theta$, and the equation of hydrostatic equilibrium is

$$(1/\rho)\,\nabla P = \nabla h = -\nabla\Phi_G - \nabla\Phi_c, \qquad (14.4.2)$$

where $h = \int dP/\rho$ is the enthalpy per unit mass. Integrating this from the surface to an interior point along the equator, one finds

$$h\,(r) - GM/r - (1/2)\,\Omega^2 r^2 = K = -GM/r_e - (1/2)\,\Omega^2 r_e^2,$$

where r_e is the equatorial radius and $h(r_e) = 0$. We assume $K = -GM/R$, the value obtained for a non-rotating configuration. The potential $\Phi \equiv \Phi_G + \Phi_c$ is maximized at the point where $\partial\Phi/\partial r\Big|_{r_c} = 0$, or where $r_c^3 = gM/\Omega^3$ and $\Phi = -(3/2)GM/r_c$. Thus, r_e has the largest possible value when $r_e = r_c = 3R/2$, or

$$\Omega^2 = \frac{GM}{r_c^3} = \left(\frac{2}{3}\right)^3 \frac{GM}{R^3}. \tag{14.4.3}$$

The revised minimum period then becomes

$$P_{min} = 1.0 \left(\frac{10\ \mathrm{km}}{R}\right)^{3/2} \left(\frac{M}{\mathrm{M}_\odot}\right)^{1/2}\ \mathrm{ms}. \tag{14.4.4}$$

Calculations including general relativity show that the minimum spin period for an equation of state can be accurately expressed in terms of its maximum mass and the radius at that maximum mass as:

$$P_{min} \simeq 0.82 \left(\frac{10\ \mathrm{km}}{R_{max}}\right)^{3/2} \left(\frac{M_{max}}{\mathrm{M}_\odot}\right)^{1/2}\ \mathrm{ms}. \tag{14.4.5}$$

It is interesting to compare the rotational kinetic energy $T = I\Omega^2/2$ with the gravitational potential energy W at the mass-shedding limit. I is the moment of inertia about the rotation axis:

$$I = \frac{8\pi}{3} \int_0^R r^4 \rho dr$$

for Newtonian stars. (In GR, one must take into account frame-dragging as well as volume and redshift corrections.) Using $\Omega^2 = (2/3)^3 GM/R^3$, we can write $T = \alpha(2/3)^3 GM^2/R$ and $|W| = \beta GM^2/R$. We have $\alpha = 1/5, \beta = 3/5$ for an incompressible fluid; $\alpha = 1/3 - 2/\pi^2, \beta = 3/4$ for an $n = 1$ polytrope; $\alpha = 0.0377, \beta = 3/2$ for an $n = 3$ polytrope; $\alpha = 1/7, \beta = 5/7$ for $\rho = \rho_c[(1 - (r/R)^2]$. We therefore find that $T/|W|$ is 0.0988, 0.0516, 0.00745 and 0.0593, respectively, for these four cases, at the mass-shedding limit. For comparison, an incompressible ellipsoid becomes secularly (dynamically) unstable at $T/|W| = 0.1375(0.2738)$, much larger values.

Chapter 15.
Galactic Chemical Evolution

An important observational input is the age-metallicity $t - Z$ relation, or AMR, which has been obtained by combining metallicity measurements with stellar ages derived from theoretical isochrones. The result can be expressed in a number of ways, given the errors in the observations:

$$\begin{aligned} \log_{10} \frac{t}{1 \text{ Gy}} =& 0.93 + 1.3 \left[\text{Fe/H}\right] - 0.04 \left[\text{Fe/H}\right]^2 \\ \left[\text{Fe/H}\right] =& 0.68 - \frac{11.2 \text{ Gy}}{t + 8 \text{ Gy}}, \end{aligned} \tag{15.1}$$

where $\left[\text{Fe/H}\right] \equiv \log_{10}(Z/Z_\odot)$. The first form is more useful when the initial metallicity is very small, but it does not have an effective upper limit. As $t \to \infty$, we expect that gas will tend to be continuously exhausted which raises Z to a terminal value, as in the second form. The second form has $Z(t \to \infty)/Z_\odot \approx 4.8$, $Z(t_1)/Z_\odot \approx 1.32$ at the present, and $Z(0)/Z_\odot \approx 0.19$ at $t = 0$. Interestingly, when one plots the second form in a linear-linear plot, one finds that it is well-approximated by a linear relation

$$Z = Z\left(0\right) + \left[Z\left(t_1\right) - Z\left(0\right)\right] \frac{t}{t_1}, \tag{15.2}$$

where $t_1 \approx 12$ Gy is the time since disk formation.

Theoretically, we can attempt to calculate the evolution of Z in the solar neighborhood. Defining the birthrate b of stars as the mass of stars born per unit time, the total stellar birthrate is:

$$\psi\left(t\right) = \int_0^\infty m b\left(m, t\right) dm.$$

If the initial mass function (IMF) is constant in time it is $\phi(m) = b(m,t)\psi(t)$ and is normalized

$$\int_0^\infty m \phi\left(m\right) dm = 1.$$

The mass of gas (usually defined in terms of a mass per unit area integrated vertically through the galactic disc) changes because of star formation (ψ), gas loss from stars $R\psi$, and inflow (f):

$$\frac{dm_g}{dt} = -\psi\left(t\right) + R\left(t\right)\psi\left(t\right) + f\left(t\right).$$

If τ_m is the lifetime of a star with mass m, which sheds at death all but a remnant mass w_m, and if $m(t)$ is the mass for which $\tau_m = t$, we have

$$\begin{aligned} R\left(t\right)\psi\left(t\right) &= \int_{m(t)}^\infty \left(m - w_m\right) \phi\left(m\right) \psi\left(t - \tau_m\right) dm \\ &\simeq \psi\left(t\right) \int_{m(t_0)}^\infty \left(m - w_m\right) \phi\left(m\right) dm \equiv R\psi\left(t\right). \end{aligned}$$

We used the *instantaneous recycling* approximation, which neglects τ_m and the integral over the IMF is from the present turnoff mass (1 $M_\odot$) to the upper limit for stars. R is about 0.2–0.4 for the local IMF.

$$\frac{dm_g}{dt} = -\left(1-R\right)\psi\left(t\right) + f\left(t\right).$$

This equation does not apply for metals, which are produced in stars. The mass fraction of a star ejected as newly synthesized metals is p_{zm}. The metallicity Z of the infalling material may not be equal to that already present in m_g: call it Z_f. Then

$$\frac{dZm_g}{dt} = -Z\left(t\right)\psi\left(t\right) + \int_{m(t)}^{\infty}\left[\left(m-w_m\right)Z\left(t-\tau_m\right) + p_{zm}m\right]\phi\left(m\right)\psi\left(t-\tau_m\right)dm$$
$$+ Z_f\left(t\right)f\left(t\right) \approx -\left(1-R\right)Z\left(t\right)\psi\left(t\right) + P_Z\psi\left(t\right) + Z_f\left(t\right)f\left(t\right),$$

again using instantaneous recycling and $P_Z = \int_{m(t_0)}^{\infty} p_{zm}m\phi(m)dm$. We can combine the previous two equations to eliminate $\psi(t)$:

$$m_g\left(t\right)\frac{dZ\left(t\right)}{dt} + \frac{P_Z}{1-R}\frac{dm_g}{dt} = \left(Z_f - Z\left(t\right) + \frac{P_Z}{1-R}\right)f\left(t\right).$$

This equation has the general solution, denoting $y = P_Z/(1-R)$, $m_{gi} = m_g(0)$, and $Z_i = Z(0)$:

$$m_g\left(t\right)e^{Z(t)/y} = m_{gi}e^{Z_i/y} + \int_0^t \left(Z_f - Z\left(t'\right) + y\right)f\left(t'\right)e^{Z\left(t'\right)/y}dt'.$$

The simplest model has $f = 0$:

$$m_g\frac{dZ}{dm_g} = -\frac{P_Z}{1-R}, \qquad Z = Z_i + y\ln\frac{m_{gi}}{m_g}.$$

This says that Z should increase steadily to a present value of about 0.075–0.1, assuming $\ln(m_{gi}/m_g) \simeq 3$ today. However, this result does not seem to fit observations: the large final value of Z is incorrect. Moreover, the total mass of stars born with $Z < Z'$ is

$$M_*\left(Z<Z'\right) = \int_0^{t'}\psi\left(t\right)dt = \frac{1}{1-R}\left[m_{gi} - m_g\left(t'\right)\right], \qquad Z\left(t'\right) = Z'$$

or

$$M_*\left(Z<Z'\right) = \frac{m_{gi}}{1-R}\left(1 - \exp\left[\frac{Z_i - Z'}{y}\right]\right).$$

This is proportional to $Z' - Z_i$ when the argument of the exponential is small, and over-predicts the number of metal-deficient G-K dwarf stars if $Z_i = 0$ (curve 1 in the figure, which shows $M_*(Z<Z')/M_*(Z<Z(t_1))$. This is the famous G-dwarf problem. However, according to the AMR (Eq. (15.1)), $Z_i(0) \approx 0.002$ when the disk formed. The new result is shown by curve 2. The situation is also not as severe as first thought (a factor of 10 or more at [Fe/H]=-0.5), due to the fact that many old, low-metallicity stars had not been

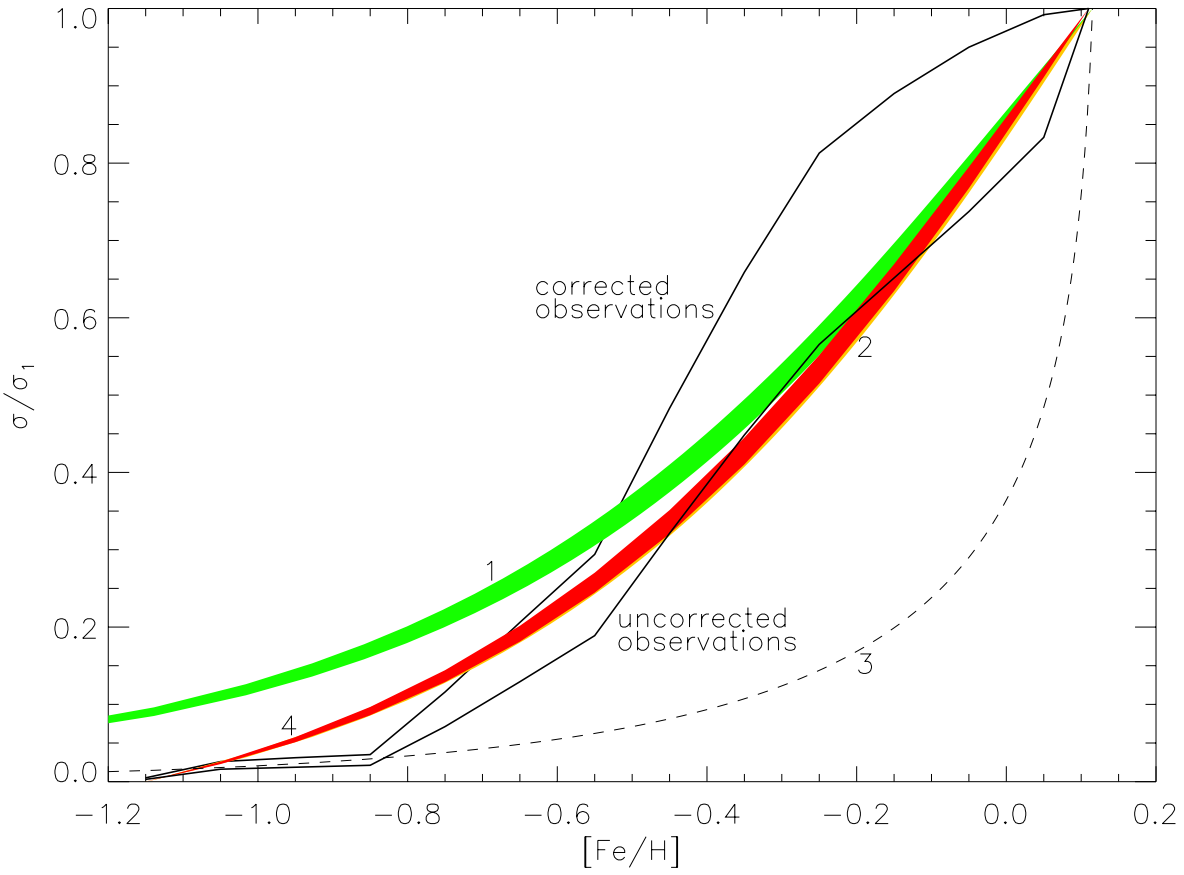

Figure 15.1: The corrected cumulative distribution of stars as a function of metallicity (labelled by uncorrected and corrected observations).

counted because they have moved outside the volume in which the number counts were made. Nevertheless, the large prediction for Z today is a failure.

Note that the star formation rate is

$$\psi\left(t\right) = \frac{-1}{1-R}\frac{dm_g}{dt} = \frac{m_g}{P_Z}\frac{dZ}{dt},$$

which shows that it is proportional to the gas mass, as one would expect. Also note that the explicit time dependence of Z in this approach is not calculable, but if we require consistency with the AMR we can establish it.

These problems point to the following solutions:

1) An early burst of star formation involving an IMF different than today's. There are very few stars of $2M_\odot$ or less involved in this burst. This can be modelled, without infall, using the above by setting $Z_i \neq 0$. The figure (dashed line) shows the case $Z_i = 0.002$, which gives agreement for extremely metal-deficient stars, but like the previous case, underpredicts the numbers of stars of higher metallicity.

2) Alternatively, there has been an appreciable inflow of metal-deficient gas into the disc up to the present time. Consider the case in which infall is enough to make m_g a constant: $f(t) = (1-R)\psi(t)$. The total mass is

$$M\left(t\right) = m_{gi} + \int_0^t f\left(t\right)dt = m_{gi} + \left(1-R\right)\int_0^t \psi\left(t\right)dt.$$

In terms of the variable

$$\mu(t) = \frac{M(t) - m_{gi}}{m_{gi}} = \frac{1-R}{m_{gi}} \int_0^t \psi(t)\, dt,$$

which ranges from an initial value of 0 to a present value of about 20, we have

$$\frac{dZ}{d\mu} = -Z + y.$$

This has the solution

$$Z = Z_i + y\left(1 - e^{-\mu}\right),$$

which tends to y as $\mu \to \infty$. In fact, Z attains an equilibrium value in a very short time (that needed for $M(t)$ to build up to a few times m_{gi}). This equilibrium value is consistent with what's observed today. The cumulative star mass in this model is

$$M_*\left(Z < Z'\right) = \int_0^{t'} \psi(t)\, dt = \frac{m_{gi}}{1-R}\left[\mu(t) - \mu(0)\right] = \frac{m_{gi}}{1-R} \ln \frac{y - Z_i}{y - Z'}.$$

Now we see from curve 3 in the figure that the mass of stars born with small metallicities is much too small.

3) It has also been suggested that there was a loss of heavy elements due to their incorporation in remnants (white dwarfs possibly, but especially neutron stars and black holes) or ejected from the galaxy as hot metal-rich gas (from supernovae). In this case, we set $f = 0$, but introduce a metal-loss term Q, so that

$$\frac{dZ m_g}{dt} = -\left(1 - R - Q\right) Z(t)\, \psi(t) + P_Z \psi(t).$$

In addition, we seek a closed form solution by setting the star formation rate proportional to the gas mass as established before:

$$\psi(t) = \frac{m_g(t)}{t_*},$$

where t_* is an effective time scale of gas exhaustion. We now find an explicit relation for $Z(t)$:

$$Z(t) = \frac{Z(0)\left[e^{Q(t_1 - t)/t_*} - 1\right] + Z(t_1)\, e^{Qt_1/t_*}\left[1 - e^{-Qt/t_*}\right]}{e^{Qt_1/t_*} - 1}.$$

The best fit between this relation and the observational AMR (Eq. (15.1)) is obtained for $Q = 0$, in which case we find Eq. (15.2)! The star formation rate is

$$\psi = \psi(0)\, e^{-(1-R)t/t_*}, \qquad \psi(0) = m_{gi} t_*^{-1},$$

and the cumulative stellar mass is

$$\frac{M_*\left(Z < Z'(t)\right)}{M_*\left(Z < Z(t_1)\right)} = \frac{1 - \exp\left[-(1-R)\, t/t_*\right]}{1 - \exp\left[-(1-R)\, t_1/t_*\right]},$$

or, expressed in terms of Z, is the same as for models 1 and 2:

$$\frac{M_*\left(Z < Z'\right)}{M_*\left(Z < Z(t_1)\right)} = \frac{1 - \exp\left[\left(Z(0) - Z\right)/y\right]}{1 - \exp\left[\left(Z(0) - Z(t_1)\right)/y\right]}.$$

Such a model is thus able to account both for the present-day metallicity and the metallicity distribution in stars.

Table of Contents